ABSTRACT

A theoretical model which permits the computation of average surface temperature trends over the whole life-time of any terrestrial planet is described. The evolution of the atmosphere is considered in detail, and the changes in the physical parameters which affect the surface temperature are discussed. The variables of particular importance are the planetary albedo, the flux factor (a parameter previously considered constant), the infrared absorption spectrum of the atmosphere, the surface infrared emissivity and the probable evolutionary changes in the solar luminosity. Each of these parameters is discussed in detail and the possible feedback mechanisms which may link them to the evolution of the planetary atmosphere/surface system are considered.

The computational techniques utilized in the development of the numerical model are described. The errors are discussed and the model is found to be widely applicable and to produce smoothed temperature tracks which agree well with present-day data for both the Earth and Mars. Numerical methods are used to extend laboratory parameterizations for the variation of absorption with absorber amount and partial pressure for two gases: carbon dioxide and water vapour. Trace constituents and the effect of broadening by neutral gases are discussed.

The resulting temperature curves exhibit a number of interesting features. In particular, a number of the model planets considered are found to exhibit remarkably stable surface

temperatures as their atmospheres evolve. This stability results, in part, from the compensatory nature of the evolution of some of the planetary parameters. The rate and mode of degassing is found to be particularly important for Mars and may also be important for Venus. The temperature curve for the Earth remains above the freezing point of water throughout the life-time of the planet, and thus the predicted results agree well with geological data. Shorter-term fluctuations leading to glaciations, etc., are also discussed.

A THEORETICAL STUDY OF THE EVOLUTION OF THE ATMOSPHERES  
AND SURFACE TEMPERATURES OF THE TERRESTRIAL PLANETS

by

Ann Henderson-Sellers, B.Sc.

Thesis submitted to the University of Leicester for the  
degree of Doctor of Philosophy, September, 1976.

UMI Number: U431235

All rights reserved

INFORMATION TO ALL USERS

The quality of this reproduction is dependent upon the quality of the copy submitted.

In the unlikely event that the author did not send a complete manuscript and there are missing pages, these will be noted. Also, if material had to be removed, a note will indicate the deletion.



UMI U431235

Published by ProQuest LLC 2015. Copyright in the Dissertation held by the Author.  
Microform Edition © ProQuest LLC.

All rights reserved. This work is protected against unauthorized copying under Title 17, United States Code.



ProQuest LLC  
789 East Eisenhower Parkway  
P.O. Box 1346  
Ann Arbor, MI 48106-1346

NOTICE IS HEREBY GIVEN THAT THE LIBRARY HAS RECEIVED A  
STIMSON, RAY TO HOLLOWAY AND CO LTD JAPANESE LIBRARY

THESIS  
521909  
31 3 77



NOTICE IS HEREBY GIVEN THAT THE LIBRARY HAS RECEIVED A  
STIMSON, RAY TO HOLLOWAY AND CO LTD JAPANESE LIBRARY

x75301590X

FRONTISPICE

The appearance of a terrestrial planet is influenced by its  
atmosphere and surface temperature.



and the first project I had

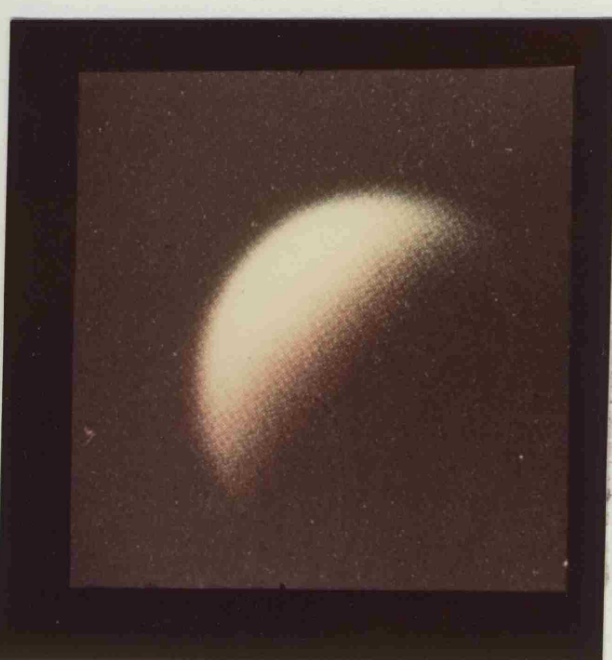
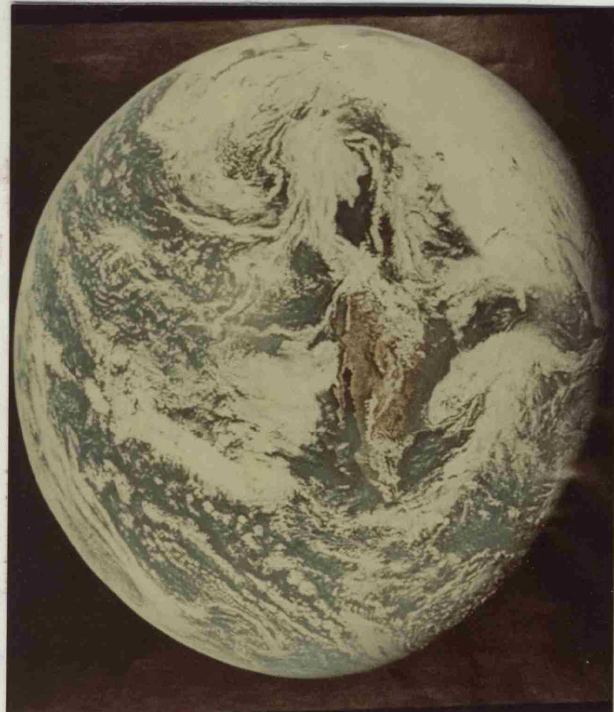
to do was to make

the Earth from clay.

It took me about

two days to make

the Earth from clay.



ACKNOWLEDGMENTS

Throughout the three years of this research project I have received assistance, support and inspiration from many sources. I wish especially to thank my husband, Brian, and my parents for their love and patience. I am deeply indebted to both my supervisors, Professor A. J. Meadows and Dr. G. E. Hunt for all the time and help they have given to me. I wish to acknowledge the Science Research Council for financial support and to thank the Director General of the Meteorological Office for access to members of the Meteorological Office staff and the library facilities.

I have received invaluable help from Professor R. Hide of the Meteorological Office, Dr. A. A. Mills of the Geology Department and Dr. K. Brodie of the Computer Laboratory at Leicester University. I am also indebted to the Astronomy Department of Leicester University and the Science Research Council for provision and financing of the computer time, without which this project would have been impossible, and also to all the members of the Computer Laboratory staff who have guided and assisted my work. I wish also to sincerely thank Mrs. Norma Corby for the efficient typing of this thesis.

Finally, I thank God with all my heart for His love and guidance throughout my life and pray for His continuing support.

ABSTRACT

A theoretical model which permits the computation of average surface temperature trends over the whole life-time of any terrestrial planet is described. The evolution of the atmosphere is considered in detail, and the changes in the physical parameters which affect the surface temperature are discussed. The variables of particular importance are the planetary albedo, the flux factor (a parameter previously considered constant), the infrared absorption spectrum of the atmosphere, the surface infrared emissivity and the probable evolutionary changes in the solar luminosity. Each of these parameters is discussed in detail and the possible feedback mechanisms which may link them to the evolution of the planetary atmosphere/surface system are considered.

The computational techniques utilized in the development of the numerical model are described. The errors are discussed and the model is found to be widely applicable and to produce smoothed temperature tracks which agree well with present-day data for both the Earth and Mars. Numerical methods are used to extend laboratory parameterizations for the variation of absorption with absorber amount and partial pressure for two gases: carbon dioxide and water vapour. Trace constituents and the effect of broadening by neutral gases are discussed.

The resulting temperature curves exhibit a number of interesting features. In particular, a number of the model planets considered are found to exhibit remarkably stable surface

temperatures as their atmospheres evolve. This stability results, in part, from the compensatory nature of the evolution of some of the planetary parameters. The rate and mode of degassing is found to be particularly important for Mars and may also be important for Venus. The temperature curve for the Earth remains above the freezing point of water throughout the life-time of the planet, and thus the predicted results agree well with geological data. Shorter-term fluctuations leading to glaciations, etc., are also discussed.

CONTENTS

Page No.

Frontispiece

Acknowledgments

Abstract

CHAPTER 1 INTRODUCTION: MODEL DESCRIPTION AND

<u>SOLAR INFLUENCE</u>	1
1.1 Introduction	1
1.2 Previous Models	4
1.3 Surface Temperature Calculation	8
1.4 Solar Evolution	12
1.5 Short-Period Variations	19
1.6 Conclusions	23

CHAPTER 2 SURFACE TEMPERATURE CALCULATION

<u>(MATHEMATICAL MODEL)</u>	26
2.1 Introduction	26
2.2 Analysis	28
2.3 Calculation of the Step Function	
Approximation to the Absorption	
Spectrum	36
2.4 Calculation of Surface Temperature	
(Computational Method)	41
2.5 Discussion of the Accuracy of the	
Calculations	44
2.6 Conclusions	49

CHAPTER 3 THE SPHERICAL ALBEDO, SURFACE INFRARED  
EMISSIVITY AND FLUX FACTOR OF A TERRESTRIAL

<u>PLANET</u>	53
3.1 Introduction	53
3.2 Planetary Albedo	55
3.3 Surface Emissivity	60
3.4 Computation of Spherical Albedo	62
3.5 Albedo Calculations for Mars and	
the Earth	68
3.6 Clouds	74
3.7 Expected Variation of the Albedo of	
a Terrestrial Planet	82

	Page No.
3.8 Variation in the Flux Factor	87
3.9 Mars and the Evolution of the Flux Factor	90
3.10 Possible Variations in the Flux Factor of the Earth	96
3.11 Conclusions	100
<b>CHAPTER 4    <u>THE ATMOSPHERIC GASES AND THEIR INFRARED                   ABSORPTION SPECTRA</u></b>	<b>101</b>
4.1 Introduction	101
4.2 The Secondary Atmosphere	102
4.3 Gaseous Absorption	110
4.4 Theoretical Band Model	118
4.5 Computational Extensions	123
4.6 Carbon Dioxide	133
4.7 Water Vapour	151
4.8 Other Absorbers	171
4.9 Neutral Gases	195
4.10 Conclusions	208
<b>CHAPTER 5    <u>MODELS OF EVOLVING PLANETARY ATMOSPHERES                   AND RESULTING SURFACE TEMPERATURES</u></b>	<b>209</b>
5.1 Introduction	209
5.2 Degassing: Mode and Rate	213
5.3 Loss of Gases from the Atmospheric Vapour Phase	219
5.4 Surface Temperature Calculations	232
5.5 Modifications and Extensions	256
5.6 A Multidimensional Method of Calculating the Evolutionary Tracks of Surface Temperatures	263
5.7 Conclusions	279
<b>CHAPTER 6    <u>CONCLUSIONS</u></b>	<b>280</b>
<b>BIBLIOGRAPHY</b>	<b>285</b>
<b>PUBLICATIONS</b>	<b>292</b>

## CHAPTER 1

### INTRODUCTION: MODEL DESCRIPTION AND SOLAR INFLUENCE

#### 1.1 Introduction

The work described in this thesis consists of the development of a theoretical model of surface temperature evolution on a terrestrial planet. The surface temperature is found to depend upon a number of parameters, and these are discussed in detail in the following chapters. However, it seems reasonable to assume that the surface temperature will always be a function of both the total available energy for surface heating and the "blanketing" effect of the atmosphere, which prevents surface cooling. It is this balance between incoming solar energy and outgoing planetary energy that determines the surface temperature. Thus two important aspects of this work will be the consideration of the evolution of the Sun (see Section 1.4) and the evolution of each planetary atmosphere. The solar energy is an external parameter for planetary surface temperature and may thus be considered without reference to the possible state of planetary evolution (which is why it is considered in this first chapter). The evolution of the planetary atmosphere, however, is strongly linked to the state of the surface characterised by its temperature. For instance, it is difficult to establish whether the majority of the volatiles around Venus were driven into the atmosphere by the high surface temperatures, or if the hot surface is a direct result of a massive atmosphere. The truth will, no doubt, be discovered to be a combination of these two possibilities involving complex feedbacks. It is the interdependence of many of

the features of surface and atmosphere of all the terrestrial planets that makes this work both complicated and interesting.

The theoretical model described here has been designed to calculate the mean, global surface temperature at any stage in the evolution of a planet. It was hoped that a successful computation of the evolutionary trend in surface temperature would be a fundamental tool for the discussion of physical, chemical and even biological evolution of the planet's atmosphere/surface system. The importance of the planetary surface temperature can be readily illustrated by consideration of the many planetary characteristics which are directly dependent upon it.

The surface temperature affects the evolution of the atmosphere of the planet. Atmospheres around all the terrestrial planets are thought to have been degassed from the surface rocks. This gaseous emission will be a function of the surface temperature. Also the survival of gases in the atmosphere will depend upon the surface temperature, since very low values lead to condensation of some constituents into polar caps. The lapse rate in the atmosphere depends upon the ground temperature; so cloud formation and precipitation, leading to lake and ocean formation, are also determined by the value of the surface temperature. Also the origin and evolution of life is believed to be closely dependent upon the average temperature of the planetary surface.

The surface temperature is, at least partially, responsible for the physical appearance of a planet. At the moment, the three terrestrial planets which possess atmospheres (Venus, Earth and Mars) are of similar overall composition and, on the scale of

the whole Solar System, are reasonably close together in space. Their outward appearances are, however, strikingly different (see frontispiece). The surface temperatures of these three planets range through approximately 500 K, although the black-body temperatures calculated for their distances from the Sun differ by only 30 K. Thus variation in the value of the surface temperature can lead to changes in the atmospheric and surface conditions on the planet.

The fundamental importance of surface temperature has thus been illustrated. The calculation of planetary surface temperature will have to be an iterative process to permit the inclusion of all the atmospheric/surface feedback mechanisms. The calculation is thus suitable for solution by computer and, indeed, the nature of programming permits both the generalization required to include a number of planets and also the large data variation necessary. The formulation of the equations and the implementation of the surface temperature calculation on the computer is discussed in Chapter 2. Chapters 3 and 4 consider the planetary characteristics which directly affect the surface temperature calculation (i.e. albedo, flux factor, surface infrared emissivity and the absorption properties of the atmosphere). In Chapter 5, the results of a number of planetary surface temperature calculations are discussed and the relative importance of the feedback mechanisms considered.

This chapter is devoted to a literature review, and initial consideration of the basis of the theoretical model. Also the only external parameter (solar luminosity) is considered and the time scales of temperature variations and particularly the applicability of this model are discussed.

## 1.2 Previous Models

Earlier theoretical calculations of surface temperature change fall into two distinct groups. The first group consists of meteorological models designed to calculate surface temperatures (more usually zonal or local, rather than global) on Earth today, which have been "modified/extended" to produce climatological calculations. The second, and very much smaller group, consists of models designed to encompass more than one planet. These models are much better suited to the task of calculation of surface temperatures over the lifetime of the Solar System, but have, in the past, failed to consider the intricacies of feedback loops between the large number of parameters involved. The model described here has been developed over the past three years, and has, I hope, benefitted from examination of both these directions of approach.

The short-term meteorological models, which have been extensively developed around the world, mainly at research institutions, are probably the least useful for this work. The reason is quite simply that the complexity of these models demands huge amounts of data in order to generate forecasts. Data on this scale are only just becoming available for the Earth today, and can never be available for earlier epochs on any planet. It may be possible to simulate atmospheric changes, and thus use these complex models in a continuous mode (i.e. requiring only initial data). However, trials designed to test the stability, over long periods, of forecast models against the real atmospheric behaviour have only recently begun (see e.g. Blumen, 1976). If it

is possible to produce a forecast model which is reasonably stable, there are interesting modes in which it could be run - to simulate a glacial period, for example. Climatic models have been developed for the Earth, but these rely heavily on initial values of parameters, relevant only for the present Earth, and should not "be expected to apply under conditions differing greatly from those existing today" (from Sellers, 1973). Even the simple climatic model suggested by Budyko (1969) has been shown mathematically to be applicable only for very small variations in the planetary surface temperature. Outside these values, the model breaks down and produces complex solutions for the surface temperature (Chylek and Coakley, 1975). Similarly, a model developed by Schneider (1972) to investigate the feedback effects of variations in cloud cover depends, both for magnitude and direction of its results, upon rather arbitrary choices of parameter values. This will be discussed in Chapter 5 (Section 5.3).

Thus both meteorological and climatological atmospheric models, developed for the Earth, are bound, by their formulation and lack of generality, to conditions very similar to those of today. Since there are very few data available for the Earth in earlier stages of its history, and almost none for any other planet, it seems better to develop a general model which can calculate probable trends in surface temperatures without requiring any more than general planetary characteristics as data. Two such models have been considered in the last decade, but neither was general enough to treat the problem satisfactorily.

The early stages of planetary evolution and atmosphere formation were considered by Rasool and De Bergh (1970) with particular reference to Venus. They considered the effect of large amounts of absorbing gas in the atmosphere of a planet, and also allowed for possible albedo variation. Unfortunately, they did not consider the evolution of the Sun. Thus their calculations are appropriate only for the present-day planets. Since it is almost certain (see detailed discussion in Section 1.4) that the luminosity of the Sun has increased since the formation of the planets, the temperatures calculated by Rasool and De Bergh, and, hence, their evolutionary sequences, were in error. The calculations were also a first-stage assessment only, since no attempt was made to consider the further evolution of the atmosphere/surface system once present-day conditions were achieved.

The other paper of importance for planetary evolution was that describing calculations for the Earth and Mars (Sagan and Mullen, 1972). This time, full account was taken of the probable variations in the solar luminosity. The greenhouse increment was calculated by using an approximation to the real transmission curve of the atmosphere. However, no variation in the amount of carbon dioxide or water vapour in the atmosphere of the Earth was considered at any stage in its evolution, although various mixing ratios of ammonia were discussed. Furthermore, the albedos of the planets were unchanged throughout the calculation. These two omissions make the temperature curves presented in their paper unrealistic.

The model described in this thesis attempts to consider the evolution of the surface temperature of a terrestrial planet allowing for all the possible variations of parameters both external and internal to the atmosphere/surface system.

### 1.3 Surface Temperature Calculation

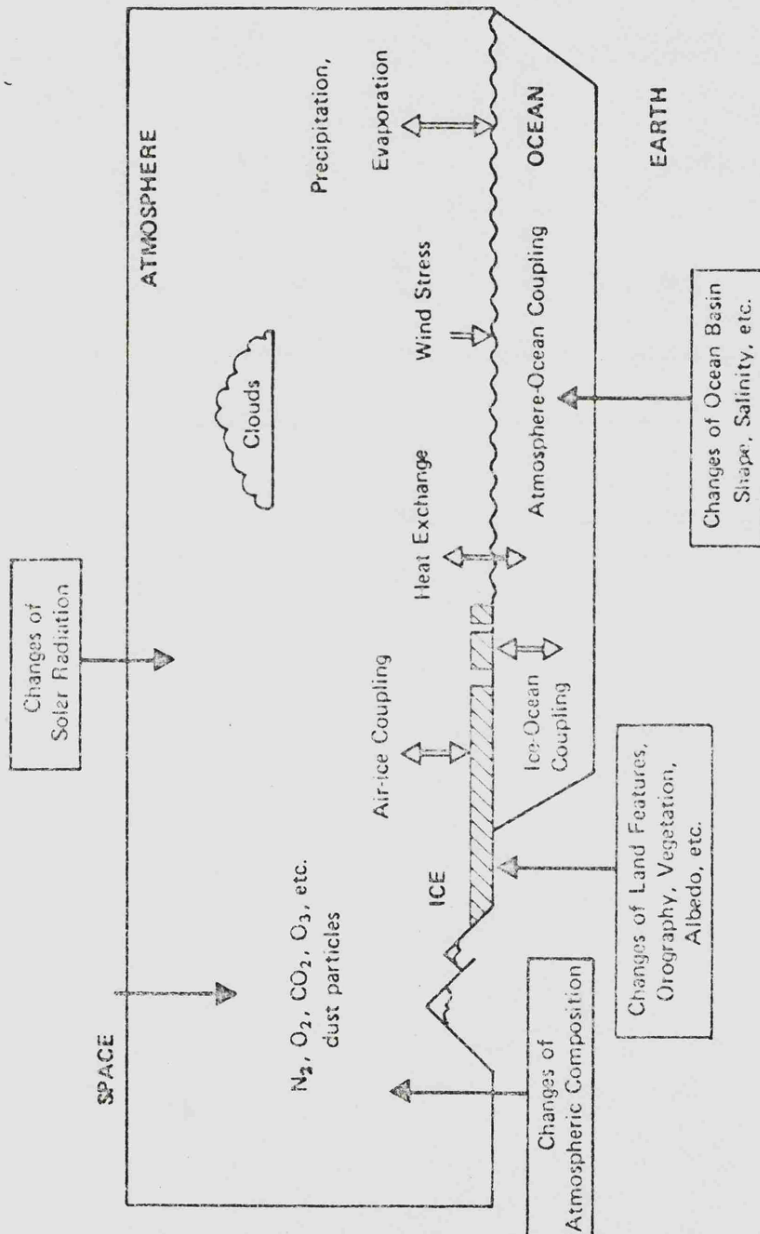
Calculation of a surface temperature depends upon knowledge of a large number of parameters. Figure 1.1 illustrates the complex processes which affect the value of the surface temperature. The figure is obviously a cartoon of a typical bit of the Earth, but many of the processes noted on it are valid for all the terrestrial planets. In particular, three of the four boxes in the figure are relevant to, and of great importance for, all the terrestrial planets. They are:

- i) changes in solar radiation
- ii) changes of atmospheric composition
- iii) changes of land features, orography, vegetation, albedo etc.

These three types of changes will be found to be of the utmost importance for surface temperature calculations. Variations in the incoming flux available to the planet are caused either by variations in the solar luminosity (which will be discussed in the following section), or variations in the planetary albedo. It is also possible that short-term orbital fluctuations will produce variations in the radiation budget, but these will not be significant over the time-spans considered in this work.

It is very important to establish the time-scale over which the calculations of any model are relevant. It was noted earlier that the problems of the climatic models available at present are due to parameter values being valid only for the present-day Earth. The model described here is designed for the long-term calculation of surface temperature. It calculates only the average surface temperature, and this average value is

Figure 1.1



Complex feedback mechanisms affecting the surface temperature. The full arrows are examples of external processes and the open arrows are examples of internal processes in climatic change.

probably not appropriate over shorter times - say  $< 10^8$  years. The problems of identifying what is meant by an 'average global temperature' will be considered in detail in the following chapters. The model does allow for variations in all parameters involved. In particular, the atmospheric constituents and their absorption properties are computed in detail. Also the probable variation in the solar luminosity, planetary albedo, flux factor and surface infrared emissivity are considered and included in the computed temperature curves. The only external variable, the solar flux, is discussed in Section 1.4, whilst all the other variables are considered in Chapters 3 and 4.

The model, which is described in detail in Chapter 2, consists of a suite of computer programs. These programs have been written in Fortran IV, and run on the Leicester University computer - a C.D.C. Cyber 72. The accuracy and self-consistency of the numerical model is discussed in Chapter 2. Calculations of present-day surface temperatures of Mars and the Earth have been performed, and the results (described in Chapter 2) are in good agreement with the observed data. Thus the model enables calculation to be made of the trends of global surface temperatures on any planet over the life-time of the planet, and may also be used predictively. Fluctuations over times very much shorter than the  $4.5 \times 10^9$  years life-time are not calculated (in fact, the curve of surface temperature is smoothed), so that any such oscillations do not appear in this type of global model. The globally averaged results are particularly useful, since they demonstrate the general planetary trend (and, as is seen in

Chapter 5, exhibit remarkable stability). It is also worth noting that calculations more complex than these (i.e. zonal or local temperature calculations) could probably never be substantiated, since geological data only serve to indicate the average global conditions.

The calculations of surface temperatures have been performed for individual planets and, in addition, a series of temperature curves have been produced. These curves (described in Chapter 5) illustrate the individual and combined effect upon the surface temperature of all the parameters of interest. They provide a method of displaying results which allows general conclusions to be drawn about planets of a given type. For example, the evolutionary sequence of the atmosphere of any planet able to support life can be plotted, taking into account the type and evolution of the star it orbits and its distance from that star. The numerical model is sufficiently flexible to allow for the inclusion of many minor constituents in the model atmospheres. The problems of predicting the dominant gases at any stage in the evolution of a planet are considerable. The atmospheres have, in general, been assumed to consist of carbon dioxide and water vapour, but the addition of other secondary components will be discussed and the appropriate calculations of surface temperature made (see Chapters 4 and 5).

1.4 Solar Evolution

The temperatures of all the terrestrial planets are directly dependent upon the radiant energy available to them from the Sun. This energy is, of course, modified both by the reflectivity of the planet and by the planet-Sun distance (see Section 1.5). But the most important factor will arise from any modifications of the solar luminosity. By the late 1950's, the models of stellar evolution and, particularly, of the evolution of the Sun were well established. Age estimates made for the Sun gave values of approximately  $5.0 \times 10^9$  years, which were in good agreement with independent estimates for the age of the Solar System. The Sun was known to be a typical G2 star, and its probable evolutionary track along the Main Sequence had been calculated. These calculations enabled estimates to be made of the likely luminosity change for the Sun over its life-time. The estimates differed slightly, but gave, in general, consistent results. For instance, Schwarzschild et al. (1957) gave

$$\frac{L_{\text{present}}}{L_{\text{initial}}} \approx 1.6$$

whilst, from a similar calculation, Haselgrove and Hoyle (1959) suggested that

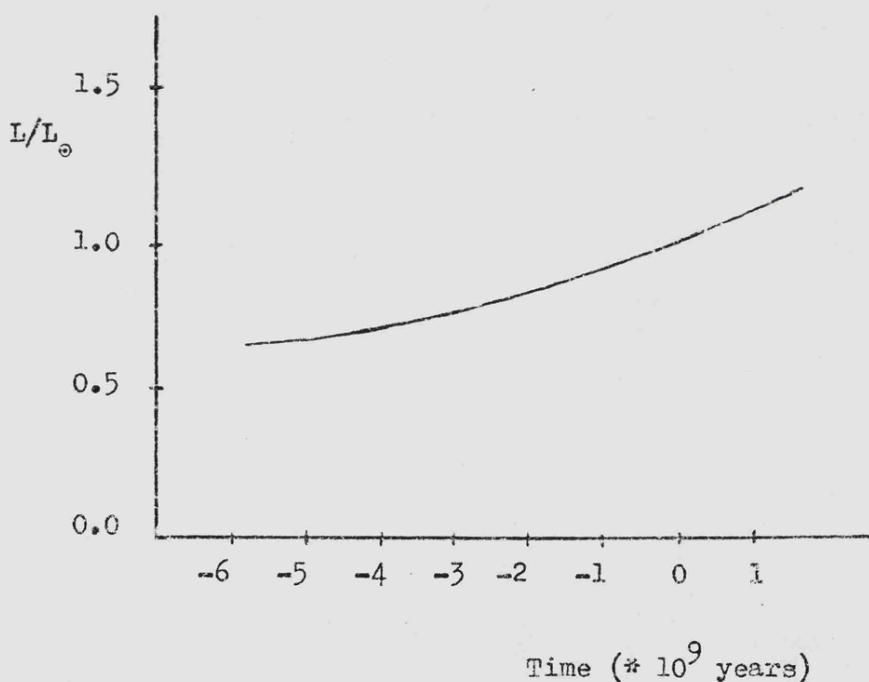
$$\frac{L_{\text{present}}}{L_{\text{initial}}} \approx 1.46$$

The second of these ratios seems to be more appropriate, because the model calculation took into account small effects neglected in the earlier work. This ratio of present luminosity to initial

luminosity gives a percentage decrease (from the present value) in the luminosity of the Sun, over its lifetime, of approximately 30 per cent. The computed values for luminosity divided by present luminosity are illustrated in Figure 1.2 as a function of time. Thus the percentage increase in the solar luminosity over the lifetime of the planets (say 4.5 to  $4.6 \times 10^9$  years) is approximately 43 per cent. It has been suggested that such a large variation in the solar luminosity could have been responsible for detectable terrestrial temperature changes (see, for instance, Schwarzschild, 1958). The magnitude of this luminosity change led Sagan and Mullen (1972) to compute temperatures for the early Earth that were unacceptably low, and, consequently, to postulate the existence of additional absorbing gases in the early atmosphere. This calculation omitted several very important considerations, however, as will be demonstrated in later chapters.

Since the development, and general acceptance, of these models of solar evolution, observational data have created a number of problems. Since 1968, an experiment has been under way to try and count solar neutrinos. Neutrinos were calculated to comprise about 3 per cent of the total energy released by the Sun. The advantage of direct capture of these particles, which are produced during weak decays of nuclei in the central core of the Sun, was that for the first time data would be available on activity deep inside the Sun. The experimental problems of detection are very great. The technique adopted by Davis (see Wick, 1971) is to capture the neutrinos by interaction with chlorine-37 isotopes and count the resulting argon-37 atoms. The

Figure 1.2

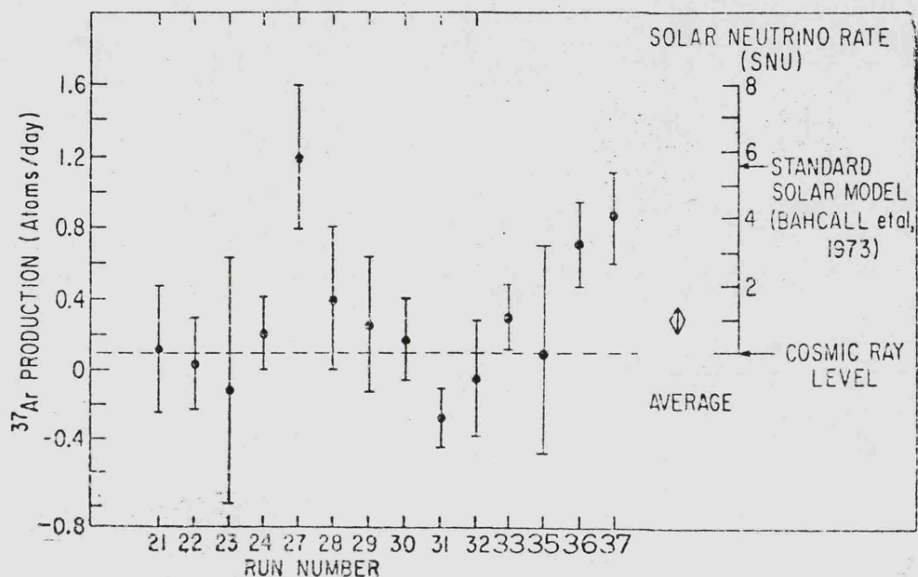


Variation of solar luminosity with time in terms of the ratio of the past luminosity ( $L$ ) to the present luminosity ( $L_{\odot}$ ), (based on the calculations of Haselgrave and Hoyle, 1959).

experiment has to be conducted down a mine (to shield the tank of cleaning fluid employed from cosmic rays). The earliest results published by Davis and his co-workers indicated a rate of detection of neutrinos considerably lower than that predicted by the conventional solar model. The count continued too low (by factors of around 6) for a number of years, and as the experimental technique was examined and improved the conventional solar models were thought to be at fault. It was conjectured that the central temperature of the Sun must be considerably lower than the value given by the standard model but this produced difficulties in dealing with the evolutionary sequence of the Sun over its known lifetime of approximately  $5.0 \times 10^9$  years. Theories were developed that involved a rapid central rotation of the Sun to produce both the observed neutrino flux and the temperatures required (Roxburgh, 1974). However, yet further improvements in the experiment seem to have led to much higher neutrino counts (Bahcall and Davis, 1976), though the new counts still fall short of the predicted values, and the average over the whole experimental period remains below expectation. Figure 1.3 illustrates Davis' results, and indicates the predicted level. The general feeling is now that these results may be reconcilable with the predictions of the standard models.

Within the last few years other observational techniques have been developed which may lead to fuller understanding of the processes acting in the solar interior. The short-period oscillations (of less than one hour) noted by Hill and Stebbins (1975) are now thought likely to be the result of acoustic waves

Figure 1.3



Results from the solar neutrino count experiment (after Bahcall and Davis, 1976). Although the most recent runs have found higher values of neutrino captures the average falls short of the level predicted by a recent solar model based upon the standard theory.

within the Sun. These waves may operate in a number of modes (e.g. radial, quadrupole, etc.) and also have overtone frequencies. The frequencies predicted for the acoustic waves by a standard solar model seem to agree well with Hill's data (see Christensen-Dalsgaard and Gough, 1976). This is further evidence in defence of the standard models of solar evolution. Other oscillations have been observed independently by Russian and by British astronomers (Severny et al., 1976 and Brookes et al., 1976). These oscillations have a longer period (approximately 2 hours 40 minutes) than those originally noted by Hill, although he has also confirmed this oscillatory mode. Initially explanations of this longer period oscillation suggested that it could be a fundamental radial mode - this would imply an almost homogeneous Sun with a very much lower central temperature than is predicted by standard models. (This, incidentally, is also incompatible with the neutrino fluxes observed by Davis.) A model which is more physically realistic than that of a homogeneous Sun has been described by Christensen-Dalsgaard and Gough (1976). They suggest that gravity waves could be excited in the Sun by interference between the seismic waves already identified by Hill. Such gravity waves could produce an oscillation of approximately the required period whilst still retaining a standard solar model.

Thus theoretical and observational work in the last year seems to have re-established the credibility of the early solar evolution models. It is for this reason that, after consideration of all the above evidence, it has been decided to compute

temperature curves for the planets assuming that the solar luminosity has increased by approximately 43 per cent, from its initial value, when the planets condensed, over the life-time of the Solar System. However it should be noted that the model is able to operate under any luminosity variation, and Chapter 5 also derives temperatures produced by other functional relationships.

### 1.5 Short-Period Variations

The model developed here is not sensitive to variations in any parameters over time periods less than  $10^8$  years. This is an intentional limitation, since the method of calculation was designed to span  $4.5 \times 10^9$  years. Thus any fluctuations in the incident radiation at a planet caused by what are often referred to as "long-period" orbital variations are, for this model, essentially short-period variations. The only radiation variation, which will be considered in the surface temperature calculations described in Chapter 5, is that due to the evolution of the Sun (discussed above). However, it is worth noting briefly the short-period variations in input solar radiation, their causes and possible consequences. The variations in available energy may occur over time periods ranging from  $10^5$  years (the eccentricity variation in the planetary orbit) to the 11 year sunspot cycle. There have been a number of attempts to correlate solar activity with meteorological and climatological patterns on Earth (for instance, there appears to be some evidence for suggesting a link between solar sector boundaries and weather patterns - see e.g. Wilcox, 1975). Even more recently the suggestion that glaciations could be brought about by the passage of the Solar System through interstellar dust clouds has been re-examined (see e.g. Dennison and Mansfield, 1976 and Begelman and Rees, 1976). There are other climatic factors, such as volcanic emission of dust, which may also be important in the triggering of glacial periods (see Kelly and Lamb, 1976). Some of the astronomical theories which predict the changes in the

physical parameters are reasonably well developed, but the climatological effects cannot yet be described. The problem lies in predicting the feedback loops which may either enhance, or dampen, slight zonal temperature changes (e.g. precipitation variation at the edge of glacial fields). Simple global circulation models are incapable of handling the zonal insolation changes originally calculated by Milankovitch in 1920. These calculations revealed periodic changes both in the total radiation incident at the planet and in the distribution of the incident radiation with latitude. Such variations could be responsible for climatic changes.

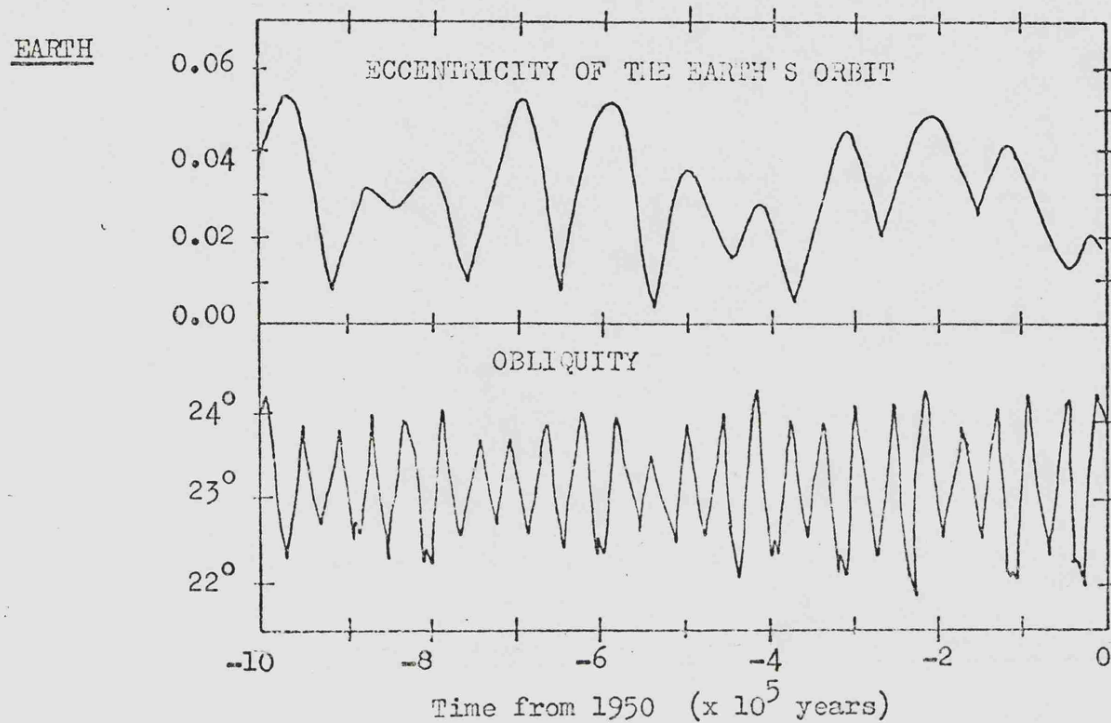
The theory is now often referred to as "Milankovitch Theory", although the idea was suggested in 1842 by Adhemar. Radiation changes are caused by the periodic variation in eccentricity of the planetary orbit, and both the obliquity and the precession of the axis of rotation. The original calculations by Milankovitch for the Earth have been corrected and improved by a number of authors (see e.g. Van Woerkom, 1953) and extended to the planet Mars (Murray et al., 1973). In fact, the calculations for Mars reveal considerably larger variations in the obliquity of the planet than is the case for the Earth. This is caused by the near resonance between the spin axis and orbital plane precession. The eccentricity of the Martian orbit is also larger than that of the Earth. Figure 1.4 illustrates the periodic variations described above for both the Earth and Mars (after Van Woerkom, 1953 and Ward, 1973, respectively).

Obviously, these systematic variations in the net radiation

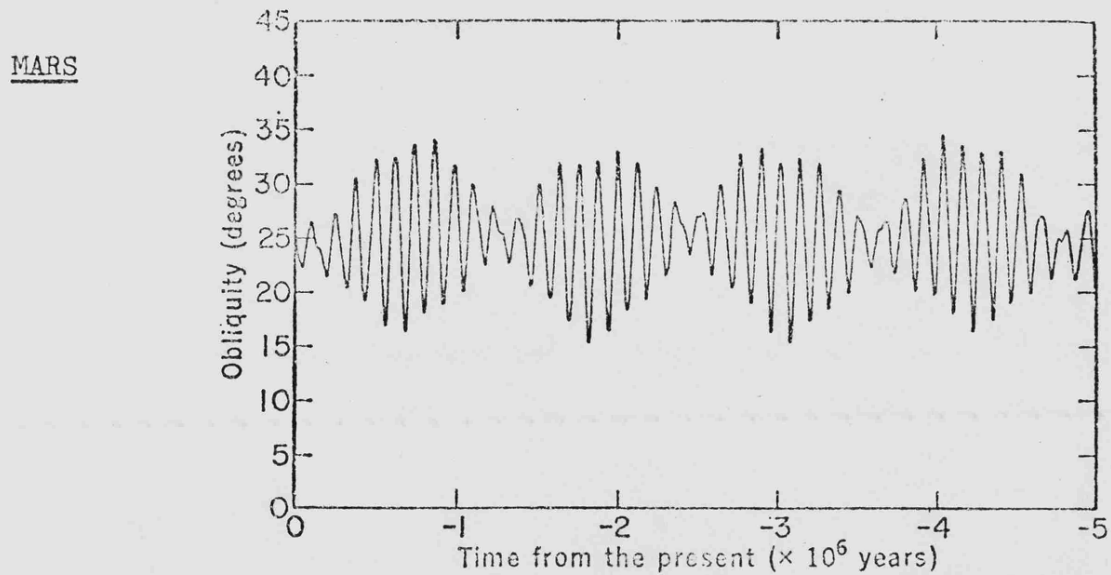
Figure 1.4

21.

Periodic variations due to Milankovitch perturbations calculated for the Earth and Mars. (note different scales).



( after Van Woerkom, 1953 )



( after Ward, 1973 )

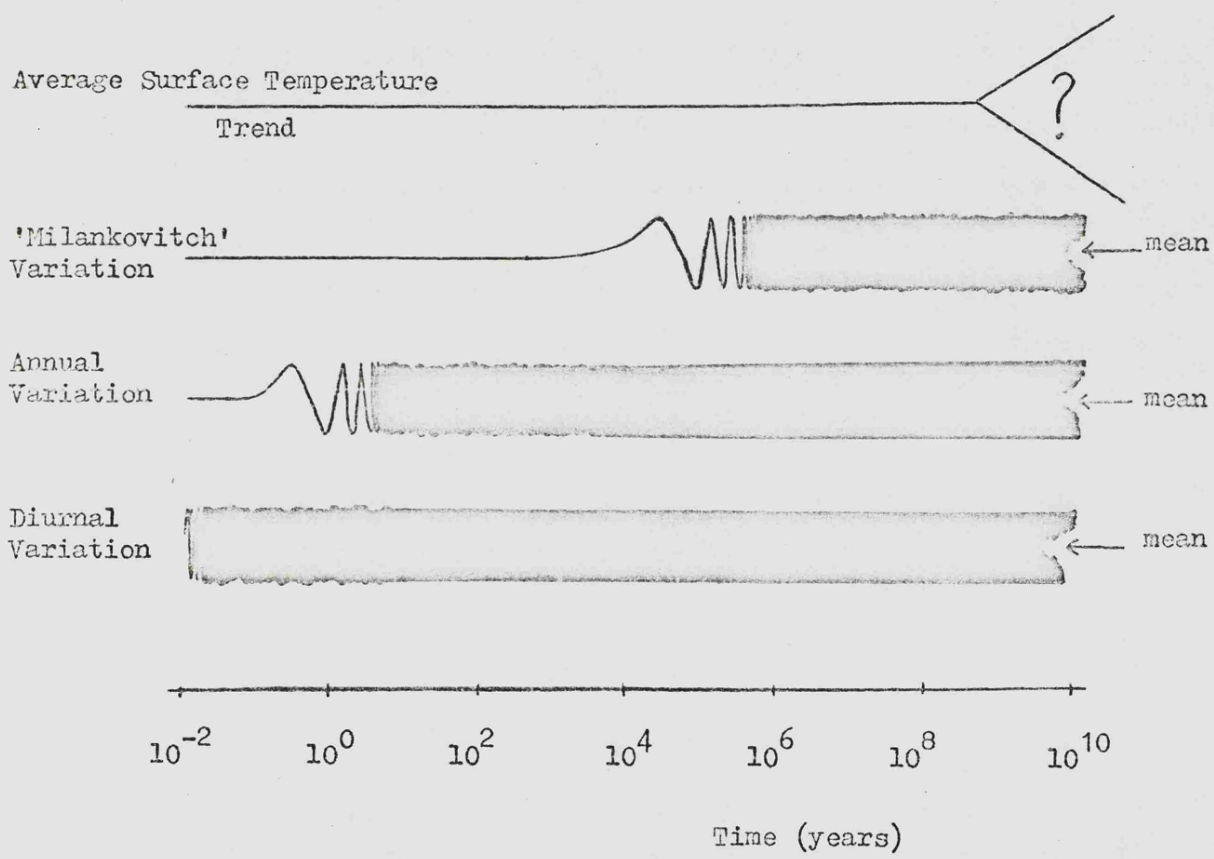
input led to attempts at correlation between radiation and temperature variation. It was argued that zonal variation (rather than global variation) would be of importance in calculation of climatic change. Variation at latitudes high enough to affect glacier formation have been studied for the Earth and in polar temperatures for Mars. The calculations for Mars seemed to indicate that the large radiation variation at the planet could, indeed, produce climatic changes (Sagan et al., 1973). However, the temperature changes produced for the Earth are small, and, it was argued (see Shaw and Donn, 1968), not great enough to produce climatic change. Very recently, work by Kukla (1975) and Weertman (1976) has indicated that even slight temperature changes may be enhanced by meteorological feedbacks to produce a change in the climatic regime. The change in the net radiation balance between polar and equatorial zones may be found to be an important forcing mechanism. This view has been supported by the Director General of the Meteorological Office (see Gribbin, 1976), who considers that the energies are of the right magnitude to produce climatic modification. It may be that future research will confirm that fluctuations in the orbital parameters of the planets can and do cause climatic variations. The time-scale of these variations (as is illustrated by Figure 1.4) are likely to be equal to or less than,  $10^5$  years, and they are almost certainly periodic. Thus, although such short-period variations are interesting and important, their effect upon the very long-term evolution of the planetary surfaces and atmospheres (i.e. the work considered here) will, because of their cyclical variation, be negligible.

### 1.6 Conclusions

This introductory chapter has attempted to describe the importance of planetary surface temperatures. The computer model is designed to calculate mean global surface temperatures over the whole life-time of the Solar System. It cannot be used to calculate local temperatures. This is not an important omission, since there is little or no data to use as input or to support the results of such local calculations for any but the present epoch on Earth. However, it is felt that reasonable deductions about temperature ranges and seasonal variations can be made from a global temperature. The advantages of the model are that it permits the calculation of values for surface temperatures over astronomical times, and that these calculations take into account all the variables which may influence the result. It is applicable to all the terrestrial planets (although the present Venus atmosphere is so massive that the simple radiative model employed cannot produce high enough surface temperatures). It will be used to describe the temperature curve of all the terrestrial planets as their atmospheres evolve (see Chapter 5, particularly Section 5.6).

The long-term nature of the computer model necessitates that parameter values required for the calculation of the surface temperature are averaged over similar time periods. The discussion of solar luminosity variation (in Section 1.4) has indicated the most probable evolutionary path for the Sun. The luminosity curve is found to be almost linear over 4.5 aeons. The following chapters (especially Chapters 3 and 4) will attempt to produce

Figure 1.5



Variations in the surface temperature caused by short-period oscillations. Those illustrated are the diurnal, annual and 'Milankovitch' variations which are all cyclic. Over times very much greater than their period of oscillation these vary too rapidly to be considered as taking anything but their mean value. The amplitude of variations has been assigned the same arbitrary value.

probable evolutionary trends for all the other variables (e.g. planetary albedo and atmospheric absorption) which will be applicable over periods of the order of  $10^9$  years. The validity of discussing values of all the parameters averaged over periods of the order of  $10^9$  years is illustrated by Figure 1.5. This figure attempts to indicate both the cyclical nature of many of the shorter-period variations (e.g. those illustrated, which are the diurnal, annual and "Milankovitch" oscillations in surface temperature) and the impossibility of ascertaining the precise position in each of these short period variations when time periods of the order of  $10^8$  to  $10^9$  years are considered. It thus seems reasonable to take a mean value for all these shorter-period fluctuations when trying to calculate very long-term surface temperature trends.

It is now considered highly probable that the surface temperature of the Earth, over most of its life, should be approximately constant (around 280 K). Is it possible that planetary evolution tends towards this type of stable situation, or is the evolution of the surface temperature of the Earth atypical? It is hoped that the investigation of long-term variations in planetary parameters in this thesis, together with the results produced by the numerical model, will be a first step towards answering this question.

## CHAPTER 2

### SURFACE TEMPERATURE CALCULATION (MATHEMATICAL MODEL)

#### 2.1 Introduction

The average surface temperature of a planet is the critical parameter which determines the present state and the future evolutionary path of the planetary surface/atmosphere system. The surface temperature enhances or inhibits the development of the atmosphere (e.g. by assisting a "runaway greenhouse" effect or by allowing surface condensation of the volatile gases). It also constrains the production or removal of surface features (e.g. by dust, wind or liquid erosion or fissures produced by a freeze/thaw effect) and determines the rates of chemical reactions on the surface and between surface rocks and atmospheric gases (e.g. the taking up of salts into solution in oceans on Earth). Both the spherical albedo and the surface infrared emissivity of the planet are functions of the surface temperature; the spherical albedo is determined by the combined reflectivities of surface and cloud layers and the surface infrared emissivity depends upon the surface types and their areal extent. All these parameters vary with the surface temperature. For example, in the case of Mars at the present time, the freezing of carbon dioxide onto the surface in the polar regions increases the albedo of the planet from approximately 7 per cent (typical of a dark, dust covered surface) to 16 or 17 per cent by the addition of highly reflective polar caps. Similarly this effect may alter the surface infrared emissivity. It can also be seen that

such a large-scale removal of the dominant gas in the Martian atmosphere will alter the infrared absorption spectrum of the atmosphere. Thus the surface temperature also determines the amounts of various gases in the atmosphere (e.g. water vapour in the atmosphere of the Earth) and thus directly affects its infrared absorption properties.

However, the surface temperature is itself a function of all the parameters discussed above. The variation of spherical albedo, surface infrared emissivity and gaseous constituents in the atmosphere all affect the planetary surface temperature. Thus it can be seen that the calculation of even the average surface temperature of a planet must involve iterative procedures. There are also external parameters upon which the surface temperature depends. The solar radiation incident upon the planet/atmosphere system, which is known to have varied during the lifetime of the solar system (as described in Chapter 1), is of particular importance. On much shorter time-scales the orbital fluctuations and short-term solar variations also produce variations in surface temperature.

The model described in this thesis is designed to calculate the average surface temperature of a terrestrial planet and describe a probable evolutionary path with time. This chapter describes the parameters affecting the surface temperature and its calculation at any stage in the evolution of the planet.

## 2.2 Analysis

The effective temperature of any planet represents a balance between the incoming solar radiation and the emitted infrared (or thermal) radiation from the planet. This equilibrium may be written as

$$S(1 - A) = f \sigma T_e^4 \quad \dots\dots 2.1$$

Here  $S$  is the solar flux, integrated over all wavelengths, at the average distance of the planet from the Sun;  $A$  is the Russell-Bond spherical albedo for the planet; and  $f$  (the flux factor) represents the ratio of the area of the planet emitting radiation to the area intercepting the solar radiative flux.

The average emitting (or effective) temperature of the planet,  $T_e$ , may thus be computed. The average surface temperature of the planet,  $T_s$ , is usually higher than  $T_e$  for planets possessing an atmosphere as discussed in Chapter 1. This discrepancy between the effective and surface temperatures is due to the "greenhouse" effect which is caused by the variation in transmissivity of the atmospheric gases with wavelength. The Earth's atmosphere is moderately transparent in the region of visible light and thus most solar radiation in this region passes unimpeded through the planetary atmosphere but the outgoing thermal radiation from the planetary surface is emitted at longer wavelengths, in the infrared region. In this region some of the atmospheric gases absorb strongly. Thus in certain wavelength regions the outgoing radiation is absorbed by the atmosphere which heats up and re-emits thermal radiation in all directions. The downward thermal

radiation adds to the heating effect at the surface leading to an increased surface temperature. The variation in absorptivity of gases in the Earth's atmosphere is illustrated in Figure 2.1. Thus the average surface temperature depends upon the absorption properties of the atmospheric gases involved. It is important to note that the surface temperature also depends upon sensible and latent heat fluxes and especially upon convection. However, the assumption of radiative equilibrium (which is used here) is a useful first order approximation and is simple enough to be applied over evolutionary time periods. The optical properties of the atmosphere must therefore be considered, in detail. At any point in the atmosphere the radiative transfer equation may be stated as:

$$\cos \theta \frac{dI_\nu(\theta, \tau_\nu)}{d\tau_\nu} = I_\nu(\theta, \tau_\nu) - S(\theta, \tau_\nu) \quad \dots \dots \quad 2.2$$

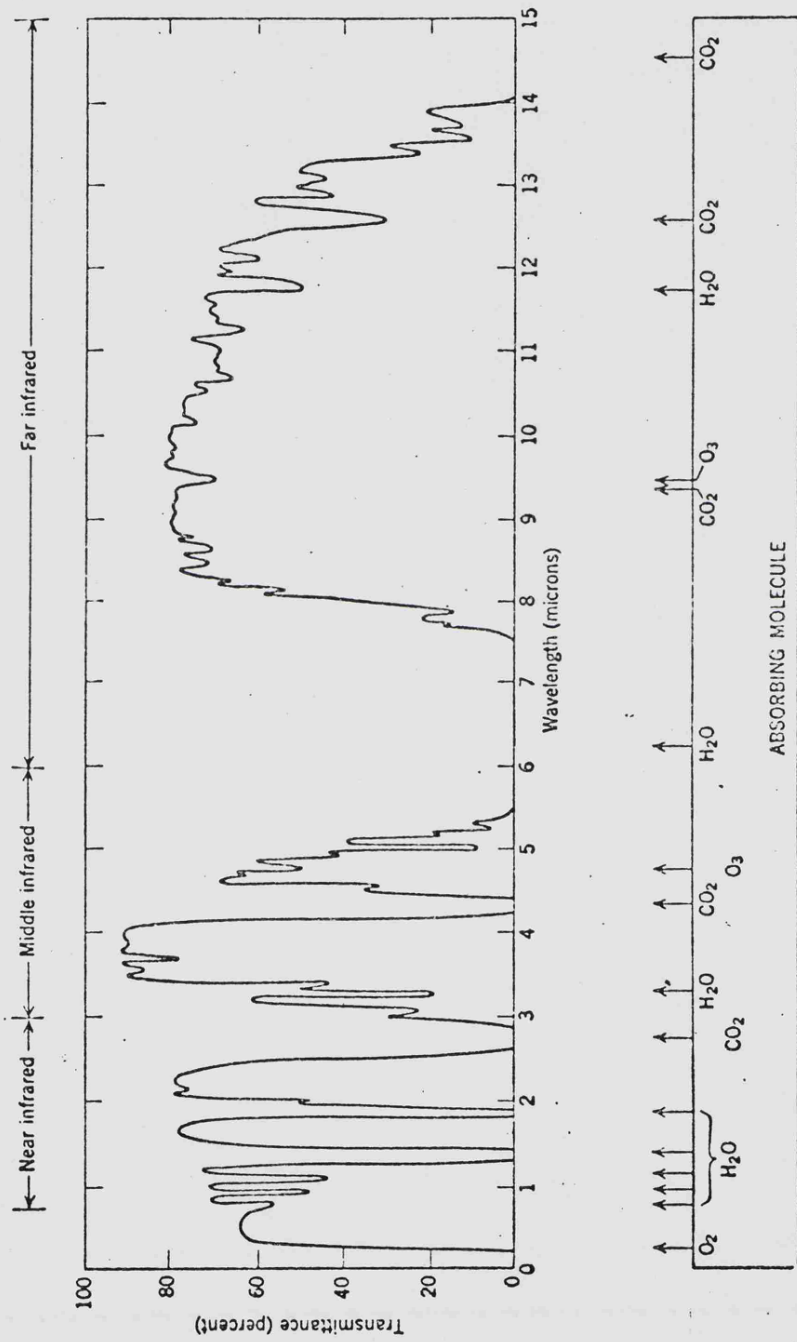
With the assumptions of local thermodynamic equilibrium and integrating over frequency (i.e. assuming the gray body case) this may be simplified so that

$$\cos \theta \frac{dI}{d\tau} = I - B \quad \dots \dots \quad 2.3$$

where  $I(\theta)$  is the intensity of radiation;  $B$  is the "black body" function and  $\tau$  is the optical depth of the atmosphere averaged over frequency. Using Eddington's two-stream approximation to the radiation field the transfer is described by

Figure 2.1

Typical variation in the percentage transmission of gases in the Earth's atmosphere in the infrared region of the spectrum.



Transmittance of the atmosphere for a 6000 ft horizontal path at sea level containing 17 mm of precipitable water

$$T^4(\tau) = \frac{F}{2\sigma} \left( 1 + \frac{3\tau}{2} \right) \quad \dots \dots 2.4$$

Where  $F$  is the constant upward thermal flux which is given by

$$F = \sigma T_e^4 \quad \dots \dots 2.5$$

in terms of the effective temperature of the planet,  $T_e$ , (from Equation 2.1).

At the top of the atmosphere  $\tau = 0$  and  $T(0) = T_{TOP}$  thus

$$T_{TOP}^4 = \frac{T_e^4}{2} \quad \dots \dots 2.6$$

$$T_{TOP} = 2^{-\frac{1}{4}} T_e \quad \dots \dots 2.7$$

This approximate value for the temperature at the top of the atmosphere will be required for a later calculation of the surface temperature. It is also interesting to note that this temperature (derived for a value of optical depth  $\approx$  zero) may be identified with the stratospheric temperature. Thus, on Earth,  $T_{TOP} \approx 207$  K which is approximately the temperature at the tropopause. At the surface of the planet there is a temperature discontinuity; otherwise there could be no upward flux. If the total optical depth of the atmosphere is  $\tau_g$  then the air temperature just above the surface is given by

$$T^4(\tau_g) = \frac{T_e^4}{2} \left( 1 + \frac{3\tau_g}{2} \right) \quad \dots \dots 2.8$$

whilst the surface temperature  $T_s$  is from

$$T_s^4 - T^4 (\tau_g) = \frac{F}{2\sigma} \quad \dots \dots 2.9$$

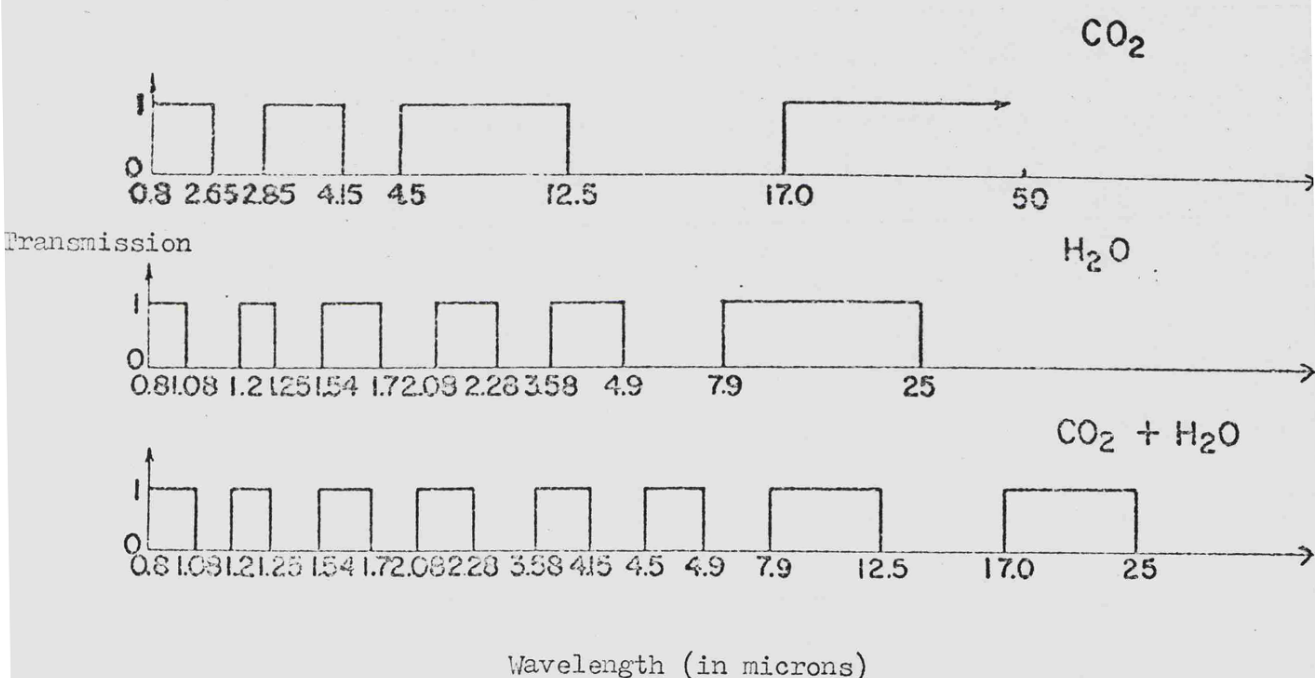
and so

$$T_s^4 = T_e^4 \left( 1 + \frac{3\tau_g}{4} \right) \quad \dots \dots 2.10$$

This temperature jump at the surface must be unstable against convection. Thus the assumption of pure radiative equilibrium is always unstable for a terrestrial planet but provides a useful approximation for  $T_s$ .

Equation 2.10 would enable a calculation of the average planetary surface temperature to be performed. However, the optical depth has been averaged over frequency and thus although it is possible to consider the effect of an evolving atmosphere upon the surface temperature (e.g. Rasool and De Bergh, 1970) the effects of combining gases with strong infrared absorption properties are not easily discerned. Such a gray body approximation to the surface temperature calculation may be considered as a zero order approximation to the real situation whilst the method employed here is a higher (first) order solution. Rather than approximate by integrating over all the frequency intervals of interest it was decided, (in this work), to approximate the transmission spectrum of each gaseous constituent by a step function approximation. Thus absorption spectra of individual gases and of combinations of gases exhibit recognizable features, as shown in Figure 2.2. In this way the transmission spectrum of the atmosphere at any stage in its development may be computed (see Chapter 5). The calculation of

Figure 2.2



Step function approximation to the transmission spectrum of carbon dioxide and water vapour and to the transmission spectrum of a combination of these two gases.

surface temperature using such a block approximation to the true absorption features of the atmosphere utilizes a method similar to that described by Sagan and Mullen (1972). In this work the calculations have been extended by use of laboratory data and semi-empirical representations of absorption. The value of this simplified approach is that it permits calculation of surface temperatures throughout the lifetime of the terrestrial planets.

The incident solar flux is balanced by a two-stream approximation to the outgoing thermal flux from the planet/atmosphere system. The thermal radiation which is emitted from the surface at temperature  $T_s$ , in "window" regions of the atmosphere is considered as passing through the atmosphere unimpeded, whilst the rest, which undergoes absorption by various gases, is considered as emitted from the 'top' of the atmosphere at a lower temperature  $T_{TOP}$ . Thus the balance may be written

$$\frac{S}{f} (1 - A) = \sum_{\lambda_i} e B \lambda_i (T_s) \Delta \lambda_i + \sum_{\lambda_j} B \lambda_j (T_{TOP}) \Delta \lambda_j \quad \dots \dots 2.11$$

From Equation 2.7 the value of  $T_{TOP}$  may be expressed in terms of  $T_e$  (which is readily calculated using Equation 2.1). The value of the average surface temperature,  $T_s$ , may now be calculated using

$$\frac{S}{f} (1 - A) = \sum_{\lambda_i} e B \lambda_i (T_s) \Delta \lambda_i + \sum_{\lambda_j} B \lambda_j (2^{-\frac{1}{4}} T_e) \Delta \lambda_j \quad \dots \dots 2.12$$

where  $e$  is the surface infrared emissivity. The Planck function in terms of wavelength  $B_\lambda(T)$  is given by

$$B_\lambda(T) = \frac{2\pi hc^2}{\lambda^5} \frac{1}{\left(e^{\frac{hc}{\lambda kT}} - 1\right)} \quad \dots \dots 2.13$$

where  $c$  is the velocity of light,  $k$  is the Boltzmann constant and  $h$  the Planck constant. The calculation of  $T_s$  is clearly iterative and requires accurate values of  $S$ ,  $A$ ,  $f$ ,  $e$  and the absorption spectrum of the atmosphere. The latter will be discussed in Chapter 4 and the other parameters are considered in Chapter 3.

### 2.3 Calculation of the Step Function Approximation to the Absorption Spectrum

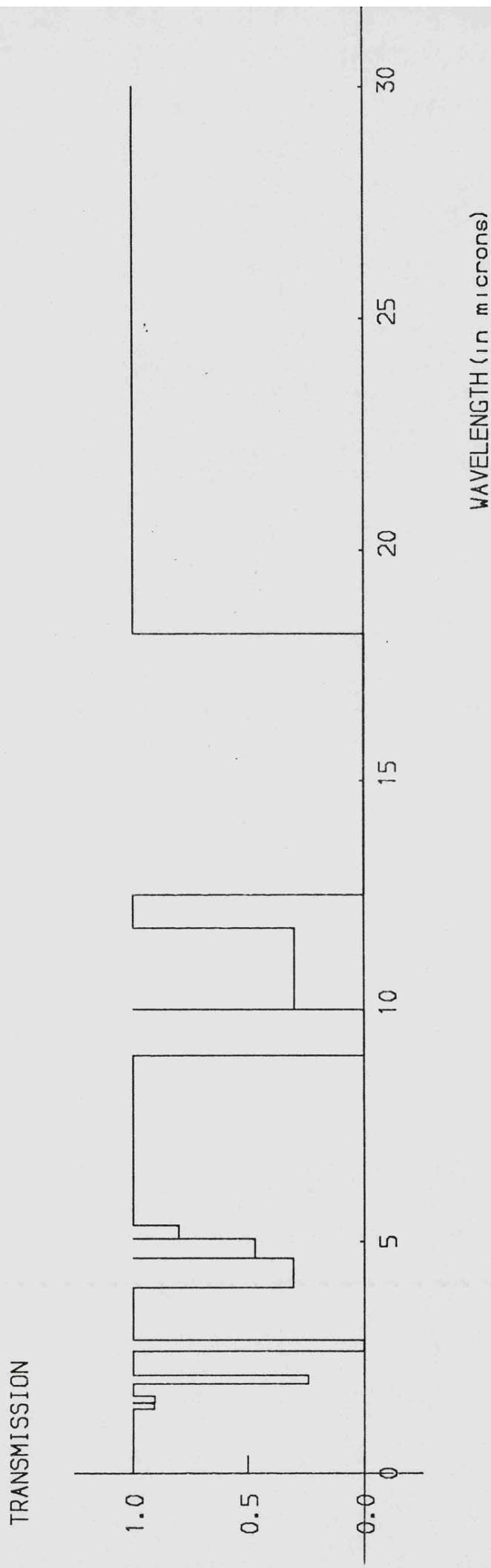
The absorption features of the infrared region are due to vibrational and rotational energy changes in the gas molecules.

The structure of the absorption bands is complex and depends critically upon the particular molecule considered. The gases of special interest in degassed secondary atmospheres are carbon dioxide and water vapour. Other possible constituents (e.g. methane and carbon monoxide) also possess absorption features in the infrared region and may exist in large enough amounts in the atmospheres to be important. The absorption properties of all the gases required are discussed in Chapter 4. Also in that chapter laboratory data are used to produce semi-empirical formulae which permit the calculation of a fractional transmission spectrum for a large range of partial pressures. The spectrum illustrated in Figure 2.3 is typical of the transmission curves produced. However, as discussed in the previous section, this fractional transmission curve must be approximated by a step function representation before computation of  $T_s$  is possible.

This step approximation which allows only total or zero transmission by the atmosphere must be produced with great care since it is necessary to weight the averaging process with respect to the Planck curve for the surface temperature under consideration. The method employed in the production of the step function curves is described in this section.

The thermal flux from the planetary surface is emitted at a temperature of  $T_s$  and thus the absorption of each band is

Figure 2.3  
 $\text{CO}_2$  ( $P_s = 50 \text{ mb}$ ) TRUE SPECTRUM



A typical transmission curve produced using laboratory data as described in Chapter 4.

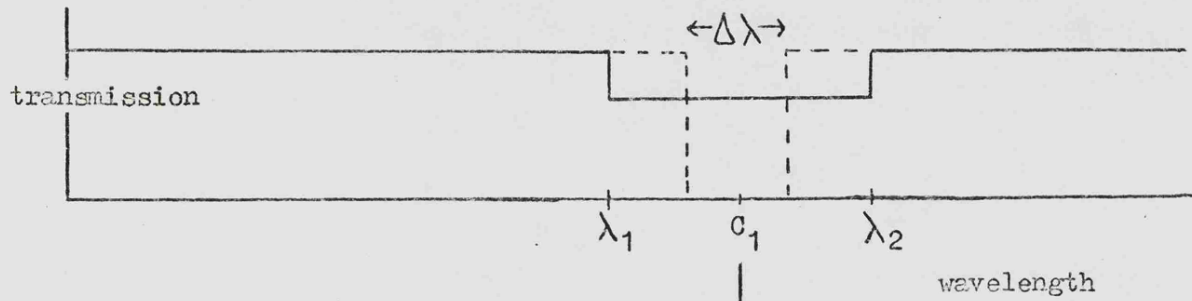
really represented by the fractional area beneath the Planck curve for  $T_s$  over the wavelength region of the band. The method used to approximate the true band is illustrated in Figure 2.4. The band is defined as extending from wavelength  $\lambda_1$  to wavelength  $\lambda_2$  and has an average percentage transmission in this region (as shown by the solid curve in part i) of Figure 2.4). The width,  $\Delta\lambda$ , of the fully absorbed step function, which will replace the band, is calculated by equating the areas under the solid and dotted curves in i). To ensure that the total energies are equal, however, it is also necessary to equate the area of the fractionally absorbed band beneath the Planck curve to the area defined by the step function (shown in ii)). Since the width,  $\Delta\lambda$ , of the step function is already determined this equating of energies may involve a recentring of the step function. The step function is repositioned so that its centre is now given by  $C^*$  rather than  $C_1$  (see iii)). The direction of movement of the fully absorbed approximation is determined by the position of the band relative to the peak of the Planck curve. This procedure is a second iteration following the first calculation of  $T_s$  since it requires the value of  $T_s$  to be well determined. It is found to produce significant variations in the second iterative calculation of  $T_s$  only for strong bands near the peak of the black body curve.

Thus the complete procedure involves initially positioning the fully absorbed steps by centring them at the centre of the partially absorbed band.  $T_s$  is then calculated using this first

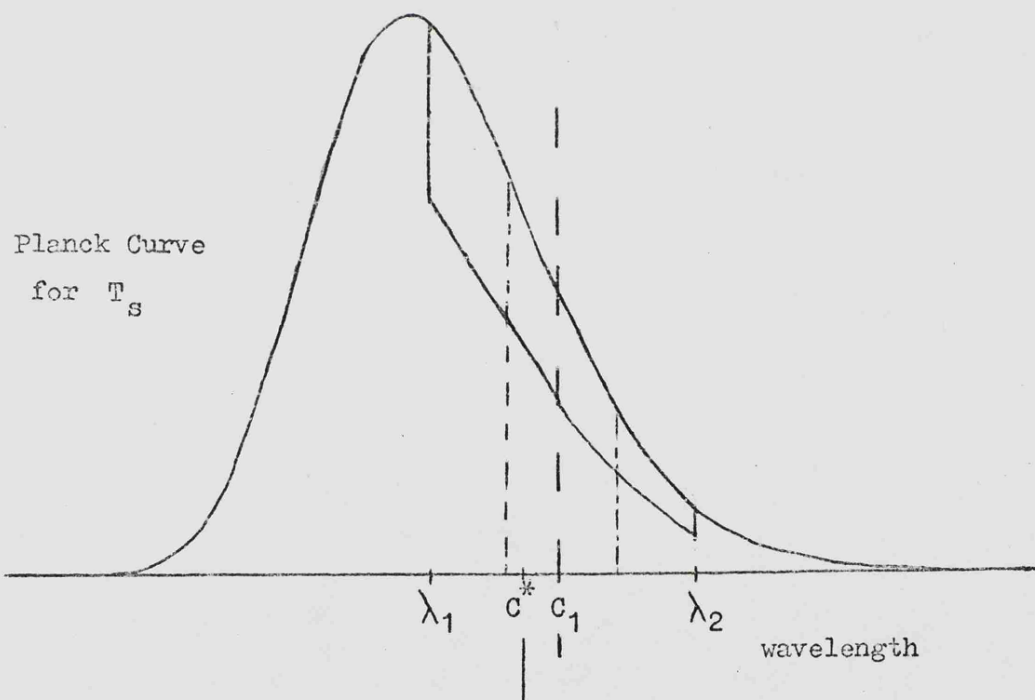
Figure 2.4

Graphical representation of the recentering procedure.

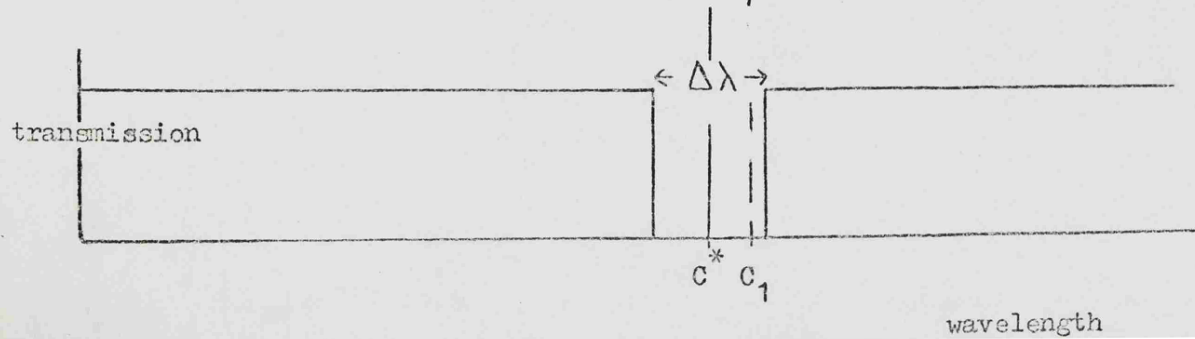
- i) Determination of block width,  $\Delta\lambda$ .



- ii) Equalizing of total energies by movement of block.



- iii) Final block position in transmission spectrum (note change of central position from  $c_1$  to  $c_1^*$ ).



step function approximation. Any strong bands near the peak of  $B_\lambda(T_s)$  are next re-positioned, as described above, and using this improved step function a better value of the surface temperature is obtained. For surface temperatures of interest in this model the iteration of  $T_s$  is found to be sensitive only to the first movement of even strongly absorbing bands.

## 2.4 Calculation of Surface Temperature (Computational Method)

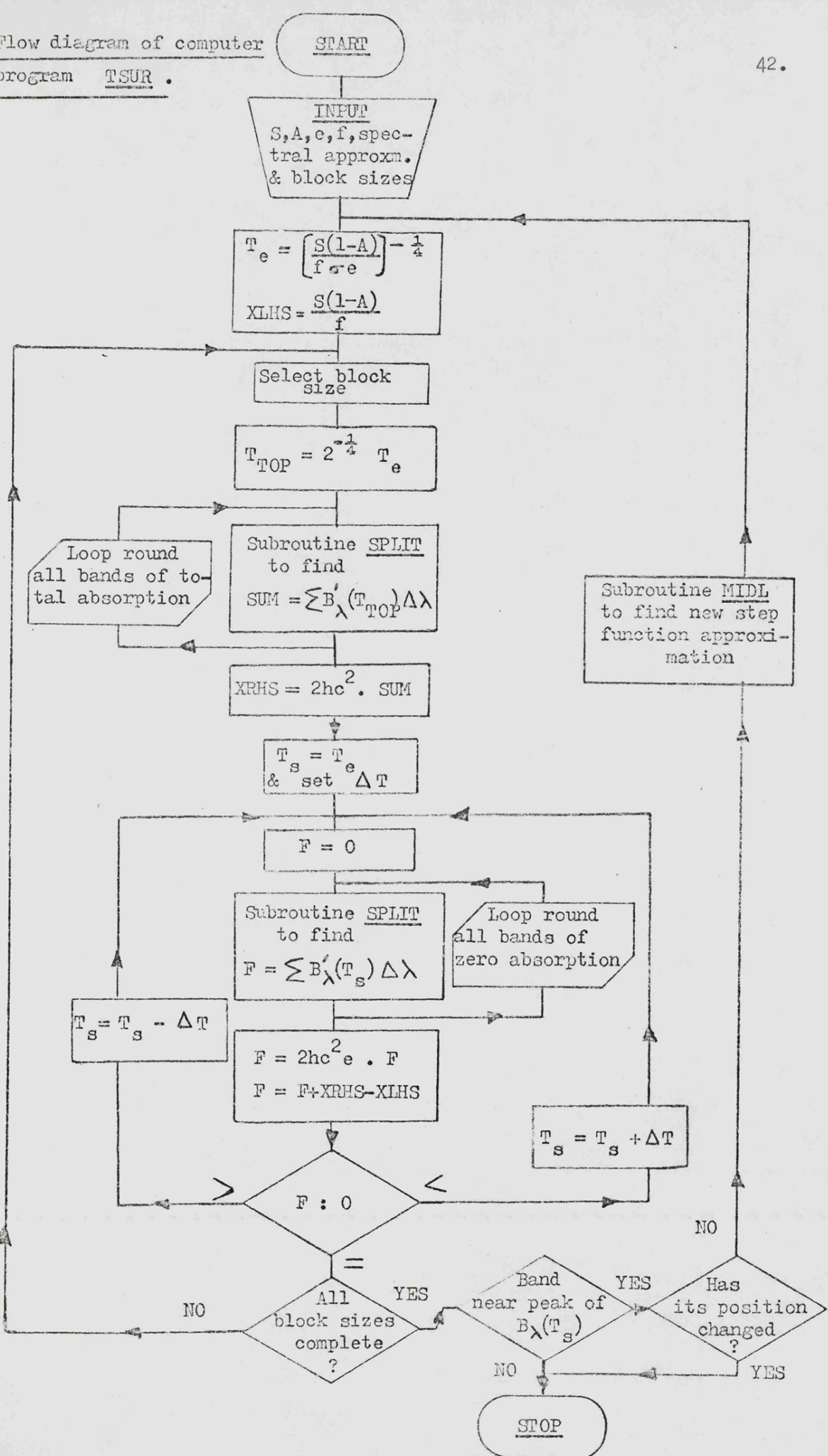
The computer program (called TSUR) which calculates surface temperature is written to solve Equation 2.12 iteratively for  $T_s$ . It was found necessary to choose carefully the widths,  $\Delta\lambda_i$  and  $\Delta\lambda_j$ , of the wavelength intervals over which the summations were performed so that the regions in which the Planck function was changing rapidly were adequately packed. Thus the wavelength region of the absorption approximation was divided into intervals of width  $\Delta\lambda$  (the block size).  $T_s$  was calculated using diminishing widths of  $\Delta\lambda$  until a further change in  $\Delta\lambda$  produced a negligible alteration in  $T_s$ . Also, as described in Section 2.3, an iterative procedure was employed to ensure the best positioning of the fully absorbed step approximations.

The final model of an evolving planetary atmosphere would involve variation of albedo, infrared surface emissivity, flux factor, absorption spectrum and solar luminosity and thus all these parameters, input as data for this program, were allowed to vary independently. Since it was intended to use an iterative method to evaluate  $T_s$  the zero-order approximation was chosen to be equal to the effective temperature,  $T_e$ , (calculated from Equation 2.1).  $T_e$  is the minimum possible value of  $T_s$ , and  $T_s$  can take this value only for a planet with no atmosphere. Equation 2.12 was rewritten in the form

$$F = \sum_{\lambda_i} e^{B_{\lambda_i}(T_s)} \Delta\lambda_i + XRHS - XLHS \quad \dots\dots 2.14$$

Flow diagram of computer  
program TSUR .

42.



where

$$XLHS = \frac{S}{f} (1 - A) \quad \dots\dots 2.15$$

and

$$XRHS = \sum_{\lambda_j} B_{\lambda_j} (2^{-\frac{1}{4}} T_e) \Delta \lambda_j \quad \dots\dots 2.16$$

Thus when the correct value of  $T_s$  has been achieved the function,  $F$ , becomes zero. This method of iteration is illustrated in the flow diagram of the program TSUR.

The subroutines called by TSUR are: i) SPLIT which divides the wavelength region passed to it into the smaller widths of size  $\Delta\lambda$  and then performs the summations indicated, and ii) MIDL which re-centres any strongly absorbed band close to the peak of  $B_\lambda(T_s)$  in the manner described in Section 2.3. The re-positioning of any strong bands by MIDL necessitated a recalculation of  $T_s$  as shown in the flow diagram. In practice both these iterative loops were suppressed after two calculations (see Section 2.5) and the centre iterative loop calculating  $T_s$  was, in general, suppressed once an accuracy of  $\pm 0.08$  K had been obtained. The whole problem of the accuracy of the results derived from this computer program will be discussed in the following section.

## 2.5 Discussion of the Accuracy of the Calculations

The method of calculation of the average planetary surface temperature outlined in this chapter incorporated variations in all the parameters (solar luminosity, albedo, surface emissivity, flux factor and absorption spectrum) to produce a model of the evolving surface conditions on a terrestrial planet. These results are discussed in Chapter 5 and the variations expected in all the parameters listed above are discussed in Chapters 3 and 4. However, the value of the results produced depends upon the accuracy of the mathematical model described in this chapter. A number of approximations are implicit in the model, itself, and thus warrant discussion here.

Probably the biggest problem in any surface temperature calculation is the complex feedback responses generated by a change in the surface temperature. An increase of surface temperature on the Earth today would probably lead to higher rates of evaporation of water vapour into the atmosphere but the combined effects of increasing the absorption by water vapour and possibly increasing the albedo by the formation of more clouds are difficult to establish. This problem is considered further in Chapters 4 and 5.

The approximations which lead to the mathematical formulation of the relationship between the average surface temperature,  $T_s$ , and the other variables have been outlined in Section 2.2. Equation 2.12 from which all the surface temperatures are derived is a gross approximation to the complex radiative balance. Thus it seems unreasonable to quote figures for the average surface

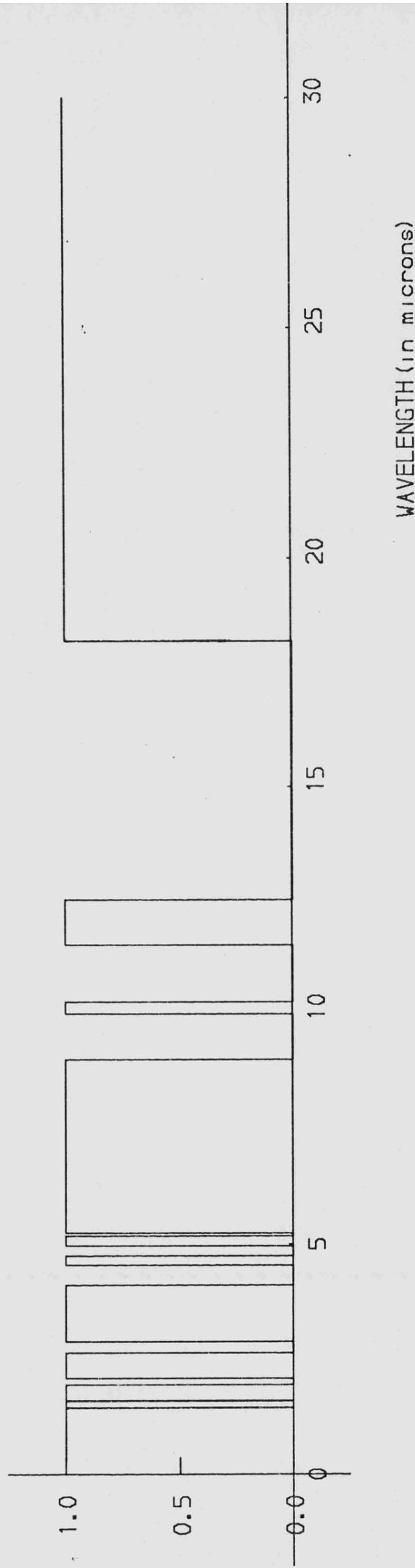
temperature to any greater accuracy than 0.1 K. This is the reason for terminating the iteration of  $T_s$  at an accuracy of  $\pm 0.08$  K as mentioned in Section 2.4.

Many other approximations have been made in an attempt to save computational time. Iterative loops are usually written so that high accuracies may be obtained, but then the last few iterations are suppressed for all but test calculations. Using this technique it was discovered that the final value of  $T_s$  was almost insensitive to further diminishing of the block size,  $\Delta\lambda$ , below one micron (a default allowed bands of width less than this to be calculated individually). Similarly, the recentring procedure discussed in Section 2.3 was found to produce significant variations in the second calculation of  $T_s$  only for bands close to the peak of the Planck curve for  $T_s$ . Table 2.1 lists the variation in  $T_s$  produced by movement of the 15 micron band of carbon dioxide. The other parameters in the calculation were assumed to be those typical of Mars at the present time, except that  $f$  had a value of 4. The atmosphere was taken as pure carbon dioxide and only the surface pressure was varied. The arithmetic centre of the 15 micron band is 15.341 microns and the table lists the displacement from this value caused by the recentring procedure. These results illustrate the increasing surface temperature with mass of carbon dioxide in the atmosphere and also the typical variation in  $T_s$  produced by the recentring procedure. Figure 2.5 is the step function approximation of Figure 2.3, and illustrates the type of block approximation produced by the routines described above.

Figure 2.5

$\text{CO}_2$  ( $P_s = 50 \text{ mb}$ ) STEP FUNCTION

TRANSMISSION



Step function approximation to the real transmission curve illustrated  
in Figure 2.3.

Table 2.1

Temperature Changes Caused by Recentering the 15 Micron Band of CO<sub>2</sub>  
for Mars

CO <sub>2</sub> surface pressure (mb)	T <sub>s</sub> (K)	New Centre (microns)	Displacement (microns)	New T <sub>s</sub> (K)
1	223.58	15.682	0.341	223.50
10	229.18	15.568	0.227	229.02
20	232.30	15.454	0.113	232.14
50	238.86	15.341	0.0	238.86

Two further approximations implicit in the program TSUR are the cut-off points for the calculation at both long and short wavelengths. The absorption spectra (which will be calculated for various gases and pressures in Chapter 4) are all assumed to begin at 0.8 microns. This is outside the wavelength region in which the Planck curves for temperatures in the range 200 K to 300 K are significant. Thus all the near infrared region is easily included. However the long-wavelength region is less easily approximated since the Planck curve may still be significant at 100 microns and beyond. At least two atmospheric gases (water vapour and ammonia) have strong absorption features in the far infrared region and thus may contribute to the "greenhouse" increment because of absorption in this region. The nature of the iteration procedure used to calculate T<sub>s</sub> actually produces values too high if part of the far infrared region is neglected. This is illustrated by the temperatures given in Table 2.2. The values of T<sub>s</sub> have been calculated for the present day Earth, but the summation process has been terminated at a number of different

wavelengths.

Table 2.2

Effect upon Surface Temperature Caused by Varying the Longwave Cut-

Off Point in the Calculation

Cut-off point (microns)	25	50	90	900
$T_s$ (K)	298.2	287.7	285.1	284.4

This table illustrates the need for care in determining the point of termination of the summations. In general, summations were discontinued at 90 microns since, as is illustrated by Table 2.2, only a slight variation in  $T_s$  is produced by continuation beyond this point. However, it should be noted that particular care was required in the precise situation of the step function approximation to the rotation band of water vapour. This problem is discussed more fully in Chapter 4.

## 2.6 Conclusions

This chapter has been devoted to a description of the mathematical and computational methods which have been used in the calculation of average surface temperatures. The accuracy of the calculations has been commented upon and the complex nature of possible feedback processes has been noted. However, the methods of computation of  $T_s$  are sufficiently reliable to enable long-term trends in surface temperatures to be modelled.

The accuracy of the model may be indicated by applying it to the present-day situations on both the Earth and Mars. For these two planets the other parameters are reasonably well established. A further difficulty arises in the case of Mars since the definition of an average surface temperature (although very useful over long time periods) cannot be readily compared with the widely differing 'spot' temperatures observed on Mars. The Martian surface temperatures vary over a range greater than 100 K between day and night time and between approximately 145 K (minimum polar cap temperature) and 305 K (maximum equatorial temperature). Using values described in greater detail in Chapter 3 for the albedo, emissivity and flux factor and assuming a pure carbon dioxide atmosphere of between 10 and 20 millibars surface pressure the model produces  $T_s$  in the range 230 K to 250 K. This value of an average surface temperature for Mars does not conflict with observed values.

The calculation of an average surface temperature for the Earth involves the infrared absorption by both carbon dioxide and water vapour broadened by a large amount of a neutral gas.

This computation will be discussed in much greater detail in Chapter 4. The results produced for present-day values of other parameters and appropriate amounts of water vapour and carbon dioxide are in the range 283 K to 288 K which seem reasonable values for  $T_s$ .

A further simple calculation, which indicates the sensitivity of this method of calculating  $T_s$ , is to double the total amount of carbon dioxide in the Earth's atmosphere. The values given in Table 2.3 are typical of the results produced by the model.

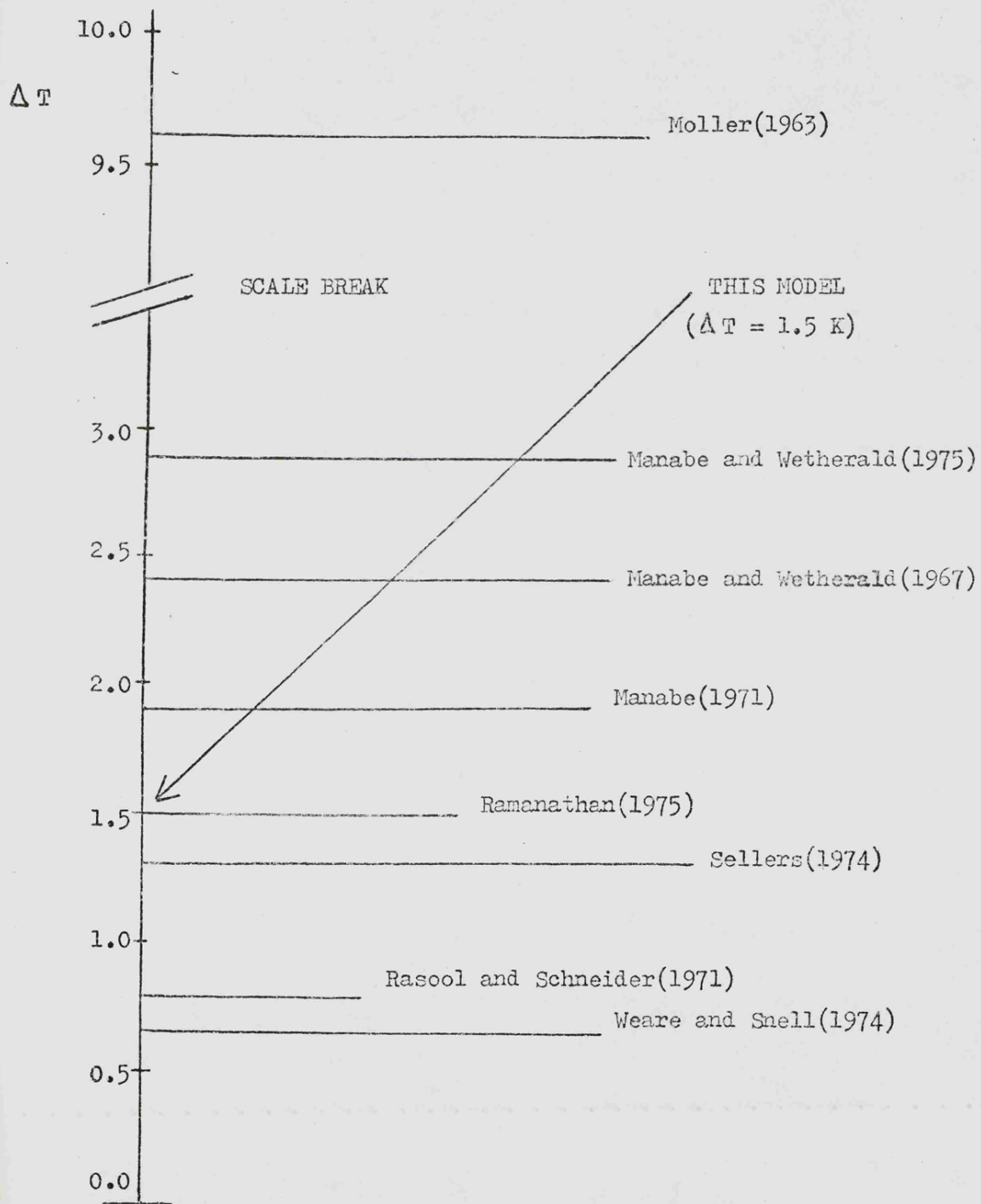
Table 2.3

The Effect upon Surface Temperature of Doubling the CO<sub>2</sub> Amount in the Earth's Atmosphere

Present Earth's atmosphere	Earth's Atmosphere with twice CO <sub>2</sub> partial pressure
$T_s$ (K)	285.1

These results indicate an increase of 1.5 K in  $T_s$  caused by doubling the amount of carbon dioxide. The real percentage increase expected in the surface temperature is generally thought to be between 1.5 K and 3 K. However the wide variation in temperature increase in current literature is illustrated in Figure 2.6 and described by Schneider (1975). Thus the model described here produces a satisfactory result which lies within the range of values produced by much more complex climatic models.

Figure 2.6



Surface temperature increments,  $\Delta T$ , caused by doubling the carbon dioxide amount in the Earth's atmosphere as predicted by a number of different climatic models. The result derived here agrees well with those of more complex models.

The model described in this thesis is intended to predict long-term surface temperature trends over the life-time of the terrestrial planets. Only average surface conditions can be studied over such long periods, but from these global averages deductions can be made about possible regional variations. The methods outlined in this chapter are an efficient means of calculating the global climatic trends over astronomical times.

CHAPTER 3

THE SPHERICAL ALBEDO, SURFACE INFRARED EMISSIVITY AND FLUX FACTOR  
OF A TERRESTRIAL PLANET

3.1 Introduction

As discussed in Chapter 2 long-term changes in the average surface temperature,  $T_s$ , of a planet with an evolving atmosphere are most readily derived in terms of an effective temperature,  $T_e$ , defined by

$$S(1 - A) = f \sigma T_e^4 \quad \dots \dots \quad 3.1$$

The average surface temperature,  $T_s$ , is then obtained, allowing for the "greenhouse" effect, by dividing the emergent flux into two parts as described in Chapter 2. This approximation permits the calculation of  $T_s$  using the expression derived as Equation

2.19 viz:-

$$\frac{S}{f} (1 - A) = \sum_{\lambda_i} e B_{\lambda_i} (T_s) \Delta \lambda_i + \sum_{\lambda_j} B_{\lambda_j} (2^{-\frac{1}{4}} T_e) \Delta \lambda_j \quad \dots \dots \quad 3.2$$

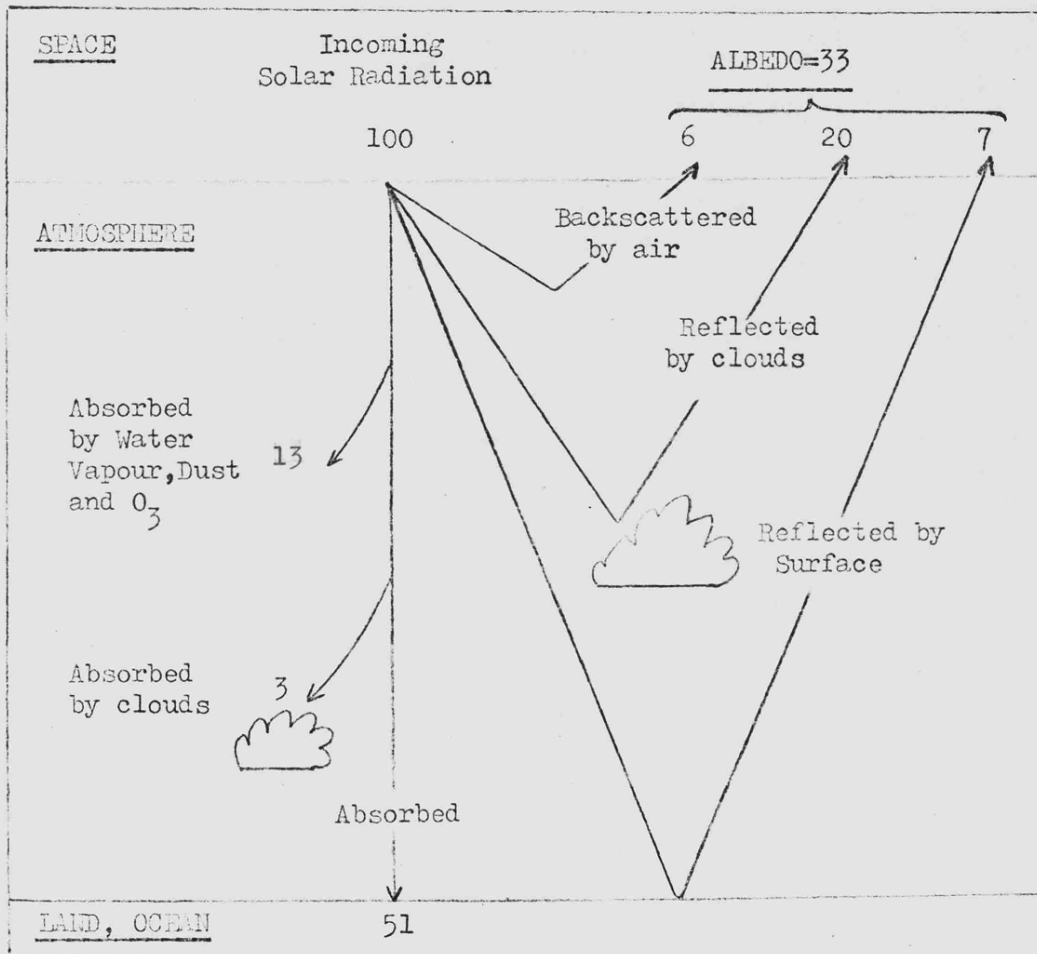
where the infrared absorption spectrum is approximated by a step function, so that there is total absorption at the wavelengths  $\lambda_j$  and zero absorption at the wavelengths  $\lambda_i$ . The emissivity of the planetary surface is given by  $e$ . All five of these factors,  $S$ ,  $A$ ,  $e$ , the infrared absorption spectrum and  $f$  are potentially variable over the time-scale of the planet's existence. Variations in the first four of these have been recognised (though not necessarily simultaneously) in previous calculations

of atmospheric evolution (e.g. Rasool and De Bergh, 1970; Sagan and Mullen, 1972). In this chapter the variation in albedo and emissivity will be discussed. The variation in the infrared absorption spectrum will be considered more fully in Chapter 4. Also in this chapter the variations in the flux factor (a parameter previously neglected in all calculations) will be considered in terms of atmospheric evolution.

### 3.2 Planetary Albedo

In any calculation of the surface temperature of a planet knowledge of the amount of input solar radiation is vital. This value depends upon two factors: the solar flux at the planet, denoted by  $S$ , and the spherical albedo of the planet,  $A$ . The solar flux is a function of the solar luminosity and the average planetary distance from the Sun. As discussed in Chapter 1 the solar luminosity will be considered to have increased linearly by a factor of approximately 43 per cent, from its initial value, over the life-time of the Solar System. The planetary albedo is a measure of the reflectivity of the planet/atmosphere system. Thus the albedo of the Moon is simply an expression of the reflectivity of its surface whilst that of Mars depends, for example, upon the area of the surface covered by the highly reflective polar caps. Venus has an albedo which is determined entirely by its cloud decks since little solar radiation penetrates to the planetary surface. The Earth is an intermediate case as the incident solar radiation may either be reflected by clouds (which cover approximately half the planetary surface) or may penetrate to the surface to be reflected by one of various surface types (e.g. ocean, desert, ice, vegetation), as illustrated in Figure 3.1. The average albedo of the Earth thus depends upon the reflectivity of these different surfaces, their relative proportions and distribution as well as upon the cloud cover. Clouds are found to be highly reflective and thus the higher the proportion of planetary surface which is cloud covered the higher the planetary albedo and consequently the smaller the

Figure 3.1



The mean annual short-wave radiation budget of the Earth and its atmosphere.

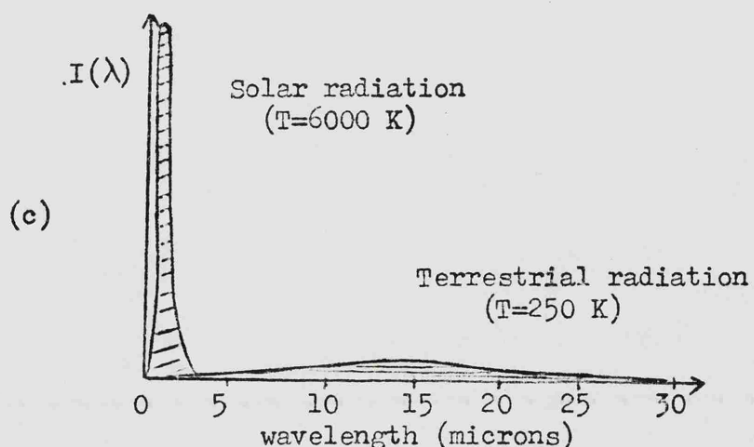
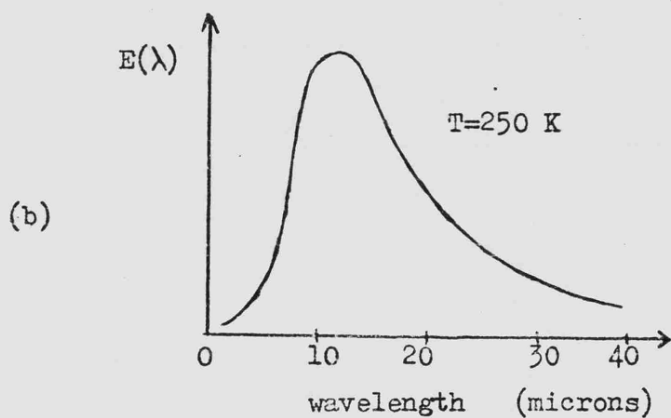
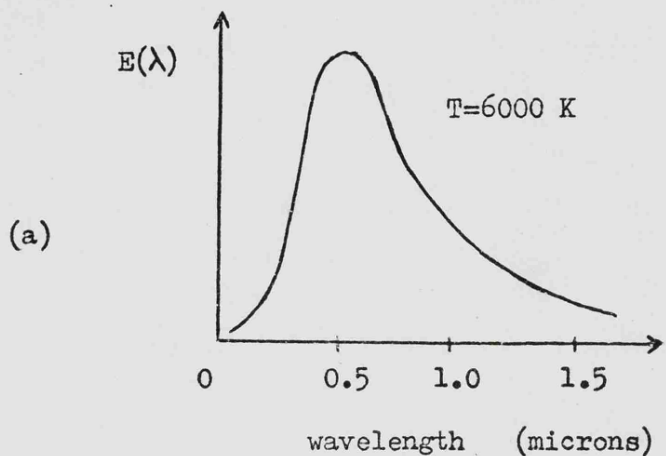
amount of solar energy able to penetrate the planet/atmosphere system. This lowering of input solar energy could lead to a lowering of the average surface temperature (see Sellers, 1973) and thus cause further feedbacks. The possibilities of such feedback mechanisms will be discussed later in this chapter.

The problems involved in the consideration of the variation in a planetary albedo are not only concerned with the type of reflecting surfaces but also with their latitudinal distribution. The planetary albedo is defined in terms of the Russell-Bond spherical albedo (at wavelength  $\lambda$ ) as

$$A_\lambda = \frac{\text{total energy emerging from the whole planet at wavelength } \lambda}{\text{total energy incident at the planet at wavelength } \lambda} \quad \dots \dots \quad 3.3$$

This spherical albedo is a measure of the radiation which has not taken part in any energy transformation at the planet as its wavelength has remained unchanged. However, the calculation of average surface temperatures requires a spherical albedo averaged over all the wavelength range of the incident solar radiation. The assessment of albedo is simplified by the fact that the Planck curves for the effective temperatures of the Sun and the planets hardly overlap, as is illustrated for the case of the Earth by Figure 3.2. Thus the solar and planetary radiative emissions may be treated as two separate streams. The values of planetary albedo have been obtained by measurement of the amount of reflected sunlight (see e.g. Kuiper, 1953). This was not, however, easily performed for the Earth until the advent of space

Figure 3.2



Electromagnetic energy radiation curves as a function of wavelength  $\lambda$ .

- (a) Black-body radiation for  $T = 6000 \text{ K}$ ,
- (b) Black-body radiation for  $T = 250 \text{ K}$ ,
- (c) Approximate relative intensities for total solar radiation and total terrestrial radiation.

vehicles, and the exact value of the Earth's albedo and its short-term fluctuations are still open to discussion (see e.g. Vonder Haar and Suomi, 1971 and 1972 and Winston, 1972).

The problem of giving a correct value to a planetary albedo for an earlier epoch is complex. The present-day values of the albedos of the Moon, Mars, Earth and Venus are respectively 0.07, 0.17, 0.33 and 0.71 and from these figures it could be suggested that the build-up of an atmosphere (typical of the terrestrial planets) will lead to an increasing albedo. Thus the calculations of evolutionary paths of surface temperatures, for any planet, which fails to consider changes in the albedo (e.g. Sagan and Mullen, 1972) neglect a vital part of the calculation. The precise way in which changes in an atmosphere, which is well developed, may produce albedo variations is not yet understood. Recently, however, possible feedback mechanisms have been described (Charney, 1975). Fortunately, the early stages of atmospheric development are less complex. A planet with little or no atmosphere must have its albedo determined solely by the surface conditions. Even when a tenuous atmosphere is established, but before clouds dominate the reflectivity, the surface materials and their distribution play a major role in the determination of the albedo. Thus a first stage in the calculation of planetary albedo is the modelling of albedo variations caused by surface alterations.

### 3.3 Surface Emissivity

The infrared emissivity of a planetary surface (denoted by  $e$ ) is defined as the ratio of thermal emission by the surface (at a known temperature) to the "black body" emission at that temperature. Thus it appears as a premultiplier in the first summation term in Equation 3.2 which is the sum of the thermal radiation emitted by the planetary surface through atmospheric "windows". Thus the accurate calculation of  $T_s$  throughout the history of the planet requires that the value and variations in  $e$  are known. In this computation the emissivity is averaged over the whole planetary surface and over the wavelength range of the emitted radiation.

The infrared emissivity is a function of the material and its surface properties: it is also found to vary with wavelength and temperature. The averaging process required for this computation must be done with care. Thus the final value of the surface emissivity of a planet will depend upon the surface materials, their areal extent and temperature. Table 3.1 gives a list of some relevant materials together with a value of their infrared emissivity and the temperature at which the measurement was made. From this it is possible to estimate the appropriate value of emissivity to be used in planetary calculations. The value of  $e$  chosen by many authors is 0.90 which can be seen to be appropriate only for a desert-covered planet. It is generally agreed that two-thirds of the surface of the Earth has been covered by oceans for much of its history. Thus a value nearer  $e = 0.95$  seems more reasonable.

Table 3.1Infrared Emissivities

(after Hudson, 1969 and Buettner and Kern, 1965)

<u>Substance</u>		<u>Temperature</u>	<u>Emissivity</u>
Concrete		20° C	0.92
Sand		20° C	0.90
Soil	dry	20° C	0.92
	saturated	20° C	0.95
Water	distilled	20° C	0.98
	ice (smooth)	-10° C	0.96
	frost	-10° C	0.98
	snow	-10° C	0.85
Water + petroleum film		10° C	0.97
Water + plastic sheet		10° C	0.96
Wood		20° C	0.90
Asphalt paving		20° C	0.96

The emissivity is found to increase as the roughness of the surface is increased since the effect of smoothing a surface (and thus increasing the reflectivity) is to decrease the emissivity. Large-scale changes in the surface features of a planet (e.g. the growth of vegetation over land, where none had previously existed, during the evolution of life on Earth; partial glaciations of the planet or the removal of vegetation by Man) will cause a small but significant second order effect in the surface temperature. For this reason the parameter  $\epsilon$  has been allowed to vary, between values of 0.88 and 1.0, with the planetary surface features throughout the evolutionary calculation.

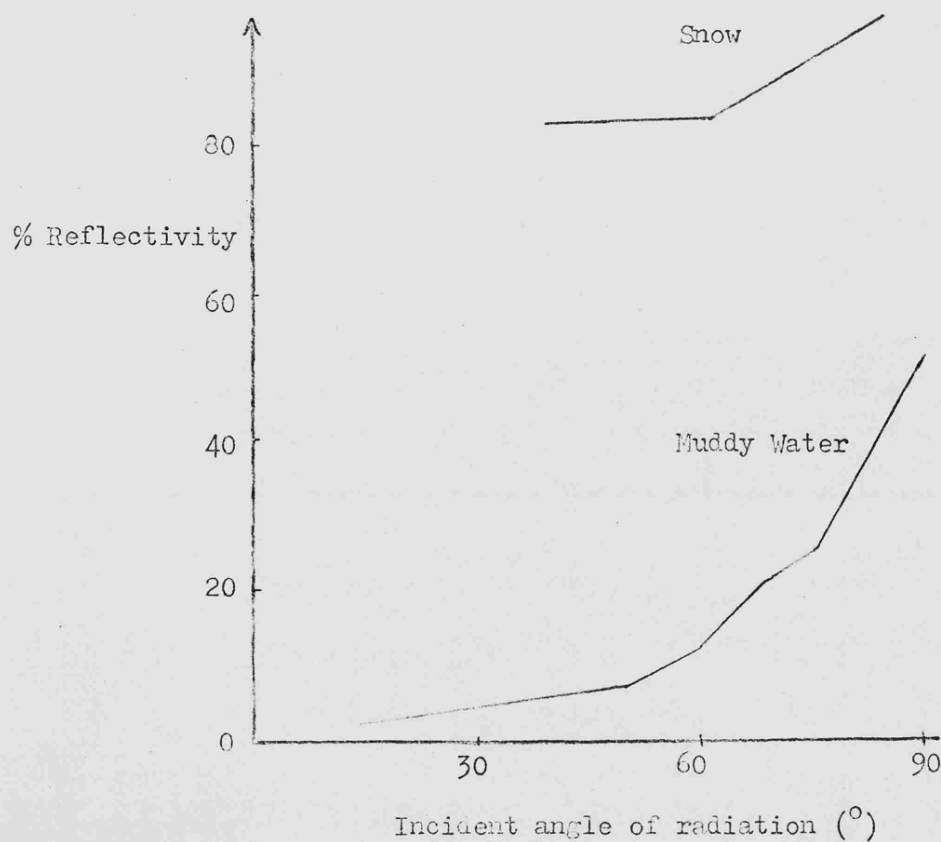
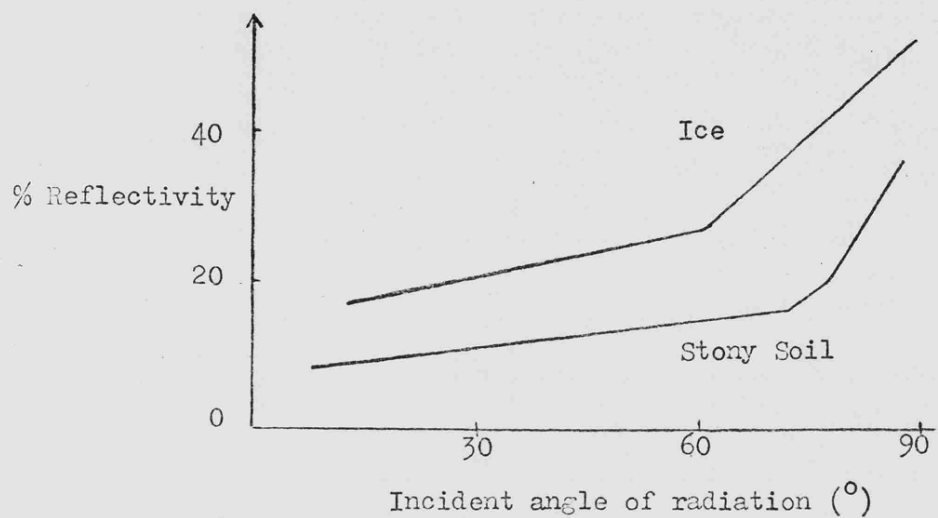
### 3.4 Computation of Spherical Albedo

The Russell-Bond spherical albedo of a planet has been defined in Section 3.2 in terms of the ratio of light reflected by the planet to that incident upon it. The proportion of monochromatic light reflected at any point will depend upon two factors: the planar reflectivity of the material and the angle of incidence of the radiation. Thus the calculation of spherical albedo depends upon the latitudinal distribution of features as well as their reflecting ability.

The computer program discussed in this section was written to permit the calculation of the surface spherical albedo. The more complex problems of scattering and reflection by clouds will be mentioned later. The variation of planar reflectivity of surface materials typical of the terrestrial planets with the angle of incidence of the radiation is not well determined. However, semi-empirical curves of reflectivity as a function of incidence angle have been constructed using various data sources (e.g. Robinson, 1966). Some of these curves are shown in Figure 3.3. The precise relationship was found not to be critical since computer results produced only minor changes in  $T_s$  for any reasonable functional dependence. The program was intended to facilitate the calculation of the surface albedo of a planet having many different configurations of surface types, thus permitting an analysis of the effect of increasing snow or ice cover, or of moving land and sea masses relative to each other. The axis of rotation of the planet was assumed to be perpendicular to the plane of the incident radiation (see Figure 3.4) and the

Figure 3.3

Variation of reflectivity of four surface types as a function of the angle of incidence of the radiation.



surface types to be grouped in latitudinal zones. These assumptions give rise to a value of the surface albedo which is also a reasonable approximation to a mean value of the albedo, for other orientations, over the long-time periods under consideration.

The spherical albedo of the planetary surface was calculated by considering the radiation incident upon, and reflected by an elemental area,  $dA$  (as shown in Figure 3.4). The amount of radiation reflected by  $dA$  is a function of the reflectivity  $R(\psi)$ ; where  $\psi$  is the angle of incidence of the radiation and also upon the foreshortening function  $f(\theta, \phi)$ ; where  $\theta$  and  $\phi$  are the co-ordinates of the element  $dA$ . The total spherical surface albedo is given by this ratio integrated over the surface of the sphere:

$$\text{spherical albedo} = \frac{1}{\pi r^2} \int_{\theta=-\pi/2}^{\pi/2} \int_{\phi=-\pi/2}^{\pi/2} R(\psi) dA f(\theta, \phi) \quad \dots \dots \quad 3.4$$

where  $f(\theta, \phi) = \cos \theta \cos \phi$

$$dA = r^2 \cos \theta d\theta d\phi$$

$$\psi = \cos^{-1} (\cos \theta \cos \phi)$$

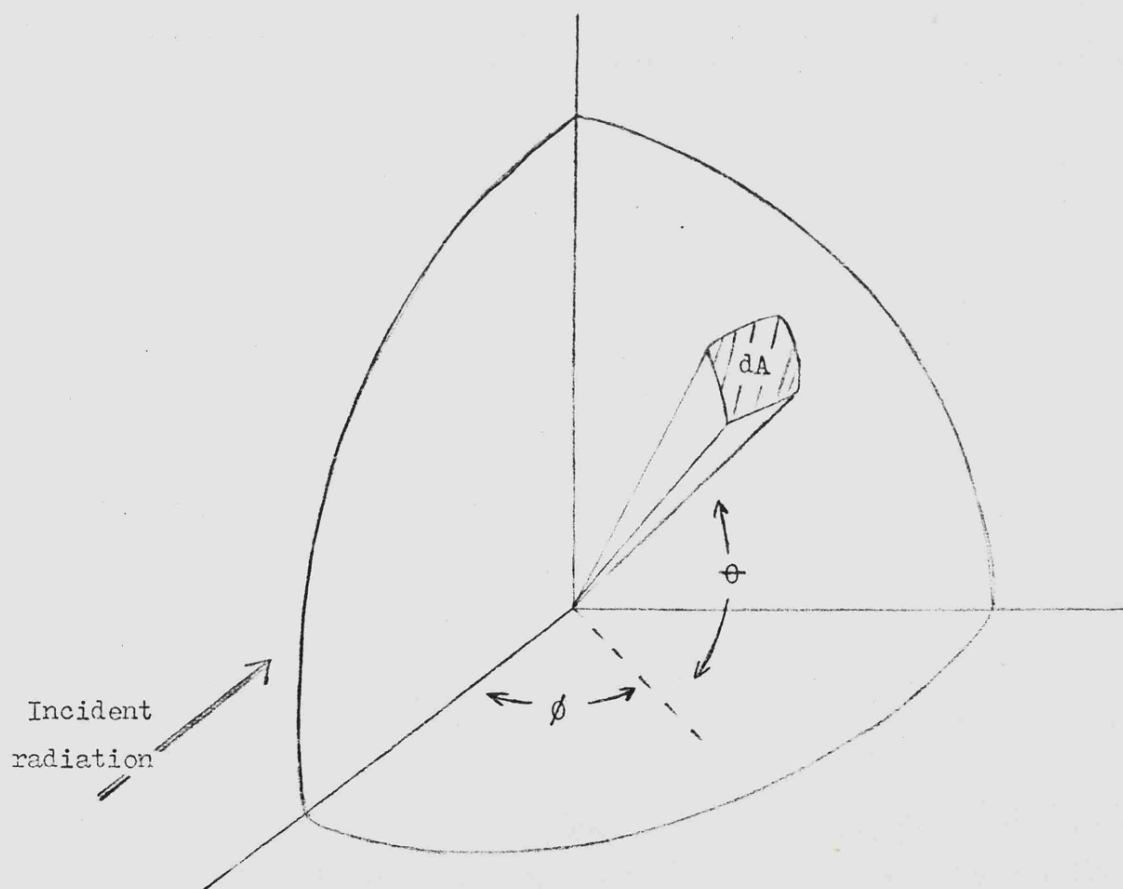
Thus Equation 3.4 becomes:

$$A = \frac{2}{\pi} \int_{\theta=-\pi/2}^{\pi/2} \int_{\phi=0}^{\pi/2} R \{ \cos^{-1} (\cos \theta \cos \phi) \} \cos^2 \theta \cos \phi d\phi d\theta \quad \dots \dots \quad 3.5$$

This double integral was evaluated for different surface configurations using the computer program described below.

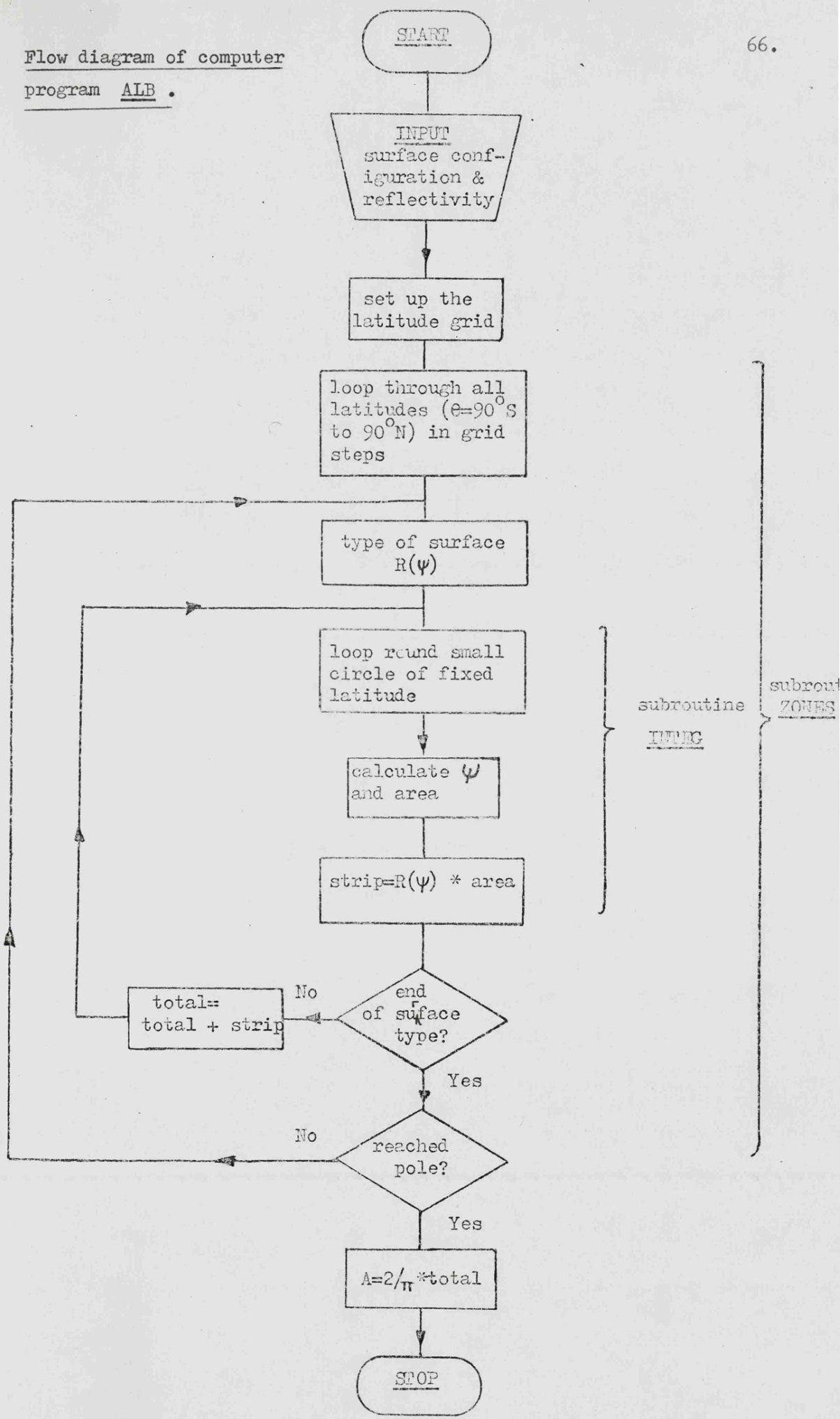
Figure 3.4

Co-ordinate system for determination of spherical albedo.



Flow diagram of computer  
program ALB.

66.



The program, ALB (Albedo), (see flow diagram) was written to permit calculation of the surface albedo of a planet possessing surface features which could be approximately represented by latitudinal belts of differing surface types. Thus at each latitude step between equator and poles the summation was undertaken round a small circle of constant surface type. This summation was performed in the subroutine INTEG (Integration) called from the subroutine ZONES which discriminated between surface types and controlled the summation through latitude values. The initial calculations performed were for the Earth. In this case the surface types were defined by allowing only one-third of the total planetary surface to be land and the remainder ocean. Land and ocean areas were moved relative to one another and the effects of glaciation considered. Later the program was extended to permit calculation of the Martian albedo. In the case of Mars this computation gives the true planetary albedo, since the atmosphere takes little part in reflection of radiation. The variation in surface features on Mars is caused by the eccentricity of its orbit, which leads to large and asymmetric variations in the extent of the polar caps. For this calculation, a further subroutine was developed called MARZON. This replaced ZONES and calculated the extent and reflectivity of the polar caps whilst the rest of the planet was assumed to be dusty desert.

### 3.5 Albedo Calculations for Mars and the Earth

The planetary albedo of Mars and the surface albedo of the Earth were calculated as described in Section 3.4. The results may be considered as illustrating two different types of albedo variation. The first would be expected to occur on a planet which possessed only a very tenuous atmosphere, particularly if one of its major constituents was at a temperature close to its frost point. In this case, the winter hemisphere would be expected to possess a large polar cap. The eccentricity of the Martian orbit adds further to this situation by producing an asymmetry in the formation of the polar caps. As the reflectivity of the Martian surface materials are not well known, the dusty cratered surface was modelled by a desert-type reflectivity and the polar caps by a highly reflective snow/ice mixture. The results obtained for various polar cap configurations are given in Table 3.2. Thus the typical variation in the Martian albedo

Table 3.2  
Variation in Martian Albedo

Latitude to which polar caps extend

<u>North polar cap</u>	<u>South polar cap</u>	<u>Global Albedo (%)</u>
from pole to $80^{\circ}$	no cap	11.69
from pole to $70^{\circ}$	no cap	12.48
from pole to $60^{\circ}$	no cap	14.48
from pole to $80^{\circ}$	from pole to $80^{\circ}$	11.81
from pole to $70^{\circ}$	from pole to $80^{\circ}$	12.59
from pole to $60^{\circ}$	from pole to $80^{\circ}$	14.63
from pole to $50^{\circ}$	from pole to $80^{\circ}$	17.92

is between a perihelion value of approximately 12.5 per cent and an aphelion value of 17.9 per cent. As this variation occurs during one orbit of the Sun an average value is required for long-term calculations of surface temperature evolution, but this extreme variation will be important in calculations of temperatures at specific positions in orbit,

The second set of results derived from the program relate to the Earth and illustrate the second type of albedo variation which occurs over time periods closer to the life-time of the planet. These variations are caused by the very large changes in the surface condition of a planet which are to be expected during its history. The geological record of the Earth indicates that throughout much of its recent history the proportions of land and ocean have varied very little. However, the relative positions of large continental and oceanic areas have changed considerably because of continental drift. Two extreme configurations of land and ocean were considered: i) in which the continents are gathered together to form a belt around the equator; ii) where most of the continental mass is close to the poles, producing either a continental polar cap or, more likely, a land-locked polar ocean. The surface albedos of these two extreme cases were computed using ALB. Case i) was found to give an albedo of approximately 9 per cent, assuming that there was little or no glaciation, whereas case ii) in which there was assumed to be an ice/snow covering on the land masses surrounding the poles gave an albedo of approximately 28 per cent. This difference in surface albedo is found to change the surface

temperature by more than  $15^{\circ}\text{C}$  (see Chapter 5 for full description of surface temperature variation). Since the difference between a glacial and interglacial period probably corresponds to a change in average temperature of only  $5^{\circ}\text{C}$  (Bryson, 1974) this albedo-dependent variation must be regarded as significant.

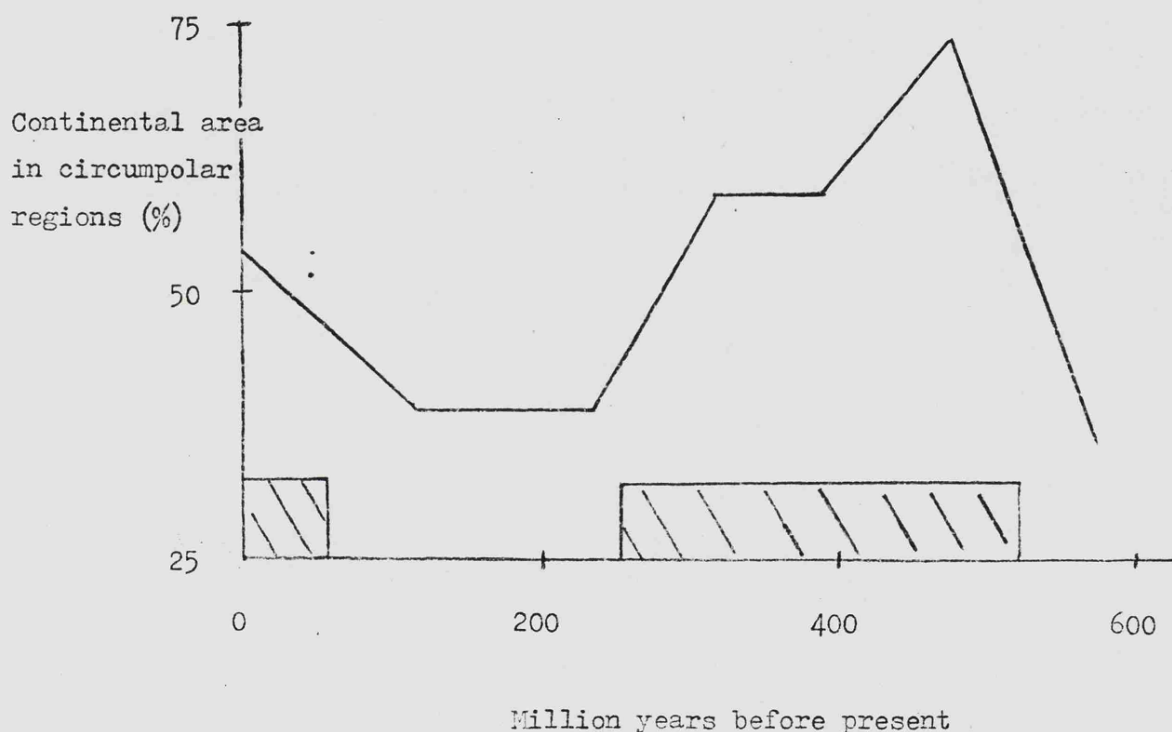
It must be noted that these extreme cases will be modified by the introduction of cloud cover, and any likely change in this will narrow the temperature difference derived above. Nevertheless, after allowing for these factors, the amount of latitudinal change postulated in reconstructions of continental drift still seems, from these results, to be capable of producing a variation in surface temperature of a few degrees. The effect of this would be to accentuate the effects of climatic conditions already prevailing on Earth. In particular, although a land-mass near one of the poles would, in any case, be expected to have an ice-snow cover, a slight lowering of the average surface temperature, as a result of the albedo effect, could turn this into a major glaciation. It has been suggested recently by Kukla and Kukla (1974) that anomalous weather patterns experienced in 1972 and 1973 may be the result of large variations in the cover of snow and pack ice in the previous year. Thus it is possible to state that the likelihood of extensive glaciation occurring should be greater when a higher proportion of the total land mass is near the poles.

An attempt was made to find geological data which might confirm or refute the hypothesis. Data cited by McElhinny (1973) were used to derive values for the latitudinal distribution

of the continents during each of the geological periods. The results were found to be best represented in terms of the percentage of Earth's surface within  $30^{\circ}$  of the poles covered by land at any time. The reason for choosing this form of presentation of the data is that continental displacements at lower latitudes, although leading to small changes in the albedo, cannot support extensive glaciation. It is this glaciation that can most readily be detected in the geological record. Some of the data on continental drift is uncertain and, in particular, the data concerning the Precambrian was found to be inadequate for the comparison required here. Nevertheless, as can be seen in Figure 3.5 (after Sellers and Meadows, 1975), the periods of extensive occurrence of global glaciation (see, e.g. Seyfert and Sirkin, 1973) correlate reasonably well with periods when a higher percentage of the circumpolar regions was occupied by continents. Within the limits of the data, therefore, predictions based upon the albedo effect are supported by the available geological evidence.

More recently, a very interesting study by Donn and Shaw (1975) has corroborated these results for a period extending from the present day to 200 million years ago. Their computations used a simplified dynamical model to compute global surface temperatures for five geological epochs. Allowing for both polar wandering and the movement of continental land-masses they produced an increasing temperature sequence for periods when the percentage of land within the polar regions was decreasing.

Figure 3.5



Variation of continental area within  $30^{\circ}$  of poles as a function of time. The shaded parts of the time axis include all extensive glaciations.

These two sets of results from the computer program ALB thus suggest that the values derived for the surface albedo of the planet are realistic. The case of Mars is confirmed by present day observations, whilst the results derived for the Earth seem to be supported by data from the geological record. The usefulness of surface albedo calculations, even on a planet where much of the reflectivity is dominated by cloud cover, has been illustrated by the case of the Earth. However, if a real evolution of the planetary albedo is to be attempted, a further consideration of the effect of cloud cover must be made. The problems of both computing and observing the spherical albedo of a whole planet have been illustrated. The controversy which persists over the exact value of the albedo of the Earth (see Section 3.6) and the need to "average" the values listed in Table 3.2 for Mars also underline this problem. Although short term variations in the spherical albedo of a planet may be important this work is concerned primarily with long-term trends. Thus present day values of the albedos of Venus, the Earth and Mars have been taken to be 0.70, 0.33 and 0.17 respectively and slight variations in these values are not considered.

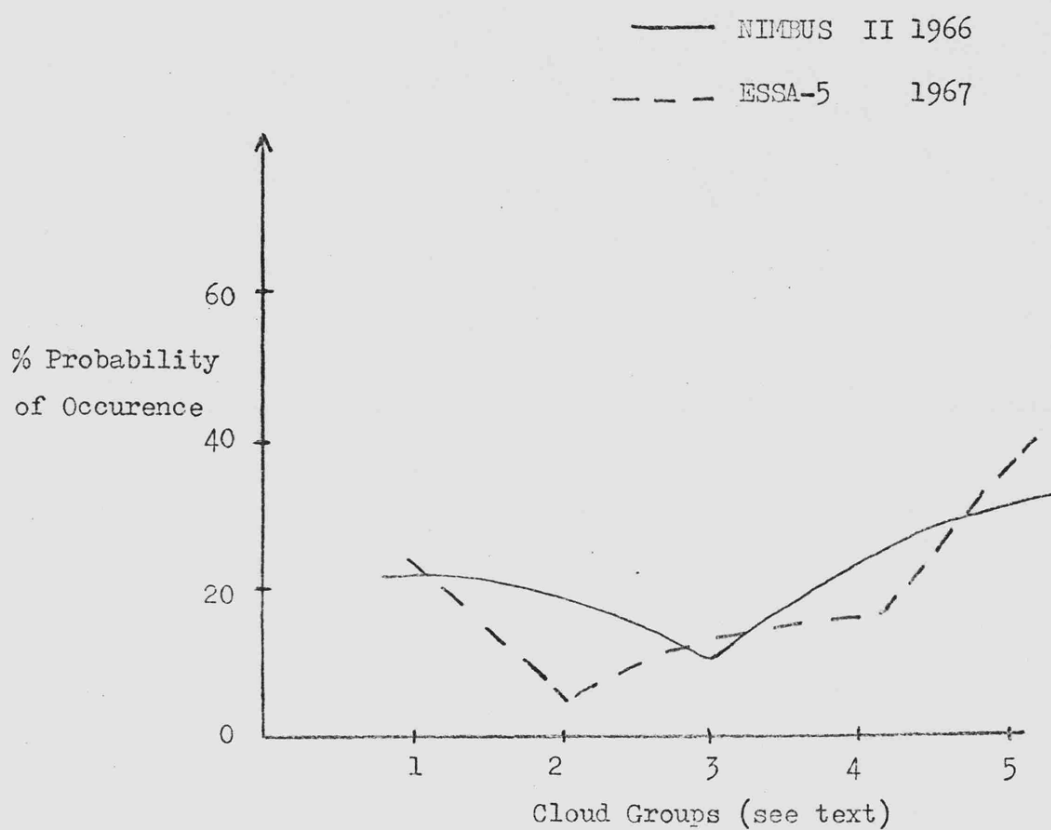
3.6 Clouds

The major degassing constituents of all secondary atmospheres of the terrestrial planets are likely to be water vapour and carbon dioxide (see Chapter 4, Section 4.2). If the average surface temperature of the planet rises above 273 K then large areas of water will be condensed onto the planetary surface, and the hydrologic cycle will develop with the condensation of water vapour clouds in the atmosphere. It is also possible that atmospheric conditions could enable the condensation of other constituents (e.g.  $\text{CO}_2$  or  $\text{H}_2\text{SO}_4$  in solution) into clouds. Any cloud is important to the planet in a number of ways: it is part of the weather system, since condensation will generally occur because of a rapid temperature change; it affects the reflectivity of the planet and is a strong absorber in the infrared, thus strongly affecting the radiation budget of the planet.

The problems involved in a discussion of clouds are immense. The formation of clouds in a developing atmosphere could lead to a sudden jump in the albedo, which would, presumably, lower the surface temperature. Formation mechanisms of clouds on the Earth, the mean, global, average cover, the feedback direction and effects of alterations in cloud cover are not well understood (see, for example, Cess, 1975). Data are a problem, since global cloud cover data have been collected for less than 50 years, whilst satellite data conflicts with ground-based observation and even with other satellite data, due to rapid changes in instrumentation and observation techniques (see Figure 3.6).

Globally, annually averaged cloud cover data is only now

Figure 3.6



Changes in cloud cover - comparison of satellite and ground-based observations.

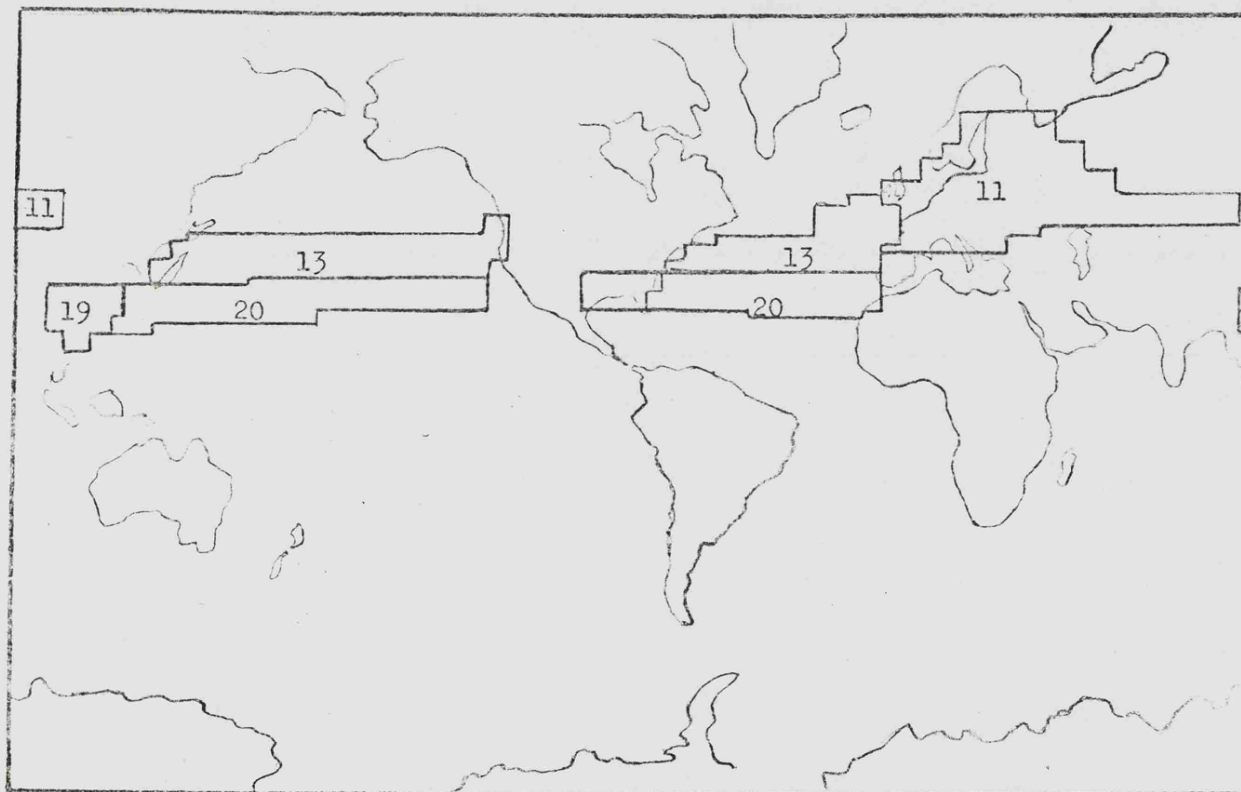
Satellite data of percentage cloud cover (categories are described in detail in the text) for a single region during the summer season (June, July, August) for two consecutive years. Ground-based observations showed no variation in cloud cover for these two years (1966 and 1967). The satellite systems had similar resolution.

becoming available to meteorologists. There seems little chance of producing adequate cloud data for past epochs (see e.g. Lamb, 1972) and thus the discussion of cloud cover changes likely over 4.5 aeons must remain theoretical.

The calculation of surface albedo discussed in the previous section (Section 3.5) led to a consideration of the possible differences (or similarities) of annually averaged cloud cover over continental and oceanic areas. If a determination of the likely position of the majority of clouds could be made, then this factor could be added to the computation. An initial consideration of cloud propagation mechanisms on Earth led to the proposition that cloud cover might fall into three major types: i) continental, ii) oceanic, iii) maritime (the interface between i) and ii) ). Little consideration has been given to the differences in cloud cover over land and ocean, but I have made a tentative study using data prepared in a N.A.S.A. report relating to projects concerned with observations of surface features from satellites (Sherr et al., 1968). The cloud cover data are determined from ground-based observations at stations considered to be typical of the region and presented in the form of a probability distribution of five possible cloud types. These cloud groups are related to more usual meteorological terminology in Table 3.3.

These probability distributions were derived for summer and winter seasons at two times of day (0400 and 1600 local time). Many of the areas in the southern hemisphere had data for only 3 or 4 years, and thus it was thought more reasonable

Figure 3.7



The positions of regions 11, 13, 19 and 20 on the world map.  
(the cloud cover data for each of these regions are presented  
in Figures 3.8 and 3.9)

11 - mid-latitude land

13 - mid-latitude ocean

19 - sub-tropical land

20 - sub-tropical ocean

Table 3.3Fractional Representation of Cloud Group Number

<u>Cloud Group</u>	<u>Eighths (Octals)</u>	<u>Tenths</u>
1	0	0
2	1,2	1,2,3
3	3,4	4,5
4	5,6,7	6,7,8,9
5	8	10

to reverse seasonal data from similar regions in the northern hemisphere. Therefore the zones discussed in this section have been chosen from the northern hemisphere and have been identified on Figure 3.7. The regions are:

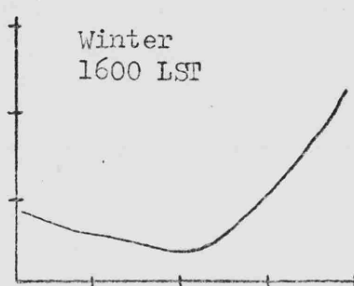
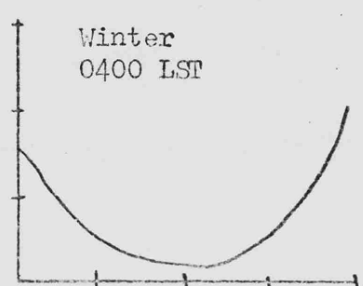
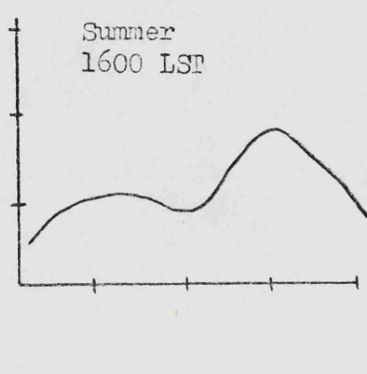
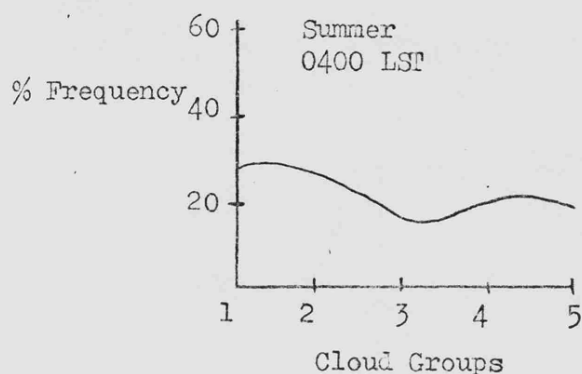
- 11 - areas of mid latitude land
- 13 - areas of mid latitude ocean
- 19 - areas of sub-tropical land
- 20 - areas of sub-tropical ocean.

Figure 3.8 shows the distributions for regions 11 and 20, and Figure 3.9 shows those for 13 and 19. The similarities exhibited by these probability distributions appear to be between regions 11 and 19 and also between 13 and 20. Thus the regions of land at different latitudes seem more likely to have similar cloud cover than land and ocean at approximately the same latitudes. However, it must be noted that the afternoon distributions of all four regions exhibit similarities, which may suggest that over a long period the variations, caused by differing underlying surfaces can be ignored. Conclusions about the effect of surface types upon cloud cover are difficult to draw from such limited data, although it should be noted that

Figure 3.8

Cloud cover frequencies for regions 11 and 20.

REGION 11



REGION 20

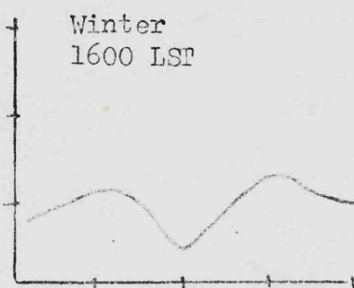
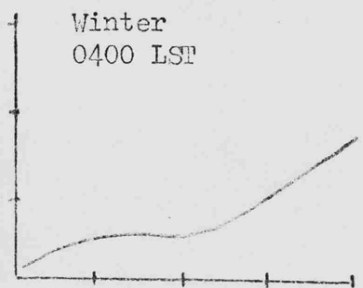
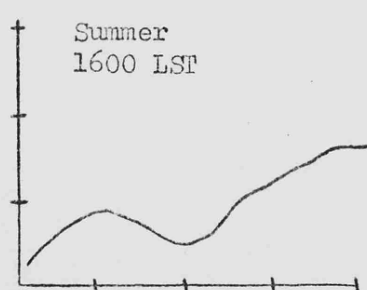
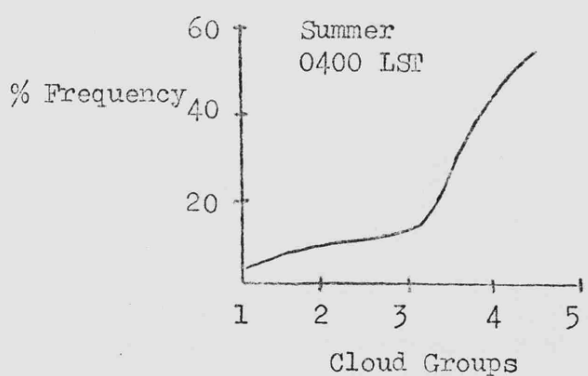
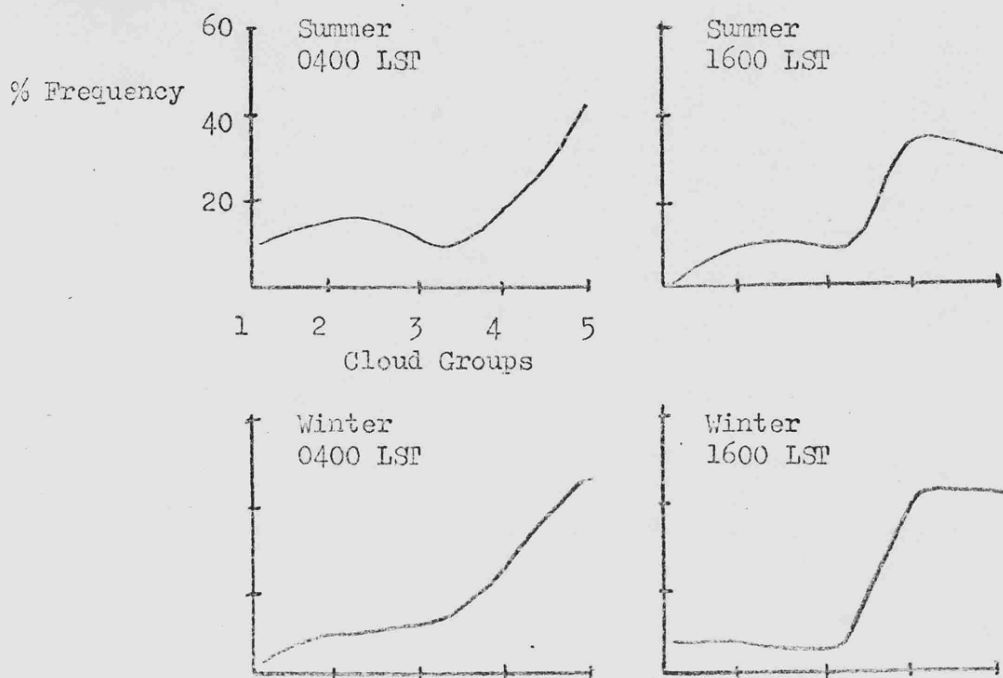


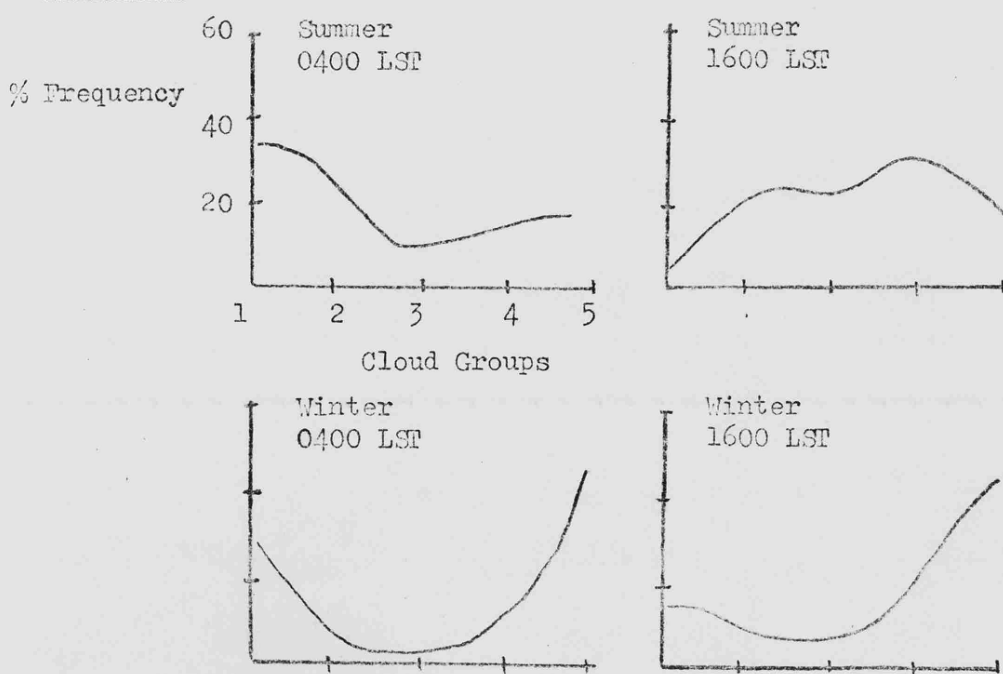
Figure 3.9

Cloud cover frequencies for regions 13 and 19.

REGION 13



REGION 19

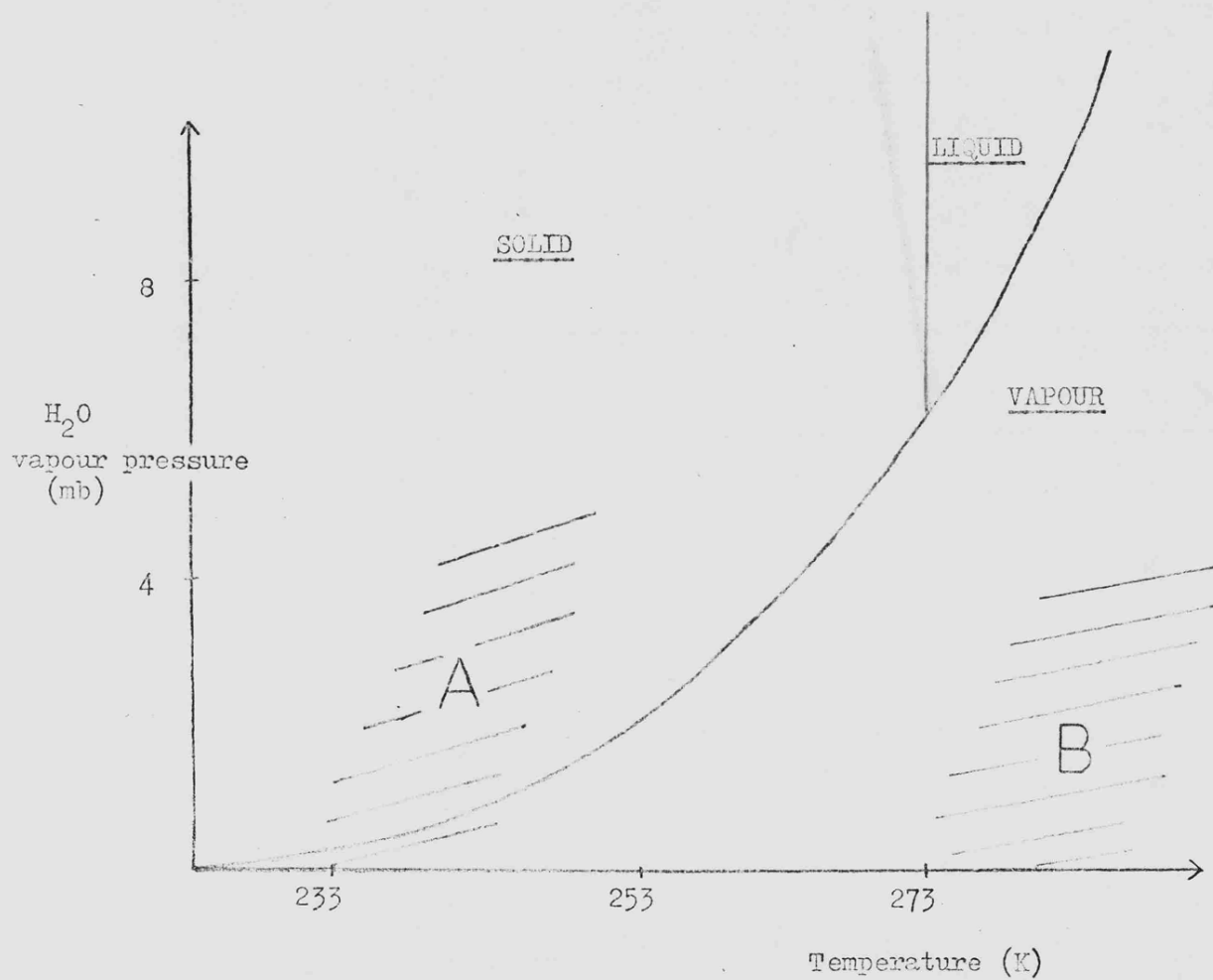


Falls (1974) has produced a single probability distribution to describe many of the regions in this report. It is possible that surface type does not directly affect the overlying cloud but the general circulation of an atmosphere is known to be forced by continental positions and thus an indirect effect may be expected. Contrary to this tentative conclusion it may also be significant to note that there seems to be a slightly higher percentage of cloud cover over the southern hemisphere of the Earth than the northern hemisphere. The modelling of cloud cover and its possible feedback effects will be discussed in Chapter 5, but the use of real cloud data to link cloud variations with climatic variations over astronomical times is not to be expected in the near future and may never be possible.

### 3.7 Expected Variation of the Albedo of a Terrestrial Planet

It has been demonstrated in Sections 3.5 and 3.6 that the variation in the planetary albedo of any terrestrial planet will be determined by a combination of the reflectivities of the surface and clouds. Thus in the initial phase of the planetary history when there is little or no atmosphere, a low albedo value of approximately 7 per cent is to be expected, determined only by the rocky or dusty cratered surface. The start of the degassing phase leads to a tenuous atmosphere around the planet. At this point the histories of all the planets will differ, since the further development of the albedo depends upon the ambient temperature which is a function of the distance of the planet from the star it orbits and also of its rate of rotation. Too high a temperature will lead to the atmosphere escaping (also a small planetary mass has similar consequences) whereas too low a temperature may lead to the immediate condensation of the gases onto the surface. If the star is assumed to have an increasing luminosity, this latter history may be changed at a later stage when the flux from the star is enough to re-evaporate the atmospheric gases. Every possible intermediate case between these two extremes exists, and the Solar System itself exhibits four terrestrial planets illustrating four possible cases. However, if it is assumed that the major atmospheric components are water vapour and carbon dioxide and also that enough degassing has taken place to form a thin atmosphere, the planetary evolution will probably depend critically upon the final state of the majority of the water vapour. The fate of the water is determined

Figure 3.10

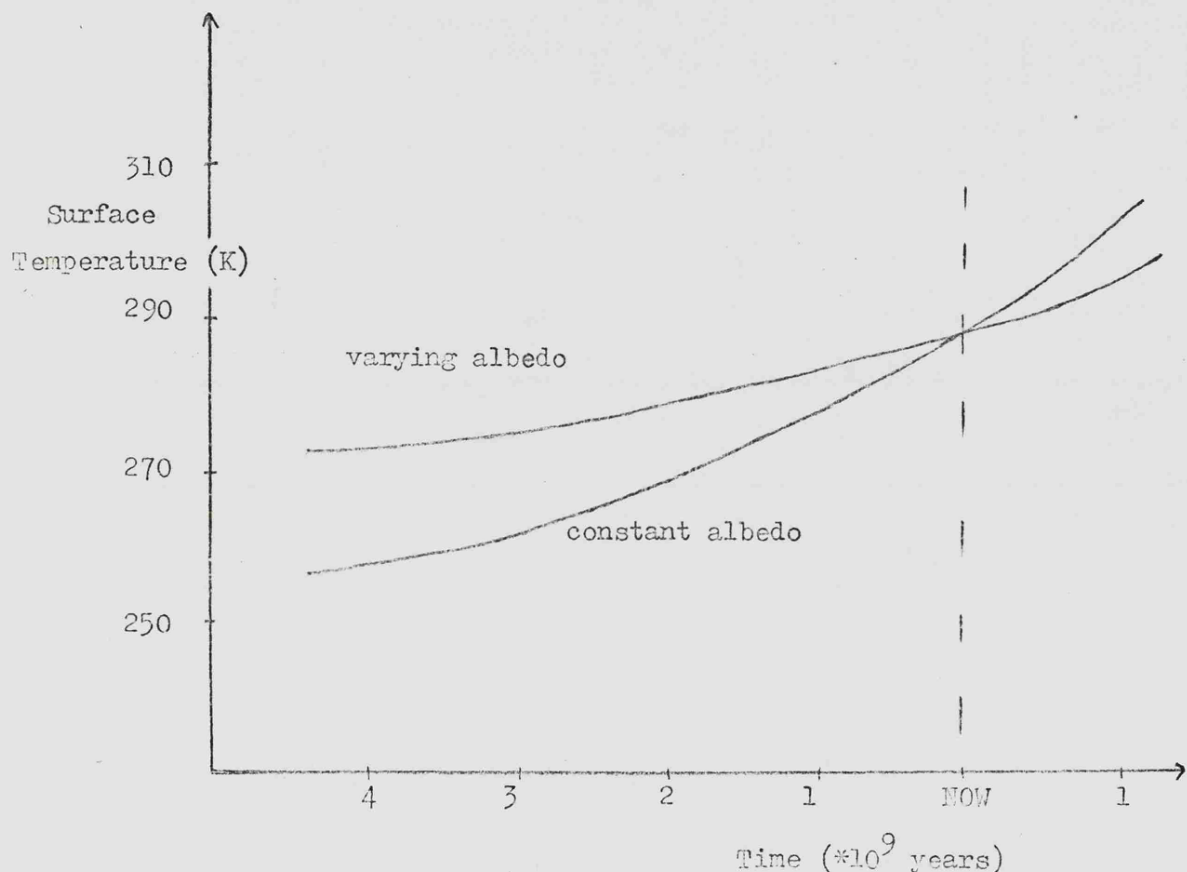


Dependence of atmospheric water vapour upon the planetary surface temperature and the triple point of water.

by the relationship between the ambient conditions on the planet and the triple point of water. If, during the early stages of degassing the average planetary temperature is below 273 K (as in region A in Figure 3.10) then most of the degassed vapour will freeze. Although later temperature rises may liberate this water, allowing liquid and vapour phases, the initial surface deposits of water (as ice, snow and oceans) may greatly modify the albedo. If, however, the surface temperature is near, or above, 273 K before the degassing (e.g. close to region B on Figure 3.10), then the vapour will remain in the atmosphere. It would thus be able to contribute to the infrared absorption, so enhancing the greenhouse effect and raising the surface temperature still higher. The formation of clouds requires that the situation resembles that of the second region, but also depends upon the lapse rate of the atmosphere. The feedback from clouds forming in such an evolution could possibly lead to a lowering of  $T_s$  since the albedo would be raised.

The precise path taken by the albedo of a planet with an evolving atmosphere is very difficult to predict since it involves feedback loops which are not well understood. However, as a very crude estimate, it seems reasonable to presume that the value of the planetary albedo will increase from around 7 per cent to approximately 35 per cent as the atmosphere evolves. The prediction of its further evolution beyond the state, typified by the present-day Earth, is difficult. The "runaway greenhouse" stage in which most of the volatile chemicals are evaporated into the atmosphere will probably only occur if the

Figure 3.11



Increase in the surface temperature of the Earth with increase in solar luminosity for cases of constant albedo and varying albedo (all other parameters are held constant).

planet is close to the star it orbits. This would seem to be the limiting case for albedo, i.e. a value similar to that of Venus - namely about 70 per cent. Thus, although the final state of the planetary albedo is difficult to foresee, it seems that the albedo will change rapidly during the early degassing phase and continue to increase for some time. Thus calculations which fail to include this alteration cannot produce meaningful results.

The importance of albedo variation is illustrated by a simple calculation conducted for the Earth. The average surface temperature  $T_s$  was computed (as described in Chapter 2) allowing only the solar luminosity to alter ( $S$  increases by 43 per cent over 4.5 aeons from initial conditions). All other parameters were held constant, and the albedo had a constant value of  $A = 0.33$  (its present-day value). The lower curve on Figure 3.11 resulted. If, however, the albedo of the Earth is allowed to vary from 0.15 through its present value to 0.40 one aeon in the future, the top curve, for  $T_s$ , is produced. It can be seen that just this variation in albedo keeps the temperatures close to the freezing point of water well back in the evolutionary history. Reasonable variation of the value of the planetary albedo is seen to be vital.

### 3.8 Variation in the Flux Factor

Variations in the value taken by the flux factor,  $f$ , (defined in Equation 3.1) lead to a reconsideration of the definition of the effective temperature of a planet. The choice of the value of  $f$  is usually dismissed as elementary. For a rapidly rotating planet with a thick atmosphere it is supposed that the area emitting radiation is  $4\pi R^2$  (where  $R$  is the planetary radius), whereas for a slowly rotating planet with a thin atmosphere the emitting area is taken to be  $2\pi R^2$  (Sagan and Mullen, 1972 and Hunten, 1971). Since the area receiving solar radiation is  $\pi R^2$ , the flux factor (defined as the emitting area to receiving area ratio) for these two cases is 4 and 2, respectively. However, for a planet which falls into neither of these two extreme categories it appears that the flux factor takes an intermediate value between 4 and 2. The planet Mars is an example of just such a situation; although it is a rapidly rotating planet, it possesses only a thin atmosphere. The consequent uncertainty over the value of  $f$  to be adopted can be detected in the recent literature (e.g.  $f = 4$  in Gierasch, Goody and Stone, 1970;  $f = 2$  in Hunten, 1971). In observational terms, this problem is reflected in the difficulty of establishing a value for the average surface temperature of Mars, owing to the large fluctuations during one rotation (for details of the observations, see Kondratyev and Bunakova, 1974; Woichenshyn, 1974).

Since the project developed in this thesis is to produce a theoretical model which derives the average surface temperature,

$T_s$ , as a function of the effective temperature,  $T_e$ , the possible variation in the value of  $f$  during the evolution of the planetary atmosphere is of the utmost importance. The usual approach effectively assumes either that  $T_e$  is a constant over the rotation period, or that it has a square-wave variation. Thus the Venus atmosphere is so massive that (although the planet rotates slowly) there is no significant difference between day and night sides, indicating that the flux factor has the value 4 and  $T_e$  has a constant value throughout. The planet Mercury takes the other extreme value of the flux factor, 2, since its proximity to the Sun and lack of atmosphere combine with a very slow rotation rate to give day-time temperatures far in excess of the night-time values. Thus, in this case, the value of  $T_e$  has a square-wave form, being almost negligible on the night-side of the planet. The obvious extension to Mars is to assume a square-wave variation again, but with a more prolonged maximum than minimum. (This corresponds physically to assuming that  $T_e$  remains at the day-side value over some specified area of the night-side).

In physical terms, the correct value to be assigned to the flux factor depends upon the ratio of two characteristic times. The first ( $\tau_h$ ) is the time required for a planetary atmosphere to radiate away its heat content. This can be written

$$\tau_h = \frac{m c_p \bar{T}}{\sigma T_e^4} \quad \dots \dots 3.6$$

where  $m$  is the mass per unit area of the atmosphere,  $c_p$  is the

specific heat at a constant pressure, and  $\bar{T}$  is the average temperature of the atmosphere. The other time with which this is to be compared ( $\tau_{\text{rot}}$ ) is the rotational period of the planet. If  $\tau_h/\tau_{\text{rot}} \gg 1$ ,  $f = 4$ ; whereas if  $\tau_h/\tau_{\text{rot}} \ll 1$ ,  $f = 2$ . For Mars, at present, both  $\tau_h$  and  $\tau_{\text{rot}} \approx 10^5$  seconds (whereas for the Earth  $\tau_h$  is two orders of magnitude larger than  $\tau_{\text{rot}}$ ). When the ratio is close to unity the value of  $f$  will lie between 2 and 4.

Thus it can be seen that during the development of a planetary atmosphere the value of the flux factor is likely to move gradually from an initial state close to  $f = 2$  to a final state  $f = 4$  as the amount of the atmosphere increases. However, the rotation rate of the planet is also of importance since a very slowly rotating planet would require a much denser atmosphere to obtain a value of  $f = 4$  than one which rotated faster. Also the possible variation in the rotation rate of the planet during its evolution must be considered since large fluctuations in  $\tau_{\text{rot}}$  could cause sudden changes in the value assigned to  $f$ .

### 3.9 Mars and the Evolution of the Flux Factor

As indicated above, the present-day state of the planet Mars is one which requires an intermediate value of the flux factor (i.e.  $2 < f < 4$ ). An appropriate value of  $f$  for Mars has been calculated by consideration of the fluxes from the observed day-time and night-time temperatures, assuming an overall radiation balance during the course of a complete rotation of the planet. This leads to a value of  $f \approx 2.7$ , corresponding to  $T_e \approx 242$  K. Table 3.4 shows the variation of  $T_e$  and  $T_s$  for different values of  $f$ , assuming the other Martian parameters to have their present-day values.

Table 3.4  
Temperature Dependence upon Flux Factor

Flux Factor	Effective Temperature (K)	Surface Temperature (K)
4.0	219	228
3.0	236	245
2.7	242	252
2.0	261	270

The importance of the value of the flux factor is illustrated by the large variation shown in these figures.

Thus the evolution of the atmosphere of Mars can be considered, and the appropriate values of  $T_e$  and  $T_s$  can be calculated, at each stage in its evolution from zero surface pressure to its present-day condition. This calculation is of special relevance to this chapter since it covers the period of

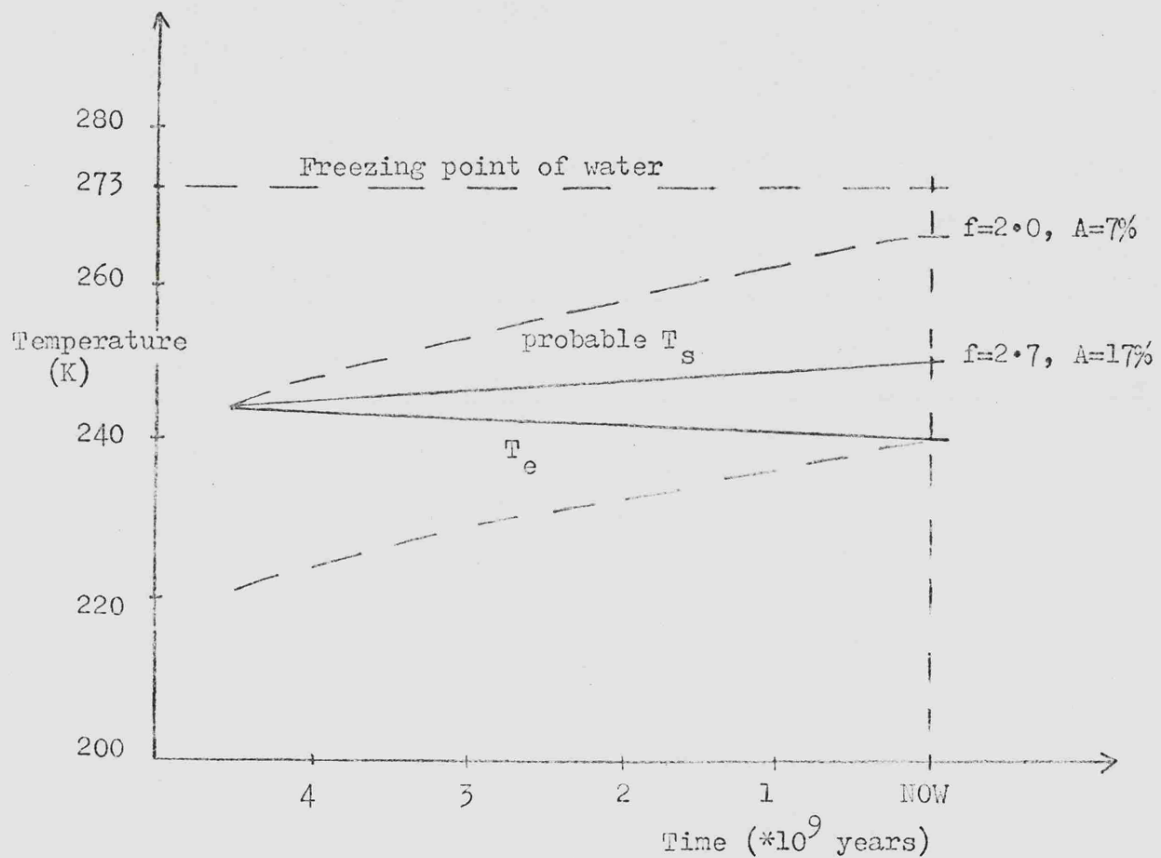
greatest variation in the value of the flux factor for Mars and also includes a variation in the albedo of 10 per cent. The calculation of  $T_s$  has been explained in detail in Chapter 2.

All the parameters ( $S$ ,  $A$ ,  $f$  and  $e$ ) in the defining equation for  $T_s$  (Equation 3.2) will vary over this period. The degassing rate is also of importance to this calculation since, although the sequence of change in  $T_e$  and  $T_s$  will remain the same, the degassing rate will determine the temperature reached at any epoch. Thus the degassing rate was modelled for three cases.

Case I assumes a rapid initial degassing, with the present Martian atmosphere essentially formed by the end of the first aeon of the planet's history. Case II assumes a constant degassing rate throughout the lifetime of the planet, and case III allows for a late degassing event in which the Martian atmosphere evolved from near zero surface pressure to the present value in the last two aeons. These three cases allow a full discussion of the effect of the variation in all the parameters, but particularly underline the importance of the albedo and the flux factor.

The chemical composition of the Martian atmosphere has been assumed to be constant throughout its history, since the evidence for a 'primary' highly reducing atmosphere is fairly tenuous (see, e.g. Margulis, 1976). The changes in the albedo and flux factor are linked to the degassing rate (since it is assumed that the rotation rate of Mars has not altered significantly over its lifetime). It has been assumed that the atmosphere-less planet will have an albedo of 7 per cent and

Figure 3.12



The evolution of  $T_e$  and  $T_s$  for Mars in Case II (a linear degassing rate). The surface temperature (in K),  $T_s$ , is seen to vary little throughout the 4.5 aeons.

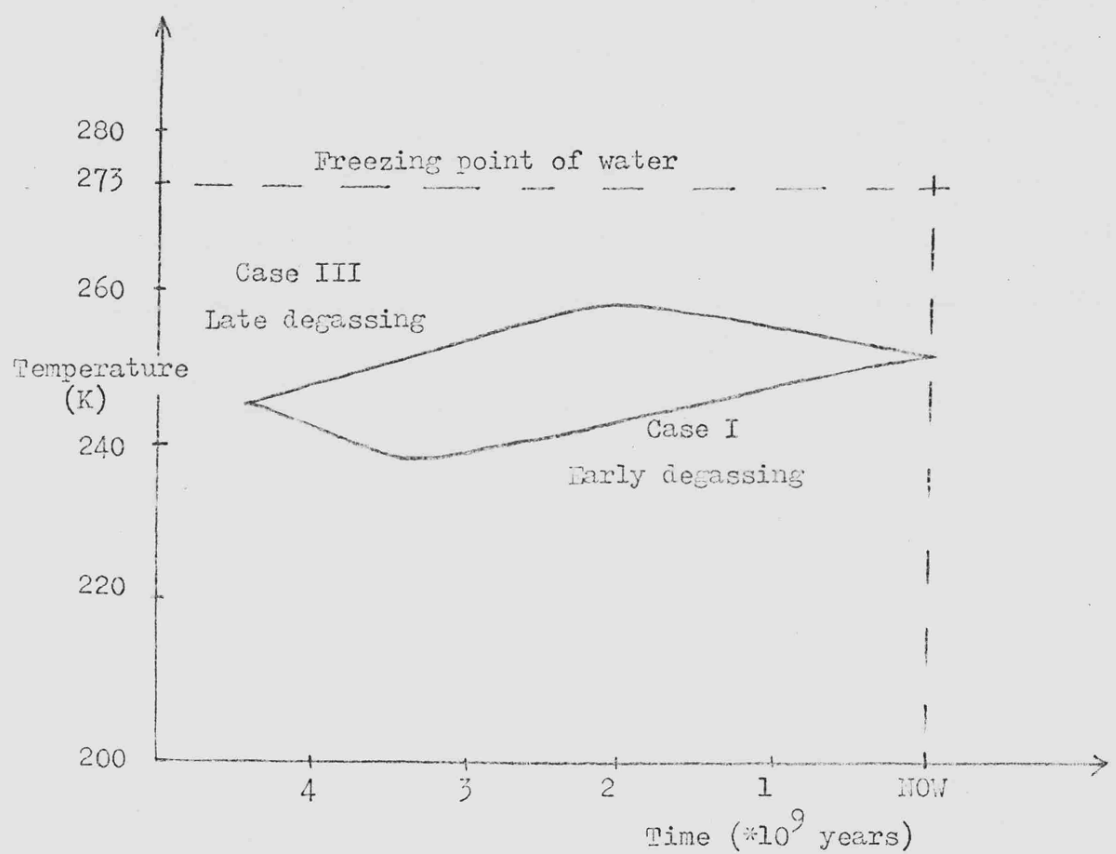
$f = 2$ . As the present-day values for  $A$  and  $f$  for Mars are respectively 17 per cent and 2.7 the increases can be directly associated with the build-up of the atmosphere. For the purposes of this calculation it has been assumed that these parameters will vary in proportion to the atmospheric mass per unit area.

Figure 3.12 (after Henderson-Sellers and Meadows, 1976) shows the results for both  $T_e$  and  $T_s$  in case II (linear degassing). The significant point to note is the way in which the changes in the albedo and the flux factor compensate for the changing solar luminosity, so that the surface temperature of Mars varies very little throughout its history.

Figure 3.13 shows the results for  $T_s$  obtained in case I (early degassing) and case III (late degassing). For these two curves the degassing rate and, thus, the rate of change of albedo and flux factor differ, so that  $T_s$  changes appreciably with time. Hence in case I, the surface temperature passes through a minimum value of about 239 K one aeon after the formation of Mars; whereas, in case III, it passes through a maximum of about 261 K at the beginning of the postulated degassing episode, two aeons ago.

Clearly, with the above assumptions all the degassing sequences considered give an average surface temperature for Mars which remains below the freezing point of water. However, in view of the large temperature fluctuations on Mars, areas of the planet can have temperatures which are above freezing point for an appreciable fraction of the time even when the mean temperature is below this figure. Consequently, the occurrence of

Figure 3.13



The evolution of the surface temperature (in K),  $T_s$ , in both Case I (early degassing) and Case III (late degassing) for Mars.

liquid water on the surface of the planet becomes increasingly possible as the mean temperature rises. It is evident from the results presented here that a late degassing episode is especially suitable for 'switching on' a liquid water phase at a particular point in the evolution of Mars. The Mariner 9 observations of the Martian surface might therefore be taken to support a link between tectonic activity and atmospheric growth in the recent history of Mars.

### 3.10 Possible Variations in the Flux Factor of the Earth

The calculation of the average surface temperature of the Earth, throughout its history, is more complex than that performed above for Mars since the albedo, surface emissivity and flux factor have varied over greater ranges and the degassing has probably been much more extensive. However, to illustrate simply the possible effect of a sudden alteration in the flux factor of the Earth due to a rotation rate change, the calculation has been simplified. It has been assumed that the chemical composition of the atmosphere has varied little since its formation, allowing a similar calculation to that described above to be performed to link  $T_e$  to  $T_s$  throughout the Earth's evolution.

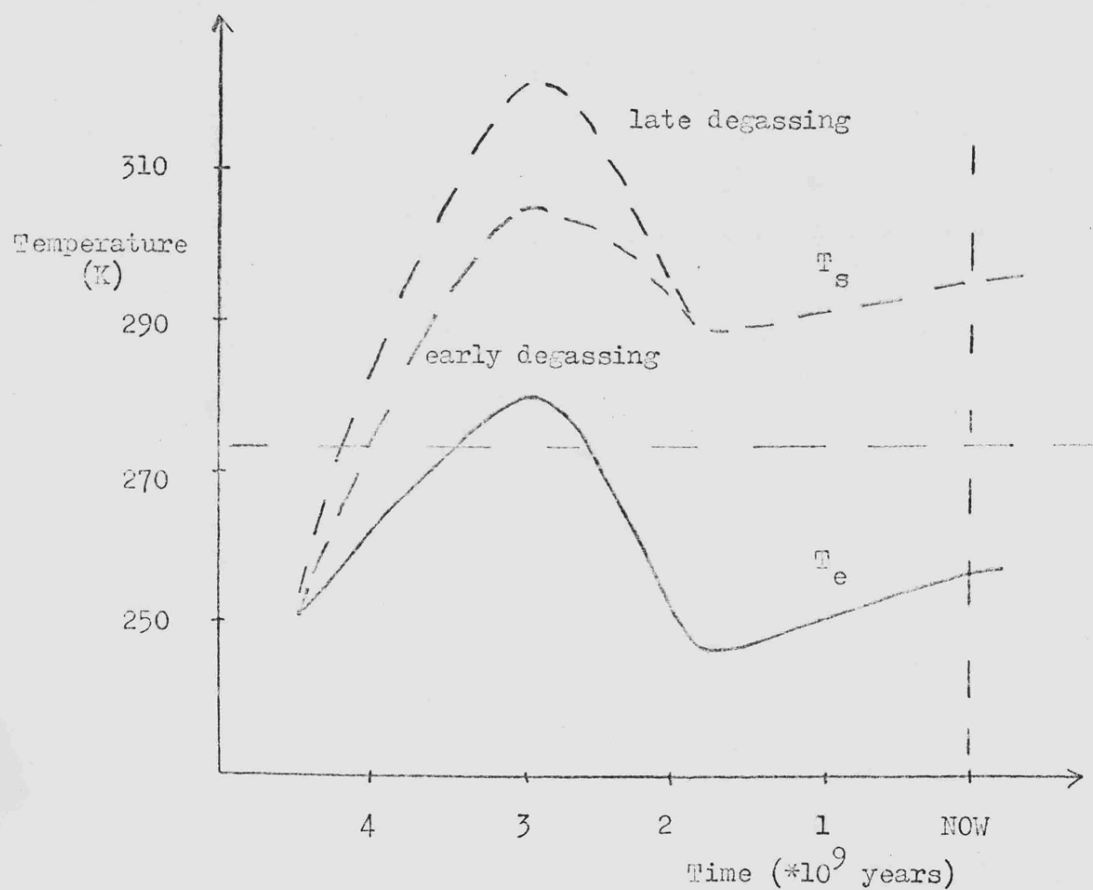
The capture of the Moon by the Earth is generally supposed to have occurred at, or soon after, the planet's formation, about 4 aeons ago. If, contrary to this assumption, the Moon and the Earth were formed in mutual gravitational fields, the slowing of the rotation rate of the Earth, caused by tidal interaction, would be less important but still a significant factor, producing a variation in the value of  $f$ . If capture occurred it probably slowed the rotation rate of the Earth from its early value of approximately 2 hours to near its present value of 24 hours. The rate of alteration would be rapid, giving a value of  $\tau_{\text{rot}} \approx 16$  hours by 3 aeons ago (see Marsden and Cameron, 1966). Such changes in  $\tau_{\text{rot}}$  would be expected to produce large changes in the value of the flux factor,  $f$ , as discussed in Section 3.8. The value of the flux

factor also depends upon the heat capacity of the atmosphere, itself a function of the degassing rate. For this calculation it has been assumed that the alteration in the rotation rate of the Earth caused by lunar capture happened before the atmosphere was very well formed. Thus, for the early, rapidly rotating Earth, possessing only a very tenuous atmosphere, the flux factor has been assumed to have a value of 4. The rapid alteration in the rotation rate over the next aeon plus slight degassing would probably imply that the Earth had a value of  $f$  similar to present-day Mars (i.e.  $f \approx 2.7$ ). Then the build-up of the atmosphere, increasing the value of  $\tau_h$  and a little further slowing of the planetary rotation would finally lead to the present day conditions of  $f = 4$ .

The variation in the albedo of the Earth is more complex than that of Mars since to achieve present-day conditions cloud cover must be considered. For this calculation, the albedo has been allowed to increase gradually with the development of the atmosphere and thus in step with the changing flux factor.

Figure 3.14 shows the results of these calculations, illustrating the possible evolutionary track of  $T_e$  given the above assumptions. As in the Martian calculation, two possible degassing sequences have been considered in the calculation of  $T_s$ . These curves serve mainly to demonstrate the large effect caused by an early fluctuation in the value of the flux factor. A complete description of the evolutionary sequence of  $T_s$  for the Earth will be given in Chapter 5. The calculations in Chapter 5 will allow for the variations in all the parameters

Figure 3.14



Possible evolution of  $T_e$  and  $T_s$  for the Earth allowing for variations in 'f' caused by rotation alteration due to the capture of the moon.

affecting surface temperatures. However, it is interesting to note (from Figure 3.14) that even with the extreme fluctuations in  $f$  postulated here the value of  $T_s$  is above the freezing point of water 3 to 3.8 aeons ago. This is of particular importance since many calculations which have attempted to evaluate  $T_s$ , allowing for the lower solar luminosity in the past, have results contradictory to the geological evidence which indicates surface water as far back as 3.9 aeons ago (see e.g. Ramsay, 1963 or Cloud, 1968). This has led to consideration of large changes in atmospheric composition to account for the discrepancy. As the calculations in Chapter 5 and even the simple  $T_s$  track outlined above illustrate, however, such exotic atmospheres are unnecessary if the correct variations in both  $f$  and  $A$  are included.

### 3.11 Conclusions

The variation in three important parameters has been considered in this chapter. The albedo and surface emissivity have both been previously acknowledged as variable, but a consistent method to allow for their variation has not been discussed. The third parameter, the flux factor, has never been considered variable before. The fact that  $f$  takes a value intermediate between 2 and 4 for Mars at the present time has been demonstrated. The relevance of the variation of both  $f$  and  $A$  has been illustrated by simplified calculations of the evolution of the effective and surface temperatures for both Mars and the Earth. It has been indicated by these calculations that the combined effects of varying  $f$  and  $A$  may compensate for the lower solar luminosity in the past.

CHAPTER 4THE ATMOSPHERIC GASES AND THEIR INFRARED ABSORPTION SPECTRA4.1 Introduction

The model developed in this work is intended to describe the evolution of a planetary atmosphere/surface system with time. Most of the parameters which influence the surface temperature have been discussed in Chapter 3. There remains the infrared absorption spectrum of the atmosphere at any stage in its evolution to be considered. In this chapter the likely evolutionary sequence of a terrestrial planetary atmosphere will be described and the effect of varying the chemical constituents and total pressure will be discussed. A parameterization of laboratory data will enable the absorption properties of individual gases to be incorporated into the mathematical model described in Chapter 2.

#### 4.2 The Secondary Atmosphere

The atmosphere of the Earth (and thus, probably, of all the terrestrial planets massive enough to retain an atmosphere) is of secondary origin; that is, not a remnant of the solar nebula. This is deduced from the marked depletion of the noble gases in the Earth's atmosphere relative to the solar abundance, which indicates that any primitive atmosphere must have been very rapidly dispersed after the formation of the planet. An internal source for the atmospheres of all the terrestrial planets has been the generally accepted theory since the comprehensive assessment of possible sources for the "excess volatiles" by Rubey in 1951. It has recently been suggested (Benlow and Meadows, 1976) that some constituents of the atmospheres of the terrestrial planets could be due to external sources. Accretion of atomic particles due to the solar wind combined with the impacting of dust and larger amounts of carbonaceous meteoritic material early in the history of the planets (possibly during the final stages of planetary accretion) may be found to be the source of atmospheric volatiles. Whichever of these processes dominated the initial stages of atmospheric formation around the terrestrial planets it seems reasonable to assume that the gases involved were similar for all these planets and that the differences apparent in the present-day atmospheres are due mainly to differences in mass and distance from the Sun of the planet itself.

Degassing processes are evident on the Earth today in volcanic events and evidence has been cited which indicates

volcanic degassing on the Moon (Moore, 1971). Surface features typical of both crustal/volcanic events and meteoritic impacts have been identified on all the terrestrial planets. The most recent evidence of surface activity is derived from radar maps of Venus (Metz, 1976). It is thus not unreasonable to construct a model which describes the general evolution of such a degassed planetary atmosphere with the aim of applying it to all the terrestrial planets.

The effect of the atmosphere upon the thermal balance of the planetary surface is determined largely by the infrared properties of the individual gases. Thus before discussing the absorption properties it is necessary to predict the gases typical of a secondary terrestrial planetary atmosphere.

The major part of the atmospheric and hydrospheric constituents of the Earth are generally assumed to have been formed by degassing. The term degassing (as used here) includes the emission of juvenile elements, the re-emission of elements previously recycled from the surface and also the emission of radiogenic isotopes which have been produced since the material containing them was last at the surface. Thus the production of an atmosphere will depend upon the amount of crustal activity (either by impact, volcanic events or crustal movement) and the atmospheric constituents will depend upon the surface rocks typical of the planet. Most theories of the evolution of the Solar System form all the terrestrial planets from similar material. Some models (Woolfson, 1976) require the break-up of one or two protoplanets for the formation of the terrestrial

planets which further indicates similarities between rocks of all the planets. The question of crustal activity is complex particularly as mechanisms for crustal movement are not yet well understood. It may be found that plate movement is peculiar to the Earth but both bombardment and crustal activity are possible on all the terrestrial planets.

The juvenile gases detected in volcanic events today on the Earth are typically  $H_2O$ ,  $CO_2$ ,  $CO$ ,  $N_2$ ,  $SO_2$  and  $HCl$  and a few other trace gases. Thus, as a first approximation, it could be assumed that these gases, probably in the given order by volume have been degassed throughout the history of the Earth. However the differentiation of the planet may have influenced, not only the degassing rate, but also the chemical state of the gases evolved. If, in the early period of degassing, there existed large amounts of iron in the mantle (through which the gases passed) the gases at the surface would probably be chemically reduced. These reduced gases are generally supposed to be a mixture of  $H_2O$ ,  $CH_4$ ,  $NH_3$  and possibly  $H_2$  compared with a later oxidized sample of  $H_2O$ ,  $CO_2$  and  $N_2$ .

The gases actually present in the atmosphere of a planet at any point in its history depend upon many factors. The rate of degassing and the possible loss rates from the top of the atmosphere and to the surface rocks will be considered in Chapter 5. Other important factors are the surface temperature, planetary mass and distance from the Sun. Perhaps the best that can be said of a general secondary atmosphere around a terrestrial planet is that most chemical combinations of the elements

carbon, hydrogen, oxygen, nitrogen and sulphur are possible plus a selection of trace elements. The atmosphere of the Earth is not typical of a secondary degassed atmosphere since it is dominated by two mechanisms which are not present on any other planets. The first is the balance made possible by the presence of large liquid water masses on the surface and the second is the balance effected by interaction with the biosphere. Photosynthesis is probably the dominant mechanism producing excess oxygen in the Earth's atmosphere, (incidentally leading to the formation of ozone in the stratosphere). A possible alternative mechanism is the photodissociation of water vapour and escape of hydrogen atoms. This will be discussed later. It is also interesting to note that ozone has been observed in the Martian atmosphere over both polar regions (Hunt, 1974). It is not yet clear how this ozone is formed; the photodissociation and chemical recombination rates of both carbon dioxide and water vapour may be important for its presence. Also the balance between free oxygen and methane in the Earth's atmosphere is controlled by reactions within the biosphere. Thus the atmosphere of the Earth is not an ideal example from which to consider all terrestrial planetary atmospheres. However, it is the atmosphere concerning which we have the most data, and the only atmosphere for which there is (at present) any data on chemical composition at earlier stages. A further interesting point is the idea (due to Margulis and Lovelock, 1974) that the biosphere has actually acted as a stabilizing mechanism for the Earth/atmosphere system: thus for a planet upon which no life

had evolved much more extreme conditions than those apparently experienced by the Earth could be expected. Table 4.1 below lists the gases found in clean, dry air (for the Earth) at ground level together with the percentage of each, by volume.

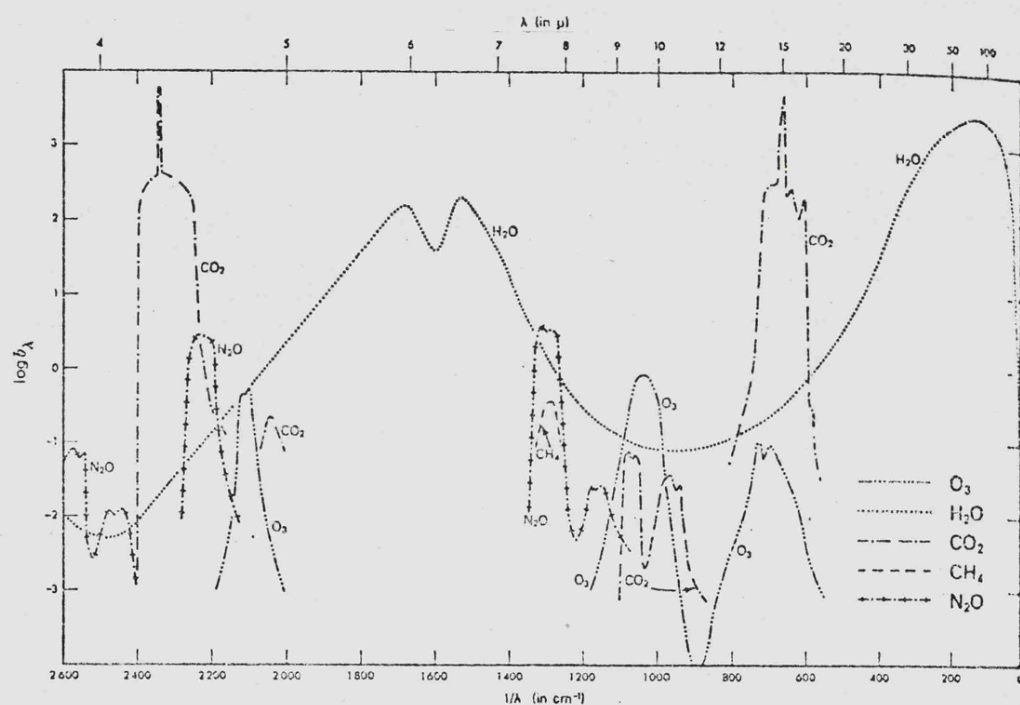
Table 4.1

Gaseous Constituents of Earth's Atmosphere at Ground  
Level (after Giddings, 1973)

<u>Constituent</u>	<u>Percent by volume</u>
Nitrogen ( $N_2$ )	78.084
Oxygen ( $O_2$ )	20.946
Argon (Ar)	0.934
Carbon dioxide ( $CO_2$ )	0.031
Neon (Ne)	$1.82 \times 10^{-3}$
Helium (He)	$5.24 \times 10^{-4}$
Methane ( $CH_4$ )	$1.5 \times 10^{-4}$
Krypton (Kr)	$1.14 \times 10^{-4}$
Hydrogen ( $H_2$ )	$5 \times 10^{-5}$
Nitrous oxide ( $N_2O$ )	$3 \times 10^{-5}$
Xenon (Xe)	$8.7 \times 10^{-6}$
Ozone ( $O_3$ )	$2 \times 10^{-6}$
Ammonia ( $NH_3$ )	$6 \times 10^{-7}$
Nitrogen dioxide ( $NO_2$ )	$1 \times 10^{-7}$
Nitric oxide (NO)	$6 \times 10^{-8}$
Sulphur dioxide ( $SO_2$ )	$2 \times 10^{-8}$
Hydrogen sulfide ( $H_2S$ )	$2 \times 10^{-8}$
Water vapour (average)	up to $1\%$

(Water amounts in the atmosphere vary considerably with latitude and season, but an average value is about 1 percent of the total). The very small mixing ratios of some of the gases listed in Table 4.1 belie properties of importance. The infrared absorption

Figure 4.1



Infrared band absorption of atmospheric gases for  
the Earth.

spectrum (also typical of the average Earth atmosphere) shown in Figure 4.1 illustrates the complex absorption features due to band absorption, not only by carbon dioxide and water vapour, but also by methane, ozone and nitrous oxide. These and other gases possessing infrared absorption bands (e.g. ammonia) may influence atmospheric and planetary surface evolution.

Even apparently inert gases, such as nitrogen and argon, which are possible components of the planetary atmospheres may be significant. Table 4.2 lists the gases present in the atmospheres of the Earth, Venus and Mars and indicates their relative abundances by giving the percentage by volume of each.

Table 4.2

Major Gaseous Constituents of the Atmospheres of the Terrestrial Planets (after Goody and Walker, 1972)

<u>Constituent</u>	<u>Earth</u>	<u>Venus</u>	<u>Mars</u>
CO <sub>2</sub>	$3 \times 10^{-2}$	95	> 50
N <sub>2</sub> , Ar	79	< 5	< 50
O <sub>2</sub>	21	$< 4 \times 10^{-3}$	$10^{-1}$
H <sub>2</sub> O	up to 1	$10^{-2}$	up to $10^{-1}$
HC1	-	$10^{-4}$	-
HF	-	$2 \times 10^{-6}$	-
CO	$10^{-5}$	$2 \times 10^{-2}$	$10^{-1}$

The amount of N<sub>2</sub> or Ar indicated for Mars is probably too high. The difficulties encountered in assessing the presence and amount of neutral gas will be discussed in Section 4.9. However, the

presence of an unknown amount of neutral gas having the ability to broaden the absorption features of other gases without itself being readily detected could be an important factor in both temperature calculations and estimates of degassing rates.

The history of a planetary atmosphere is seen to be vital in any calculation of the surface conditions with time. Since it is possible that the amounts of most of the gases mentioned in this section have varied considerably with time, the properties of all the gases of interest which possess significant infrared features will be discussed individually together with the effect of adding varying amounts of neutral gases. The combination of these gases into model atmospheres will be considered in Chapter 5.

4.3 Gaseous Absorption

The difference between the effective temperature and the surface temperature of a planet possessing an atmosphere is due to the "greenhouse" effect. The effect (as discussed in Chapter 2) is due to the variation of molecular absorption of the atmospheric gases with wavelength. Thus in the case of the Earth the atmosphere is almost completely transparent to visible light but some atmospheric constituents absorb strongly in the spectral region of the re-emitted heat radiation from the surface. This absorption of infrared radiation heats the atmosphere which, in turn, radiates, thus enhancing the surface temperature. It is thus the absorption features in the infrared region that are of significance for the "greenhouse" temperature increment. In this section the general properties of gases exhibiting absorption features in the infrared will be discussed.

It is worth noting, incidentally, that the term "greenhouse" effect has recently been the subject of some controversy. In 1973, Lee suggested that although the generally accepted theory for surface temperature enhancement caused by variations in opacity was correct for planetary atmospheres, it was not the dominant mechanism responsible for increased temperatures inside a garden glasshouse. Thus the name "greenhouse" effect may be unfortunate. However, in reply to this paper Berry (1974) concludes that the blocking of infrared radiation is responsible for both planetary and glasshouse heating.

The absorption of radiation depends upon the wavelength of the radiation, and also upon the type and amount of gas

Figure 4.2

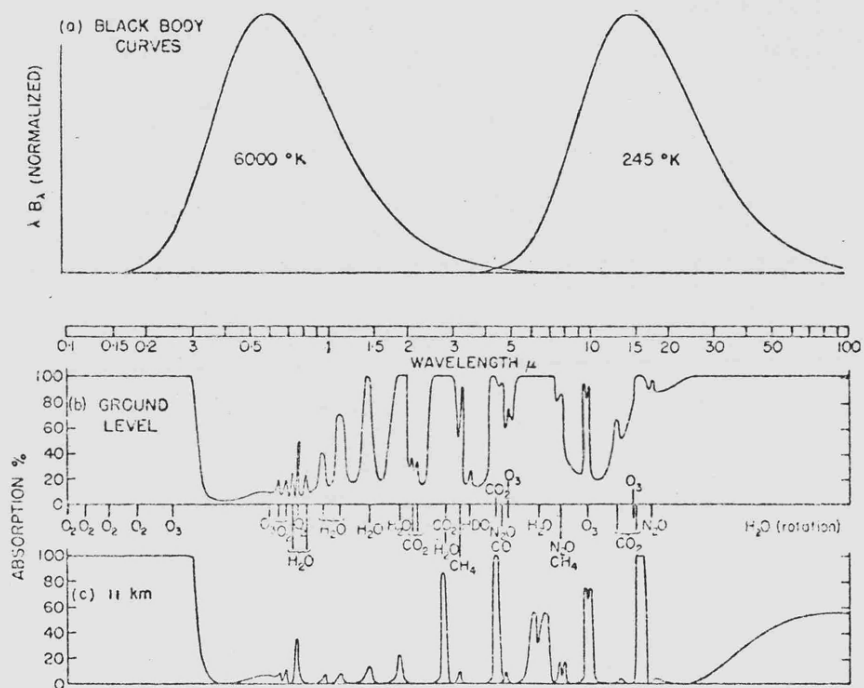


FIG. 1.1. Atmospheric absorptions.

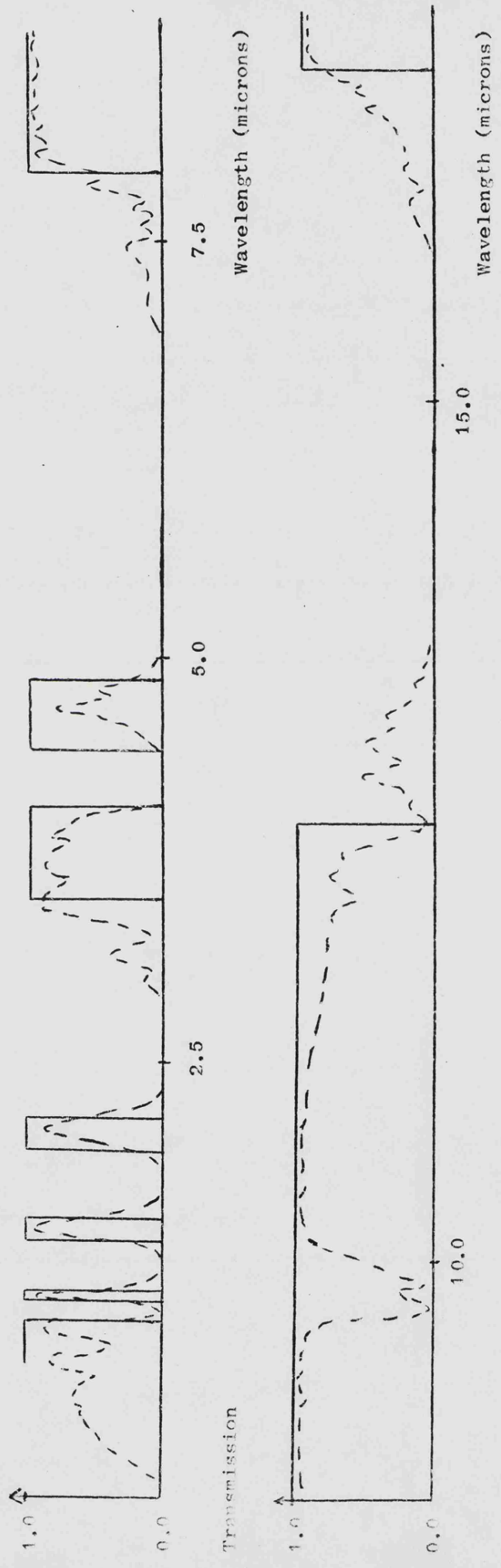
(a) Black-body curves for 6000° K and 245° K. (b) Atmospheric gaseous absorption spectrum for a solar beam reaching ground level. (c) The same for a beam reaching the temperate tropopause. The axes are chosen so that areas in (a) are proportional to radiant energy. Integrated over the earth's surface and over all solid angles the solar and terrestrial fluxes are equal; consequently, the two black-body curves are drawn with equal areas beneath them. An absorption continuum has been drawn beneath bands in (b). This is partly hypothetical because it is difficult to distinguish from the scattering continuum, particularly in the visible and near infra-red spectrum. Conditions are typical of mid-latitudes and for a solar elevation of 40° or diffuse terrestrial radiation.

Atmospheric gaseous absorption for the Earth  
(after Goody, 1964).

present in the atmosphere. Figure 4.2 shows the Planck curves for the effective temperatures of the Sun and the Earth, and thus indicates the wavelength regions over which most of their energy is emitted. The absorption curves for the Earth's atmosphere are shown at ground level and at a height of 11 kilometres in the atmosphere. The highly energetic ultra-violet radiation from the Sun is absorbed high in the Earth's atmosphere (by ozone in the stratosphere). Little absorption is present (even at ground level) in the visible region, but the atmosphere can be seen to exhibit rapidly varying opacity in the infrared region. Long wave of approximately twenty-five microns, the rotation band of water vapour absorbs almost all the radiation in the microwave region. Figure 4.2 also illustrates the effect of varying the amount of absorbing gas, since higher in the Earth's atmosphere the solar radiation has penetrated less gas and is (with the exception of the ultra-violet) less well absorbed.

The combined curves of intensity of planetary thermal radiation and varying atmospheric opacity indicate the importance of the infrared region in the calculation of the "greenhouse" increment for the surface temperature. If radiation is emitted from the surface of the planet in one of the regions of near zero absorption it will pass almost unhindered through the atmosphere, whereas radiation emitted in regions of strong absorption will contribute to the enhanced surface heating by re-emission. This "step-like" appearance of the infrared absorption features has led to a method of approximating the

Figure 4.3



A step approximation to the real transmission curve of the Earth's atmosphere. Note that this approximation (derived for  $\text{CO}_2$  and  $\text{H}_2\text{O}$  only) ignores the 9.6 micron feature due to ozone absorption.

true transmission curve of the atmosphere by steps of zero or one hundred percent transmission first suggested by Sagan and Mullen in 1971. Figure 4.3 illustrates part of the real transmission spectrum of the Earth's atmosphere (dotted curve) and the step approximation to it. The method of producing this type of block approximation will be discussed in this chapter.

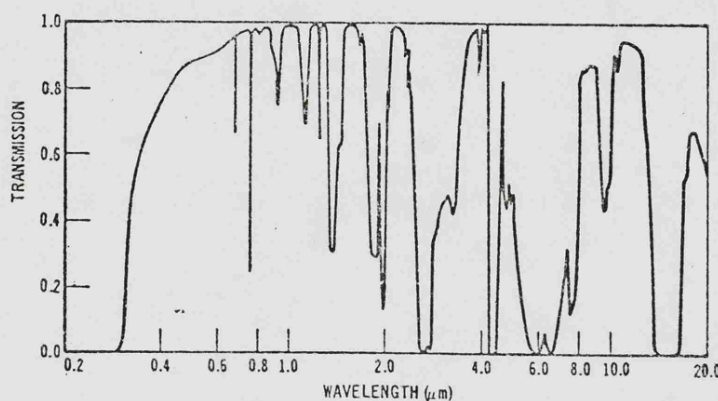
The primary cause of atmospheric extinction in the infrared is absorption by molecules. The molecules responsible for absorption features in the Earth's atmosphere are indicated in Figure 2.1 (Chapter 2). It can be seen from this illustration that the molecules of water vapour and carbon dioxide dominate the absorption spectrum of the Earth's atmosphere. Figure 4.4 illustrates that the combination of transmission curves of water vapour (of a fixed amount) and carbon dioxide approximates the real transmission curve of the Earth's atmosphere.

Molecules can possess energy in four forms: translational, electronic, vibrational and rotational. The last three are quantized and can thus take part in the exchange of energy between matter and the radiation field. Quantum theory permits the prediction of discrete spectral lines from the Planck relation:

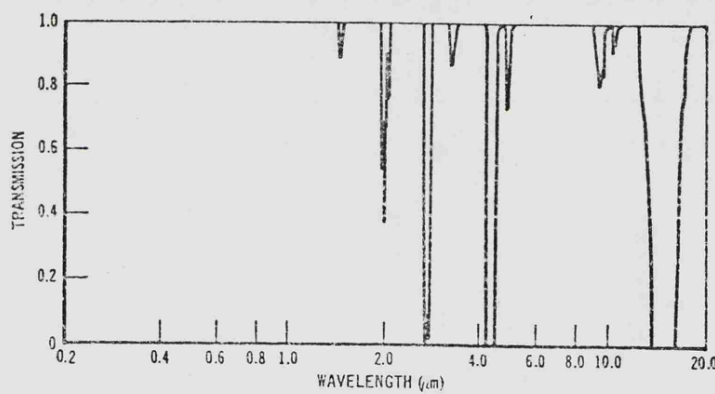
$$\Delta E = h \nu \quad \dots\dots 4.1$$

which gives the energy difference,  $\Delta E$ , between two stationary states of a molecule absorbing/emitting radiation of frequency  $\nu$ . Thus if large photon energies are available the electronic states of the molecule may be excited causing absorption/emission

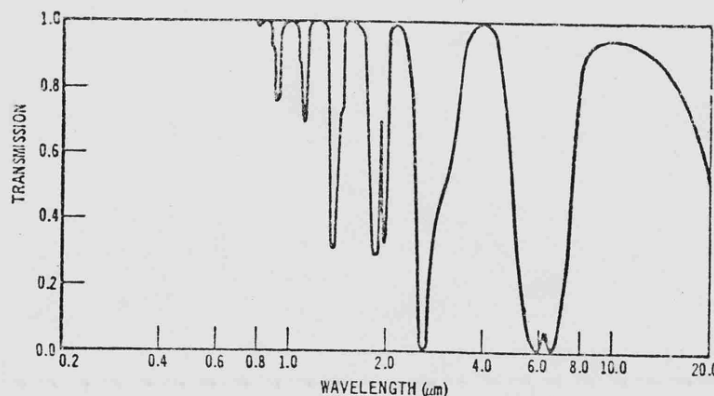
Figure 4.4



Atmospheric transmission (smoothed). At 2 km altitude (zenith), 0.25 cm precipitable water vapor.



Atmospheric transmission ( $\text{CO}_2$ ). At 2 km altitude (zenith).

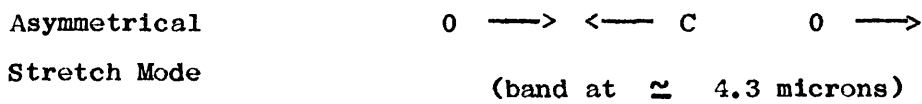
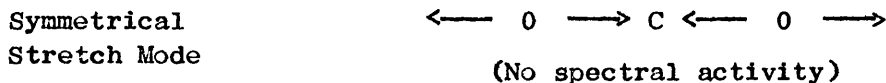


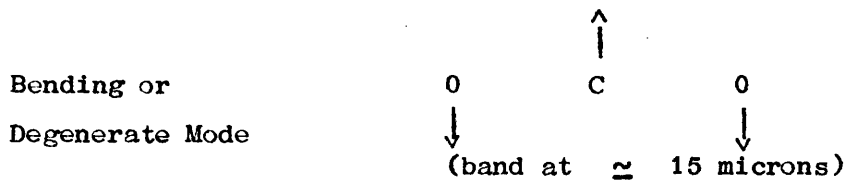
Atmospheric transmission ( $\text{H}_2\text{O}$ ). At 2 km altitude (zenith), 0.25 cm precipitable water vapor.

The combination of transmission curves of water vapour and carbon dioxide is a good approximation to the real atmospheric transmission curve.

in the ultra-violet and visible regions. The rotational spectrum of a molecule shows small energy differences between states indicating that absorption/emission occurs in the far infrared. Changes in the vibrational energy of a molecule result from absorption/emission of radiation of frequencies typical of the near and middle infrared. Thus the region of interest in the calculation of planetary surface temperatures (the infrared region) is dominated by groups of lines which constitute vibrational-rotational bands. The modelling of such bands will be discussed in Section 4.4.

Spectral activity means that an interaction has occurred between the incident radiation and the molecule. This interaction can only take place by a change in an electric or magnetic dipole or multipole moment. Thus the type of activity of any species will be a function of the charge displacement of the molecule: no vibrational spectra are expected from the symmetric vibrations of N<sub>2</sub>, O<sub>2</sub> (the most abundant constituents of the Earth's atmosphere) or Ar. Similarly the carbon dioxide molecule, which is linear and symmetric, has no permanent dipole moment and thus only two of the three possible vibrational modes produce spectral features, as is illustrated below. There is no pure rotation absorption.





The spectral activity of each of the gases of interest will be discussed in detail in Sections 4.6 to 4.9. However, the theoretical models of band absorption can be discussed prior to the consideration of individual absorption features.

The general method of approach is to construct a theoretical model of band absorption for the gas from representations of the line absorption and an assumed spacing. The absorption band models produced in this way involve numerical summation. This is often highly time consuming, although such models have been shown to be extremely accurate (e.g. the Mayer-Goody random band model, which has been shown to produce transmission functions that agree well with observations, Hunt and Mattingly, 1976). There are further problems, particularly spectral anomalies which cannot be identified without resort to spectroscopy. An alternative approach to these complex analytical models is a semi-empirical approach utilizing direct observations of band absorption. These models allow a restricted number of chosen parameters to vary with varying laboratory conditions and hence produce a useful representation of absorption under different conditions.

4.4 Theoretical Band Model

The band model used in this thesis was derived by J. N. Howard, D. E. Burch and D. Williams in a series of papers in 1956, later continued and expanded by Burch, Gryvnak, Singleton and France (1962). The aim was to produce a reasonable empirical formulation of band absorption for a general gaseous absorber and then by laboratory observation to construct a table of parameters which would enable the absorption characteristics of each band to be well represented. The experimental technique was designed to measure total band absorption of gaseous absorbers under simulated atmospheric conditions, and no attempt was made to resolve individual lines. The empirical representation was based upon a theoretical model for band absorption assuming a Lorentz line shape with:

$$k_{\nu} = \frac{S}{\pi} \frac{\alpha}{(\nu - \nu_0)^2 + \alpha^2} \quad \dots \dots 4.2$$

where  $\nu_0$  is the frequency of the line centre,  $\alpha$  the half width of the line. S (the line strength) is given by:

$$S = \int_{-\infty}^{\infty} k_{\nu} d\nu \quad \dots \dots 4.3$$

The total absorption or equivalent width,  $\int A_{\nu} d\nu$ , of a single line, although difficult to measure experimentally, reduces to a simple expression in the two limiting cases of a weak or a strong line. The weak line case, for which  $S_w \ll \alpha$ , (where w is the absorber concentration) has

$$\int A_\nu d\nu = S_w \quad (\text{weak line}) \quad \dots \dots \dots 4.4$$

whereas the strong line, for which  $S_w \gg \alpha$  has

$$\int A_\nu d\nu = 2 \sqrt{S \alpha w} \quad (\text{strong line}) \quad \dots \dots \dots 4.5$$

The effects of temperature and pressure for regions of interest were assumed to be negligible for the line strength,  $S$ . The half width,  $\alpha$ , may be expressed as a function of both temperature and pressure, but for the comparatively small temperature range involved in planetary thermal emission it was expressed simply as proportional to pressure such that

$$\alpha = \beta P \quad \dots \dots \dots 4.6$$

The band absorption was considered as being of two types: weak band absorption and strong band absorption with a transition zone between. Both these bands were assumed to be composed of strong lines: the weak bands consisting of strong lines far enough apart so that the effects of overlapping could be ignored and the strong band of closely packed strong lines. From Equations 4.5 and 4.6 above, the total absorption by a strong line may be expressed as

$$\int A_\nu d\nu = 2(S \beta)^{\frac{1}{2}} (wP)^{\frac{1}{2}} \quad \dots \dots \dots 4.7$$

Thus the total absorption of a weak band is given by

$$\int A_\nu d\nu = (wP)^{\frac{1}{2}} \sum_i 2(\beta S_i)^{\frac{1}{2}} \quad ) \quad ) \quad ) \quad \dots \dots \dots 4.8$$

i.e.  $\int A_\nu d\nu = \text{'CONSTANT'} w^{\frac{1}{2}} P^{\frac{1}{2}} \quad ) \quad )$

It was found that a more reasonable empirical representation could be achieved if extra weight was given to the partial pressure of the absorbing gas, 'p'. Also the index of both the pressure term and the absorber concentration term were allowed to vary so that the final representation of weak band absorption was

$$\int A_\nu d\nu = c w^d (P + p)^k \quad \dots \dots 4.9$$

where  $c$ ,  $d$  and  $k$  are empirical parameters which take different, experimentally determined, values for each band of each gas.

The strong band representation of absorption derived by Howard, Burch and Williams (1956) attempts to represent regions of the spectrum where the effects of overlap of strong lines becomes severe, and was determined semi-empirically to be

$$\int A_\nu d\nu = C + D \log_{10} w + K \log_{10} (P + p) \quad \dots \dots 4.10$$

where  $C$ ,  $D$  and  $K$  are empirical parameters which must be determined experimentally for each band. Values of these empirical parameters for all the gases discussed in this chapter may be found in Tables 4.5, 4.7, 4.10 and 4.11. The pressure term which occurs in both these representations was generalised and called the effective pressure ' $P_e$ ' where:

$$P_e = P + (B_c - 1) p \quad \dots \dots 4.11$$

The broadening coefficient, ' $B_c$ ', was allowed to take the values determined in the later work of Burch, Gryvnak, Singleton and France (1962) for minor atmospheric gases (e.g.  $\text{CH}_4$ ), but the original value implicitly assumed by Howard, Burch and Williams

(1956) of  $B_c = 2$  was used for both carbon dioxide and water vapour. Thus the final representation of the total absorption by an atmospheric gas was given by:

$$\text{or } \int A_\nu d\nu = C + D \log_{10} w + K \log_{10} P_e$$

(strong band) .... 4.13

Some bands had characteristics suited to only one of these representations over the whole range of the laboratory experiments. The alternative equation was, thus, not required and the parameters relating to it are arbitrarily given as zero in the tables. The region of discontinuity between the weak and strong band representations was determined experimentally and the critical absorption tabulated for each band together with the values of all the empirical parameters. Since the change from one representation to the other is not continuous it was necessary to interpolate between the weak and strong regimes.

The empirical equations together with the experimentally derived values of the parameters allowed computation of the absorption characteristics of the gases concerned. The results of these computations will be discussed in Sections 4.6 to 4.9. For each band of each gas the value of the weak band absorption was calculated using Equation 4.12 and was compared with the critical absorption. If the values were close, interpolation was required. If the weak band absorption was very much greater than the critical absorption the band absorption was recomputed using Equation 4.13. The fractional transmission for each band

was given by

$$\text{transmission} = 1 - \frac{\int A_\nu d\nu}{\text{band width}}$$

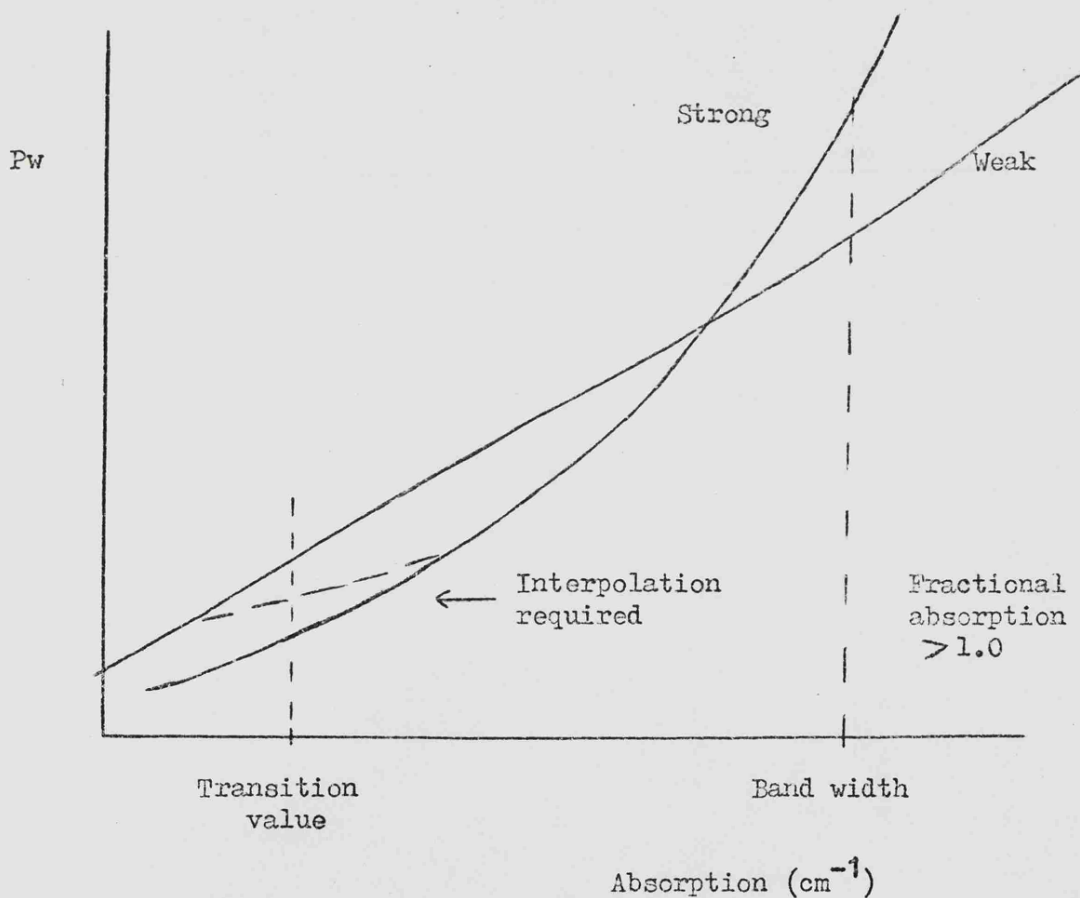
Thus these empirical relations allowed the calculation of a fractional transmission spectrum for each gaseous absorber under consideration. However both the empirical relations and the laboratory data had certain severe restrictions. Thus extensions had to be made to allow computation of spectra over a wider range of pressures and absorber concentrations. These extensions are discussed in Section 4.5.

4.5 Computational Extensions

The empirical representations of band absorption derived by Howard, Burch and Williams (1956) and later extended by others were found to be useful for the calculations performed in this work. They expressed band absorption in terms of total pressure, partial pressure of the absorbing gas and absorber concentration but without the need for complex numerical summations. This simplified representation was particularly suitable for the model described in this thesis since the calculations performed are of global temperatures extended over the whole life-time of the terrestrial planets. Additionally the simplified model considered only the general absorption features of the changing atmospheric spectra thus saving upon the otherwise large amounts of computational time required. However, since the theme of this work is the evolution of a secondary atmosphere it is necessary to consider the absorber amounts which may be required. If, for instance, the secondary atmosphere was dominated by carbon dioxide then the ranges of partial pressure of CO<sub>2</sub> considered in the laboratory experiments (typically between 1 and 50 millimetres of mercury) would not be adequate. In fact it was decided to extend the band model so that it became appropriate over larger ranges of both carbon dioxide and water vapour partial pressures although the ranges for the other gaseous absorbers considered in detail were deemed to be adequate.

Although the band representations were considered accurate (within the limits required by this work) there were two obvious discrepancies. Firstly, as already mentioned, the curve of

Figure 4.5



Variation of the Weak and Strong Band representations with  $P_w$ .  
 The area around the transition value requires interpolation and  
 large values of  $P_w$  can produce values of absorption  $>$  the band  
 width and thus a fractional absorption  $> 1.0$ .

absorption was discontinuous and secondly the strong band representation was logarithmic and thus inappropriate application of the model could lead to values of absorption greater than one hundred per cent! Both these discrepancies are illustrated in Figure 4.5. Extension of the model required a slightly different representation of absorption. The function chosen was an exponential form similar to one suggested by Plass (1960) and given by:

$$A_3 = \int A_\nu d\nu = 1 - e^{-B\sqrt{P_e w}} \quad \dots\dots 4.14$$

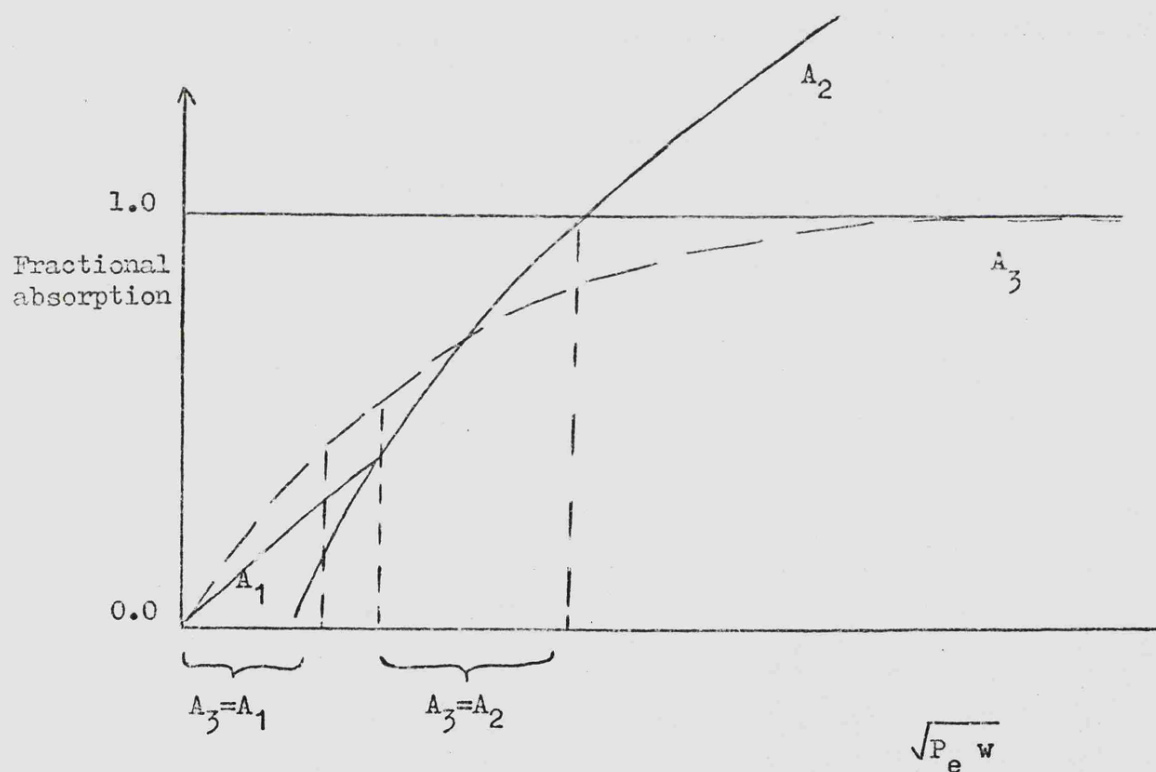
This function had to be fitted to the strong and weak band representations to find the best-fit value of 'B' for each band of the two gases considered. The two empirical relations given in Equations 4.12 and 4.13 are

$$A_1 = \int A_\nu d\nu = c w^d P_e^k \quad \dots\dots 4.12$$

$$A_2 = \int A_\nu d\nu = C + D \log_{10} w + K \log_{10} P_e \quad \dots\dots 4.13$$

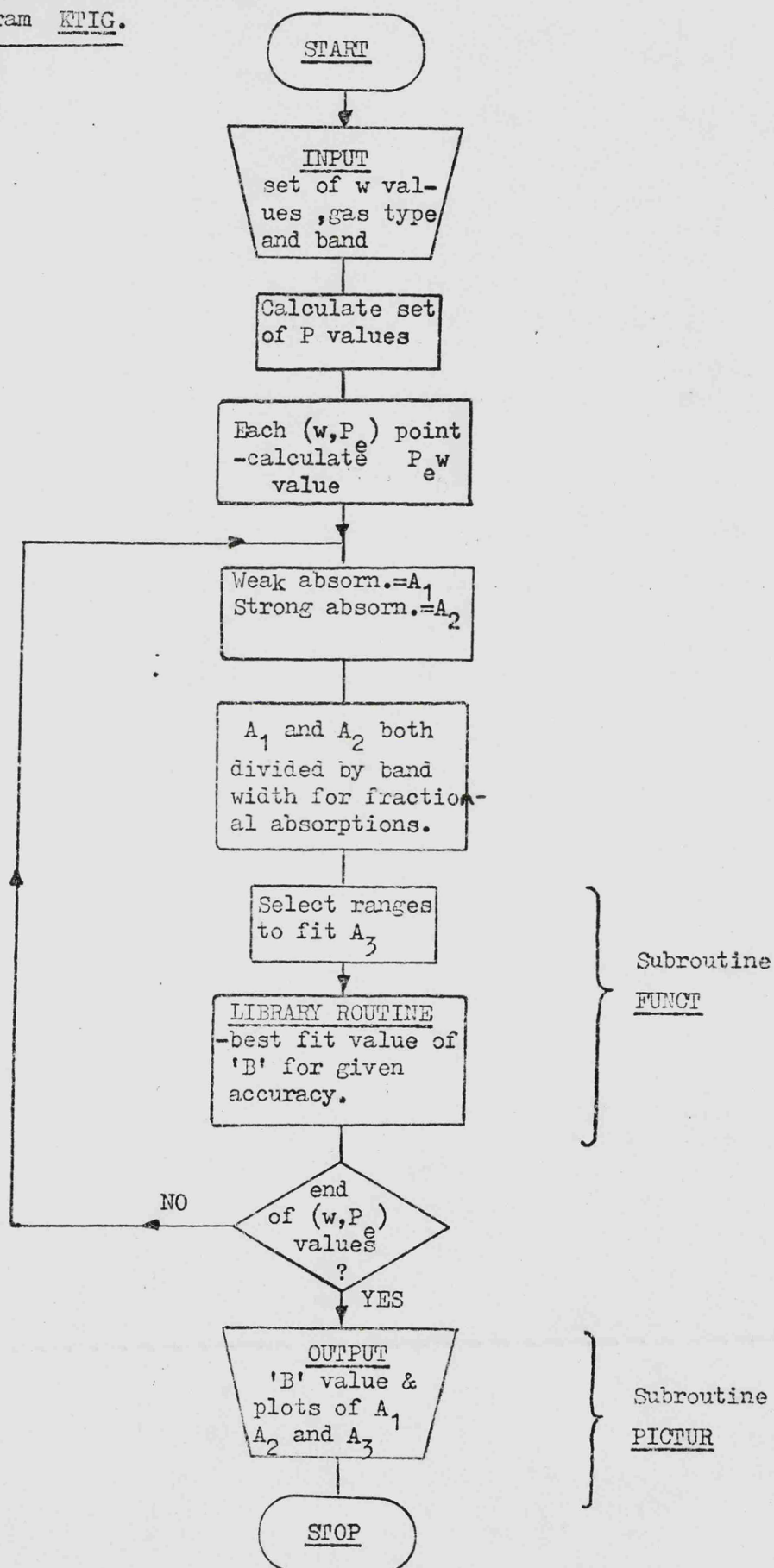
and are sketched (as functions of  $\sqrt{P_e w}$ ) together with the exponential form,  $A_3$ , in Figure 4.6. The ranges on the  $\sqrt{P_e w}$  axis are those over which the fitting procedure was used. These were made as large as possible without infringing the region of discontinuity or extending beyond the laboratory ranges of either pressure or absorber concentration. The computation of the best value of the parameter 'B' for each band of water vapour and carbon dioxide was performed using a computer program (KTIG) which is described below, together with the results of

Figure 4.6



Comparison of the three forms of band absorption:  $A_1$ ,  $A_2$  and  $A_3$ .  
 Areas indicated on the axis are the ranges of  $\sqrt{P_e w}$  over which  
 the fitting procedure was employed.

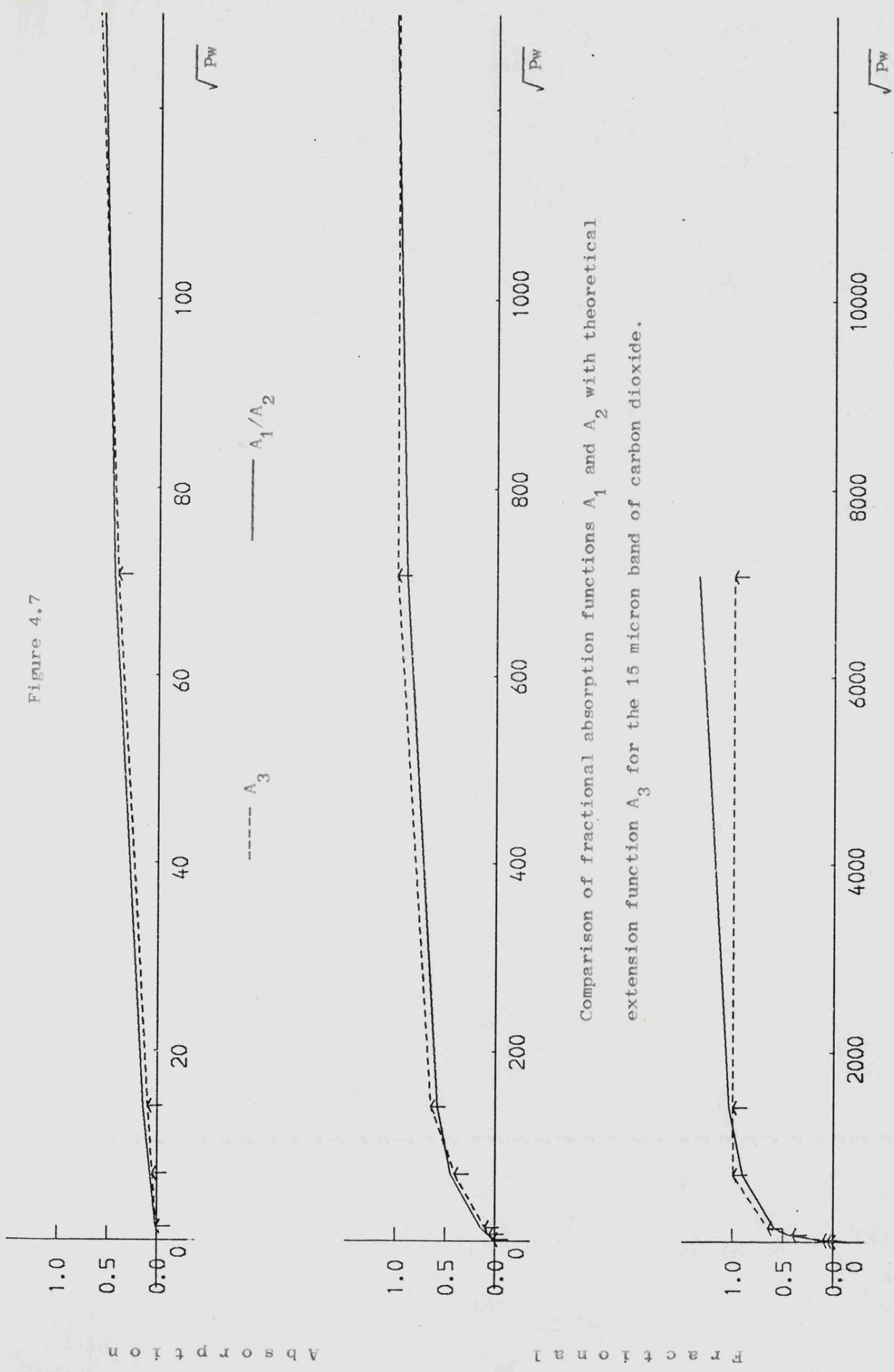
## Flow diagram of computer

program KTIG.

the calculations.

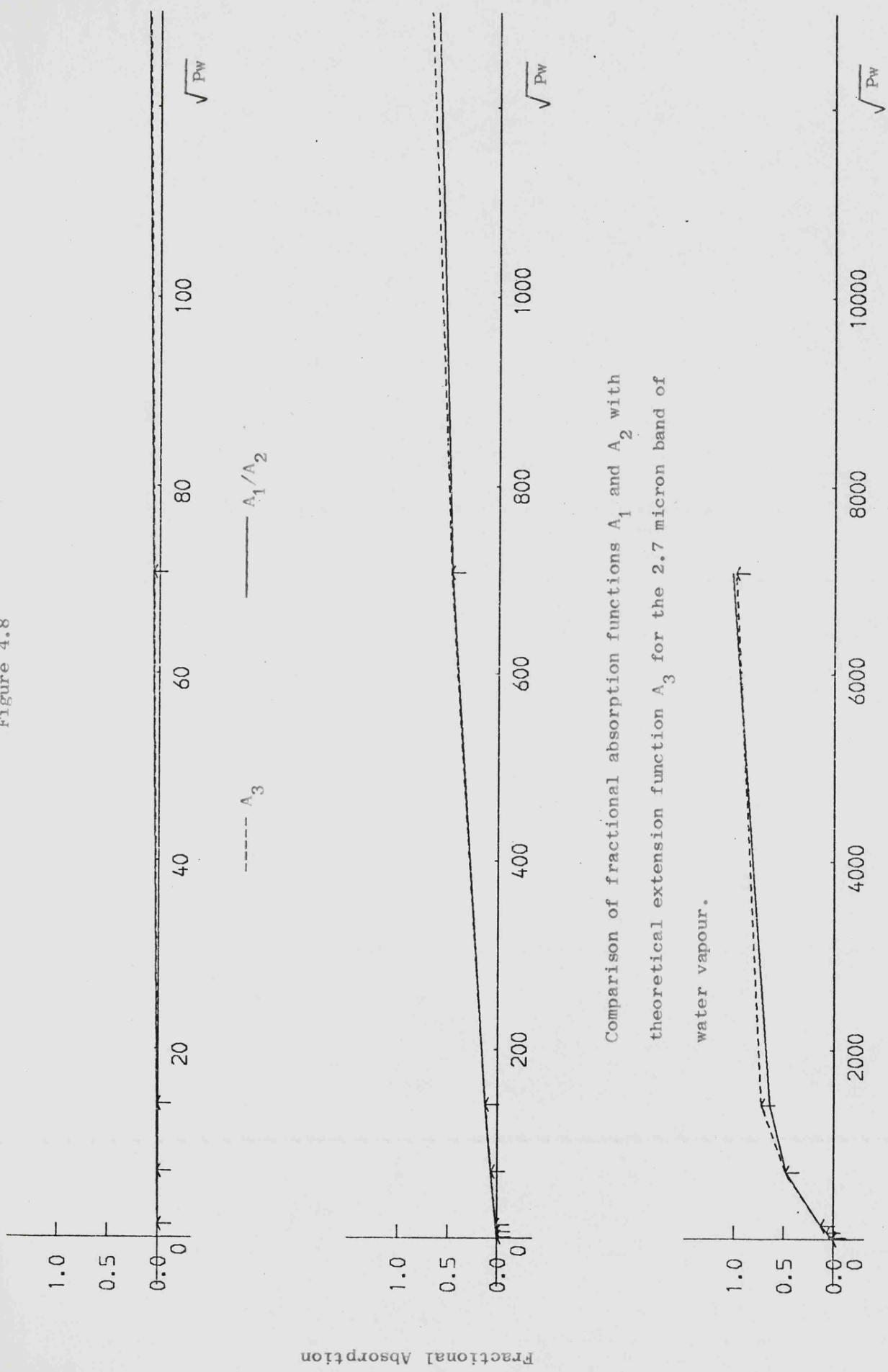
The computer program 'KTIG' fitted the chosen function,  $A_3$ , over selected ranges of  $\sqrt{P_e w}$  and determined a 'best' value of 'B' for each band of carbon dioxide and water vapour. Since the ranges of the absorber concentration,  $w$ , were different for the two gases in the laboratory experiments performed by Howard, Burch and Williams, the fitting procedure in the program was for  $10 < w < 10^4$  (atmosphere centimetres) for carbon dioxide and  $0.05 < w < 100$  (precipitable centimetres) for water vapour. The final value of 'B' determined for each band was output and also the three functions (denoted by  $A_1$ ,  $A_2$  and  $A_3$  above): the weak band absorption, the strong band absorption and the exponential function curves were plotted against  $\sqrt{P_e w}$ . The flow diagram for the program 'KTIG' illustrates the iteration necessary for each band. An accuracy of 1 in  $10^4$  was selected for the library routine, indicated in the flow diagram, which computed the best value of B. The absolute difference between the curves  $A_1$  and  $A_2$  (from the laboratory data) and the exponential curve  $A_3$  was, in general, less than 5 per cent. This was thus the maximum error in the new function for the fractional absorption. Figures 4.7 and 4.8 show typical plots of the functions  $A_1$ ,  $A_2$  and  $A_3$  generated by 'KTIG'. The error in the fitting is shown to be, as indicated above, no greater than 5 per cent. This error led to temperature differences (when the surface temperature computation was performed using the exponential function throughout rather than the weak and strong representations) of no more than 2.4 K. The reason for

Figure 4.7



Comparison of fractional absorption functions  $A_1$  and  $A_2$  with theoretical extension function  $A_3$  for the 15 micron band of carbon dioxide.

Figure 4.8



Comparison of fractional absorption functions  $A_1$  and  $A_2$  with theoretical extension function  $A_3$  for the 2.7 micron band of water vapour.

the derivation of the exponential representation of the absorption was to permit an extension of calculations beyond the ranges of the laboratory data. The original representations were to be used as far as they were applicable (i.e. in the early stages of the evolution of the atmosphere). If the atmosphere became dominated by a neutral gas (as the Earth) then the partial pressures of the absorbing gases would remain small and the original functions would still be applicable (the effect of the neutral gas will be discussed in Section 4.9). If the evolving atmosphere became dominated by a strongly absorbing gas then the surface temperature would rise rapidly. In this situation the exponential representation  $A_3$  would allow surface temperature calculations to be extended further than would be possible using the laboratory data. Since the application of this representation will only be appropriate for rapidly increasing absorber concentration and surface temperatures the possible error of up to 2.4 K was considered negligible.

The values of 'B' for each band of carbon dioxide and water vapour are given in Table 4.3. The value of  $B = 10^5$  for the rotation band of water vapour long wave of a pre-determined wavelength was chosen arbitrarily to give total absorption for very small mixing ratios of water vapour. The problems of a satisfactory representation of the rotation band of water vapour will be discussed in greater detail in Section 4.7.

Using these values of 'B' and the exponential form of the absorption:

$$A_3 = \int A_\nu d\nu = 1 - e^{-B\sqrt{P_e w}} \dots\dots 4.14$$

the fractional absorption of any band of carbon dioxide and water vapour may be calculated. This extension of the laboratory-derived functions will be used to derive some of the surface temperatures discussed in Chapter 5.

Table 4.3

Computed 'B' Values for Carbon Dioxide and  
Water Vapour Absorption Bands

BAND ( $\mu$ )	$\text{CO}_2$	BAND ( $\mu$ )	$\text{H}_2\text{O}$
15	$0.8980 \times 10^{-2}$	long wave of given wave- length	$10^5$
10.4	$0.5857 \times 10^{-3}$	6.3	0.1442
9.4	$0.9105 \times 10^{-3}$	3.7 (HDO)	$10^{-5}$
5.2	$0.2367 \times 10^{-3}$	3.2	$0.1662 \times 10^{-2}$
4.8	$0.6129 \times 10^{-3}$	2.7	$0.1166 \times 10^0$
4.3	$0.6428 \times 10^{-2}$	1.87	$0.2887 \times 10^{-2}$
2.7	$0.7307 \times 10^{-2}$	1.38	$0.3254 \times 10^{-2}$
2.0	$0.9214 \times 10^{-3}$	1.1	$0.5448 \times 10^{-3}$
1.6	$0.3557 \times 10^{-4}$	0.94	$0.1686 \times 10^{-2}$
1.4	$0.2672 \times 10^{-4}$		

4.6 Carbon Dioxide

In Section 4.2 the possible chemical constituents of a degassed terrestrial atmosphere have been discussed. It was also noted that the dominant gases released in volcanic events on Earth today are water vapour and carbon dioxide (the amount of water vapour released being up to an order of magnitude greater than the amount of carbon dioxide). However Table 4.2 which gave the atmospheric constituents of Venus, Mars and the Earth in percentage form indicates that carbon dioxide rather than water vapour dominates the atmospheres of both Mars and Venus. This apparent discrepancy between the degassing ratios and the atmospheric constituents may be considered in one of two ways: either the degassing events on both Mars and Venus favour carbon dioxide rather than water vapour or the ratios are similar on all three planets and some other mechanism is responsible for the apparent lack of water vapour in the Martian and Cytherean atmospheres. The former hypothesis seems unlikely since differing degassing ratios would presumably be attributable to differences in chemical composition of the surface rocks. Although it is reasonable to suppose that the formation of Venus, the Earth and Mars would allow such differences, their respective distances from the Sun would seem to imply that the Earth would take an intermediate composition rather than (as the atmospheres seem to indicate) Venus and Mars being depleted in water compared with the Earth. However, it has been suggested that this apparent depletion is real and that the small amount of water vapour detected in the upper atmosphere of Venus is compatible

with model predictions (McElroy and Hunten, 1969). The feeling that the  $H_2O/CO_2$  ratio of the Earth required explanation rather than those of Venus and Mars appears to be contradicted by recent observations of cometary  $H_2O/CO_2$  ratios. Delsemme (1976) has suggested that observations of Comet Kohoutek and Comet West reveal ratios very similar to the terrestrial value. The second possibility is that the same or different mechanisms are responsible for removing almost all the degassed water vapour from the atmospheres of both Mars and Venus. The most probable methods of removal from the atmosphere are either condensation onto or incorporation into the surface or escape from the top of the atmosphere. The escape of gases from the atmospheres of the terrestrial planets will be considered in greater detail in Chapter 5 (Section 5.3). There is a possibility that the degassing of water vapour from Mars has been particularly inefficient because of the low surface temperatures compared with 273 K and this will be considered further in Section 4.9. The apparent lack of similarity between the Earth and the other two planets of interest is due to the cyclic processes allowed by the presence of the biosphere and the hydrosphere. The depletion of carbon dioxide in the Earth's atmosphere compared with Venus (a planet of similar size and composition) is due to the oceans on Earth acting as a sink for atmospheric  $CO_2$ . In fact, at the present time, the rate of taking of  $CO_2$  into solution and the loss rate back into the atmosphere are almost identical but the carbonaceous sedimentary rocks on Earth indicate that a large amount of atmospheric carbon dioxide has been converted into

bicarbonate ions and thus into carbonate sediments over the history of the Earth. Table 4.4 lists the probable amounts of carbon dioxide and water vapour in the atmospheres of Venus and Mars (including its polar caps) and compares these figures with estimates of the amounts of these volatiles present in the atmosphere, hydrosphere and sediments on Earth - all the figures are in kilograms per square metre.

Table 4.4

Volatile Inventories for the Terrestrial Planets (kgms/m<sup>2</sup>)

(after Meadows, 1972)

<u>Planet</u>	<u>Water vapour</u>	<u>Carbon dioxide</u>
EARTH	( atmosphere	30
	(	5
	( atmosphere + hydrosphere	$3 \times 10^6$
	( atmosphere	$4.5 \times 10^6$
VENUS	( + hydrosphere + sediments	$8 \times 10^5$
	atmosphere	$100$
MARS	atmosphere + polar caps	$2.5 \times 10^{-2}$
		650

These figures indicate that the amount of carbon dioxide degassed on the Earth and Venus are very close whilst the amount of water vapour seems low for Venus compared to the Earth.

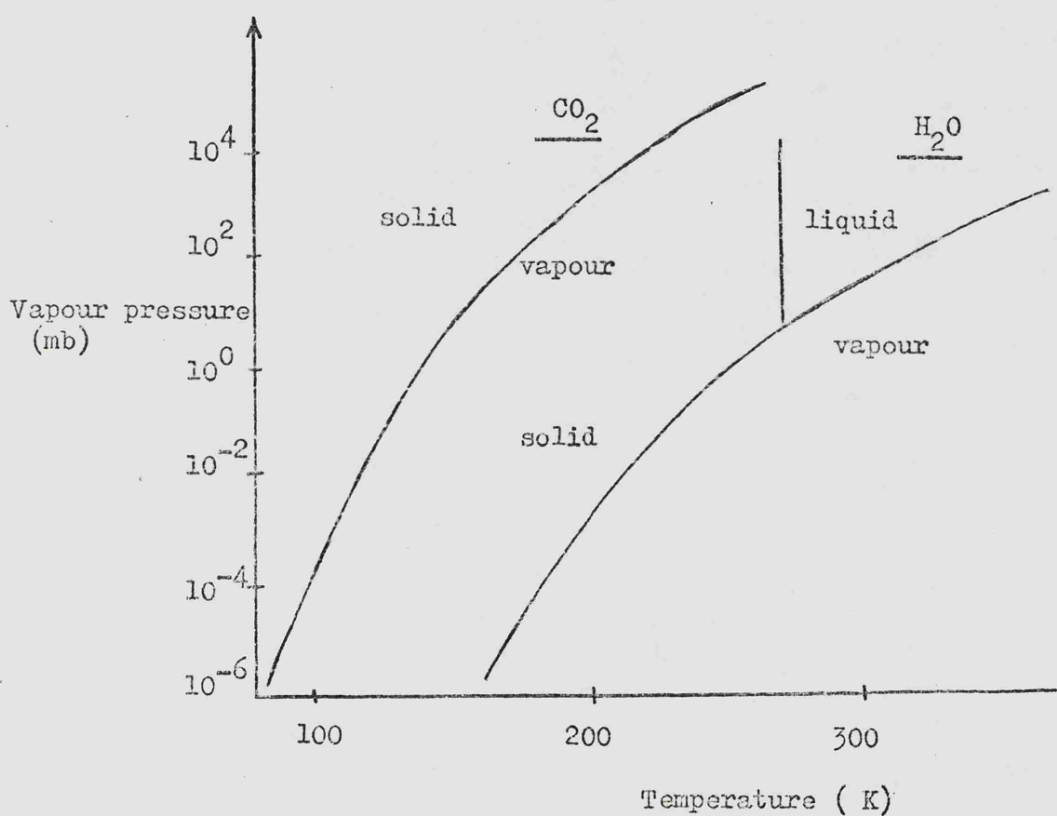
Thus it seems reasonable to assume that for a planet which has neither a hydrosphere (i.e. liquid, surface water) nor a biosphere the probable removal mechanisms (for atmospheric gases) would act more efficiently for water vapour than for carbon dioxide. This would mean that the dominant atmospheric gas would be carbon dioxide even though in the degassing sequences more

water vapour than carbon dioxide had been emitted. This assumption has been made for the calculations of possible surface temperature evolutionary tracks discussed in Chapter 5. The assumption that carbon dioxide emitted into the atmosphere of a terrestrial planet will remain there is reasonable since within the temperature and pressure ranges typical of an evolving atmosphere (say 200 K to 300 K and 1 to 1000 millibars) carbon dioxide is a vapour as is illustrated by Figure 4.9 whereas water can take any of its three phases.

As well as its significance as the major degassed constituent likely to remain in the atmosphere, carbon dioxide is of particular importance in studies of atmospheric evolution because of its infrared absorption bands. In the Earth's atmosphere, for instance, carbon dioxide accounts for only 0.03 per cent of the total atmosphere but its influence in controlling the outgoing thermal emission from the surface of the Earth is second only to water vapour. The Martian "greenhouse" increment is due predominantly to the absorption by carbon dioxide in the infrared region.

The usual carbon dioxide molecule (i.e.  $\text{C}^{12}\text{O}_2^{16}$ ) is linear and symmetric; its bonding structure being  $\text{O}=\text{C}=\text{O}$ . Owing to its symmetry the molecule has no permanent dipole moment and thus no pure rotation spectrum, consequently the infrared absorption is confined to the rotation/vibration activity. The strongest bands are due to the fundamental 'bending' and 'stretching' frequencies and lie at approximately 15 microns and 4.3 microns respectively (see Section 4.3). However the spectrum

Figure 4.9



Comparison of the phase diagrams of water vapour and carbon dioxide. In the temperature and pressure ranges of interest  $\text{CO}_2$  is usually a vapour whereas  $\text{H}_2\text{O}$  can take any of its three phases.

(after Goody and Walker, 1972 )

is complex, having a number of combination bands and also "hot bands" (i.e. bands which are weak at temperatures of interest for work in planetary atmospheres but become very much stronger at higher temperatures). The whole structure is further complicated by combinations of isotopes of both carbon and oxygen into carbon dioxide. The molecules  $C^{13}O_2$ ,  $CO^{16}O^{17}$  and  $CO^{16}O^{18}$  are all present in the Earth's atmosphere and, whilst they form less than two per cent of the total carbon dioxide, the shift of band centre frequency of up to  $60 \text{ cm}^{-1}$  (particularly in the region of the 15 micron bands) is the cause of complexity in the spectrum. As has already been indicated (see Section 4.4) it is not the intention in this work to consider the complexities of infrared band structure but rather to utilize simple theoretical models of total band absorption in order to compute long-term trends in atmospheric absorption and thus in planetary surface temperatures.

The band model used here has already been described in Section 4.4. The total absorption in a specified band region is expressed in terms of a number of parameters giving the weak and strong representation of absorption thus (from Equations 4.12 and 4.13)

$$\int A_\nu d\nu = c w^d P_e^k \quad (\text{weak}) \dots 4.12$$

$$\text{or } \int A_\nu d\nu = C + D \log_{10} w + K \log_{10} P_e \quad (\text{strong}) \dots 4.13$$

where 'w' is the absorber concentration, expressed in atmosphere centimetres for carbon dioxide, and ' $P_e$ ' is the effective pressure (in millimetres of mercury). For carbon dioxide this

takes the form (given in Equation 4.11)

$$P_e = P + (B_c - 1) p \quad \dots\dots 4.11$$

The broadening coefficient ' $B_c$ ' for carbon dioxide has been assigned a value of 2. Table 4.5 below lists the bands considered, together with the band limits (in wavenumber), the values of all the empirical parameters and the value of the absorption (in  $\text{cm}^{-1}$ ) at which the transition between weak and strong representation must take place. When only one of these two representations is available the parameters for the other are given the arbitrary value zero. The single representation should not be extended beyond the region in which it is appropriate.

The exponential representation, described in detail in Section 4.5, has been used to extend the range of the above parameters. The values used for this extension have already been listed in Table 4.3. Thus these representations of band absorption could be used to produce transmission spectra for carbon dioxide pressures from 1 to 1000 millibars. Figures 4.10 to 4.17 illustrate the computer-drawn fractional transmission spectra for pure carbon dioxide atmospheres of pressures ranging from 1 to 1000 millibars. The variation in the transmission caused by the addition of a broadening gas will be discussed in much greater detail in Section 4.9 but Figure 4.18 has been included here so that a direct comparison may be made between it and Figure 4.10.

The importance of carbon dioxide as a major constituent of terrestrial atmospheres has been discussed in this section.

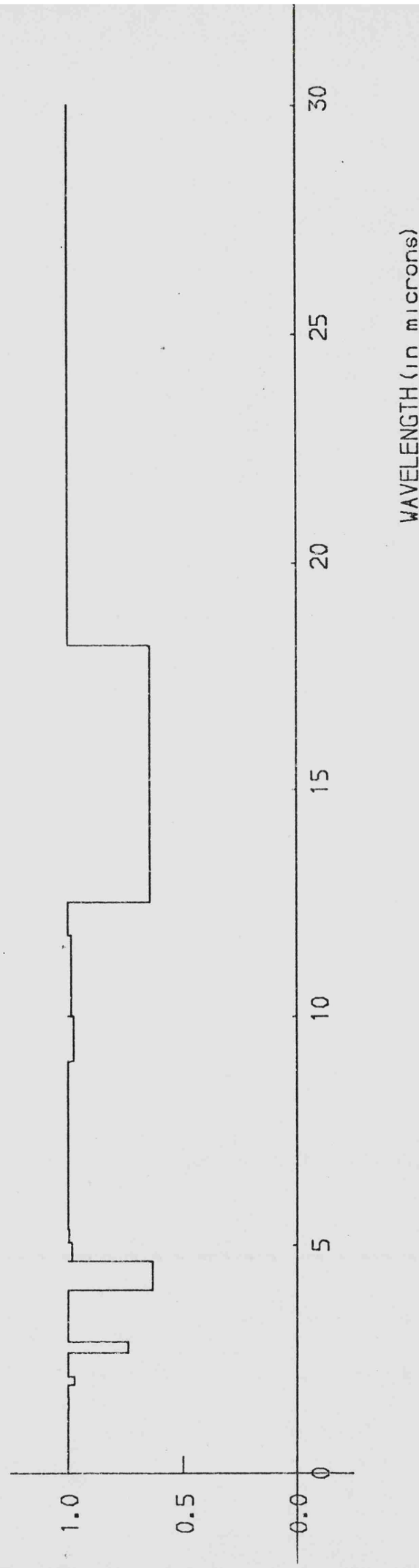
Table 4.5Empirical Parameters for All Carbon Dioxide Absorption Bands

BAND CENTRE (microns)	BAND LIMITS (cm <sup>-1</sup> )	C	d	k	C	D	K	TRANSITION VALUE $\int A_\nu d\nu$ (cm <sup>-1</sup> )
15	550-800	3.16	0.5	0.44	-68	55	47	50
10.4	850-1000	0.016	0.78	0.20	0	0	0	35
9.4	1000-1110	0.023	0.75	0.23	0	0	0	40
5.2	1870-1980	0.024	0.5	0.40	0	0	0	30
4.8	1980-2160	0.12	0.5	0.37	0	0	0	60
4.3	2160-2500	0	0	0	27.5	34	31.5	50
2.7	3480-3800	3.15	0.5	0.43	-137	77	68	50
2.0	4750-5200	0.492	0.5	0.39	-536	138	114	80
1.6	6000-6550	0.063	0.5	0.38	0	0	0	80
1.4	6650-7250	0.058	0.5	0.41	0	0	0	80

Figure 4.10

CO<sub>2</sub> ( P<sub>s</sub> = 1 mb ) TRUE SPECTRUM

TRANSMISSION



141.

Figure 4.11

CO<sub>2</sub> ( P<sub>s</sub> = 2 mb ) TRUE SPECTRUM

TRANSMISSION

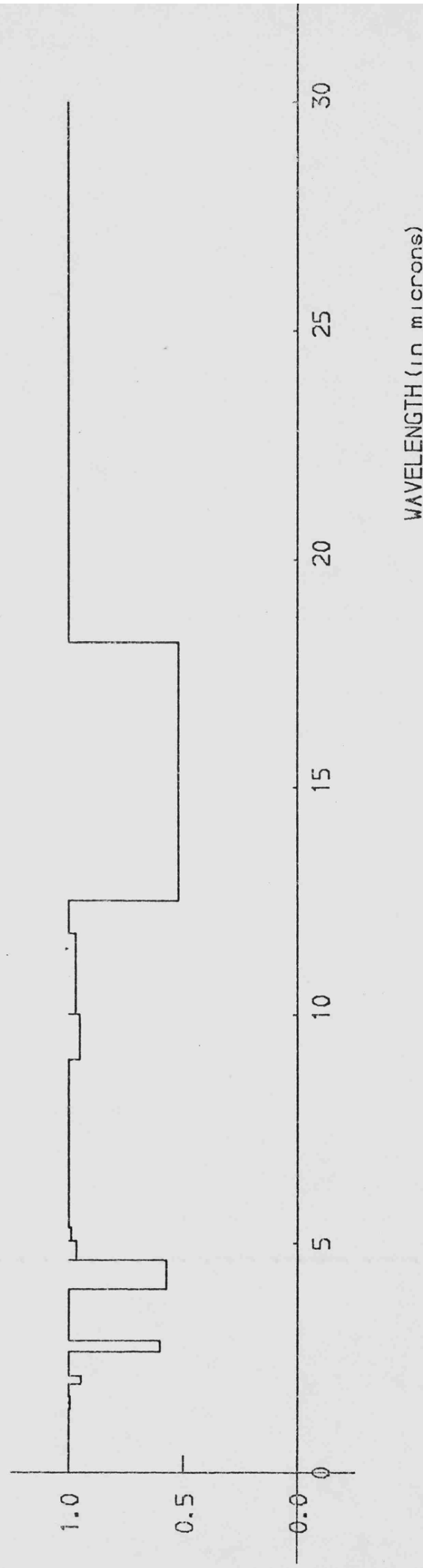
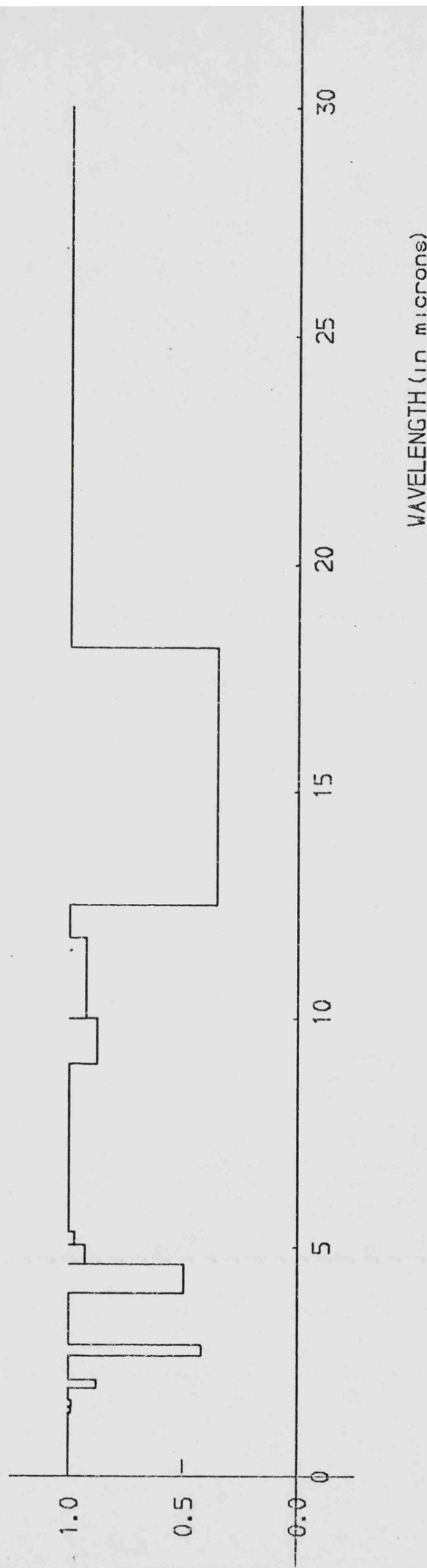


Figure 4.12

$\text{CO}_2$  ( $P_s = 5 \text{ mb}$ ) TRUE SPECTRUM

TRANSMISSION



143.

Figure 4.13

$\text{CO}_2$  ( $P_s = 10 \text{ mb}$ ) TRUE SPECTRUM

TRANSMISSION

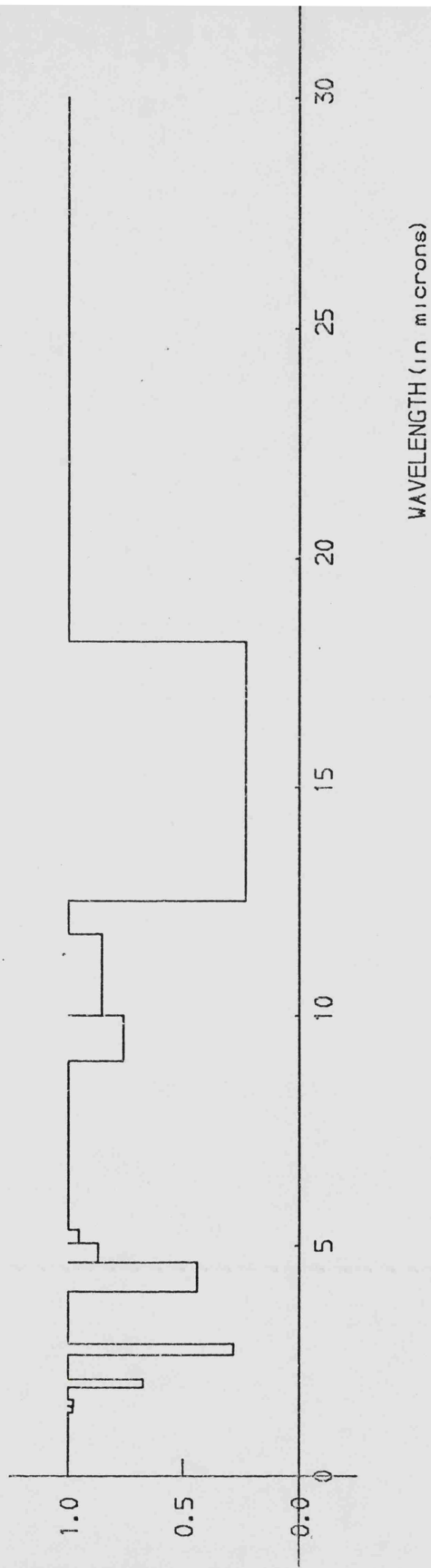


Figure 4.14

$\text{CO}_2$  ( $P_s = 20 \text{ mb}$ ) TRUE SPECTRUM

TRANSMISSION

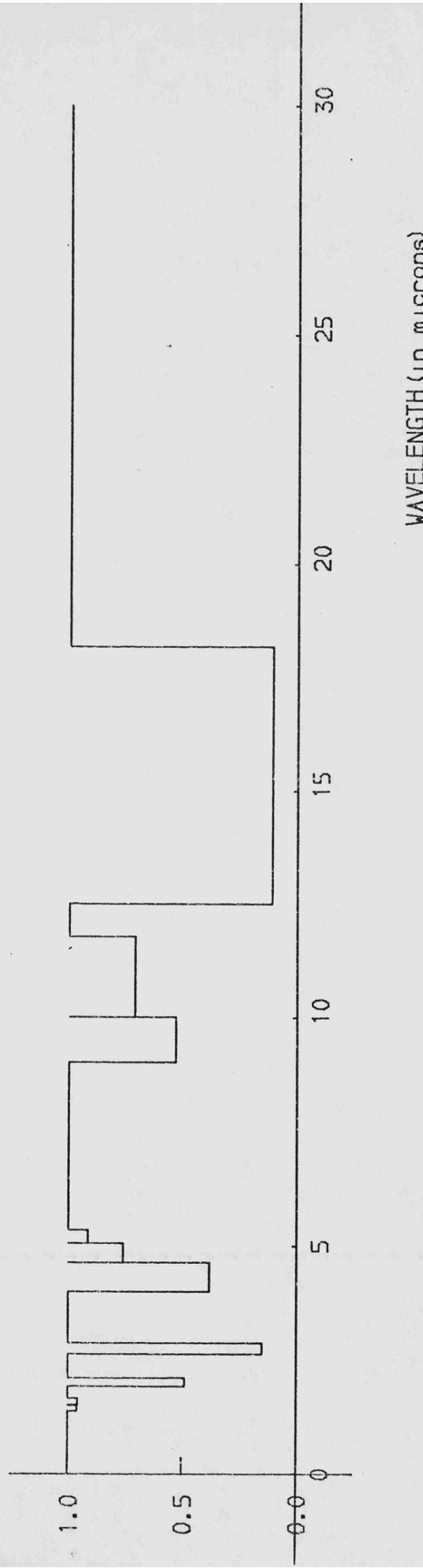


Figure 4.15

$\text{CO}_2$  ( $P_s = 50 \text{ mb}$ ) TRUE SPECTRUM

TRANSMISSION

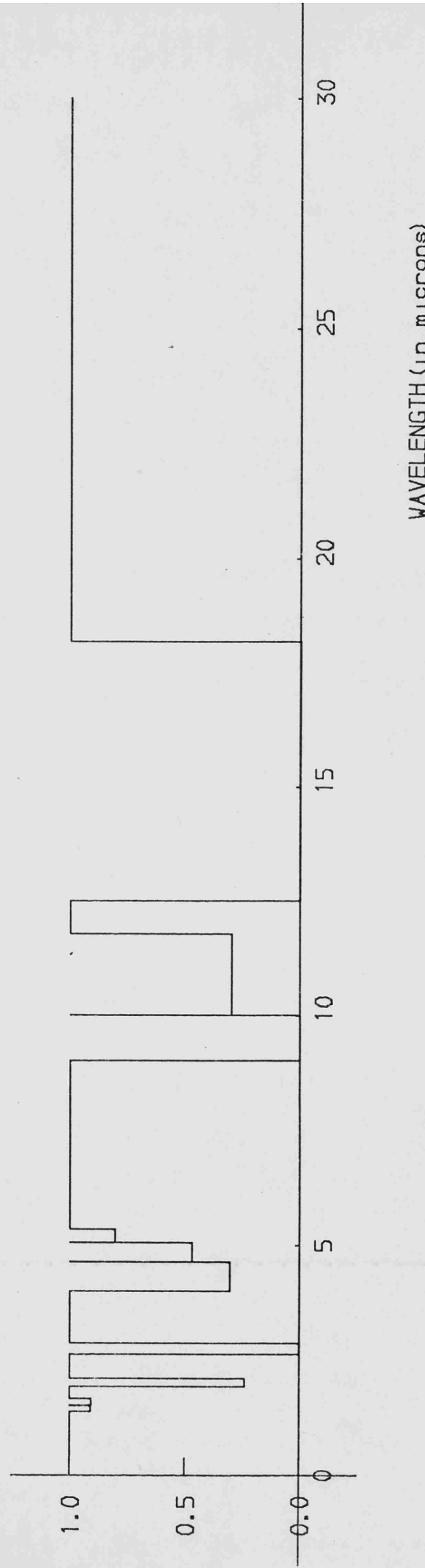


Figure 4.16

$\text{CO}_2$  ( $P_s = 100 \text{ mb}$ ) TRUE SPECTRUM

TRANSMISSION

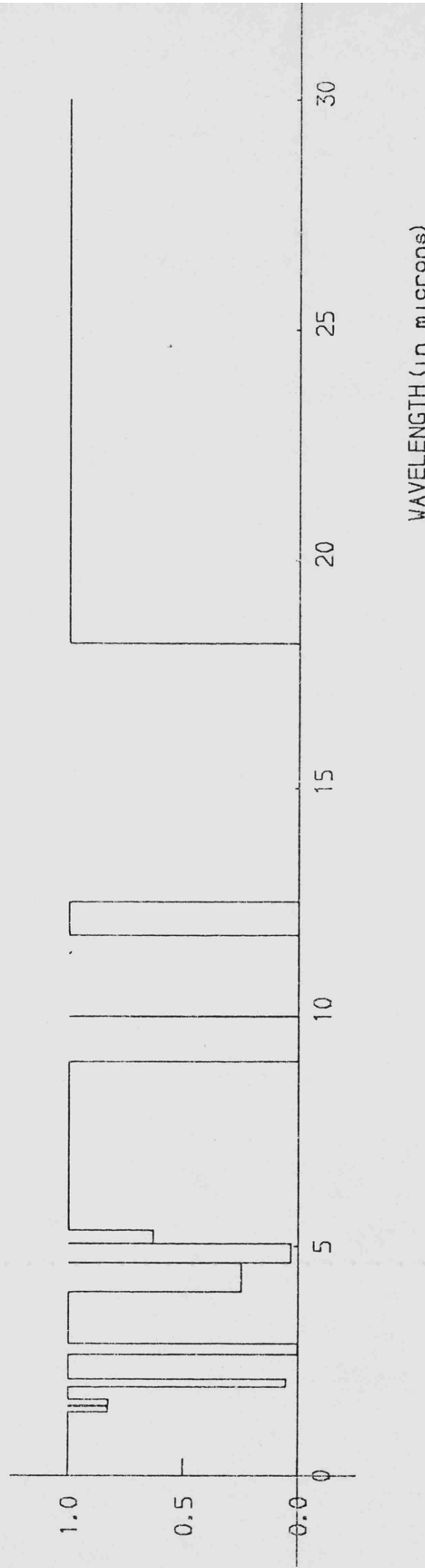


Figure 4.17

$\text{CO}_2$  ( $P_s = 1000 \text{ mb}$ ) TRUE SPECTRUM

TRANSMISSION

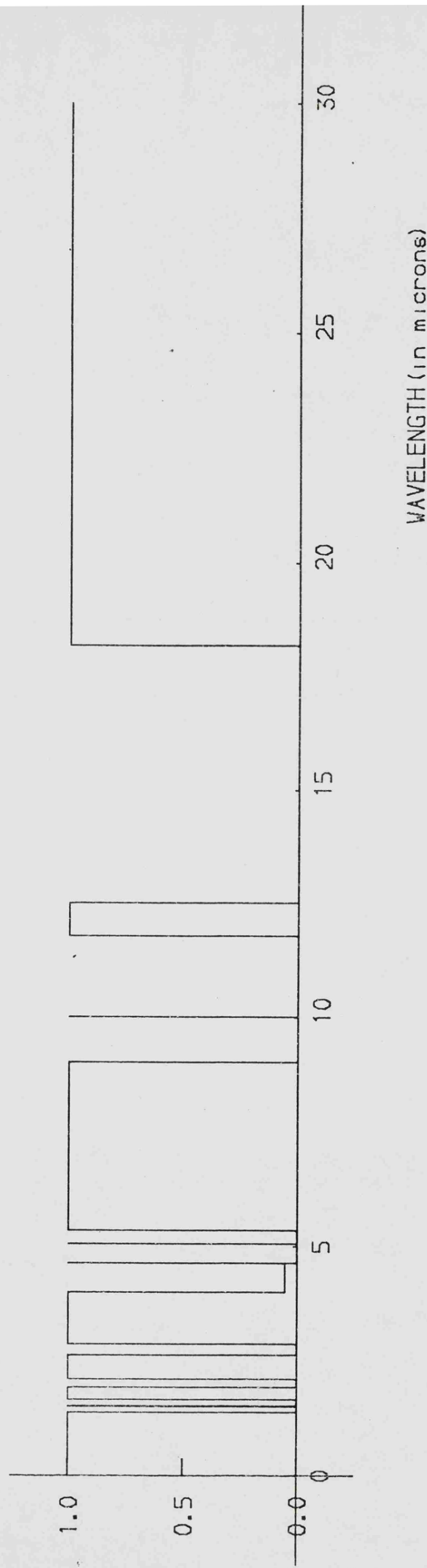
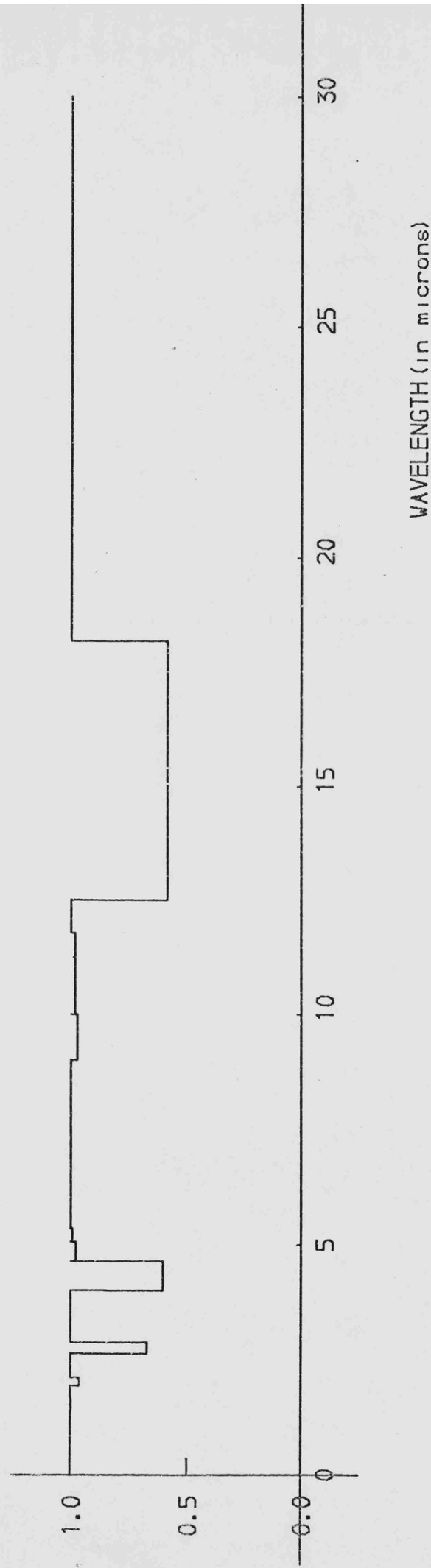


Figure 4.18

$\text{CO}_2$  (  $P_s = 1 \text{ mb}$  [absorber] + 2 mb [broadener] ) true spectrum

TRANSMISSION



The parameters which are required by the band model have been listed and typical spectra have been illustrated. These results will be utilized in Chapter 5 to produce surface temperatures for planets possessing pure carbon dioxide atmospheres and also combinations of carbon dioxide and other gases.

4.7 Water Vapour

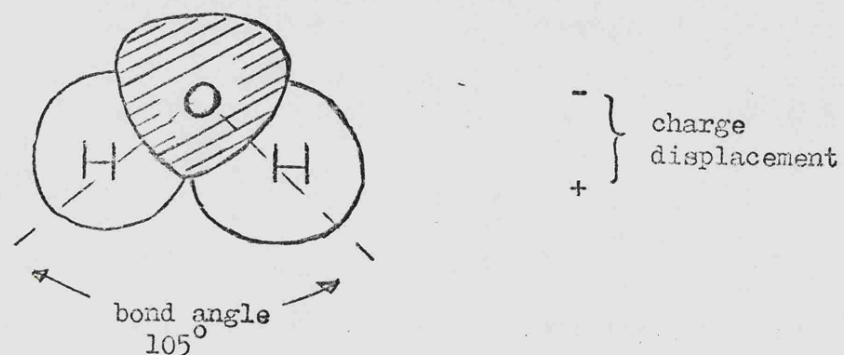
The presence of water vapour in a degassed terrestrial atmosphere has already been discussed in Sections 4.2 and 4.6. It is quite possible that more water vapour is emitted than any other gas. The small amount of water vapour in the atmosphere of the Earth (compared with nitrogen) is, of course, due to the condensation and freezing of water both into clouds and onto the surface. Figure 4.9 illustrated the saturated vapour pressure curves of both carbon dioxide and water vapour and from this it can be seen that in the temperature range 200 K to 300 K considerably less water vapour than carbon dioxide may be present in a typical atmosphere. Also the molecular weight of water vapour is less than that of carbon dioxide and thus the smaller influence of gravitational forces allows water molecules to rise higher in the atmosphere. In an early atmosphere, devoid of ozone, and thus open to energetic ultra-violet radiation some of the atmospheric water vapour will become photodissociated. The very light hydrogen atoms produced by this dissociation will escape from the atmosphere very readily. This escape mechanism, which is often invoked to account for the apparent lack of water vapour in the atmosphere of Venus, will be discussed further in Chapter 5. All these removal mechanisms will combine to limit the amount of water vapour in the atmosphere. Thus a typical terrestrial planetary atmosphere might be expected to consist primarily of carbon dioxide, but with the addition of up to approximately 50 millibars of water vapour. This amount of water vapour (although smaller than the carbon dioxide content) will

be very important in the heat balance of the atmosphere. The early evolution of all the terrestrial planetary atmospheres may have been controlled by spatial location and phase of the degassed water vapour. This is because the albedo (and thus the solar radiation input to the planetary surface) is a function of both the cloud amount and the areal extent of ice and snow cover (as already discussed in Chapter 3) and also because the role of clouds (particularly water clouds) is believed to be of importance to the radiation balance of the atmosphere even though the feedback mechanisms are not yet well understood. The possible nature of these mechanisms and their effects upon the surface temperature will be commented upon in Chapter 5.

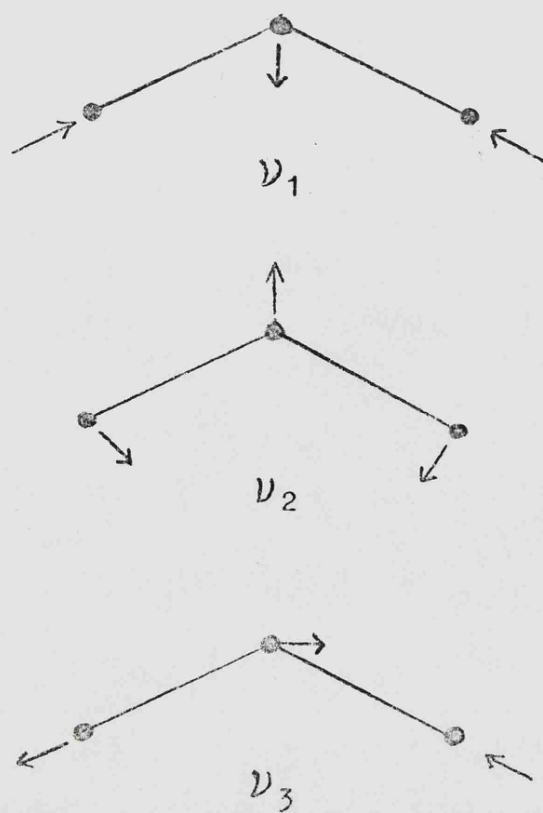
The aim of this chapter is to study the effect of differing amounts of gases in the atmosphere upon the surface temperature. Thus although the presence of water in either its liquid or solid phase is important as a parameter in a heat balance calculation it is also a direct indication of the presence of water vapour in the atmosphere since the solid or liquid form, open to the atmosphere, must be buffered by the saturated vapour pressure of water vapour in the atmosphere. Since the tropospheric temperature will fall off with height there is an approximate upper limit to the amount of water vapour in the atmosphere, given by the saturated vapour pressure, for the surface temperature. Thus an average value for the total water vapour of a vertical path through the Earth's atmosphere is 3 precipitable centimetres, but in the tropics the value can rise as high as 30 precipitable centimetres.

Figure 4.19

Structure of the water vapour molecule.



Fundamental vibrations of the water molecule.



The effect of water vapour in the atmosphere depends upon its infrared absorption characteristics. These are a function of the molecule, itself, and of the absorber amount. The water vapour molecule is an asymmetric triatomic molecule, as is illustrated in Figure 4.19, with a bond angle of  $105^{\circ}$  and three unequal, non-zero moments of inertia. It possesses a permanent charge displacement, giving rise to a dipole moment. The molecule has both a pure rotation spectrum and a highly complex vibration/rotation spectrum. The rotation band will be discussed in the following paragraphs. The vibrational modes are also illustrated in Figure 4.19; the bending vibration  $\nu_2$  having the lowest frequency and the  $\nu_1$  and  $\nu_3$  modes having approximately twice this frequency. This coincidence leads to complex combination bands, particularly around 2.7 microns. The  $\nu_2$  fundamental at 6.3 microns is important: of lesser importance are the higher frequency combination bands around 1 micron. The vibration/rotation spectrum is further complicated by the presence of a number of isotopic species. In particular, the  $\text{HDO}^{16}$  molecule has completely different vibration/rotation band centres from the  $\text{H}_2\text{O}^{16}$  molecule. Table 4.6 lists the frequencies of the fundamentals for both these molecules.

The band of  $\text{HDO}^{16}$ , due to the  $\nu_1$  fundamental, centred at approximately 3.7 microns was found to be strong enough to warrant individual study and parameterization in the work by Howard, Burch and Williams (1956). As well as the  $\text{HDO}^{16}$  molecule there are also two other isotopic forms of water found in the Earth's atmosphere. The spectra of the  $\text{HHO}^{17}$  and  $\text{HHO}^{18}$

Table 4.6Frequencies of Fundamentals of HHO<sup>16</sup> and HDO<sup>16</sup> Molecules

BAND	BAND CENTRE (cm <sup>-1</sup> )	
	HHO <sup>16</sup>	HDO <sup>16</sup>
$\nu_1$	3657.05	2723.66
$\nu_2$	1594.78	1403.3
$\nu_3$	3755.92	3707.47

molecules are much more closely related to that of the usual form of water vapour than the HDO<sup>16</sup> molecule and the variations caused amount to only a shift of up to 11 cm<sup>-1</sup> in band centre frequency. Water vapour in the atmosphere is also responsible for two other regions of absorption in the infrared. Between 8 microns and 12.5 microns there is weak continuum absorption which was believed to follow Lambert's law. More recently (Hunt and Mattingly, 1976) it has been confirmed that the water vapour dimer (H<sub>2</sub>O)<sub>2</sub> causes some of this absorption. Dimer absorption is also responsible for spectral features in the far infrared/submillimetre region. The complexity of the infrared spectrum and the importance of water vapour absorption in the Earth's atmosphere has led to much detailed observation of its absorption characteristics.

Since the theme of this work is the calculation of general trends in atmospheric absorption with varying absorber amount the aim has been to construct a simplified representation of the band structure. For the near infrared this has been performed by Howard, Burch and Williams (1956), but the far infrared pure

rotation bands were found to be highly complex. The representation used by Burch and his co-workers (1962) has been described in detail in Section 4.4. It gives the total band absorption (either weak or strong) in terms of the absorber amount,  $w$ , (in precipitable centimetres for water vapour) and the effective pressure,  $P_e$ , which is given by Equation 4.11. For water vapour, the broadening coefficient ' $B_c$ ' has been assigned the value 2. The total absorption is expressed in terms of the parameters already discussed in Equations 4.12 and 4.13. Table 4.7 below lists the values of the parameters for the vibration/rotation bands studied by Howard, Burch and Williams (1956).

These parameters permit the calculation of the total absorption of each of the bands listed. The exponential representation described in Section 4.5 permits the calculation of total absorption for values of absorber concentration higher than those originally studied. From the total absorption values, a fractional transmission spectrum can be derived for each value of the absorber concentration and total pressure,  $P$ . This form of calculation of the vibration/rotation structure of water vapour is particularly useful as it relates the variation in band absorption directly to the variation in both the water vapour amount and the total gas pressure. Thus the effect of addition of water vapour to an already established carbon dioxide atmosphere may be readily considered. This will be discussed in Chapter 5.

The rotation band of water vapour is of the utmost importance in the calculation of the "greenhouse" effect, since

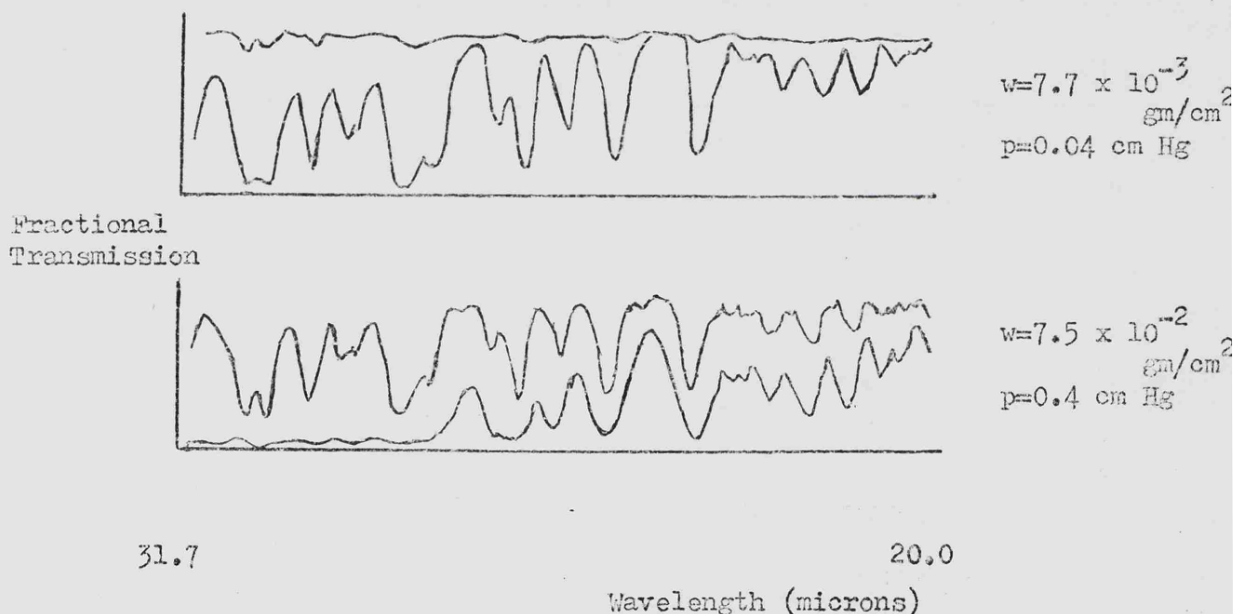
Table 4.7

Empirical Parameters for All Water Vapour Absorption Bands

(except the pure rotation band)

BAND CENTRE (microns)	BAND LIMITS ( $\text{cm}^{-1}$ )	C	d	K	C	D	K	TRANSITION VALUE $\int A_\nu d\nu$ ( $\text{cm}^{-1}$ )
6.3	1150-2050	356	0.5	0.30	302	218	157	160
3.7 (HDO)	2670-2770	0.325	0.5	0.37	0	0	0	-
3.2	2800-3340	40.2	0.5	0.30	0	0	0	500
2.7	3340-4400	316	0.5	0.32	337	246	150	200
1.87	4800-5900	152	0.5	0.30	127	232	144	275
1.38	6500-8000	163	0.5	0.30	202	430	198	350
1.1	8300-9300	31	0.5	0.26	0	0	0	200
0.94	10100-11500	38	0.5	0.27	0	0	0	200

Figure 4.20



Complex dependence of the features of the rotation band of water vapour upon absorber amount,  $w$ , partial pressure,  $p$ , and total pressure. The values of  $w$  and  $p$  are given beside the spectra - the upper curve on each spectrum is for the pure absorber and the lower curve is for the absorber plus 60 mm Hg of a neutral gas. (after Goody, 1964)

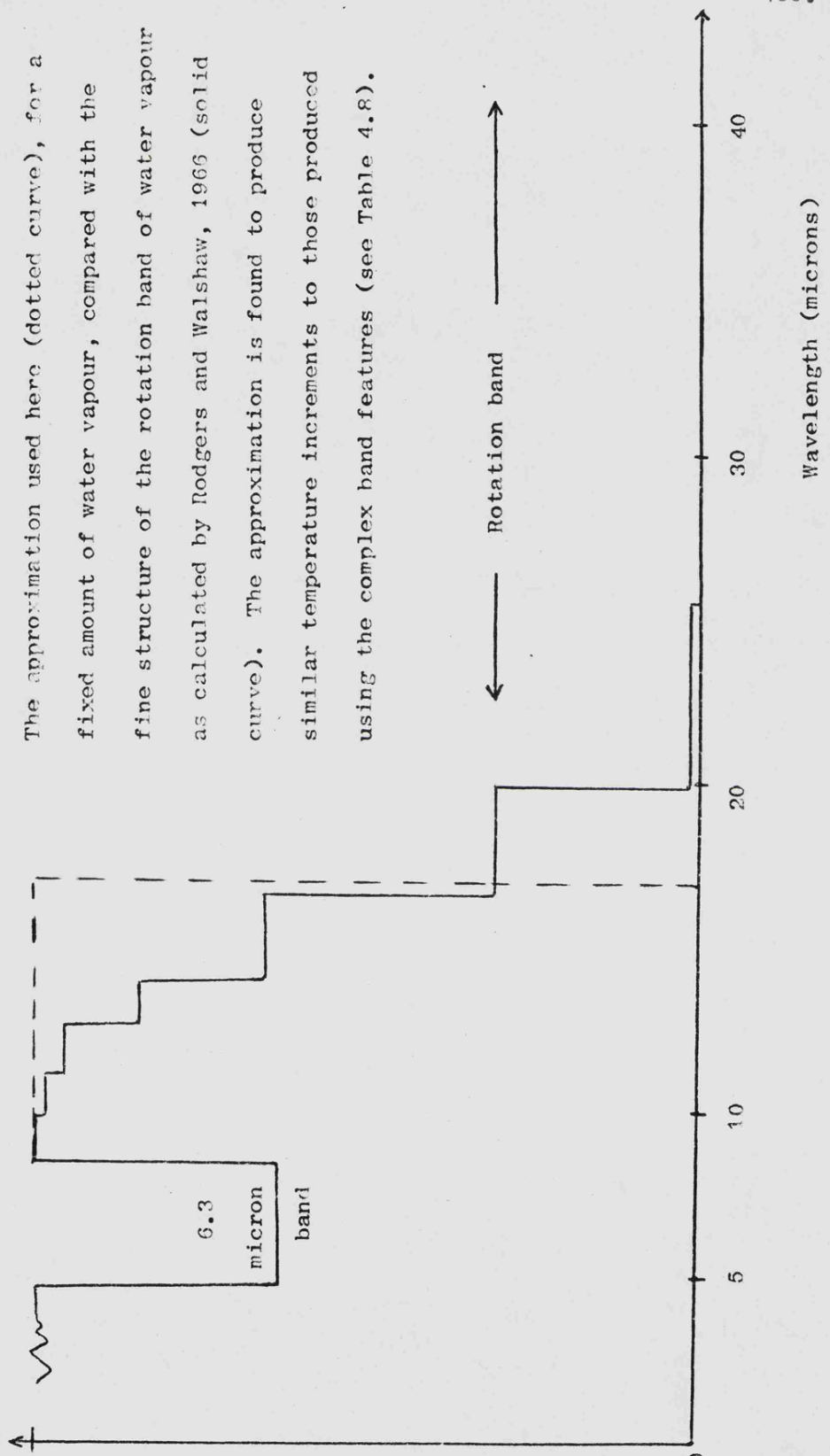
it determines the cut-off point in transmission by an atmosphere containing only a small amount of water vapour. It may overlap the strong 15 micron band of carbon dioxide in atmospheres containing large amounts of both CO<sub>2</sub> and H<sub>2</sub>O vapour.

Unfortunately, the structure of the rotation band is highly complex and its variation with temperature as well as partial pressure of the absorber and total gas pressure is less easily modelled than that of the other bands considered here. (The variation of absorption with temperature has been small enough to be ignored for all the other spectra considered.) The dependence upon absorber amount and gas pressure is illustrated by Figure 4.20 which shows the observed variation of transmission with wavenumber for the shorter wavelength region of the band. No simple representation seemed appropriate for this absorption region, but as the treatment of the other bands of water vapour and other absorbers had not been rigorous it seemed unreasonable to utilize complex (and time-consuming) modelling for this region of the spectrum alone.

To solve this problem it was decided to fit an empirical representation to a much more complex model devised by Rodgers and Walshaw in 1966. In this model they used data from unpublished work by Benedict and Kaplan which had been tabulated by Goody (1964). Their model enabled them to calculate the transmission through an atmosphere containing varying amounts of water vapour and to consider the fine structure of the rotation band by dividing it into ten regions by wavelength. Figure 4.21 illustrates the type of transmission features produced by their

Figure 4.21

The approximation used here (dotted curve), for a fixed amount of water vapour, compared with the fine structure of the rotation band of water vapour as calculated by Rodgers and Walshaw, 1966 (solid curve). The approximation is found to produce similar temperature increments to those produced using the complex band features (see Table 4.8).



calculations. This complex structure was approximated by the modification shown as a dotted line and discussed below.

To allow surface temperature calculations to proceed with reasonable accuracy it was decided to model the rotation band of water vapour longwave of approximately 11 microns by one band only. This band would be considered as fully absorbed and would extend to wavelengths beyond which the outgoing thermal flux from the planetary surface was negligible. Thus only the starting point of this fully absorbed region was allowed to vary with absorber amount. This variation was computed by comparing surface temperatures produced by a calculation using the accurate model of Rodgers and Walshaw (1966) with a calculation using the approximation (starting at a chosen wavelength) for the same absorber concentration. The correlation between these two sets of calculations is indicated in Table 4.8 below.

Table 4.8

Comparison of Temperature Increments Calculated by Approximate Model and by Rodgers and Walshaw (1966)

	<u>Water Vapour Partial Pressure</u>		
	0.1 mb	1 mb	10 mb
Temperature increment-complex model	12.0 K	22.1 K	37.8 K
Approximate cut-off point	$20\mu$	$16\mu$	$13.5\mu$
Temperature increment-approximation	11.8 K	22.2 K	38.3 K

Figure 4.22

$H_2O$  ( $P_s = 0.01 \text{ mb}$ ) TRUE SPECTRUM

TRANSMISSION

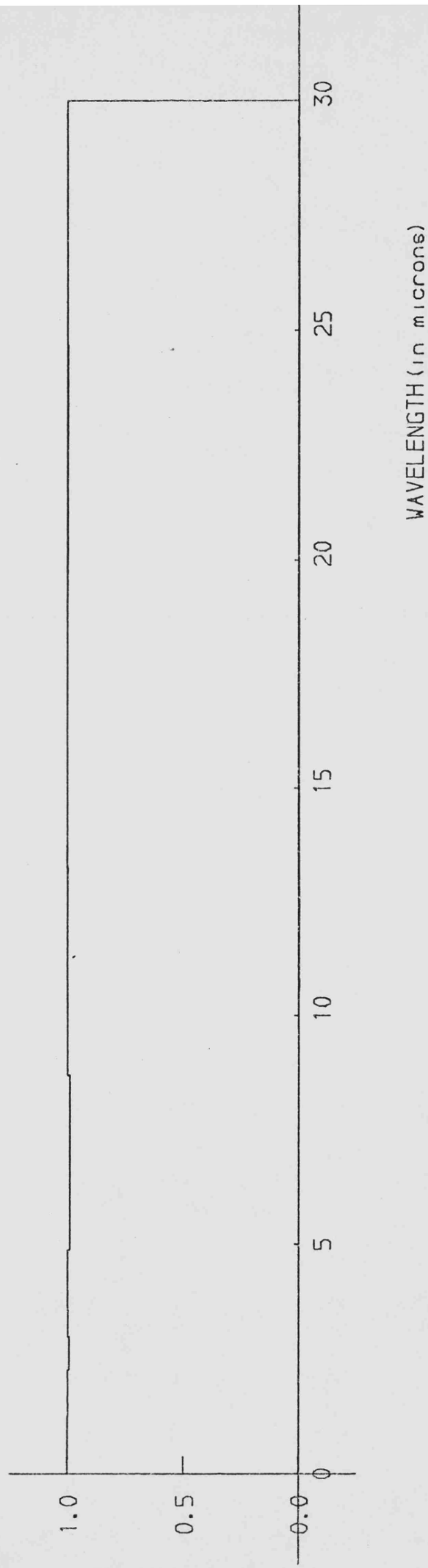


Figure 4.23

$H_2O$  ( $P_s = 0.1 \text{ mb}$ ) TRUE SPECTRUM

TRANSMISSION

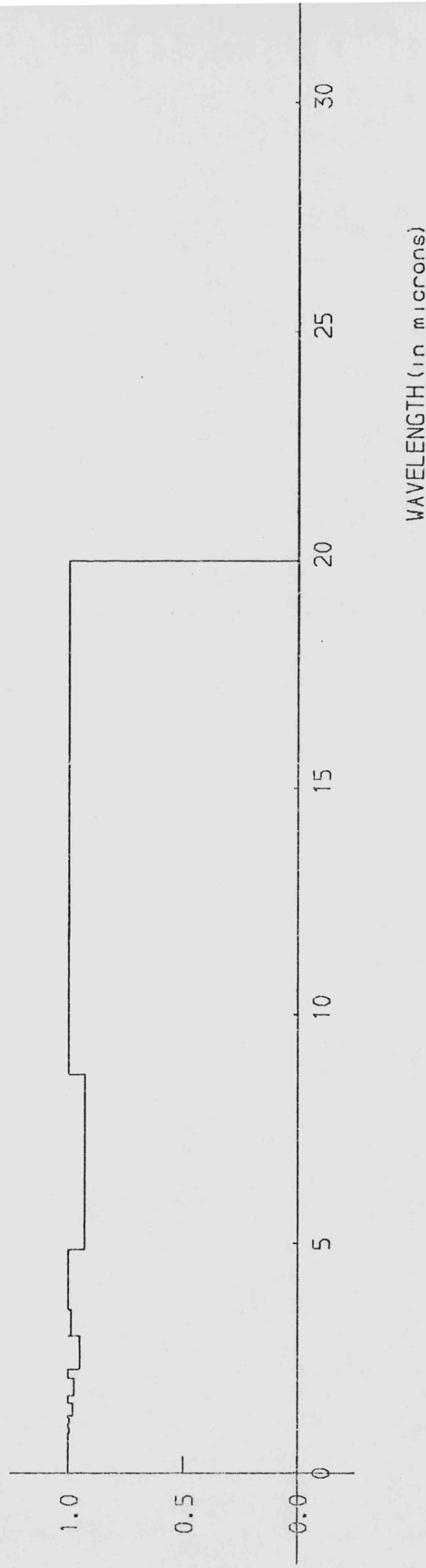


Figure 4.24

H<sub>2</sub>O ( P<sub>s</sub> = 1 mb ) TRUE SPECTRUM

TRANSMISSION

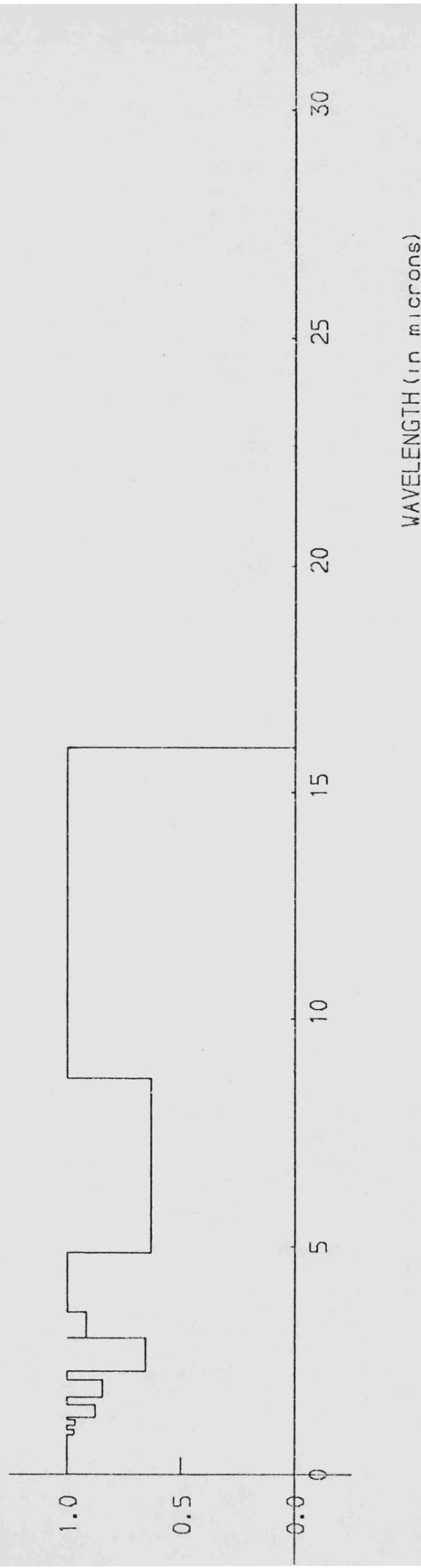


Figure 4.25

$H_2O$  ( $P_s = 2 \text{ mb}$ ) TRUE SPECTRUM

TRANSMISSION

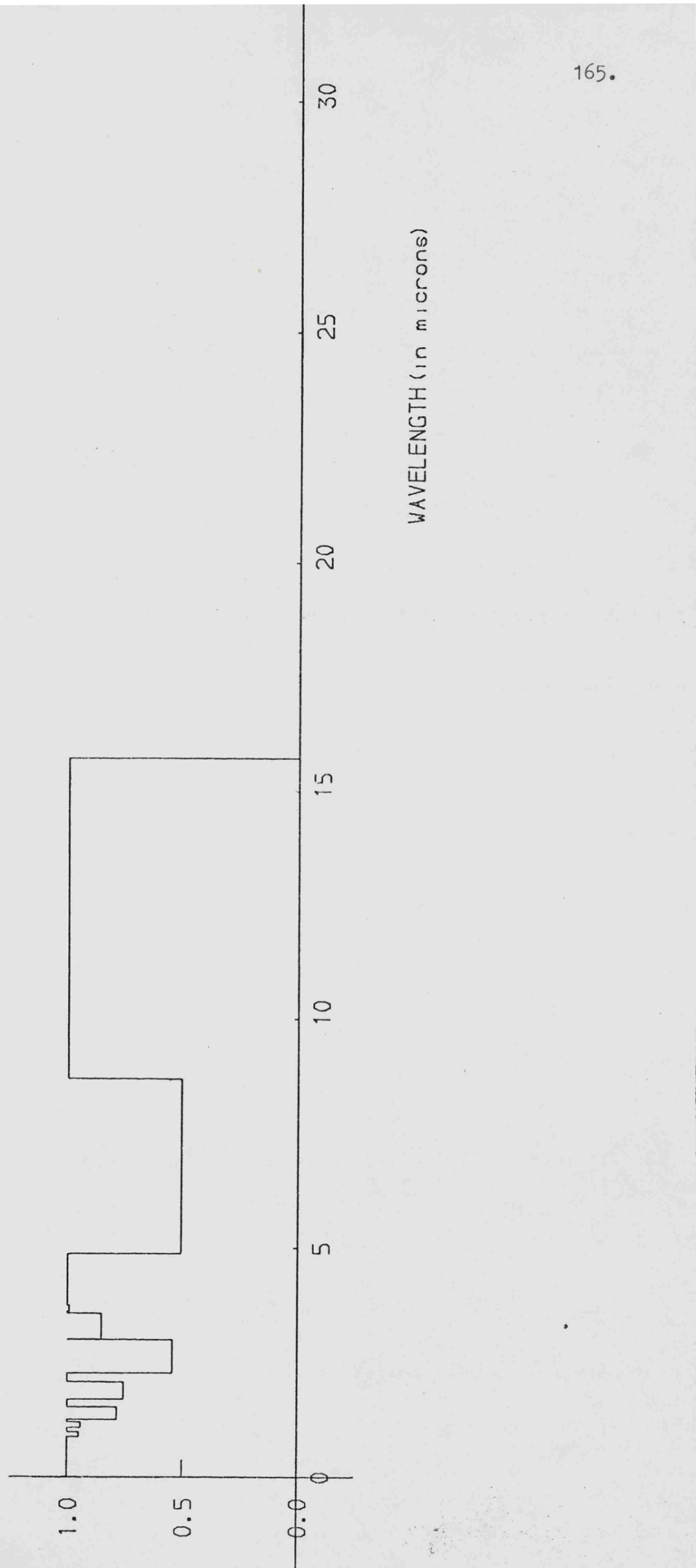


Figure 4.26

H<sub>2</sub>O ( P<sub>s</sub> = 5 mb ) TRUE SPECTRUM

TRANSMISSION

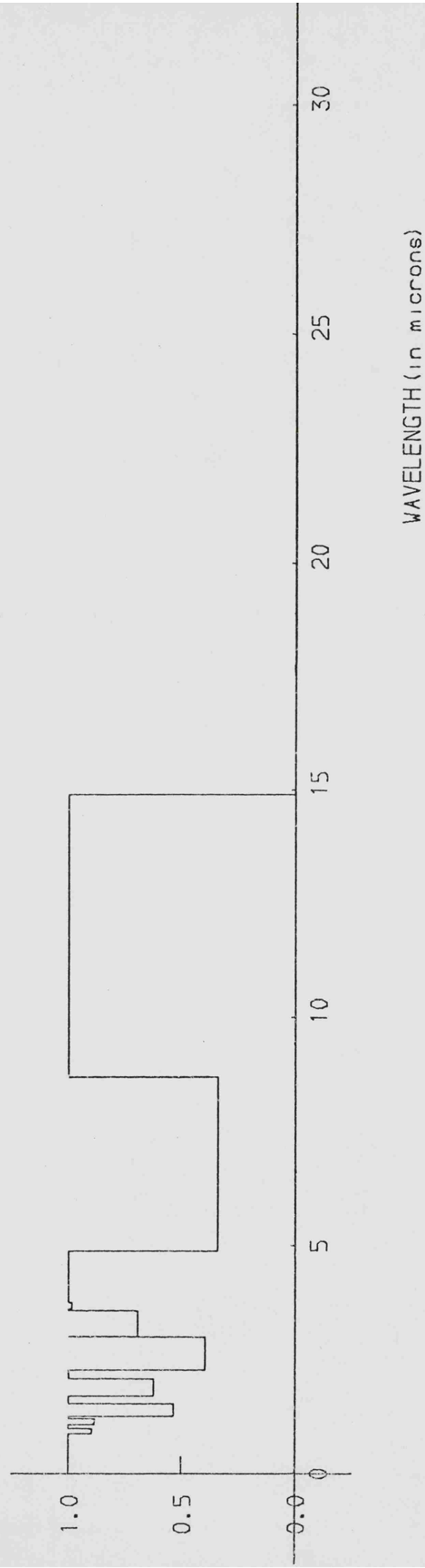


Figure 4.27

$H_2O$  ( $P_s = 10$  mb) TRUE SPECTRUM

TRANSMISSION

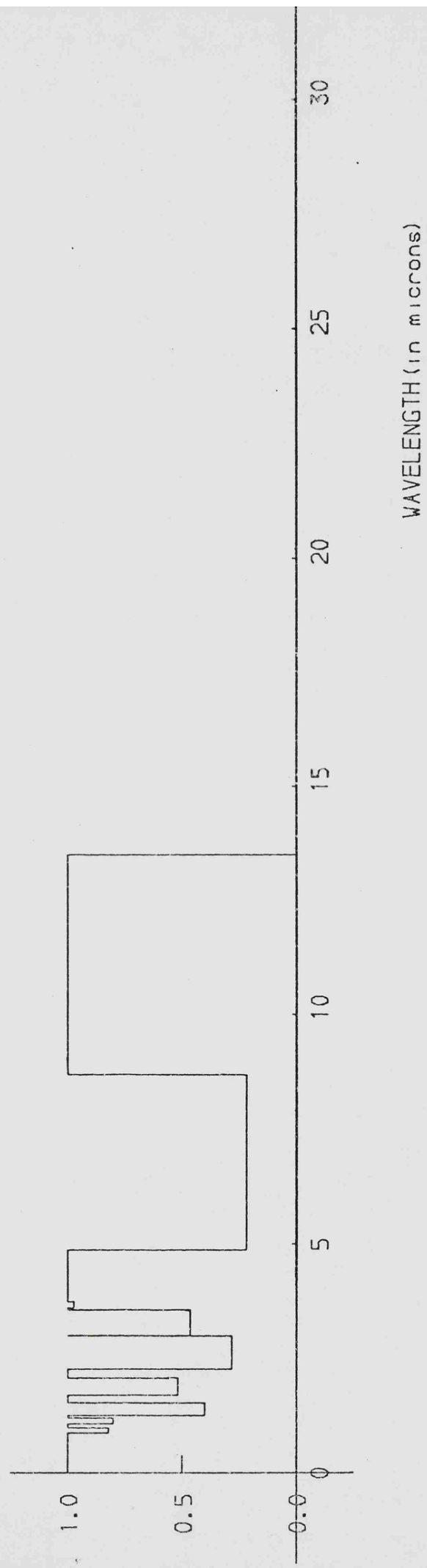


Figure 4.28

$H_2O$  ( $P_s = 20 \text{ mb}$ ) TRUE SPECTRUM

TRANSMISSION

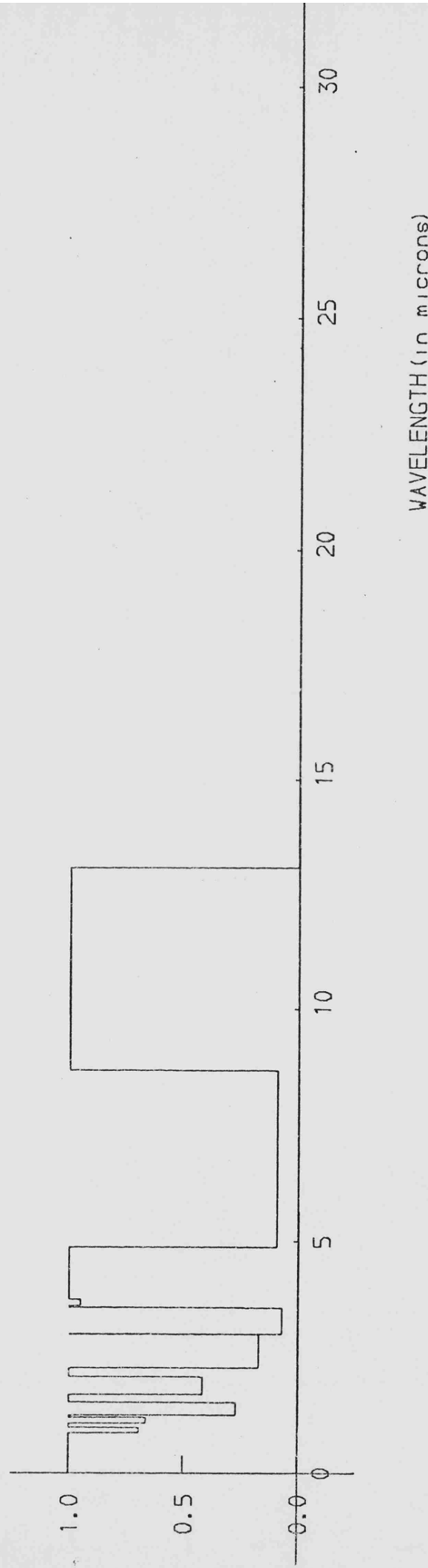
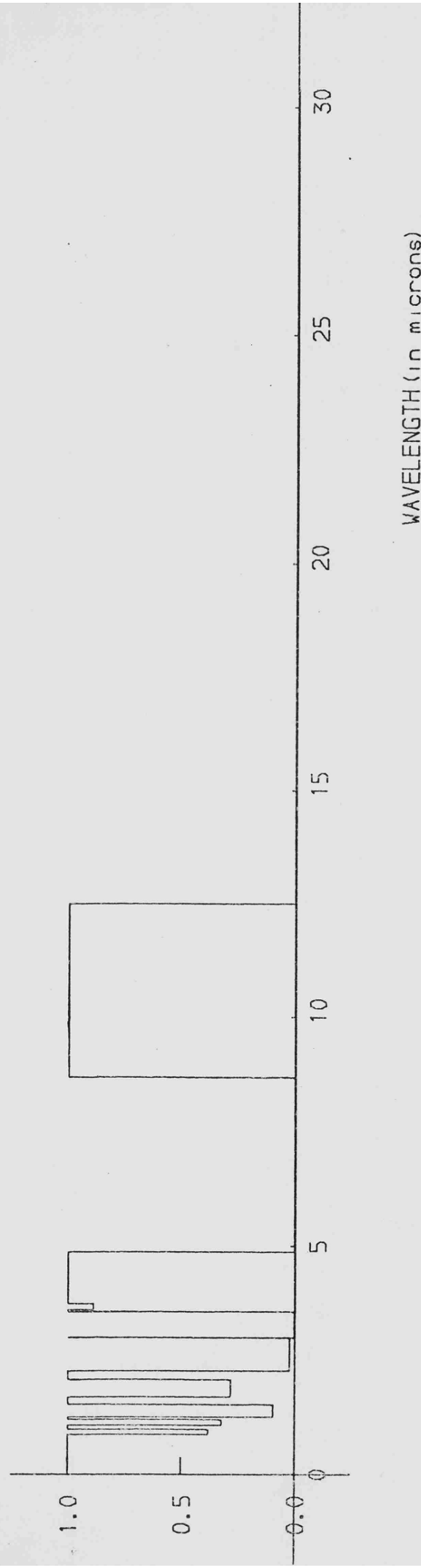


Figure 4.29

H<sub>2</sub>O ( P<sub>s</sub> = 50 mb ) TRUE SPECTRUM

TRANSMISSION



The weak and strong band representations for the vibration/rotation bands together with the approximate model described above for the rotation band permitted the calculation of absorption characteristics for varying amounts of water vapour. The exponential parameterization described in Section 4.5 was used when the absorption curve was required for amounts of water vapour outside the ranges studied in the laboratory experiments by Burch and his co-workers (1962). As there was no weak or strong representation of absorption for the rotation band, however, it was impossible to fit an exponential curve. This is the reason for the first entry in the water vapour column of Table 4.3 in Section 4.5 which is chosen arbitrarily to give one hundred per cent absorption from the wavelength indicated and is thus consistent with the model used for the rotation band.

These models have been combined to produce fractional transmission spectra for varying amounts of water vapour as illustrated by Figures 4.22 to 4.29. The absorption features due to water vapour may be calculated using the models described in this section and the effects of combining water vapour with other absorbing and non-absorbing gases will be discussed in detail in Chapter 5.

#### 4.8 Other Absorbers

In Sections 4.6 and 4.7 of this chapter the absorption characteristics of carbon dioxide and water vapour have been discussed in detail. The model atmospheres which will be considered in Chapter 5 and for which surface temperatures are to be computed will be assumed to be carbon dioxide atmospheres. The addition of different amounts of water vapour will depend upon the degassing rates, mixing ratios of the gases and the surface temperatures. However, it is possible that the evolution of the atmospheres and surface temperatures of some of the terrestrial planets could have been influenced by the addition to the atmosphere of other gases possessing strong infrared absorption features. This section will discuss the possibility of the occurrence of other absorbers and also consider two of them in detail.

The degassing of an atmosphere around a terrestrial planet was discussed in Section 4.2 and it was noted there that the chemical nature of the gases evolved from the surface may depend upon the state of differentiation of the planet. Thus prior to the removal of iron from the mantle of the Earth the gases passing through these surface rocks may have become chemically reduced. The postulate of an early, reduced atmosphere has been supported by the belief that the origin of life required a highly reducing atmospheric environment. It is supposed that the Earth's atmosphere must have passed from this early reduced state, through some intermediate phase to its present-day oxidized state. Such a model was described in detail by Holland (1962) and Table

4.9 lists the gases he suggests were present during each phase.

Table 4.9  
Postulated Atmospheric Evolutionary Stages and  
Gaseous Constituents (after Holland, 1982)

	Stage 1	Stage 2	Stage 3
Major components ( $P > 10^{-2}$ atm)	CH <sub>4</sub> H <sub>2</sub> (?)	N <sub>2</sub>	N <sub>2</sub> O <sub>2</sub>
Minor components ( $10^{-4} < P < 10^{-2}$ atm)	H <sub>2</sub> (?) H <sub>2</sub> O N <sub>2</sub>	H <sub>2</sub> O CO <sub>2</sub> Ar	Ar H <sub>2</sub> O CO <sub>2</sub>
Trace components ( $10^{-6} < P < 10^{-4}$ atm)	He	Ne He CH <sub>4</sub> NH <sub>3</sub> (?) SO <sub>2</sub> (?) H <sub>2</sub> S (?)	Ne He CH <sub>4</sub> Kr

However more recent investigations have revealed the fact that prebiotic molecules may readily be built in an atmosphere containing H<sub>2</sub>O, N<sub>2</sub>, CO<sub>2</sub> and CO. Observations of complex organic molecules in interstellar space may also indicate that the highly reducing conditions originally postulated are unnecessary.

Indeed, the evidence for liquid water on the Earth seems to imply that not only was there water vapour in the atmosphere, but also that the amount of other efficient infrared absorbers (particularly ammonia) must have been very small. Even the apparently small mixing ratios of ammonia postulated by Sagan and Mullen (1972) give surface temperatures much too high for the condensation of water onto the Earth's surface, when appropriate values of the other parameters (e.g. albedo) are used. There is a further reason why large amounts of ammonia cannot have been present after the formation of the oceans on the Earth and this is the very high solubility of ammonia.

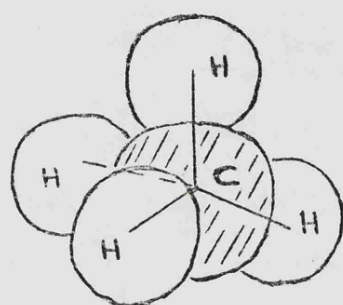
The data, for the Earth, seem to indicate that the early atmosphere resembled that of the present day and the general feeling (reported, recently, by Margulis, 1976) of both atmospheric scientists and geologists is in favour of a gradual evolution rather than the violent fluctuations of both pressure and chemical state previously postulated. It has already been noted that the degassed atmospheres of the other terrestrial planets may differ from that of the Earth because of differences in planetary mass, surface chemistry and solar distance. However, it seems reasonable to postulate that a typical degassed sample would provide carbon dioxide and water vapour and this is the way in which the model atmospheres discussed in Chapter 5 will be developed. The possibility of an atmosphere around a terrestrial planet composed predominantly of hydrogen and ammonia will not be considered. However there are gases present in the Earth's atmosphere today which contribute to the complex infrared

absorption features (see Section 4.2 and particularly Figure 4.1).

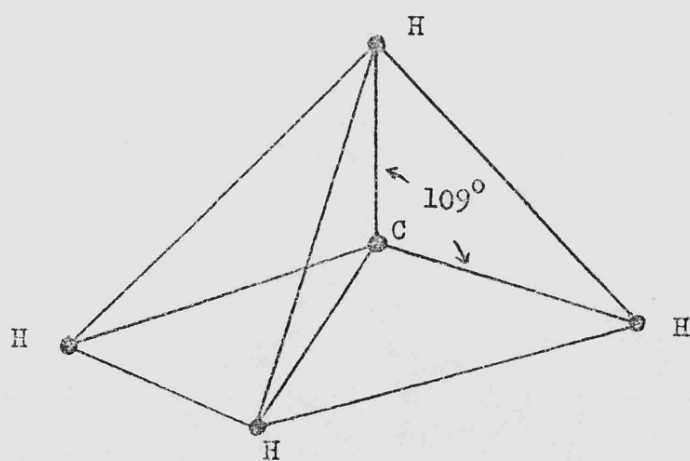
Two gases have been chosen for further study in this work; methane and carbon monoxide. They were chosen for a number of reasons which will be discussed in the following paragraphs. It should be noted that the computer model can incorporate any gas (absorbing or neutral) if adequate data are available and secondly that no attempt has been made in this study to use the extension described in Section 4.5 for these gases since it was felt that they were unlikely to be the dominant gases in the atmospheres considered.

Methane (the simplest organic compound) is formed by the covalent bonding of one carbon atom with four hydrogen atoms. It is readily formed in an oxygen-depleted environment. Thus it could form a non-negligible percentage of an early reduced degassing episode and possibly persist long enough to be significant. Methane is also produced within the "biosphere" on Earth as a product of anaerobic fermentation in both the soil and the oceans and persists as a trace gas in the Earth's atmosphere (see Table 4.1). Indeed it has been suggested that the simultaneous presence of methane and oxygen in the atmosphere of a planet may be an indication of a life-system operating on the surface. It has, however, been pointed out by several authors that methane can be produced by geochemical reactions as discussed by alone (e.g. Lovelock, 1975). The amount of methane in a carbon dioxide/water vapour atmosphere is unlikely to be great and thus the only contribution to the thermal balance of the planetary surface likely to be made is the addition of absorption in regions

Figure 4.30



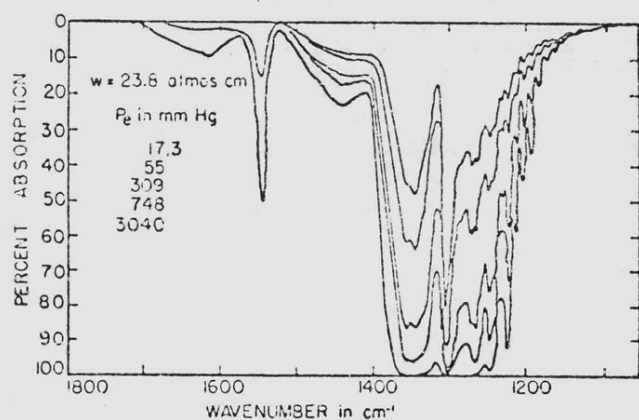
Structure of the methane molecule.



of the infrared not already dominated by bands due to other absorbers.

The infrared spectrum of methane is determined by the atomic configuration within the molecule (illustrated in Figure 4.30). The molecule is a spherical top. The hydrogen atoms are symmetrically placed around the carbon atom; thus there is no charge separation and hence no permanent dipole moment. It therefore has no rotational spectrum. The vibration spectrum has fundamentals  $\nu_1$  at 3.43 microns ( $2914.2 \text{ cm}^{-1}$ ),  $\nu_2$  at 6.55 microns ( $1526 \text{ cm}^{-1}$ ),  $\nu_3$  at 3.31 microns ( $3020.3 \text{ cm}^{-1}$ ) and  $\nu_4$  at 7.66 microns ( $1306.2 \text{ cm}^{-1}$ ) although only the  $\nu_3$  and  $\nu_4$  fundamentals are strong enough to be of importance in infrared studies for the terrestrial planets. Other bands (e.g.  $3\nu_3$  at 1.1 micron) of methane are very important in the study of the atmospheres of the Jovian planets. The coincidence that  $2\nu_2 \approx \nu_1 \approx \nu_3$  adds to the complexity of the absorption features. Both the regions of absorption considered here occur on the edge of window regions in the  $\text{H}_2\text{O} + \text{CO}_2$  spectrum and thus may be important for the thermal balance calculation. The data are derived from measurements made by Burch and his co-workers (1962). The measurements were made in two distinct spectral regions: between  $3400 \text{ cm}^{-1}$  and  $2200 \text{ cm}^{-1}$ , called the 3.3 micron band and between  $1750 \text{ cm}^{-1}$  and  $1100 \text{ cm}^{-1}$ . Almost all the absorption of interest in atmospheric studies occurs within these two regions although as Figure 4.31 illustrates the latter region incorporates both the strong  $\nu_4$  fundamental and the much weaker  $\nu_2$  fundamental. In the laboratory experiments this region was

Figure 4.31



Spectral absorption of  $\text{CH}_4$  in the vicinity of its strong  $\nu_4$  fundamental at  $1306 \text{ cm}^{-1}$  and its weak  $\nu_2$  fundamental near  $1534 \text{ cm}^{-1}$ .

arbitrarily divided at  $1535 \text{ cm}^{-1}$ . The region from  $1100 \text{ cm}^{-1}$  to  $1535 \text{ cm}^{-1}$  incorporating absorption due to both the  $\nu_4$  fundamental and due to the P-branch of the  $\nu_2$  fundamental was called the 7.7 micron band and the rest of the region was neglected.

Empirical relations linking the total absorption over the two band regions to the absorber concentration,  $w$ , and the effective pressure,  $P_e$ , were derived in the same form as those already described for carbon dioxide and water vapour. They are given by Equations 4.12 and 4.13 in Section 4.4 and the effective pressure,  $P_e$ , is given by Equation 4.11. Now for methane the best values of the broadening coefficient,  $B_c$ , were found to be

$$B_c = 1.30 \quad \text{for 3.3 micron band}$$

$$\text{and } B_c = 1.38 \quad \text{for 7.7 micron band}$$

The other empirical parameters are listed in Table 4.10 below for the two bands. These representations permitted the calculation of the total absorption of both the bands for varying values of  $w$  and  $P_e$ . However there are limited ranges over which these empirical functions are valid and no attempt was made to extend the parameterization. Thus the range of partial pressure that could be studied was limited. Calculations were made for methane partial pressures from 0.001 millibars to 0.1 millibars, taking it to be a trace absorber in atmospheres consisting of neutral gas of total pressures ranging from 20 millibars to 1000 millibars. Even as a trace absorber methane exhibits well defined regions of absorption as is illustrated by the transmission spectra in Figures 4.32 to 4.34. Figure

Table 4.10Empirical Parameters for the Two Methane Absorption Bands Considered

BAND CENTRE (microns)	BAND LIMITS $\text{cm}^{-1}$	C	d	k	C	D	K	TRANSITION VALUE $\int A_\nu d\nu$ ( $\text{cm}^{-1}$ )
7.7	1100-1535	7.3	0.45	0.27	-190	115	69	130
3.3	2200-3400	15.5	0.55	0.22	-375	272	108.8	250

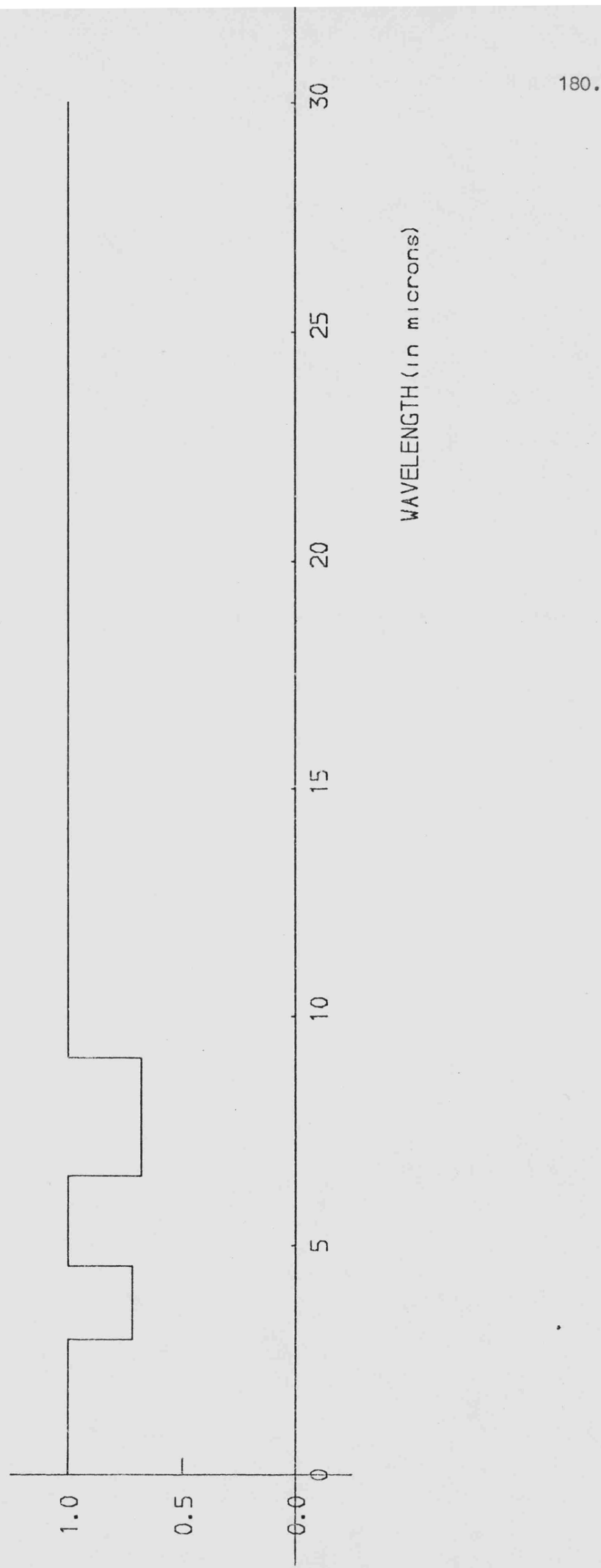
Table 4.11Empirical Parameters for Carbon Monoxide Absorption Band

BAND CENTRE (microns)	BAND LIMITS $\text{cm}^{-1}$	C	d	k	C	D	K	TRANSITION VALUE $\int A_\nu d\nu$ ( $\text{cm}^{-1}$ )
4.65	2000-2250	3.2	0.43	0.43	-106	61	61	120

Figure 4.32

$\text{CH}_4$  ( $P_s = 0.1 \text{ mb}$  [absorber] +  $20.0 \text{ mb}$  [broadener]) true spectrum

TRANSMISSION



180.

Figure 4.33

$\text{CH}_4$  ( $P_s = 0.01 \text{ mb}$  [absorber] +  $100.0 \text{ mb}$  [broadener]) true spectrum

TRANSMISSION

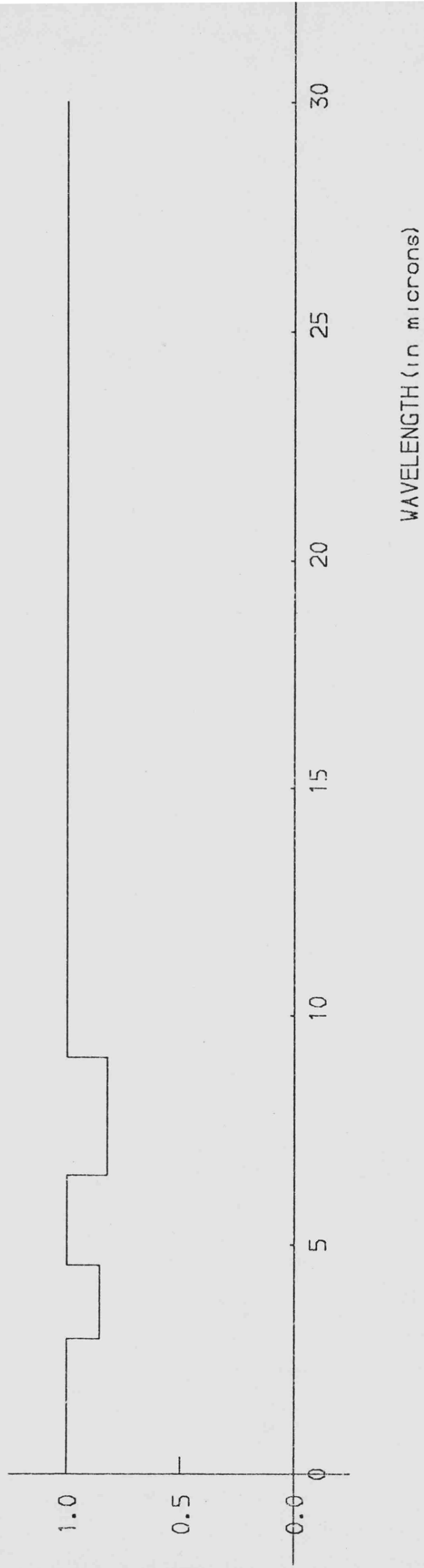
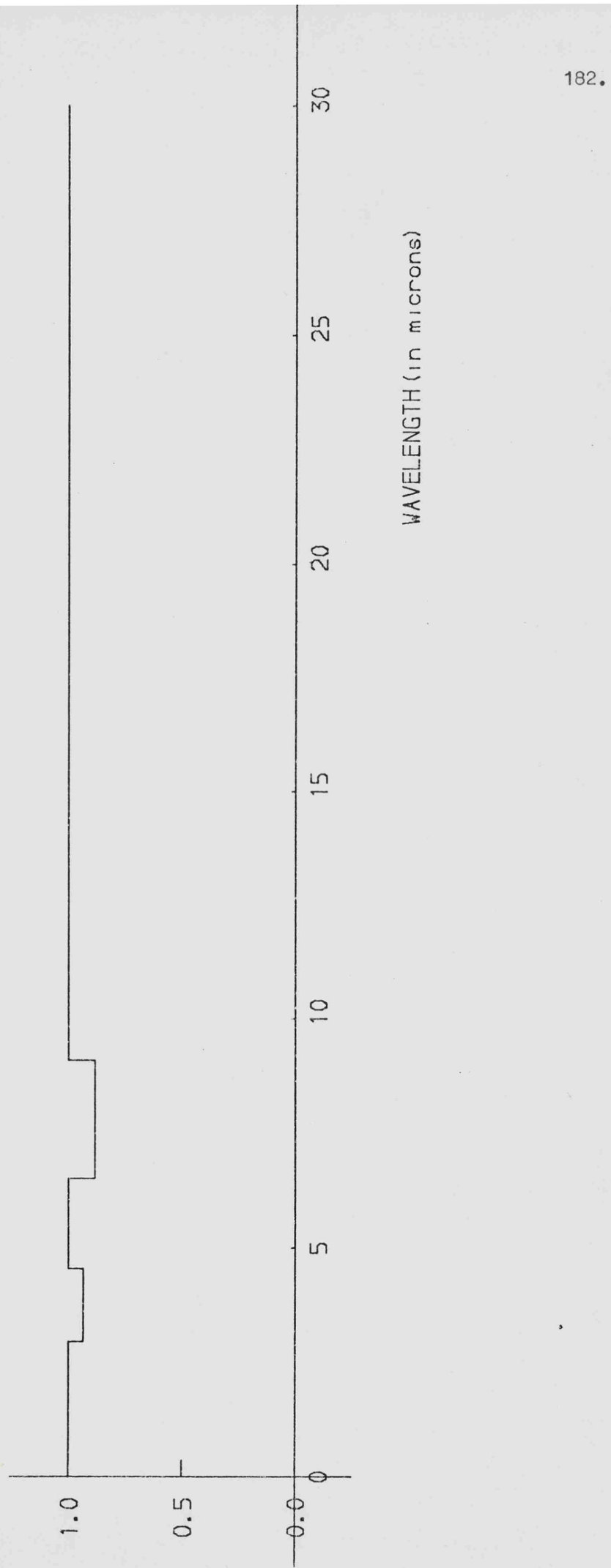


Figure 4.34

$\text{CH}_4$  ( $P_s = 0.001 \text{ mb}$  [absorber] +  $1000.0 \text{ mb}$  [broadener]) true spectrum

TRANSMISSION



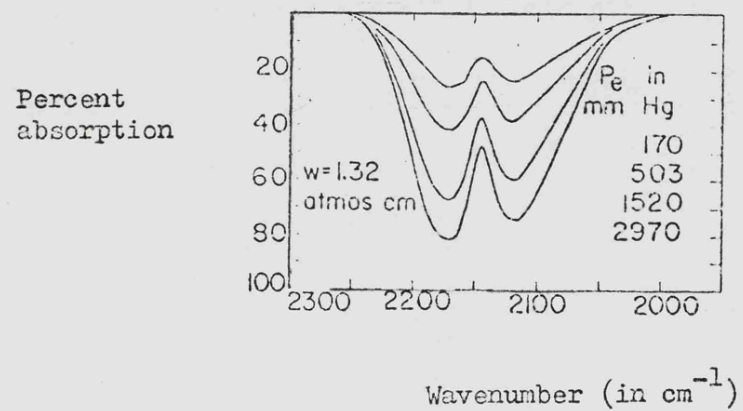
4.34 represents approximately the same amount of methane as is present in the Earth's atmosphere today. Under similar total pressure conditions (i.e. total pressure = 1000 millibars), the fractional transmission is seen to be 0.93 and 0.88 for the 3.3 micron and the 7.7 micron bands respectively. For the absorber amounts studied here the fractional transmission never fell below 0.41 and thus it is reasonable to assume that the addition of methane, as a trace gas, to the atmospheres to be studied in Chapter 5, although of interest, will not produce large variations in the surface temperatures.

The second absorbing gas studied in detail here is carbon monoxide. The reasons for choosing this were twofold. Firstly there is a large amount of evidence which points to a much higher concentration of carbon monoxide in an early carbon dioxide dominated atmosphere. Volcanic gases contain significant mixing ratios of carbon monoxide (Brancazio and Cameron, 1964). Also carbon monoxide is a significant secondary component of the Martian atmosphere. It has been found to exist in relatively large amounts in meteoritic material and has recently been observed in cometary tails. Thus, whether a secondary atmosphere was formed by outgassing or impacting, the proportion of carbon monoxide could reasonably be expected to be higher than on Earth now. The second reason for interest in carbon monoxide as a trace gas is ecological. Recently much interest has centred around the possible increased temperatures that could result from the release of large amounts of carbon dioxide into the atmosphere. However, the internal combustion engine is plagued

by under-oxidation problems and thus releases large amounts of carbon monoxide as well as carbon dioxide into the atmosphere. The addition of large amounts of a gas which is both toxic and possesses infrared absorption features could result in the balance, ~~controlled by the biosphere~~ on Earth, being upset. The major removal process of CO from the atmosphere of the Earth is ~~biological (being aided by catalysts present in several soil organisms)~~ whilst the oxidation of CO to CO<sub>2</sub> in the free atmosphere is ~~a slow process requiring a very high activation energy.~~ Thus On a sterile planet the level of carbon monoxide in a neutral atmosphere could be very much higher than the value of 0.1 ppm on the Earth today.

Carbon monoxide is a very stable molecule since the carbon and oxygen atoms are bonded by a triple electron bond (this stability has recently been underlined by the detection of free carbon monoxide in space). It has a dipole moment and rotational lines have been detected between 100 microns and 600 microns. This activity in the far infrared is of little importance for atmospheric studies since it lies beyond the range of significant thermal emission from planetary surfaces. The only fundamental lies at 4.65 microns ( $2143 \text{ cm}^{-1}$ ) and there is an overtone band at approximately 2.40 microns ( $4260 \text{ cm}^{-1}$ ). The vibration/rotation features are slightly complicated by the presence, in the atmosphere, of isotopic species particularly C<sup>13</sup>O<sup>16</sup>. The absorption features due to the fundamental are weak in the Earth's atmosphere but could be significant in an atmosphere containing larger mixing ratios of CO. However the

Figure 4.35



Spectral absorption in the vicinity of  
the CO fundamental at 4.65 microns ( $2145 \text{ cm}^{-1}$ ).

overtone band is very much weaker. As it lies at approximately 2.4 microns (further from the peak of the Planck function for temperatures lying in the range 200 K to 300 K than the stronger fundamental), it has been neglected in this work.

Thus only one band (centred at approximately 4.65 microns) was studied for carbon monoxide. The observed transmission curves for this band over the given ranges of effective pressure and absorber concentration are illustrated in Figure 4.35. These curves are from the laboratory data of Burch and his co-workers (1962) as are the empirical representations of band absorption described below. The band absorption was parameterized in the same way as for the other absorbing gases studied; given in Equations 4.11, 4.12 and 4.13. The value of  $B_c$ , the broadening coefficient, for carbon monoxide was found to be 1.02. The values of the other parameters are listed in Table 4.11 (see p.179).

As for methane, no attempt was made to use the exponential extension to the absorption parameterization and so calculations of absorption could only be made within the ranges of pressure and absorber amount originally studied in the laboratory. These allowed a variation in partial pressure of carbon monoxide from 0.001 millibars to 1 millibar and a variation in the total atmospheric pressure of 50 millibars to 1000 millibars. As the absorption feature is displaced from the peak of a Planck curve corresponding to, say, 240 K the temperature increment caused by it alone was found to be small. However the variation in the transmission with pressure and absorber concentration was well defined as Figures 4.36 to 4.38 demonstrate. Within the limits

Figure 4.36

CO (  $P_s = 1.0 \text{ mb} [\text{absorber}] + 50.0 \text{ mb} [\text{broadener}]$  ) true spectrum

TRANSMISSION

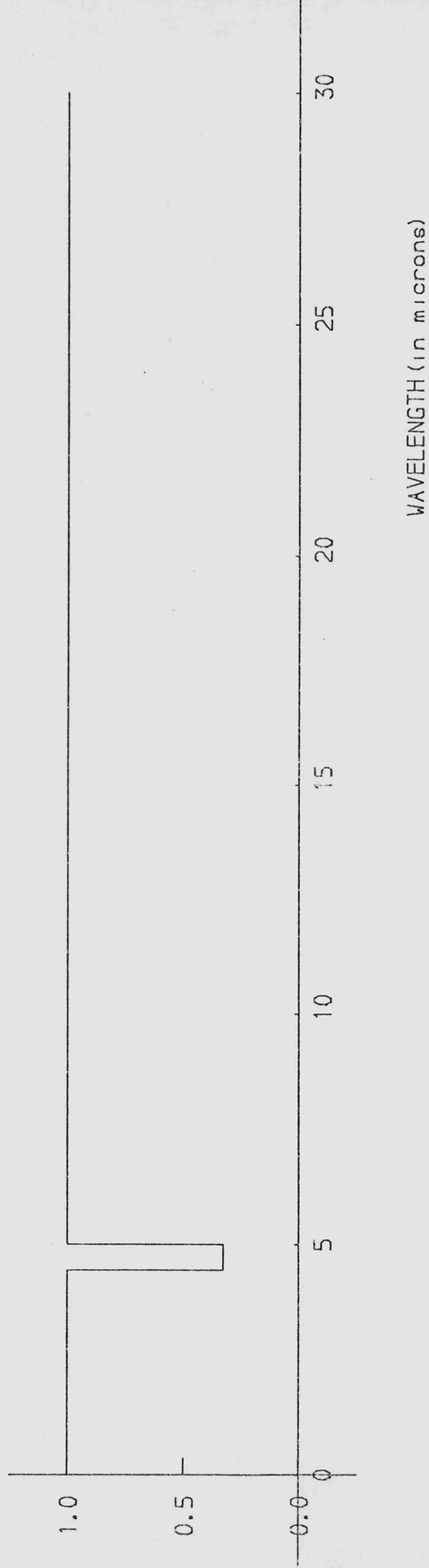


Figure 4.37

CO (  $P_s = 0.1 \text{ mb} [\text{absorber}] + 100.0 \text{ mb} [\text{broadener}]$  ) true spectrum

TRANSMISSION

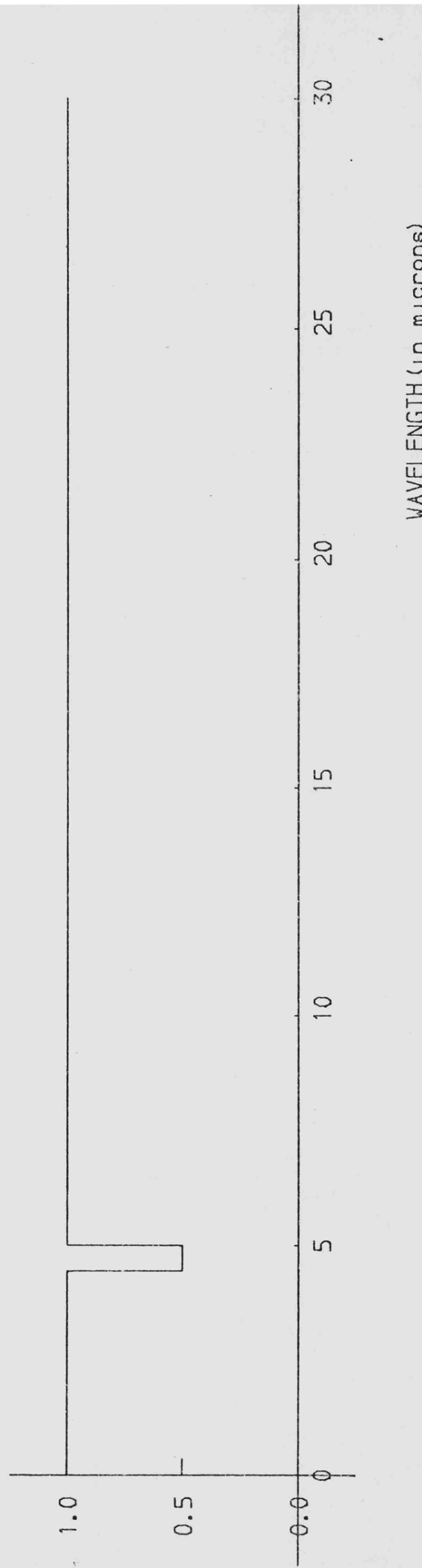
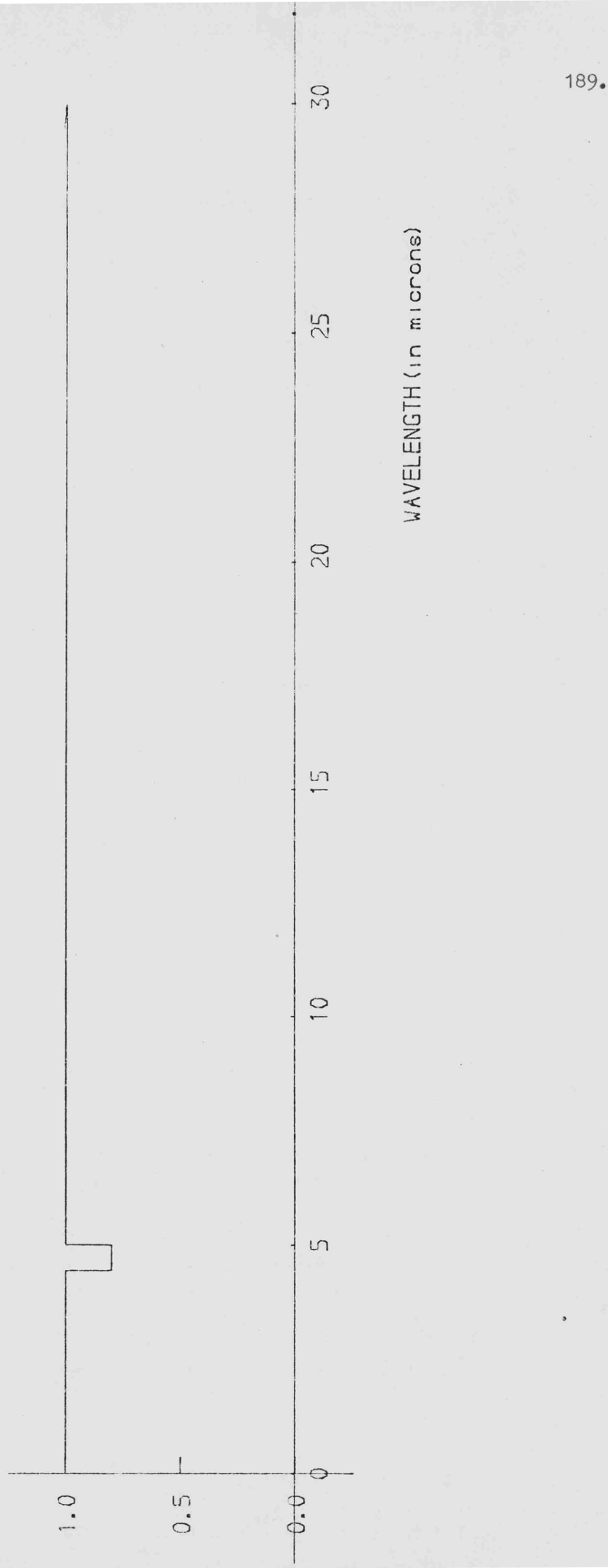


Figure 4.38

CO ( $P_s = 0.001 \text{ mb}$  [absorber] +  $1000.0 \text{ mb}$  [broadener]) true spectrum

TRANSMISSION

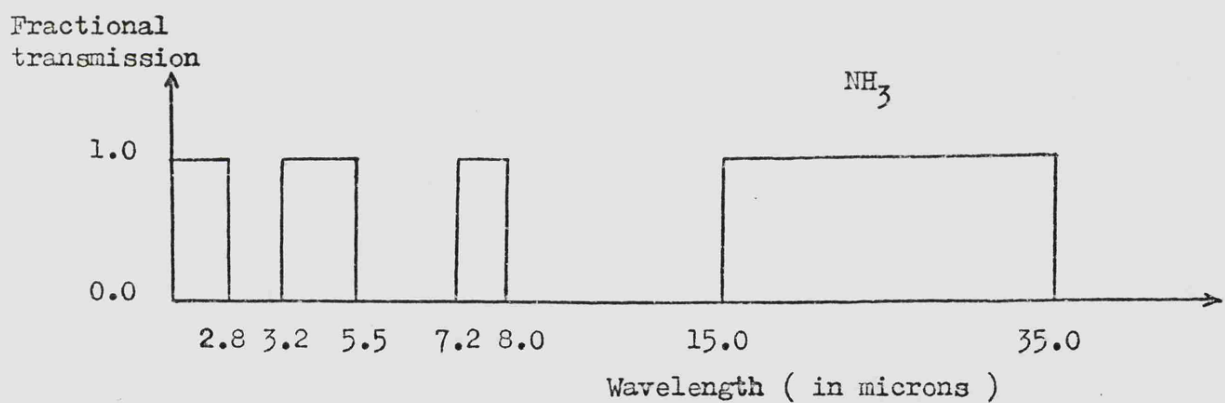


set by the laboratory data the fractional transmission was found to vary between 0.25 and 0.8.

The amounts of carbon monoxide considered in these calculations are higher than that present in the Earth's atmosphere today but consistent with the expected mixing ratios in an early atmosphere dominated by CO<sub>2</sub> or in any atmosphere around a planet without a life-system. These parameterizations will be used for both methane and carbon monoxide to allow the addition of these gases to the model atmospheres to be considered in Chapter 5.

There are a number of other gases which possess important absorption features in the infrared region: notably ozone and nitrous oxide in the Earth's atmosphere and possibly ammonia in a postulated early reducing atmosphere around any of the terrestrial planets. However, as has already been mentioned, the origin of life on Earth is no longer believed to require reducing atmospheric conditions typical of the Jovian planets. The fact that the dominant gas in the atmospheres of both Venus and Mars is carbon dioxide seems to indicate that the first stage of atmospheric evolution listed in Table 4.9 was never attained. Since it is only this early phase for which ammonia is a probable atmospheric component it may be reasonable to ignore it in atmospheric calculations. A further reason for not requiring or even expecting ammonia in large enough amounts to be of importance is the very strength of its absorption features. Figure 4.39 illustrates the block approximation used for the transmission curve of ammonia (volume mixing ratio of 10<sup>-5</sup> in 1 bar of a broadening gas) by

Figure 4.39

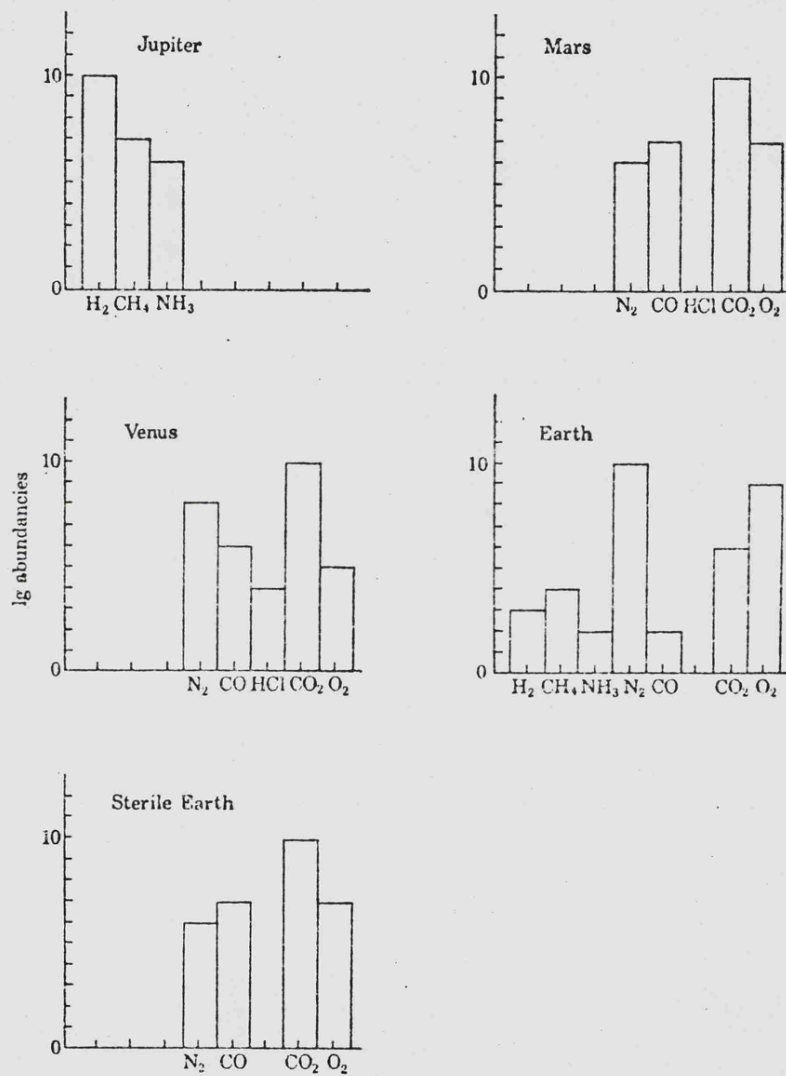


Step function approximation to the transmission curve of ammonia used by Sagan and Mullen (1971). Even for the small mixing ratio considered ( $10^{-5}$  by volume of  $\text{NH}_3$  in 1 bar of  $\text{H}_2$ ) ammonia is seen to be a very efficient absorber - particularly around the peak of Planck curves for the temperature ranges of interest. Addition of even small amounts of  $\text{NH}_3$  would lead to large temperature increments.

Sagan and Mullen (1971). The absorption is very efficient between 8 microns and 15 microns and longwave of 35 microns so that the temperature increment produced by the addition of these small amounts of ammonia would be very large (of the order of 20 K). The feedback effects upon albedo and atmospheric constituents have never been considered. The main argument in favour of ammonia in the atmosphere of the Earth (and hence the other terrestrial planets) has been based upon miscalculation of surface temperatures. The failure of Sagan and Mullen (1972) to vary the planetary albedo in calculations spanning 5 aeons naturally led to incorrect calculation of the surface temperature and hence they found it necessary to postulate the addition of very efficient absorbing gases to the early atmosphere. More appropriate calculations of surface temperature allowing for variations in albedo, flux factor and surface infrared emissivity will be made in Chapter 5. Since ammonia produces rather high surface temperatures (in contradiction to confirmed geological data) and there are no incontrovertible reasons for its inclusion it has not been considered in detail in this work.

The other gases which exhibit infrared features large enough to influence the spectral characteristics of the Earth's atmosphere are probably due to the presence of the biosphere. It is generally agreed that the large amount of molecular oxygen in the Earth's atmosphere (21 per cent) is due almost entirely to processes within the biosphere although a secondary source (probably responsible for the oxygen in the atmosphere of Mars) is the photodissociation of water molecules and the escape of the

Figure 4.40



The abundance of gases in planetary atmospheres.

Vertical scale logarithm to the base 10 of the abundances,  
(after Lovelock, 1975).

hydrogen leaving free oxygen. The build-up of oxygen in the Earth's atmosphere brought about by photosynthetic plants has led to the formation of the ozone layer in the stratosphere and has also allowed nitrous oxide to be formed. Figure 4.40 (from Lovelock 1975) is a histogram showing the abundances of gases (on a logarithmic scale) in the atmospheres of Jupiter, Mars, Venus, the Earth and a postulated sterile Earth. Since this work attempts to describe the evolution of a planetary atmosphere and the ambient surface temperature ignoring the effects of a life-system the gaseous abundances of a sterile Earth are particularly interesting. As well as underlining the importance of carbon dioxide in the atmospheres of sterile terrestrial planets these histograms also indicate the abundances of methane and especially carbon monoxide which have already been discussed. The other effect, which will be considered in Section 4.9 is that of a neutral gas in an evolving atmosphere. The histograms indicate the large amount of molecular nitrogen in the atmospheres and Table 4.2 lists the amounts of nitrogen and argon as percentages of the total atmospheric pressure. The effect of neutral gases upon the spectral characteristics are discussed below.

4.9 Neutral Gases

Of the neutral gases detected and predicted in the atmospheres of the terrestrial planets nitrogen is probably the most important and argon possibly the most interesting. The presence of a neutral gas in an alien atmosphere is difficult to establish, particularly if there is only a small amount, since, by definition, it is stable against chemical reactions within its environment and exhibits little or no spectral activity. Usually the amount of "other gas" present is assessed either by radio occultation (which establishes the surface pressure and may be compared with the absorber amount deduced from spectra) or by very careful study of spectral characteristics of absorbing gases which may reveal the presence of a broadening agent. The immense difficulty of positively identifying even large mixing ratios of inert gases in alien atmospheres is comprehensively discussed by Moroz (1976). The problem is particularly relevant to data on the Martian atmosphere. Apparently contradictory observations predicting respectively large and negligible amounts of argon are easily reconciled.

Collisional broadening is the most important line broadening effect for tropospheric studies. It is caused by large electric fields that act during molecular collisions. It depends upon the rotational quantum numbers and thus will vary from line to line. The frequency of molecular collisions is related to pressure but the term "pressure broadening" includes effects which generally only occur under very high pressure conditions. Collision broadening is responsible for increased

line widths at the pressures and chemical compositions of interest in an evolving terrestrial atmosphere and is encountered when the times between collisions are large compared with the times spent in collision. Since the effects of collision broadening vary from line to line within each band it is difficult to allow for it, in any simple way, in the parameterization already described for the absorption bands.

Howard, Burch and Williams (1956) tried to express the total band absorption (for a weak band) in the form

$$\int A_\nu d\nu \propto w^d p^k \quad \dots\dots 4.15$$

where 'P' was the total pressure. However they found that when the absorber partial pressure was of the same order as the neutral gas partial pressure self-broadening effects became important and it was necessary to express the pressure term as an effective pressure,  $P_e$ , where

$$P_e = P + p \quad \dots\dots 4.16$$

which allowed more weight to be given to the partial pressure of the absorbing gas. In later studies in the 1960's by Burch and co-workers (1962) the effective pressure term was rationalized using collisional theory.

The half-width of any collision-broadened spectral line is proportional to the collision frequency F. Kinetic theory enables the half-width to be given by:

$$\alpha = \frac{F}{2\pi} = \frac{1}{4\pi} \sum_i N_i (D_{a,i})^2 \left[ 2\pi kT \left( \frac{1}{M_a} + \frac{1}{M_i} \right) \right]^{\frac{1}{2}} \quad \dots\dots 4.17$$

where  $N_i'$  is the number of molecules of the  $i^{\text{th}}$  type per unit volume, ' $D_{a,i}'$ ' is the sum of the optical collision diameters of the absorbing molecule and a molecule of the  $i^{\text{th}}$  type, ' $M_a'$ ' is the mass of an absorbing molecule and ' $M_i'$ ' is the mass of a molecule of the  $i^{\text{th}}$  type. Thus for a simple binary mixture of an absorbing and a neutral gas, Equation 4.17 reduces to:

$$\alpha = \frac{1}{4\pi} \left[ \frac{2\pi kT}{M_a} \right]^{\frac{1}{2}} \left\{ N_a (D_{a,a})^2 \left[ \frac{2}{M_a} \right]^{\frac{1}{2}} + N_b (D_{a,b})^2 \left[ \frac{M_a + M_b}{M_a M_b} \right]^{\frac{1}{2}} \right\} \quad \dots \dots \quad 4.18$$

and by substituting for  $N_a$  and  $N_b$  in terms of partial pressures

$$\alpha = \frac{1}{4\pi} \left[ \frac{2\pi kT}{M_a} \right]^{\frac{1}{2}} \left\{ C_{a,a} P_a + C_{a,b} P_b \right\} \quad \dots \dots \quad 4.19$$

where  $C_{a,a}$  and  $C_{a,b}$  are constants involving the optical collision diameters and the masses of absorbing and broadening gases. This can be rewritten since the total pressure  $P$  is:

$$P = P_a + P_b \quad \dots \dots \quad 4.20$$

thus

$$\alpha = \frac{1}{4\pi} \left[ \frac{2\pi kT}{M_a} \right]^{\frac{1}{2}} C_{a,b} \left\{ (P_a + P_b) + \left[ \frac{C_{a,a}}{C_{a,b}} - 1 \right] P_a \right\}$$

∴

$$\alpha = \frac{1}{4\pi} \left[ \frac{2\pi kT}{M_a} \right]^{\frac{1}{2}} C_{a,b} \left\{ P_e + (B_c - 1) P_a \right\} \quad \dots \dots \quad 4.21$$

The pressure term in this equation is called the effective pressure  $P_e$  such that

$$P_e = P + (B_c - 1) p \quad \dots \dots \quad 4.22$$

where 'P' is the total pressure and 'p' is the partial pressure of the absorbing gas.

All the empirical equations for band absorption were derived in terms of this effective pressure which itself depended upon a laboratory derived value of  $B_c$  (the broadening coefficient). The later work by Burch and co-workers (1962) produced different values of  $B_c$  for carbon dioxide and water vapour. Since the empirical parameters were derived from laboratory results rather than the theory described above it was decided to allow

$$P_e = P + p$$

for carbon dioxide and water vapour, i.e.  $B_c = 2$  and to use the original results derived by Howard, Burch and Williams (1956). For the representations of methane and carbon monoxide, however, the more recent work was used and here the values of  $B_c$  were 1.30 and 1.38 for the methane bands and 1.02 for carbon monoxide.

The expression of the pressure dependence in terms of a broadening coefficient permitted computations to be carried out which considered the effect of binary mixing of gases. Some of these results have already been illustrated in the form of fractional transmission curves derived for all the absorbing gases considered in detail (see Figure 4.18 and all the methane and carbon monoxide curves). Although the binary mixtures studied in the laboratory were of an absorbing gas and a neutral gas (usually nitrogen - which is particularly appropriate for the atmosphere of the Earth) it was considered reasonable to use the same expression of pressure dependence for mixtures of two

absorbing gases and thus the mixtures of carbon dioxide plus small amounts of other absorbers discussed in Chapter 5 will use these same values of  $B_c$ .

Collisional broadening is thus dependent upon the total gas pressure and also upon the gases themselves since they determine the collisional cross-sections. In the Earth's atmosphere the 21 per cent of the total volume which is oxygen is an important factor in the collision broadening although it is not a neutral gas since it takes part very readily in chemical reactions in the atmosphere. The most important neutral, broadening gas will be nitrogen and results derived for the present-day Earth's atmosphere and surface temperature (at the end of Chapter 2) indicate the accuracy of the method outlined above.

As well as the very significant role of neutral gases as broadening agents it is important to note that the rare gases (particularly argon) are significant indicators of degassing activity. It is well established that 99.6 per cent of the argon in the Earth's atmosphere is  $^{40}\text{Ar}$  released by the radioactive decay of  $^{40}\text{K}$ . Once released into the atmosphere argon is likely to remain there. It does not take part in any chemical reactions nor is thermal escape likely even from a planet as small as Mars since its atomic weight is approximately that of carbon dioxide which is not rapidly lost from the Martian atmosphere. Thus the amount of  $^{40}\text{Ar}$  in any atmosphere must be a measure of the amount of degassing activity which has led to its release.

Particular interest has been aroused by the possibility of predicting the degassing rates and ratios from the amounts of rare gases found in planetary atmospheres since the Soviet Mars 6 spacecraft reported detecting, "several tens of percent of the surface pressure of an inert gas" (see Moroz, 1974). A number of papers were published which attempted to use this observation as an indicator of the amount of carbon dioxide that should have been degassed from the Martian surface and thus to derive limits upon the volume of solid CO<sub>2</sub> trapped in the polar caps and regolith (e.g. Levine and Riegler, 1974; Owen, 1974).

Consideration of the two extreme states of the carbon dioxide inventory, namely i) most of the CO<sub>2</sub> ever degassed is present in the atmosphere now or ii) a large percentage of the CO<sub>2</sub> degassed is in a polar cold trap (this could be up to a bar of carbon dioxide) yield <sup>40</sup>Ar amounts in the range i) 0.002 millibars to ii) 2 millibars.

It is not unreasonable that either of these two extreme possible regimes should prove to be correct since an added partial pressure of up to 2 millibars of an inert gas in the predominantly CO<sub>2</sub> Martian atmosphere would produce little variation in the fractional transmission curve of the carbon dioxide as is illustrated by Figures 4.41 and 4.42. The problem of detection of small amounts of an inert gas is enhanced on Mars by the topography. This leads to variations in surface pressure of approximately 5 millibars and thus a discrepancy of up to 2 millibars could be overlooked.

Figure 4.41

$\text{CO}_2$  ( $P_s = 10 \text{ mb}$ ) TRUE SPECTRUM

TRANSMISSION

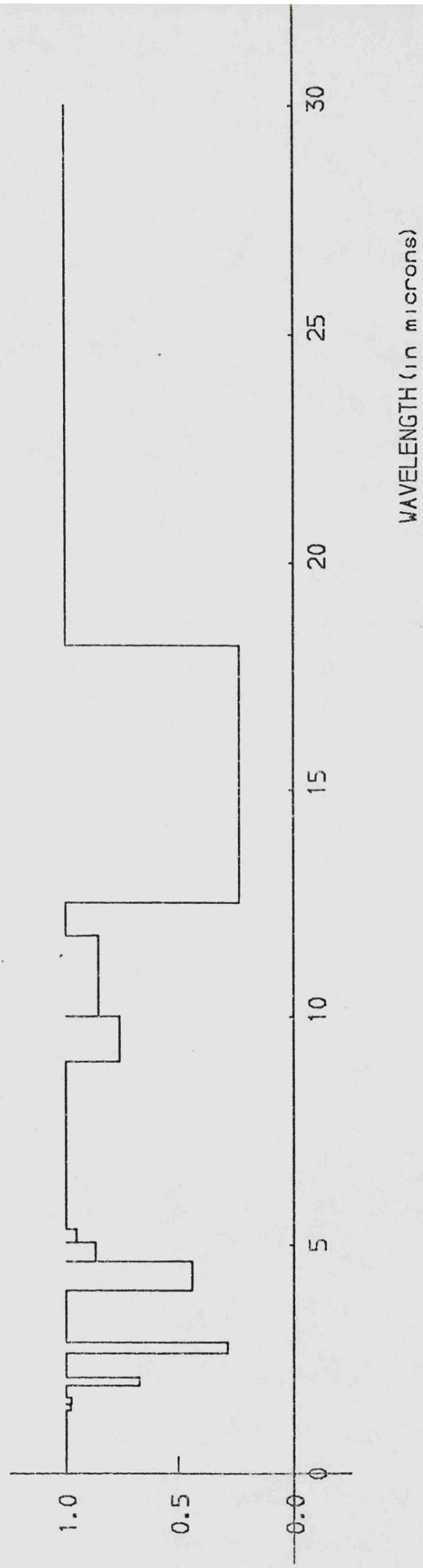
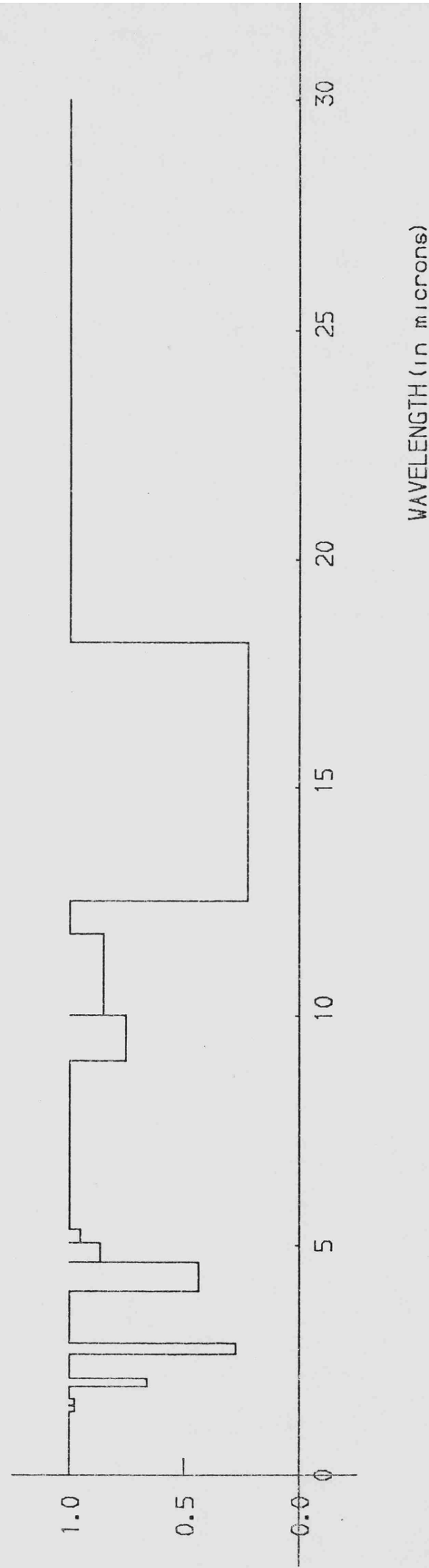


Figure 4.42

$\text{CO}_2$  (  $P_s = 10 \text{ mb} [\text{absorber}] + 2 \text{ mb} [\text{broadener}]$  ) true spectrum

TRANSMISSION

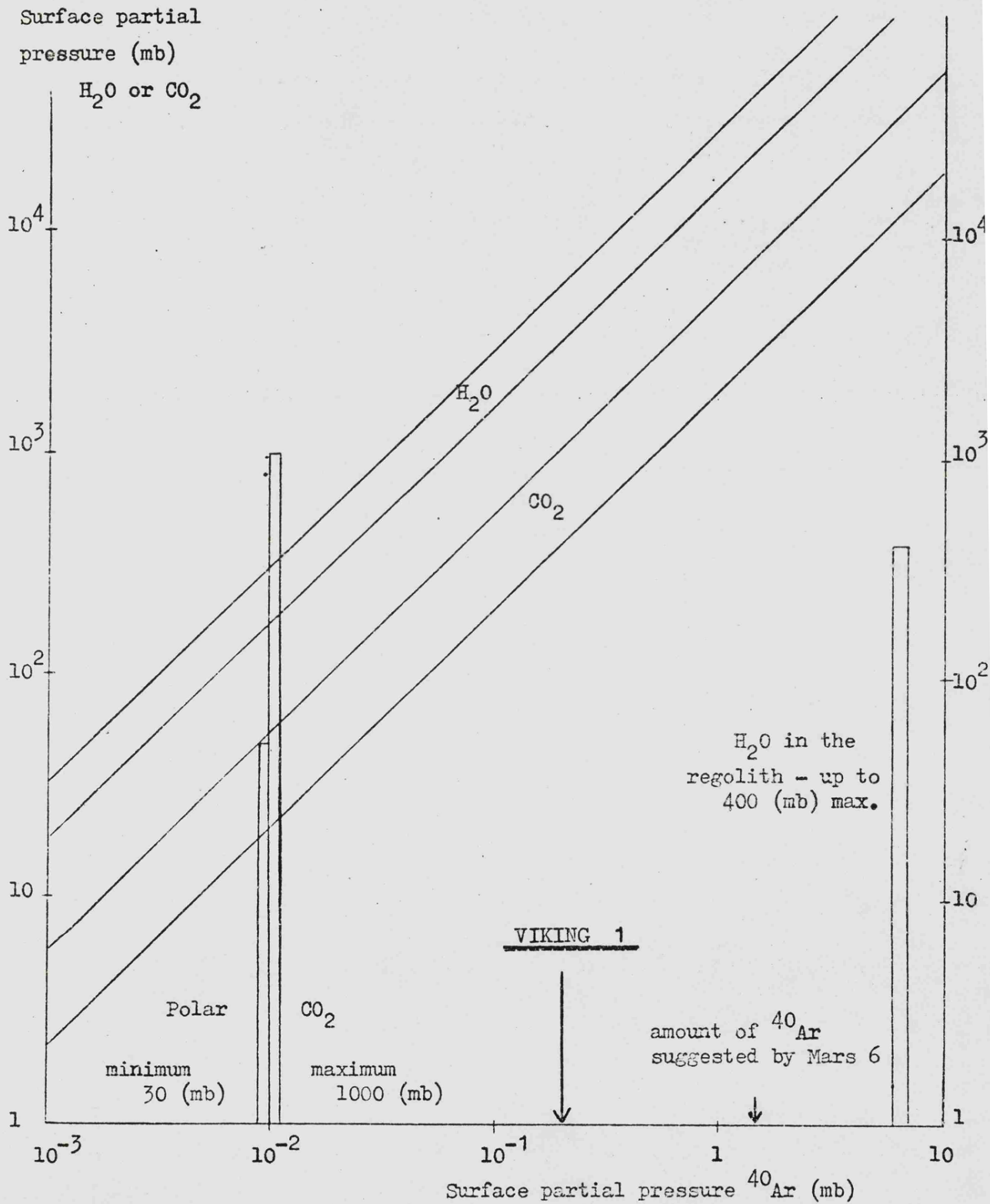


202.

A further, very interesting possibility is the extrapolation of the degassing ratio theory to water vapour. This depends upon a slightly shaky premise; namely that the ratios of  $^{40}\text{Ar}/\text{CO}_2/\text{H}_2\text{O}$  degassed from the surface of the Earth and the surface of Mars are similar. Account must, of course, be taken of the differences in mass and surface area of the planets but the extrapolation involves the assumption that both the chemical composition and the degassing histories are similar. It is important to note (see Owen, 1976) that positive detection of large amounts of  $^{40}\text{Ar}$  in the Martian atmosphere may not necessarily imply huge amounts of lost or hidden volatiles. The extrapolation of degassing ratios has, however, led to some interesting and important discussions.

Figure 4.43 has been drawn to illustrate the amounts of both carbon dioxide and water vapour likely to have been degassed for argon amounts in the ranges already discussed. The scales (of partial pressures in millibars) are logarithmic. Huge amounts of both volatiles would need to be considered in the case of a large argon abundance (i.e. similar to the "observed" values of Mars 6). An interesting point to note is the fact that if the very low amounts of argon, and hence of carbon dioxide and water vapour, are correct then the chances of a cyclic variation of climatic conditions on Mars, as suggested by Sagan, Toon and Gierasch (1973), are very slender. This is because the lower the amount of water vapour degassed the greater is the probability that it will be rapidly lost by photodissociation and escape. Such an early "one-off" hospitable atmosphere could have

Figure 4.43

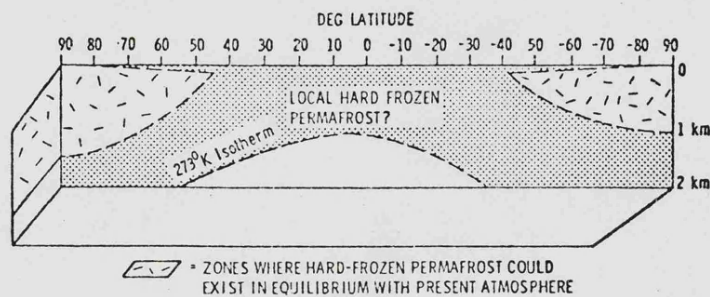


Comparison of amounts of  $^{40}Ar$ ,  $CO_2$  and  $H_2O$  degassed by Mars - assuming similar ratios to those for the Earth apply. The width of lines predicted for  $H_2O$  and  $CO_2$  indicates the uncertainty in the ratios.

produced the surface erosion features observed by Mariner 9 but the cyclic freezing and vaporization of much larger amounts of water vapour is a more exciting speculation. A further possibility is that if a large partial pressure of argon is discovered by Viking the measurement may indicate that very large amounts of water vapour are available for degassing but that the final surface outgassing has been inhibited by temperatures below 273 K. This may imply reservoirs of water under the surface of Mars. Such hidden reservoirs have been discussed very recently by Fanale (1976). Figure 4.44 illustrates a possible subsurface structure which would allow permafrost deposits at near equatorial latitudes. These would be uncoupled from the atmosphere. However closer to the polar regions Fanale suggests that equilibrium between water—ice and the Martian atmosphere is possible. The lower illustration on Figure 4.44 is the water vapour saturation curve over ice, after Farmer (1976). This curve allows the calculation of maximum water vapour amounts in the Martian atmosphere assuming the frost deposits are open to the atmosphere at some stage in the seasonal cycle.

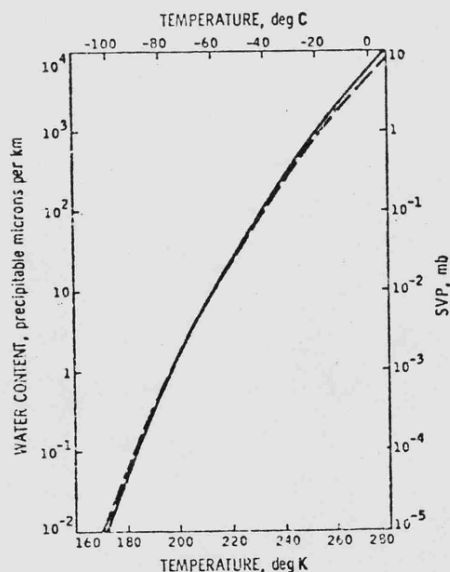
Long period variations in the Martian characteristics, caused by orbital fluctuations and solar luminosity variations (see Chapter 1) may cause improved conditions. The present atmospheric regime is somewhat less than hospitable, however, but this fact has led Sagan and Lederberg (1976) to postulate macro-organisms rather than micro-organisms as a possible Martian biology, since larger Martians may be better able to acquire and retain water from permafrost deposits.

Figure 4.44



The possible distribution of hard-frozen regolith permafrost on Mars is shown. Arguments given in the text suggest that a regolith of unconsolidated material as much as 2 km thick may exist on Mars. Within this regolith, hard-frozen permafrost could occur anywhere above the 273 K isotherm which, in the figure, is that calculated on the basis of the surface mean annual temperature as a function of latitude (Table I), and an internal thermal gradient of  $40^\circ/\text{km}$ . The thermal gradient assumed is that for a Mars with bulk chondritic [ $^{40}\text{K}$ ] and [ $\text{U}$ ] concentrations, and a regolith conductivity ( $K$ ) of  $8 \times 10^4 \text{ erg cm}^{-1} \text{ sec}^{-1} \text{ K}^{-1}$  (a reasonable value for hard-frozen permafrost). If the pores in the regolith are assumed to be largely unfilled, then  $K$  would be lower and the 273 K isotherm could occur at a more shallow position in the regolith. The existence of such permafrost at latitudes  $<\pm 40^\circ$  depends on the ability of the overlying regolith to prevent preexisting ground ice from subliming into the atmosphere (see text). However, in the "equilibrium" zones, as shown, ground ice could exist even if physical equilibrium were achieved with the present lower atmosphere; the total amount of ground ice in the Martian regolith could be as high as  $5 \times 10^7 \text{ km}^3$ , or  $4 \times 10^4 \text{ g/cm}^2$  averaged over the surface of Mars.

(after Fanale, 1976)



Water-vapor saturation pressure over ice (solid line) and equivalent maximum atmospheric water vapor content (dashed line).

(after Farmer, 1976)

The data collected by Viking 1 and 2 this summer should permit much more fruitful discussion of these important questions.

Note added in proof:

The first results produced by Viking 1 indicate a considerably lower concentration of  $^{40}\text{Ar}$  in the Martian atmosphere than suggested by the Mars 6 spacecraft, (New Scientist, 29 July, 1976). The true concentration of argon is now believed to be less than 2 per cent of the total atmosphere.

This new value has been indicated on Figure 4.43. It can be seen, immediately, from the figure that this amount of radiogenic argon implies approximately 1000 millibars of carbon dioxide and close to 5 bars of water vapour available for degassing or already degassed from Mars. The polar caps on Mars may contain up to 1000 millibars of  $\text{CO}_2$  and thus the new argon data seems to be in reasonable agreement with the carbon dioxide inventory. The large amount of water vapour implied may not have been degassed or may have been lost after degassing as has already been discussed.

#### 4.10 Conclusions

This chapter has concentrated upon the parameterizations used in this work and in particular upon the properties of atmospheric gases. The model atmospheres to be discussed in Chapter 5 will utilize the empirical representations of band absorption for each of the gases considered in detail in this chapter. Comment will also be made upon the possible feedback effects which might modify the surface and the chemical nature of the atmosphere.

CHAPTER 5MODELS OF EVOLVING PLANETARY ATMOSPHERES AND  
RESULTING SURFACE TEMPERATURES5.1 Introduction

In the earlier chapters, the dependence of planetary surface temperatures upon a number of parameters has been described. A method for calculating the average, global surface temperature,  $T_s$ , in terms of the effective temperature,  $T_e$ , the albedo, surface infrared emissivity, flux factor and also the infrared absorption properties of the atmosphere was described in Chapter 2, and is summarized by Equations 5.1 and 5.2 below:

$$S(1 - A) = f \sigma T_e^4 \quad \dots \dots \quad 5.1$$

$$\frac{1}{f} S(1 - A) = \sum_{\lambda_i} e B_{\lambda_i} (T_s) \Delta \lambda_i + \sum_{\lambda_j} B_{\lambda_j} (2^{-\frac{1}{4}} T_e) \Delta \lambda_j \quad \dots \dots \quad 5.2$$

Chapters 3 and 4 described the variations possible in all these parameters during the evolution of a planetary atmosphere. The feedback effects between these parameters and the surface temperature itself, have been mentioned, and the effect upon the surface temperature of specific alterations in some of these parameters has been described in detail.

In this chapter, the evolution of an atmosphere of a terrestrial planet will be considered in detail, and the surface temperature evolutionary track calculated. The only long-term external parameter likely to contribute to the surface temperature calculations is the solar luminosity. The gradual

increase in the luminosity of the Sun over the life-time of the Solar System has been described in Chapter 1. In the following calculations a simple linear increase of 43 per cent over the 4.5 aeon life-time of the planets will therefore be assumed.

In Chapter 4 the build-up of the atmosphere by degassing was described, and, in particular, the chemical constituents of the outgassed material were discussed at length. However, no attempt was made to estimate the degassing rate. The total atmospheric mass at any stage during the evolution of the planet will be a function of the degassing rate and mode, and also of the removal rates to the surface and to space. The mechanisms which permit loss of gases from the atmosphere (particularly condensation and chemical reactions with surface rocks) are clearly a function of the surface temperature, whereas cloud condensation and escape to space depend upon the temperature profile of the atmosphere. The dependence of emission rates of gases from surface rocks upon temperature is not obvious, but it seems reasonable to assume that frozen and molten planetary surfaces would degas differently. Thus the feedback mechanisms extend to the atmospheric mass itself. This mass will probably depend upon the planetary mass, since both degassing and escape rates may be related to the surface area and total mass.

The problems of the direction and magnitude of the many feedback mechanisms are immense. Most of the parameters required for the successful calculation of a planetary surface temperature

are themselves functions of that surface temperature. It is possible that atmospheres are stable against many of these perturbations. However, dynamic modelling of even the present-day Earth's atmosphere has not yet produced universally acceptable results on the effect of, for instance, albedo, snow/ice cover, or cloud cover, modifications upon global climate (see e.g. Ghil, 1976).

As the discussion in Chapter 1 indicated, it is unreasonable to hope for a dynamical model that can be used to describe conditions on all the terrestrial planets over 4.5 aeons. It is for this reason that the simplified model described here has been developed. Obviously, these simplifications have drawbacks. The vertical structure of the atmosphere is not considered by this model. Consequently, the formation of clouds, which depends upon both the vertical distribution of gases and the temperature profile, is difficult to represent. Similarly, the exospheric temperature, upon which the gaseous escape depends, is not calculated by this model. Photochemical reactions, which are functions of both the vertical distribution of gases and the penetration of solar radiation, are also difficult to discuss.

The calculations described later in this chapter have been performed for selected ranges of values of all the parameters previously discussed. It is believed that the most important temperature is that of the surface, and that vertical temperature variations are only a second order effect for the important parameters (e.g. albedo and total absorber concentrations).

However, the computational results will indicate probable temperature trends rather than exact climatic regimes. Such average global calculations may be an ideal starting point for an investigation of (for instance) climatic stability during a glacial period in a more complex dynamical model. Such models will probably be available within the next decade, but limitations of computer-time and money will restrict their use to distinct geological epochs. Thus this type of first-order global computation (calculating past and future surface temperatures) will, I consider, be a vital tool.

## 5.2 Degassing: Mode and Rate

The assumption that the atmospheres of the terrestrial planets were formed by degassing from surface rocks has been justified in Chapter 4. Also in Chapter 4 the dominant gases have been discussed and their effect upon the evolution of the surface temperature considered. It is important to note, however, that the mode and rate of degassing are probably as important in the calculation of surface temperatures as the gases involved. It was suggested in the discussion in Chapter 4 that degassing was associated with surface movement and/or impact features on the Earth, and thus a degassing mechanism for production of an atmosphere might be invoked for Mars and Venus (for which there is evidence of similar features). The Moon and Mercury (both with highly cratered surfaces and evidence of linear features and lava flows) could be considered as capable of similar degassing, though having lost almost all the gases by gravitational escape.

It now seems likely that a combination of the infall and degassing hypotheses will most successfully describe the evolution of the secondary atmospheres around the terrestrial planets. If an inhomogeneous accumulation model is adopted for the formation of the Solar System (see, e.g. Turekian and Clark, 1975) the final layers accreted by the terrestrial planets are likely to be of a volatile-rich carbonaceous material similar to that of a (C - 1) carbonaceous chondrite meteorite. It is possible that vaporization during impact was adequate to produce some of the volatile constituents of the atmospheres (Benlow and Meadows,

1976). However, it seems more reasonable to conclude that most atmospheric build-up has been by degassing, in the form of gases emanating from surface rocks, for all the terrestrial planets (Walker, 1976).

The major volatiles, water and carbon dioxide have probably not been fully degassed from this volatile-rich veneer, since both are soluble in silicate melts (Fanale, 1971). In fact, there is evidence of a high volatile content in the upper mantle (Sylvester-Bradley, 1972). The three distinct classes of atmospheric gases (volatiles, non-radiogenic inert and radiogenic inert) will probably have behaved in different ways. The radiogenic inert gases, which are produced by the decay of elements not confined to the surface layers, must have been continuously produced within the solid Earth. The rate and mode of their release has been the cause of recent controversy (see e.g. Sabu and Manuel, 1976). It is possible that the ratios of, for instance,  $^{40}\text{Ar}$  to water vapour and carbon dioxide may be a useful indication of degassing rates (see Section 4.9). Recent comparison of radiogenic gas amounts with non-radiogenic amounts in mantle rocks seem to support the hypothesis of an early rapid degassing for the Earth (Ozima, 1975). Before firm conclusions can be drawn, it is vital that more analyses should be performed upon both mantle rocks from the Earth and also Martian surface rocks. One of the more important factors for the computation of surface temperatures is the likely ratio of carbon dioxide to water vapour released. Studies of volcanic gases on Earth today suggest that up to 90 per cent of the total

gas released is water vapour, but this is now believed to be the result of near surface contamination by ground water (see e.g. Fielder and Wilson, 1975). Nevertheless, the total release of volatiles from the surface of the Earth almost certainly involved a larger amount of water vapour than carbon dioxide. This is supported by the volatile inventory given by Meadows (1972) for the planets Earth, Mars and Venus and listed in Chapter 4 (Table 4.4). It is important to note that the ratio of  $H_2O$  to  $CO_2$  for both Mars and Venus is very much lower than the value for the Earth; although very recent studies of volatiles in two comets suggest that this is similar to the terrestrial value (see Chapter 4). It is possible to argue (see Section 4.6) that most of the water vapour degassed from Venus has been photodissociated and lost by the escape of hydrogen. It can also be argued that either Mars was formed deficient in water, or that temperatures have restrained the degassing of water vapour into the Martian atmosphere. The consequences of such arguments have already been noted in Chapter 4 and will also be discussed in Section 5.4.

The oxidation state of the gases evolved into the atmosphere is also very important. It has already been established (see Chapter 4) that the evidence for an early, highly reducing atmosphere is not convincing (Section 4.8). The data seem to indicate that  $H_2O$  vapour and carbon dioxide were always the major degassed constituents: probably in a ratio of at least 4 to 1 (in favour of  $H_2O$ ), though this ratio may not be valid for the other terrestrial planets. The rate of degassing is still more difficult to establish. Geological evidence for the Earth has

permitted assessment of conditions as far back as 3.7 to  $3.8 \times 10^9$  years ago. The conditions on the other terrestrial planets (especially Venus and Mars) earlier in the history of the Solar System are impossible to establish at present. Analysis of lunar rocks indicates that they are ancient compared with those on Earth; this is reasonable since there is little erosion, and there are no recycling mechanisms at work. The surfaces and atmospheres of both Mars and Venus must interact. This may occur on time scales considerably shorter than the life-time of the planet (possibly forced by the perturbations discussed in Chapter 1, Section 1.5), (see e.g. Sagan, Toon and Gierasch, 1973). Over long-periods the averaged trends will smooth such fluctuations. It has been suggested that a planet possessing life-forms may be modified by them (Margulis and Lovelock, 1974). Such biological modification will, I believe, serve to dampen these shorter-term (say less than  $10^6$  years) fluctuations. The long-term surface temperature evolution is demonstrated to be stable by the results presented in Section 5.6.

Evidence for the Earth seems to indicate an early (possibly catastrophic) degassing, as originally urged by Fanale (1971). Geological data, particularly that from the Precambrian, now enables limits to be set upon the evolution of the atmosphere and hydrosphere on Earth. Carbonate sedimentary deposits date from between 3.5 to  $3.8 \times 10^9$  years ago (Schidlowski et al., 1975), and thus it is considered that the amount of free carbon dioxide in the Earth's atmosphere attained at least its present level by  $4.0 \times 10^9$  years ago. Similarly, evidence in chert deposits

(Holland, 1975) dates large, open water masses at between 3.7 and  $3.75 \times 10^9$  years ago, which limits the surface temperature and amount of water vapour degassed. It is generally agreed that no free oxygen existed in the atmosphere earlier than approximately  $2 \times 10^9$  years ago.

Models for the rate of degassing on Earth have been suggested by many authors. It now seems reasonable to assume an early degassing sequence (certainly of carbon dioxide and water vapour) for the Earth. However there may also have been an exponentially decreasing amount of gas emitted to the present day; thus allowing modifications throughout the history of the Earth. Li (1972) has proposed a family of degassing models ranging from a linear sequence over the lifetime of the Earth to a rapid exponential rate. It may be that the degassing rate has varied from planet to planet in the Solar System, so that a slower, or more rapid, sequence might be more appropriate for Mars and Venus. It is possible that the degassing sequence was not triggered until very much later in the history of the Solar System on Mars (possibly because of its greater distance from the Sun). It was for this reason that the three degassing sequences considered in Chapter 3 were used: I - an early, almost total, degassing; II - a linear degassing with time over the lifetime of the planet; III - a late degassing over the last two aeons of the planet's history. A further possible modification might be introduced by the effect of very low surface temperatures upon the degassing of water vapour. This is particularly important for Mars, and may be responsible for

the apparent lack of water vapour compared with carbon dioxide.

The degassing of volatiles into a planetary atmosphere does not, of course, imply that they will remain there. In fact, it is reasonable to assume that loss of gases from the atmosphere by escape or condensation into clouds or onto the surface may be equally as important in the evolution as emission. The possible loss mechanisms will be discussed in Section 5.3.

### 5.3 Loss of Gases from the Atmospheric Vapour Phase

The major mechanisms allowing escape of gases from planetary atmospheres have been mentioned above. They are escape, condensation either into clouds, or onto the surface, and chemical reactions between atmospheric gases and the surface. The possibility of chemical reactions taking place will depend both upon the surface temperature and partial pressure of the gas concerned and also upon the planetary surface. Over long periods the loss of volatiles through combination with the surface may be important. For instance it has been suggested by Budyko that buffering of the carbon dioxide in the Earth's atmosphere by surface reactions may be an important effect in temperature calculations. On Mars the removal of water vapour by photodissociation and escape of hydrogen will only continue if the remaining free oxygen is removed - this will probably be by reaction with the surface. Similarly chemical reactions at the Venus surface may affect the atmospheric constituents. The first two of these are difficult to discuss in terms of this model since, as indicated in Section 5.1, it does not readily permit consideration of the vertical structure of the atmosphere. However, the problems of condensation of volatiles either onto the surface or into clouds will be limited to the troposphere, and here it may be possible to estimate temperatures. The important temperature for surface condensation is the lowest surface temperature (the cold-trap temperature) which may be estimated from the global mean temperature,  $T_s$ . The condensation of clouds (solid and liquid) will depend upon both the vertical

distribution of the volatile (about which very little can be said in terms of this model) and the temperature structure. Convection is not considered here and temperature structures determined in terms of radiation alone are readily shown to be unrealistic. It is still interesting to note that the temperature derived in Chapter 2 (see Equation 2.7) as the temperature of the "top" of the atmosphere:

$$T_{TOP} = 2^{-\frac{1}{4}} T_e$$

was calculated, using Eddington's approximation, for zero optical depth. This value may be identified with the stratospheric temperature. The value of  $T_{TOP}$  for present-day Earth is found to be approximately 210 K which is in good agreement with temperatures typical of the tropopause; (above this level the very efficient absorption by ozone increases the temperature indicating the problems of a physical model unable to consider chemical distribution and reactions). It can be seen that the comparison of computed values of  $T_s$  and  $T_{TOP}$  for any model atmosphere will give an approximate description of temperature variation in the troposphere of the planet, if the chemical composition remains constant with height. From this temperature distribution a simple consideration of cloud formation may be possible (Weare and Snell, 1974). This simple cloud condensation model would be an interesting development for planetary climatic modelling (e.g. Henderson-Sellers and Henderson-Sellers, 1975). The effects of changing cloud amount will be discussed later in this section.

The problem of escape of gases from the top of an atmosphere

is difficult to consider in terms of the simple model described here. The brief summary presented here will indicate the secondary importance of escape to the model discussed. Thermal loss of gas is probably the most important mechanism for planetary atmospheres, although it has also been suggested that, for a planet devoid of a magnetic field, sweeping by the solar wind could remove hydrogen. Non-thermal mechanisms (such as the increasing of kinetic energy of atoms by direct irradiation) have been discussed - particularly in connection with the apparent lack of nitrogen on Mars (McElroy, 1972). Escape, rather than removal, from the top of the atmosphere will obviously depend upon the velocities of the atoms and ions. Velocities are a function of the temperature of the exosphere, which, in turn, depends upon the efficiency of absorption and loss of solar energy, and thus upon the chemical composition of the upper atmosphere. Absorption in the thermosphere and exosphere is of extreme ultraviolet radiation by photoionization. Thus high temperatures may be expected for the exospheres of some planetary atmospheres. However, the atoms likely to be lost will depend upon the species able to diffuse high enough into the atmosphere to pass the critical level, above which thermal escape is possible. For instance, in the case of the Earth's atmosphere, the cold trap at the tropopause prevents large amounts of water vapour diffusing into the stratosphere. Similar mechanisms have been postulated for Venus to explain the low mixing ratio of water vapour above the cloud level. It is also possible that the 'trap' which prevents H<sub>2</sub>O diffusing into the high Venus atmosphere

may be chemical rather than physical. For instance large amounts of  $H_2SO_4$  (which has a high affinity for water) in the cloud deck could prevent diffusion (see, e.g. Fink et al., 1972). Escape velocities from the terrestrial planets are given by:

$$v_e = \sqrt{\frac{2g' R^2}{r}} \quad \dots\dots 5.3$$

where  $R$  is the radius of the planet and  $g'$  its gravitational force at the level of escape measured from the centre of the planet,  $r$ .

These are listed in Table 5.1 below.

Table 5.1

Escape Velocities from the Terrestrial Planets

<u>Planet</u>	<u><math>v_e</math> (km/sec)</u>
Mercury	4.3
Venus	10.3
Earth	11.2
Moon	2.3
Mars	5.0

Any species which has atoms in the higher regions of the atmosphere will have a few with velocities in excess of the escape velocity, and thus some will escape from the influence of the planet. The velocity of atoms will, in general, depend upon their mass, and so must be considered in terms of the most probable velocity for the element. This is given, for a Maxwellian distribution, by:

$$v_o = \sqrt{\frac{2kT}{m}} \dots\dots 5.4$$

where k is Boltzman's constant, T the temperature and m the atomic mass. The values of  $v_o$  for three temperatures and three elements are listed below in Table 5.2.

Table 5.2

Most Probable Velocities (for three elements) in km/sec

Atom	Temperature		
	300 K	600 K	900 K
H	2.24	3.16	3.87
He	1.12	1.58	1.94
O	0.56	0.79	0.97

The number of atoms likely to escape over the lifetime of the Solar System is a function of this velocity distribution, and thus escape times may be computed. Table 5.3 below lists the escape times, in years, from the Earth of the three elements considered here.

Table 5.3

Escape Times from the Earth (in years)

(after Brandt and Hodge, 1964)

Exospheric temperature	Atomic species		
	H	He	O
1000 K	$8 \times 10^4$	$4 \times 10^{13}$	$4 \times 10^{51}$
2000 K	$3 \times 10^3$	$3 \times 10^7$	$8 \times 10^{25}$

It is evident from these values that the escape times are highly sensitive to the value of the exospheric temperature. In fact, calculations indicate that the exact values of these unknown parameters are relatively unimportant since only two atmospheric constituents (hydrogen and helium) are likely to have been lost in large amounts from the Earth's atmosphere. It is also important to note that the values given in Table 5.3 were derived for the Earth's atmosphere in its present-day state. The observed exospheric temperatures of Mars and Venus are lower: 350-450 K and 400-650 K respectively. These lower values are probably due to the domination by carbon dioxide, rather than oxygen and nitrogen as for the Earth. It is possible that during the early history of the Earth the temperatures of the upper atmosphere were lower, and consequently escape rates may have been different.

A great deal of work has been done recently on the possible escape mechanisms from atmospheres, particularly in connection with observations of the atmosphere of Venus. It may transpire that loss rates are determined by diffusion processes within the atmosphere rather than by Jean's escape (see, e.g. Hunten, 1973). It seems reasonable to assume, in the context of the model discussed in this work, that loss from the top of the atmosphere falls into one of three categories: i) so rapid that an atmosphere will not develop (e.g. the Moon); ii) approximately equivalent to the degassing rate and thus allowing quasi-equilibrium or iii) negligible compared with the degassing rates, so that evolution is solely determined by the degassing rate. Similar

assumptions have been used by Walker et al. (1970) in a discussion of the deep-mantle degassing rate of both the Earth and Venus. Thus the loss of vapour/gas by condensation (into clouds or onto the surface) will produce a much greater variation in the values computed for the surface temperature than losses from the top of the atmosphere.

Condensation of a major volatile from the atmosphere into clouds or onto the surface is determined by temperature. Cloud formation and its consequences will be discussed later in this section. Condensation onto the planetary surface, as has already been mentioned, will depend upon the lowest local temperature (or cold trap temperature) which will usually be considerably lower than the average global temperature,  $T_s$ . It is important to note that the problems of condensation are unlikely to arise if the planetary surface temperature has remained below the freezing point of the volatile concerned throughout its evolution. A planet which has always had  $T_s$  below 270 K is probably not glaciated, but rather only partially degassed, since water vapour (and, for much lower values of  $T_s$ , carbon dioxide also) will not escape from the surface layers. Such a "sub-surface glaciation" will evolve into a more hospitable environment as the surface temperature increases. This picture simplifies the evolutionary sequence by requiring that the non-degassed volatiles take little or no part in the feedback loops (i.e. in albedo modification or surface partial pressures). Once surface temperatures rise high enough to liberate large amounts of carbon dioxide and, later, water vapour then this liberation,

probably over large areas of the planetary surface, will rapidly modify the average surface temperature by infrared absorption. The surface condensation of volatiles will be determined by the new average and local temperatures, but the partial vapour pressure remaining (and thus further modifying the temperature) will itself be a function of the amount of condensation which takes place. The feedback loops are seen to be highly complex. However, over long time periods (i.e. of the same order as the life-time of the planet) many, if not all, of these rapid oscillations can be ignored, so revealing the general temperature trends. The present-day partial pressure of both carbon dioxide and water vapour on Mars is believed to be buffered by the polar caps and also by sub-surface ice deposits (see, e.g. Leighton and Murray, 1966).

The surface temperature curves developed in Section 5.4 will assume a volatile to be absent (or almost absent) until the temperature is high enough (over most of the planet) to liberate significant amounts from the sub-surface layers. Once there is an established partial pressure of a volatile, it is possible that some may condense onto the surface (probably initially in polar regions), altering the albedo and the surface infrared emissivity (as has been described in Chapter 3). It is important to note that even if the global average temperature is suitable for condensation of a volatile, topography and local temperature variations will limit the areas of condensation (as is the case for liquid water on the Earth and carbon dioxide ice on Mars). Thus the likelihood of a totally glaciated planet developing seems

small.

Cloud formation is a function of both the temperature profile of the atmosphere and the vertical distribution of the volatiles. The effect of clouds upon global climatic change has been believed to be of the utmost importance, as discussed in Chapter 3 (Section 3.6). However, very recently, computations seem to have indicated that the two roles of clouds in the climatic regime may be mutually compensatory (Cess, 1976): that is, there may be a balance between their highly reflective property and their efficient thermal absorption. This possibility is illustrated by a simple modification of the calculation of Schneider (1972).

Schneider considers the effect of changing cloud amount (i.e. percentage cloud cover),  $A_C$ , upon the global surface temperature. The total outgoing infrared flux, denoted by  $F_{IR}$ , is calculated from a model atmosphere for various values of cloud top height and cloud cover. This outgoing flux is compared with the absorbed solar flux,  $Q_{ABS}$ , which is also a function of the total cloud cover, since this modifies the planetary albedo.

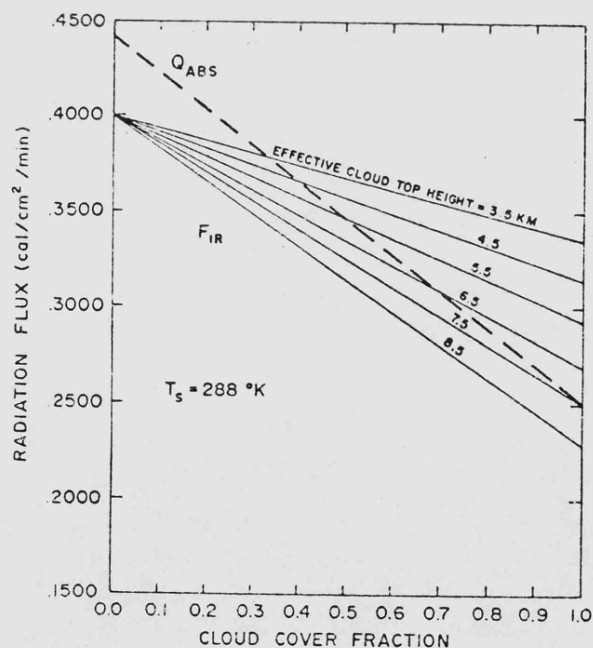
Figure 5.1 lists the parameters used in the paper to define the standard atmosphere, and also illustrates the curves derived for  $F_{IR}$  and  $Q_{ABS}$ . It will be noted that for the present-day values of  $A_C = 0.5$  and cloud top height = 5.5 km the curves intersect, implying a balance between incoming and outgoing radiation.

However, from these curves Schneider develops the theory that even a small increase in cloud cover must lead to non-equilibrium conditions, and thus (for a constant atmosphere) to a decrease in

Figure 5.1

TABLE 1. Parameters used for the global-average model atmosphere.

Parameter	Value
Surface temperature ( $T_s$ )	288K
Surface pressure ( $p_s$ )	1013 mb
Tropospheric lapse rate ( $\partial T_s / \partial z$ )	-6.5K km <sup>-1</sup>
Stratospheric temperature	218K
Relative humidity, surface	75%
Vertical distribution of water vapor mixing ratio ( $w_z$ )	$w_s (p_t / p_s)^4$
CO <sub>2</sub> amount	300 ppm



The infrared flux to space,  $F_{IR}$ , emitted from the earth-atmosphere system (described in Table 1) and the absorbed solar energy,  $Q_{ABS}$ , as a function of amount of cloud cover and for several values of effective cloud top height.

(after Schneider, 1972)

Note the different gradients of the emitted flux functions,  $F_{IR}$ , and the absorbed energy function,  $Q_{ABS}$ .

the average surface temperature. The values of  $F_{IR}$  are model-dependent and a function of the cloud cover,  $A_C$ . Schneider finds that

$$\frac{\partial F_{IR}}{\partial A_C} \approx -0.107 \quad \dots \dots \quad 5.5$$

The functional relationship between the value of  $Q_{ABS}$  and  $A_C$  is simple; we have:

$$Q_{ABS} = \frac{Q_{SC}}{4} (1 - \alpha_p) \quad \dots \dots \quad 5.6$$

where  $Q_{SC}$  is the solar flux at the top of the atmosphere and  $\alpha_p$  is the albedo of the Earth, which is given by:

$$\alpha_p = \alpha_C A_C + \alpha_S (1 - A_C) \quad \dots \dots \quad 5.7$$

Schneider chooses values for the cloud albedo,  $\alpha_C$ , and the clear sky albedo,  $\alpha_S$ , of 0.5 and 0.12, respectively. He then derives the curve for  $Q_{ABS}$  given in Figure 5.1. These values seem to be arbitrarily chosen. A more appropriate value for  $\alpha_S$  (which is really the albedo of a cloudless Earth, rather than a "clear sky" albedo) is 0.20 (see Section 3.5 of Chapter 3, which discusses, at length, computations of such surface albedos for the Earth and Mars). To achieve the global albedo of 0.31, which is required by this model for  $F_{IR} = Q_{ABS}$  at the present-day values, we must choose  $\alpha_C = 0.42$ . This value for cloud albedo is not unreasonable if it is noted that the cloud modelled is an "effective cloud" which replaces clouds of all heights and types. The value of  $Q_{ABS}$  now derived differs widely from that

of Schneider. We find:

$$\frac{\partial Q_{\text{ABS}}}{\partial A_C} = -0.11 \quad \dots\dots 5.8$$

which compares favourably with the value of -0.107 for  $\partial F_{\text{IR}} / \partial A_C$ . Also the curve for  $Q_{\text{ABS}}$  lies almost exactly on that derived for  $F_{\text{IR}}$  for a cloud top height of 5.5 km. This simple modification of Schneider's original calculation (using more reasonable values of albedo) seems to indicate a much more stable regime, for the present-day Earth, at least. The variation in global albedo caused by increasing the cloud cover seems to be almost entirely compensated for by the change in the infrared radiation budget.

Although this and other similar calculations indicate that the two large feedback effects of cloud cover variations (albedo variation and infrared flux variation) are certainly in opposite directions and probably of the same magnitude, another variation, cloud cover, the cloud height, may be found to greatly affect the radiation budget. Schneider's model produces a lowering of surface temperature for a decreased cloud height (even with the modification in albedo values described above). Meteorologists are particularly interested in the effect upon the atmospheric heat balance of high Cirrus clouds (e.g. Hunt, 1976). The variation in cloud height is a function of the tropospheric temperature gradient and the vertical distribution of volatiles, neither of which are derivable from the model developed here. Over very long periods it may be found that even this cloud feedback mechanism is compensated by others: certainly

nothing can yet be said about the magnitude of such a feedback on a global scale.

This discussion of the loss mechanisms of gases from the atmospheres of the terrestrial planets has been, in general, qualitative. Loss from the top of the atmosphere has been considered, and will no doubt be invoked as an explanation for the apparent lack of water on Venus for many years to come. It is probably not an important factor in surface temperature trends. Cloud formation, once believed to be an important factor in the calculation of surface temperature, may in fact, be found to produce mutually compensatory feedback loops. Thus it seems that surface condensation and, particularly, polar cap formation with consequent modification of global albedo may be the primary forcing function for surface temperatures. The calculation of planetary albedos for various surface types and distributions was discussed in Chapter 3. These calculations will be utilized in the following section.

#### 5.4 Surface Temperature Calculations

The model derived in this work was designed to compute average planetary surface temperatures over the whole life-time of the Solar System, and to permit extension of these calculations into the future. The model is based upon a number of computer programs which were written to solve Equation 5.1 iteratively for  $T_s$ . The main program (TSUR) which calculated the temperature has already been described in Chapter 2, and its accuracy has been discussed. It was also necessary to transform the fractional transmission spectra produced by the calculations from laboratory data described in Chapter 4 into a step function. The numerical methods used for this were also discussed in Chapter 2. However, a most important facility of the suite of programs has not yet been described. This is the subprogram which permits the transmission spectrum of a total atmosphere, rather than only one gas, to be constructed.

Model atmospheres composed of a number of absorbing gases and a neutral (broadening) gas will be considered. In Chapter 4, the dependence of the fractional absorption of each band upon the effective pressure,  $P_e$ , was given. This pressure term included the broadening effect of other gases upon the spectral lines of the gas considered. Thus for any given atmospheric composition the fractional transmission spectrum may be calculated for each absorbing gas. The combination of all these individual spectra into one which represented the absorption properties of the whole atmosphere was a complex operation, requiring a numerical solution.

The program which allowed the transmission functions to be combined, utilized the multiplicative property of transmissions. This property has been demonstrated experimentally for overlapping bands of carbon dioxide and water vapour by Burch, Howard and Williams (1956). The relation between the fractional transmissions,  $T_\nu$ , of two components of a gaseous mixture and the resulting total transmission of the mixture is given by:

$$T_\nu(1,2) = T_\nu(1) \times T_\nu(2) \quad \dots \dots \quad 5.9$$

This is illustrated by the observed fractional transmission variation with frequency of carbon dioxide and water vapour separately, and their combined transmission curve shown in Figure 5.2 (after Burch, Howard and Williams). The experimental results obtained by Burch, Howard and Williams showed that at low pressures the broadening effect of carbon dioxide upon water vapour was similar to that of nitrogen. Theoretical calculations by Goody (1964) have indicated that the multiplication property is valid whenever absorption by two different gases is involved. It was therefore felt reasonable to extend the use of this property to permit the simple calculation of the fractional transmission at any wavelength by multiplication of the transmissions due to all the absorbing gases. This formulation was preferred to use of the empirically derived function linking the total absorption over given frequency intervals to the observed absorption for individual components (given by Burch et al.), since these results did not allow for the addition of either carbon monoxide or methane to the model atmosphere.

Figure 5.2

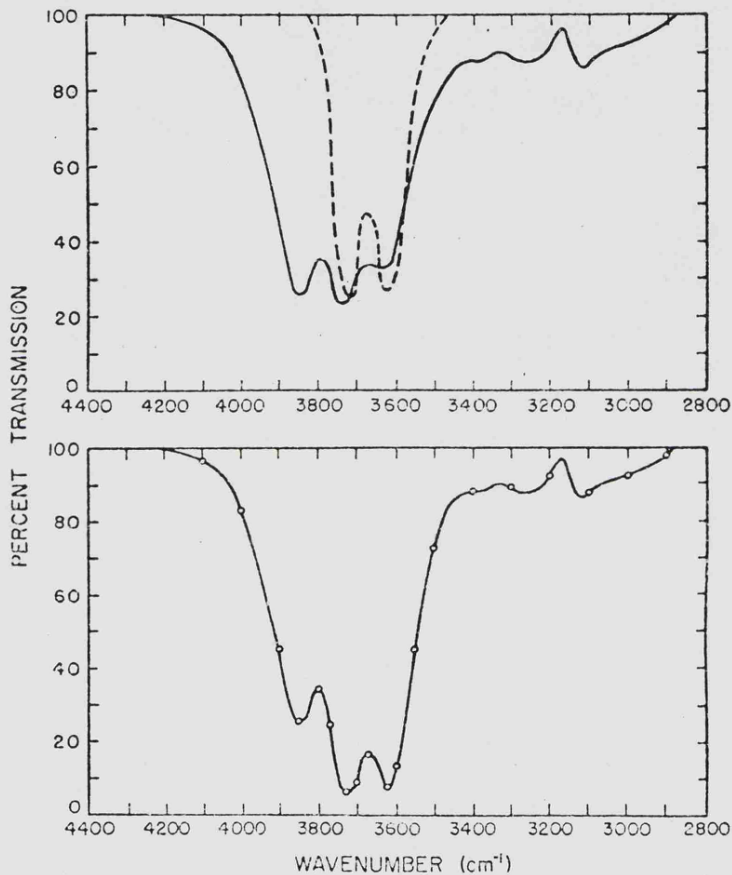


FIG. 4.1. The multiplication property of band transmission at low resolution. The upper spectra are those for CO<sub>2</sub> and H<sub>2</sub>O individually. The lower spectrum is for the mixture; the full line is observed and the points are obtained by multiplying the two transmissions in the upper panel. Path length 88 m, H<sub>2</sub>O pressure 5 mm Hg, CO<sub>2</sub> pressure 4 mm Hg. The total pressure is made up to 140 mm Hg with nitrogen. The dilution is sufficient for interaction between absorbing molecules to be neglected. After Burch, Howard, and Williams (1956).

Multiplication property of band transmission,  
(after Goody, 1964).

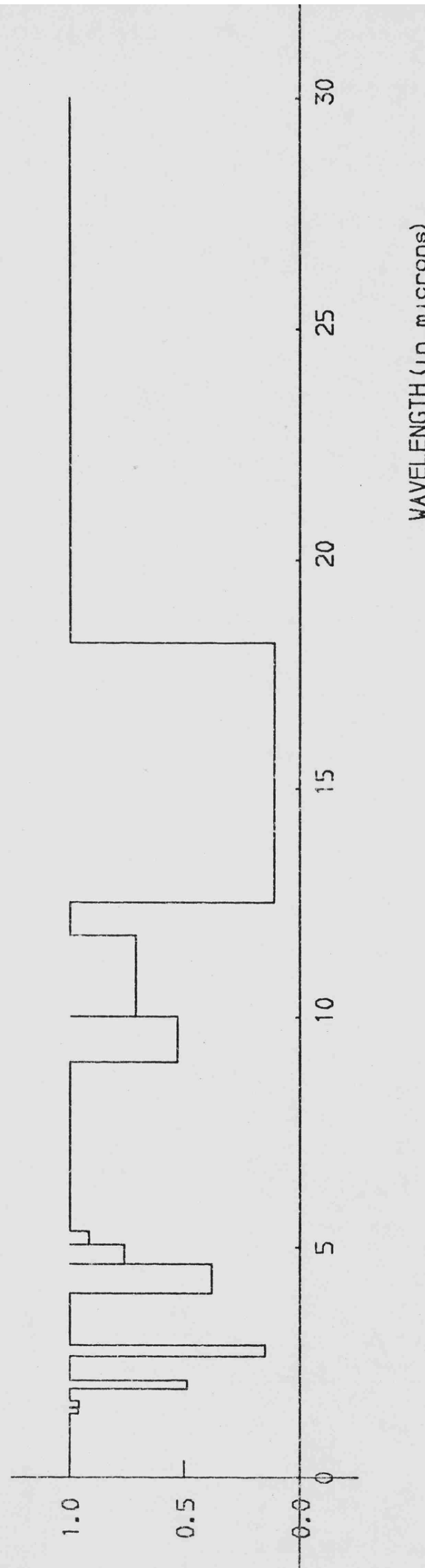
The computer program (TWO) required input data which listed the components of the atmosphere (any or all of the absorbing gases considered here: water vapour, carbon dioxide, carbon monoxide and methane and a neutral gas) and the partial pressures of each. From this, the effective pressure and absorber concentration of each gas was computed, and, hence, the absorption spectrum of each (using the formulae derived in Chapter 4). The fractional transmission spectra were combined sequentially. The overlapping of bands produced a much more fragmentary spectrum than for a single gas, as is illustrated by Figures 5.3 - 5.7. Once the total atmospheric transmission spectrum had been produced the computation continued as described in Chapter 2. The step-function approximation was produced (e.g. Figure 5.8), so the value of  $T_s$  could be calculated. A second iteration was required, since bands near the peak of the Planck curve were re-centred to ensure that the total energy remained constant. This final addition to the program library, developed over the three years, permitted the calculation of  $T_s$  for a planet having known atmospheric composition. Thus the degassing sequences and chemical modifications of the atmosphere could now be included in the surface temperature calculations.

A number of the results produced by the computer programs have already been listed. The discussion of the accuracy, and so the usefulness of the method employed (in Chapter 2) included calculations of the present-day surface temperature of the Earth, and the effect upon global temperatures of increasing the carbon dioxide amount (see Section 2.6 especially). Chapter 3 has used

Figure 5.3

$\text{CO}_2$  ( $P_s = 20 \text{ mb}$ ) TRUE SPECTRUM

TRANSMISSION



236.

Figure 5.4  
 $H_2O$  ( $P_s = 1 \text{ mb}$ ) TRUE SPECTRUM

TRANSMISSION

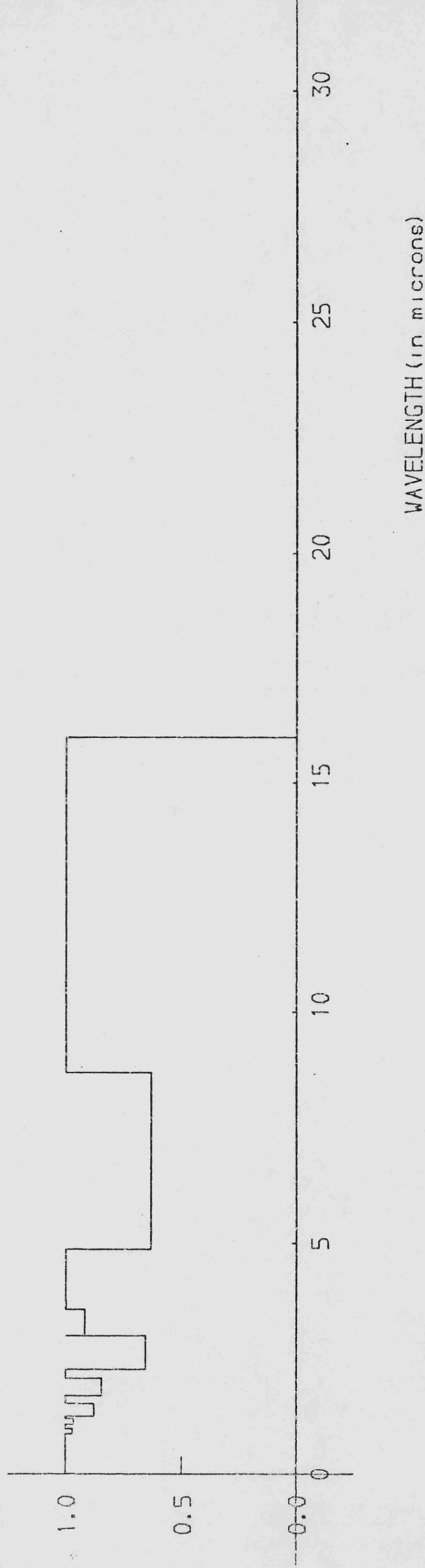
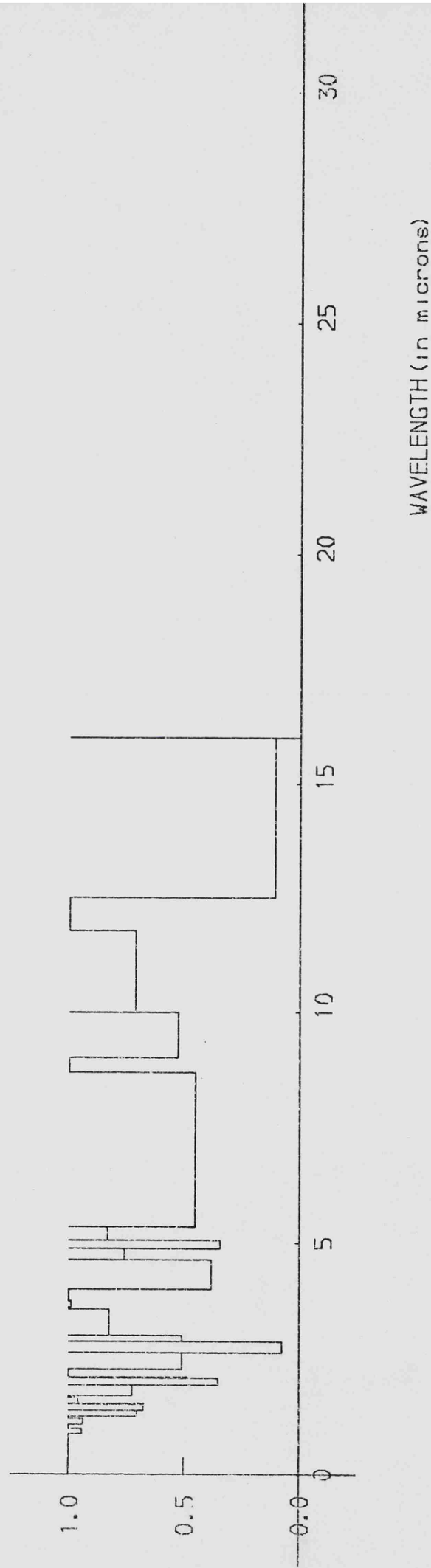


Figure 5.5

COMBINATION OF  $\text{CO}_2$  ( $P_s = 20.0 \text{ mb}$ ),  $\text{H}_2\text{O}$  ( $P_s = 1.0 \text{ mb}$ ) TRUE SPECTRUM

TRANSMISSION



Combined transmission spectrum produced by the computer program TWO. Compare with Figures 5.3 and 5.4.

Figure 5.6

$\text{CH}_4$  ( $P_s = 0.1 \text{ mb}$  [absorber] +  $20.0 \text{ mb}$  [broadener]) true spectrum

TRANSMISSION

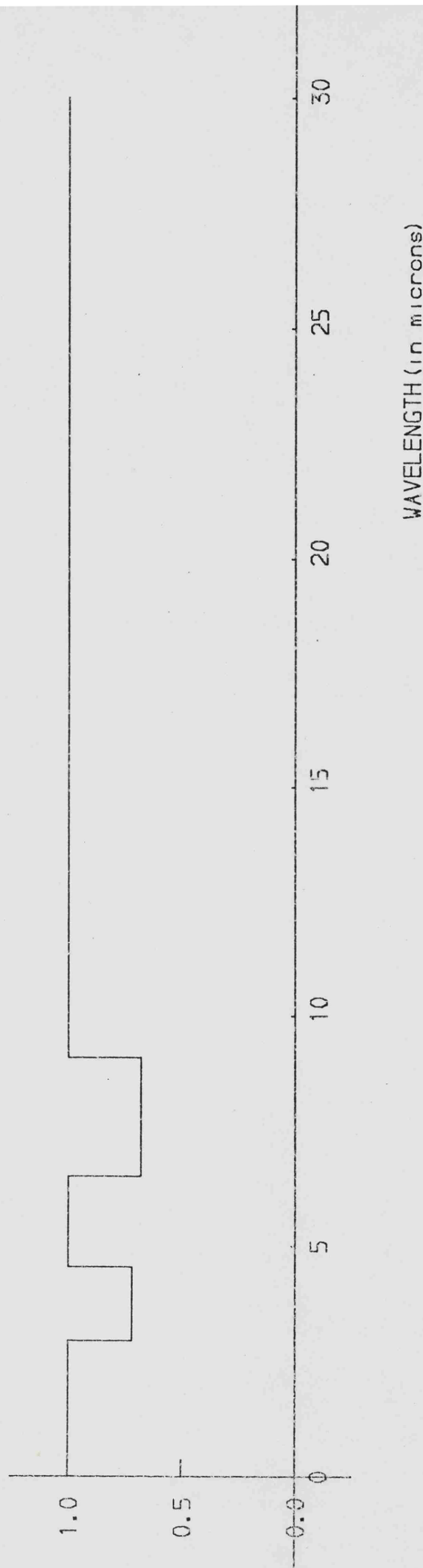
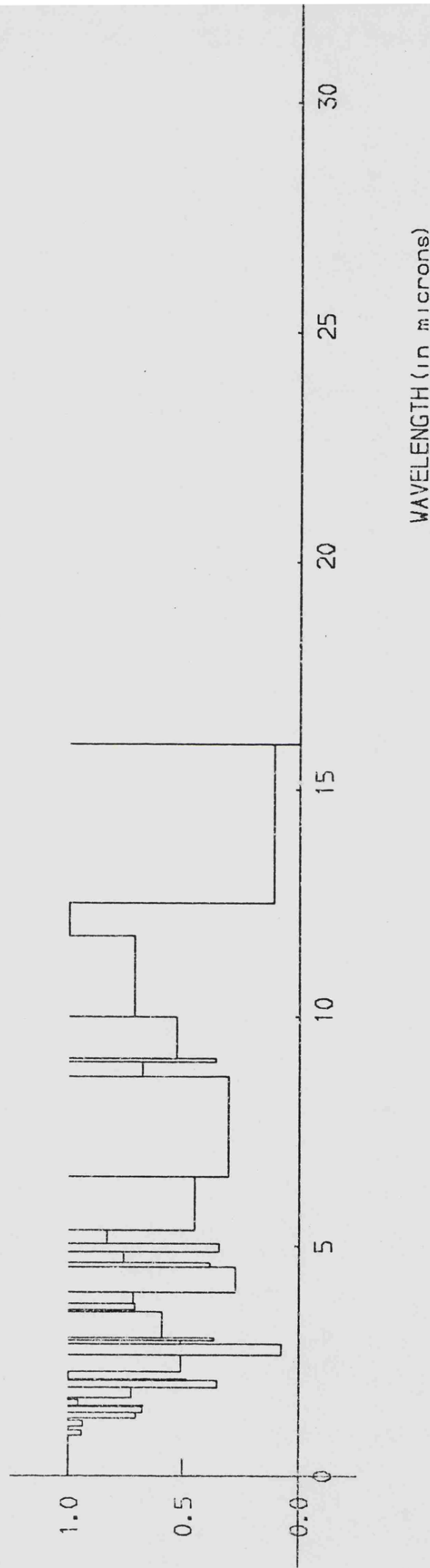


Figure 5.7

COMBINATION OF  $\text{CO}_2$  ( $P_s = 20.0 \text{ mb}$ ),  $\text{H}_2\text{O}$  ( $P_s = 1.0 \text{ mb}$ ) &  $\text{CH}_4$  ( $P_s = 0.1 \text{ mb}$ ) TRUE SPECTRUM

TRANSMISSION

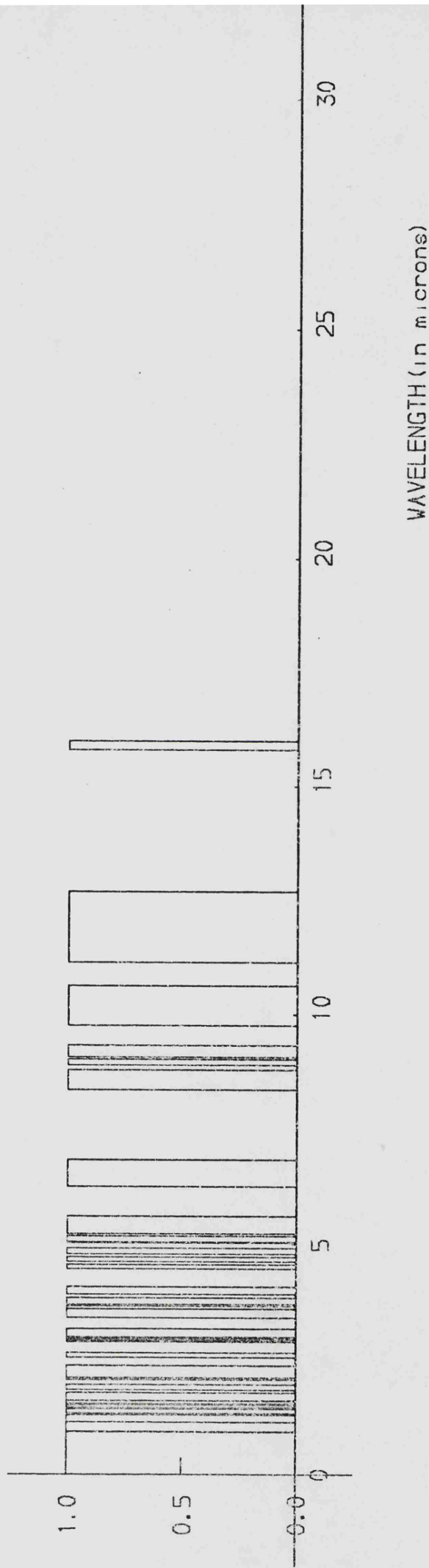


240.

Typical atmospheric transmission spectrum produced by the computer program TWO. This combines the individual absorption features shown in Figures 5.3, 5.4 and 5.6.

Figure 5.8  
COMBINATION OF  $\text{CO}_2$  ( $P_s = 20.0 \text{ mb}$ ),  $\text{H}_2\text{O}$  ( $P_s = 1.0 \text{ mb}$ ) &  $\text{CH}_4$  ( $P_s = 0.1 \text{ mb}$ ) STEP FUNCTION

TRANSMISSION



Step function approximation from the transmission spectrum in Figure 5.7

approximate temperature increments to illustrate temperature trends forced by variations in both the albedo and the flux factor of a planet with an evolving atmosphere.

The results presented in this chapter will attempt to model the evolution of a "typical" terrestrial planetary atmosphere. This will be assumed to be dominated by carbon dioxide in its earliest stages, and possibly throughout its evolution. The reasons for this have been indicated throughout this work. They are primarily that two out of the three terrestrial planets have considerably more carbon dioxide present in their atmospheres than any other gas. The evolutionary track of the Earth has certainly been atypical since the development of the biosphere (approximately  $2 \times 10^9$  years ago), and may not be representative of the terrestrial planets at all. It is, of course, vital to note that there may not be any justification for attempting a study of a typical terrestrial planet, since the mode of formation and solar distance may have removed all similarities between the planets. This, I feel, is probably not the case. Most models of the formation of the Solar System consider the condensation of the terrestrial planets as a sequence of closely linked events; and the most widely accepted mechanism explaining formation of the surfaces, atmospheres and remaining debris (meteors and comets) seems to be the final infall of carbonaceous material to all the accreting planets. This would imply a strong similarity between the atmospheres of the terrestrial planets. The other important factor is the solar-planetary distance (which is unlikely to have

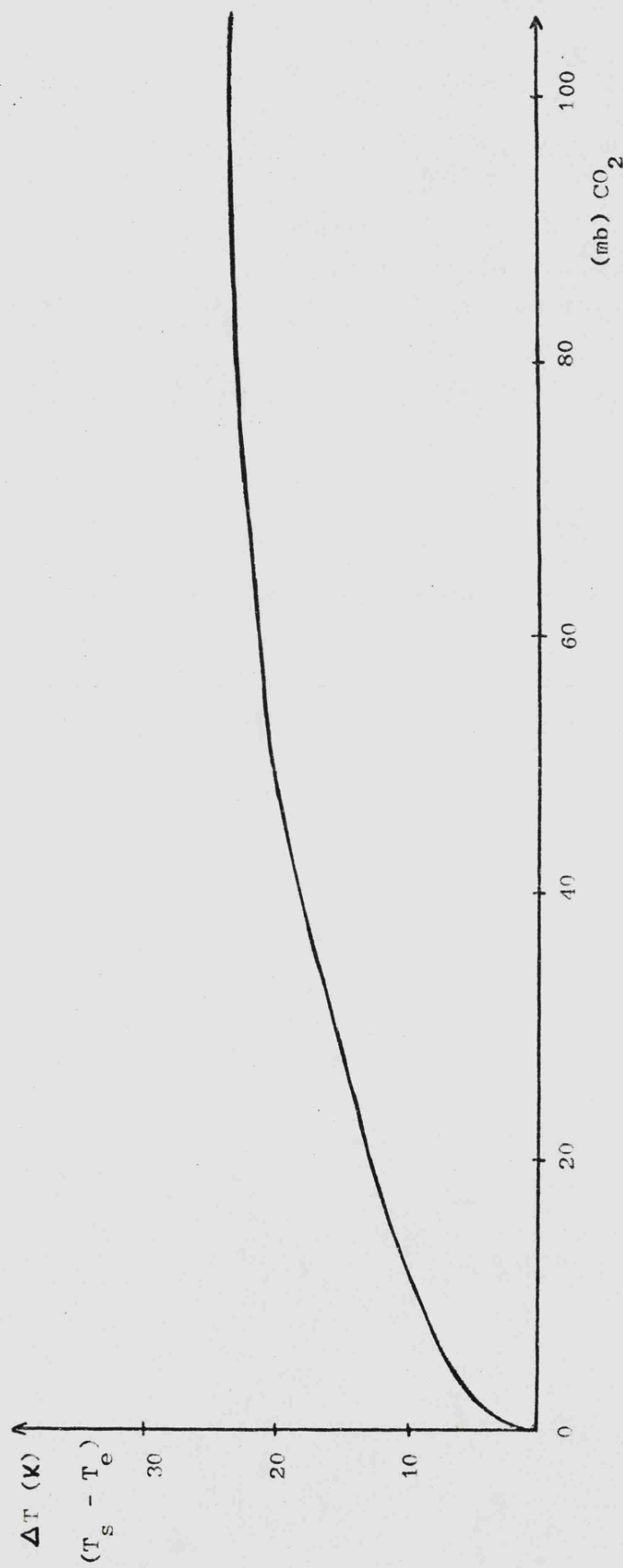
undergone anything more than cyclic fluctuations since the atmosphere began to evolve) and the solar luminosity. Chapter 1 discusses possible evolutionary tracks for the Sun. The most widely accepted theory still seems to be the traditional model of stellar evolution, implying a steady increase in luminosity of the Sun of approximately 43 per cent over the lifetime of the planets. This will be assumed for all the following calculations, except where otherwise indicated. It is important to note that this variation in luminosity, whilst a major forcing function for the atmosphere, is only input data for the computer programs, and so could be readily modified in the light of any further developments. Once the most probable evolutionary sequences, based upon carbon dioxide and monotonically increasing solar luminosity, have been considered, results can be computed for other possible regimes (e.g. early steam atmospheres, highly reducing atmospheres and constant solar luminosity).

Carbon dioxide is not as important an absorber in the infrared as water vapour, since it possesses no pure rotation band. However, its freezing point (approximately 140 K) is considerably lower than that of water and (in general) it passes from solid to gas without a liquid phase. Thus, on any terrestrial planet with a surface temperature less than 273 K, the predominant gas in the atmosphere will be carbon dioxide. This is true for Mars, and would have been the case for the Earth also, if surface temperatures had not permitted the condensation of liquid water, followed by the solution of CO<sub>2</sub>. The most useful evolutionary sequence to follow is therefore that for a planet which develops

a carbon dioxide atmosphere. How such an evolution is modified by the other parameters involved in the surface temperature calculation will be described below.

Figure 5.9 illustrates the greenhouse temperature increments produced by surface pressures of a pure carbon dioxide atmosphere ranging from zero to 100 millibars for temperatures in the region  $T_s \approx 250$  K. These are the temperature increments likely to occur on a planet early in its atmospheric evolution. The curve is in good agreement with the present-day situation on Mars which has an almost pure carbon dioxide atmosphere of between 5 and 12 millibars surface pressure, giving rise to a greenhouse increment (averaged over the whole planet) of between 5 K and 10 K. The gradient of this temperature curve drops to almost zero as the surface pressure nears 100 millibars. This is because the dominant 15 micron band is fully absorbed, and the other weaker bands are able to produce only slight further temperature increases. It is also important to note that in this pure carbon dioxide atmosphere only the effects of self-broadening are considered. If the carbon dioxide were a minor absorbing constituent in a predominantly neutral atmosphere, the curve would be modified by further broadening (computed from the dependence of the band absorption upon the effective pressure term). The evolution of the surface temperature of a model planet will depend upon its initial temperature. In the temperature range where planetary degassing activity is expected (approximately 200 K to 300 K), two initial effective temperatures have been considered: Model I with  $T_e = 200$  K and Model II with

Figure 5.9

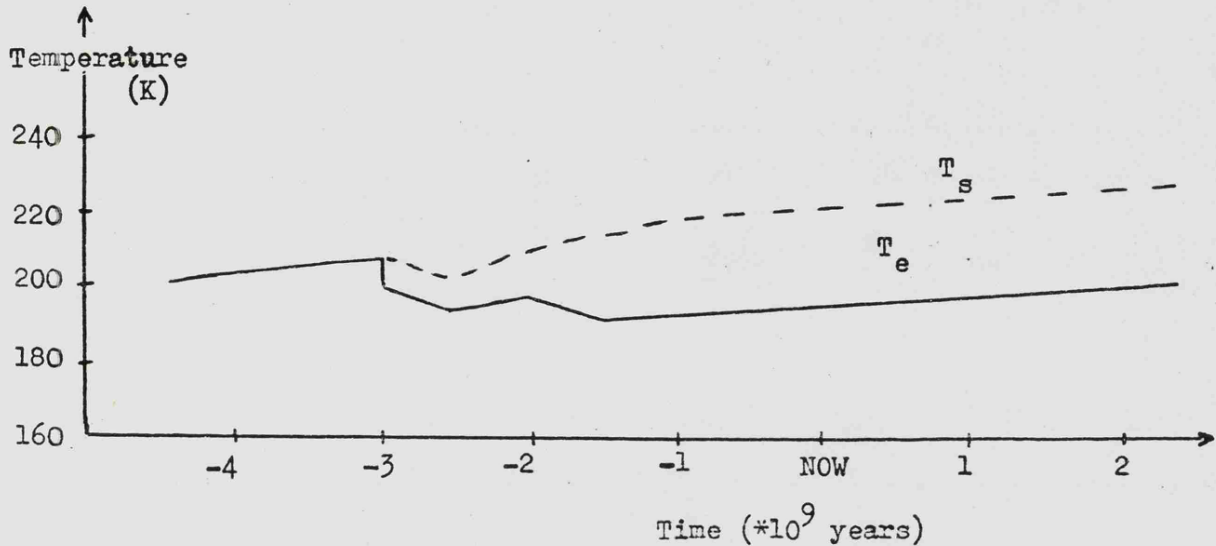


Temperature increment ( $T_s - T_e$ ) calculated by TSUR for a planet with a pure carbon dioxide atmosphere. Note the change in gradient as the surface pressure increases.

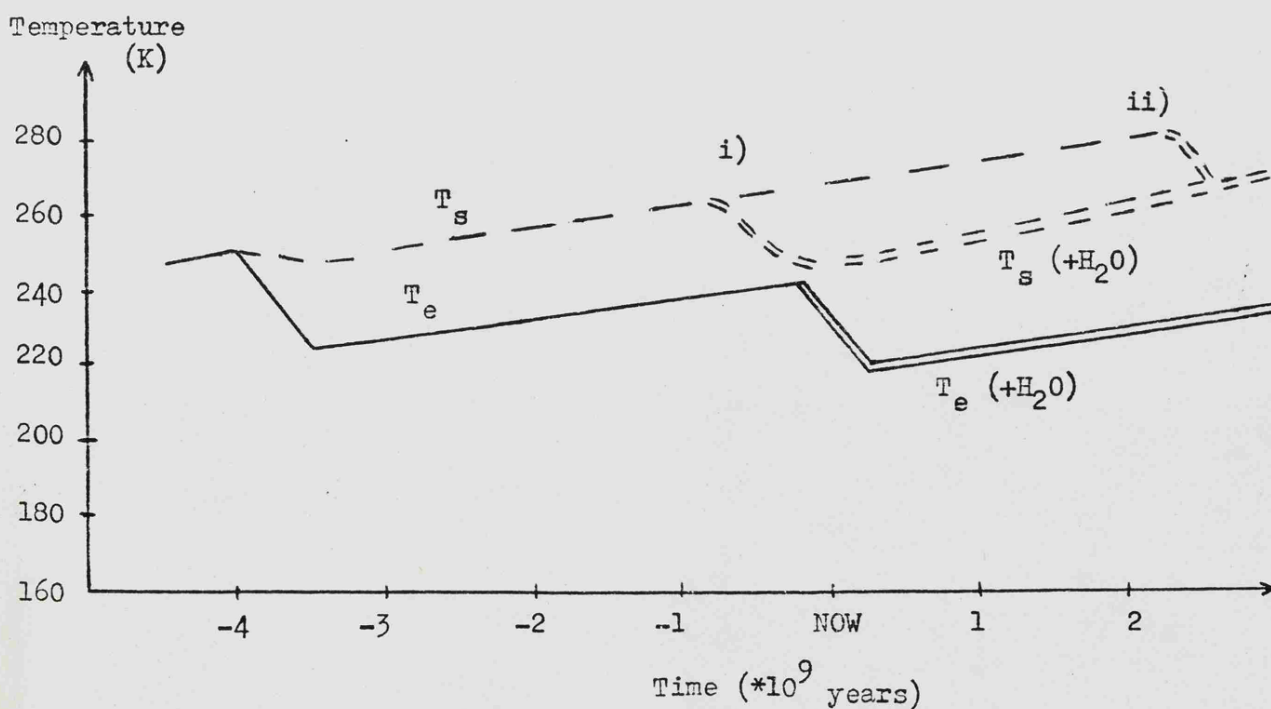
$T_e = 250$  K. (Initial values of  $T_e$  of the order of 300 K would imply a water vapour dominated atmosphere from the start). Both model planets have been assumed to form without an atmosphere and with a rotation rate similar to that of the Earth or Mars today. Thus they initially have values of  $f = 2$ ,  $e = 0.93$  and  $A = 0.07$ . These parameters, together with the chosen initial effective temperature ( $T_e$ ), define the incident solar flux at the planet 4.5 aeons ago, and so, in a sense, its distance from the Sun. The solar luminosity has been assumed to have increased by 43 per cent over 4.5 aeons. The curves of effective temperature,  $T_e$ , and average surface temperature,  $T_s$ , were then computed for each model.

Figure 5.10 shows the resulting temperature curves for the two model planets. The results are particularly interesting as they demonstrate the importance of the initial temperature for the atmospheric evolution. Model I fails to achieve surface temperatures high enough to initiate degassing of water vapour, and so the greenhouse increment is, at most, only 22 K caused by carbon dioxide absorption (see Figure 5.9). Even a further aeon into the future the surface temperature has only just risen above 220 K. Model II is probably able to degas carbon dioxide soon after its formation and, by the present day, may have water vapour in its atmosphere although its average surface temperature is still below the freezing point of water. This model planet will presumably evolve an Earth-like atmosphere, hydrosphere (and possibly biosphere!) at a time several aeons into the future. Another interesting point derived from these models is with

Figure 5.10

Model I

Surface and effective temperature curves for Model I. Carbon dioxide is degassed approximately 3 aeons ago causing a temperature increase.

Model II

$T_s$  and  $T_e$  curves for Model II. The single curves are for atmospheres of  $\text{CO}_2$  and the double curves are for  $\text{CO}_2 + \text{H}_2\text{O}$  atmospheres. Two possible values of surface temperature are indicated for the degassing of water vapour into the atmosphere: i)  $T_s \approx 265\text{K}$  and ii)  $T_s \approx 285\text{K}$ . Note the very slow temperature increase under the

reference to Mars. The choice of an initial effective temperature for Model II of 250 K actually leads to a planet positioned between the Earth and Mars (but closer to Mars). Thus its evolution may well be mimicked by Mars at some later epoch. These two model calculations seem to indicate that any terrestrial planet (starting life far enough from the Sun to ensure an initial  $T_e \approx 260$  K) will evolve in a similar way modified only by the solar distance. This generalization, of course, assumes that both carbon dioxide and water vapour are available to be degassed.

Both curves are necessarily affected by the increasing solar luminosity, but any degassing (which enhances the greenhouse effect) will produce increases in the values of both  $A$  and  $f$  and, consequently, decreases in the effective and surface temperatures. The precise values of  $A$ ,  $f$ ,  $e$ , and the absorption properties of the atmosphere are difficult to establish at a single point in time. Since the effective temperature is really a mathematical concept rather than a physical temperature (see Chapter 3), it has been allowed to be discontinuous as changes in  $e$ ,  $A$  and  $f$  occur. The surface temperature would also respond to these changes in parameter values, but the curves on Figure 5.10 have been smoothed. This may not be a realistic representation of the time period required for an increasing atmosphere to cause changes in  $A$ ,  $f$  and  $e$ , but the resulting temperature trends are reasonable. Sudden (say over time periods less than  $10^8$  years!) changes in the surface temperature may be the cause of surface features (freeze/thaw effect) and possibly glacial periods.

The double lines on the curves for Model II indicate the evolutionary trend with water vapour in its atmosphere. This addition produces an increase in  $A$  and  $f$  and a consequent decrease in  $T_e$  and  $T_s$ ; but the greenhouse increment (even for vapour pressure over ice) caused by water vapour is considerable, so the surface temperature increases rapidly. Two possible tracks have been illustrated: i) degassing of water vapour when an average surface temperature of 265 K is achieved, and ii) degassing for  $T_s \approx 285$  K. It is clearly seen that the precise  $T_s$  value at which water vapour is degassed is a particularly important parameter.

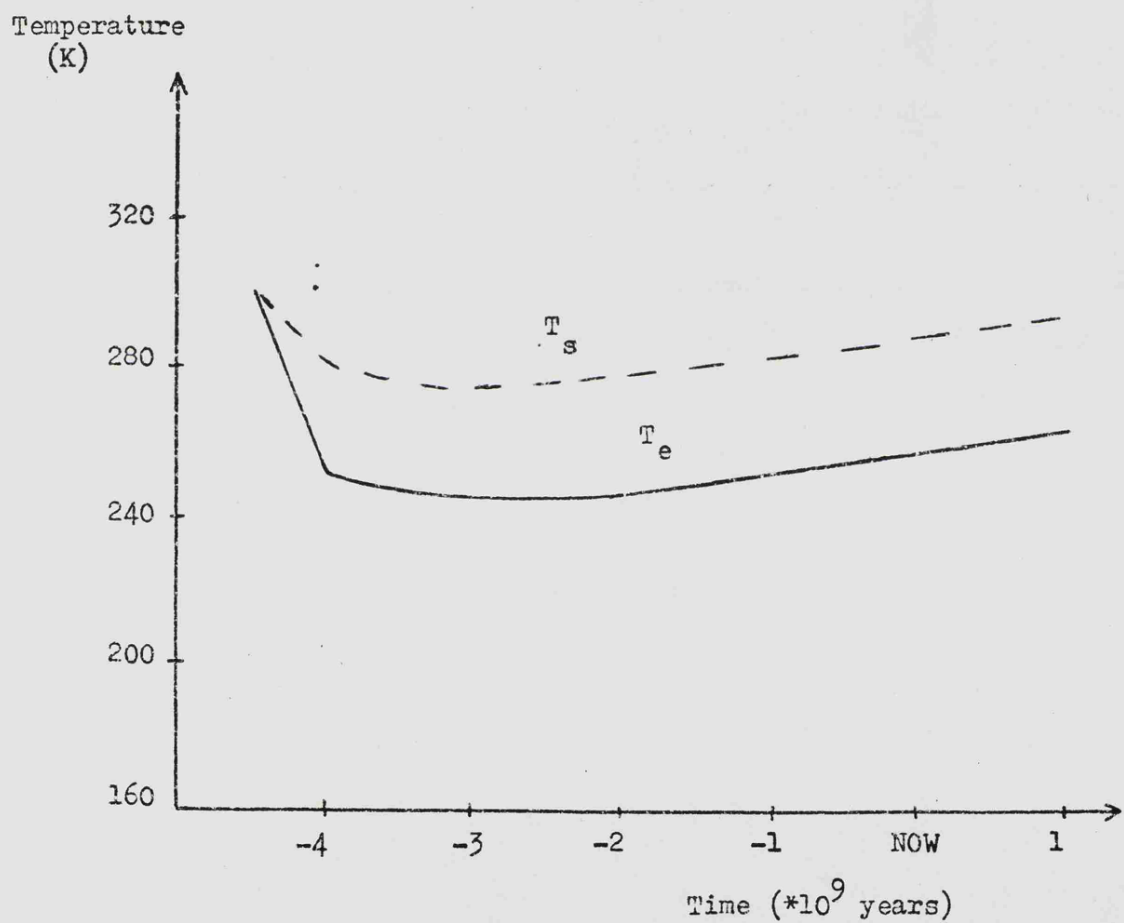
The possible variations of all the parameters permit the discussion of the evolutionary sequence for each of the terrestrial planets. Mars and the Earth have already been considered in Chapter 3. The calculations of the possible evolutionary tracks for the surface temperature of Mars allowed for different degassing rates. This consideration is more appropriate for carbon dioxide than water vapour since once surface temperatures are high enough to allow evolution of water vapour into the atmosphere the enhanced greenhouse effect which results must imply high values of both albedo and flux factor. Under these circumstances feedback mechanisms will be at least as important as the degassing rate. Figures 3.12 and 3.13 illustrate the probable evolutionary tracks for Mars in detail. The calculation of surface temperatures for the Earth is performed in the same way as those for the model planets I and II. The standard solar luminosity evolution (as discussed previously) is assumed and the initial effective temperature of an atmosphere-less

Earth is calculated for values  $A = 0.07$ ,  $f = 2$  and  $e = 0.93$ .

This gives a starting temperature for the Earth of almost 300 K (as illustrated in Figure 5.11), and consequently implies a rapid degassing of both carbon dioxide and water vapour. The probable evolutionary tracks of  $T_e$  and  $T_s$  shown in Figure 5.11 stabilize within an aeon of the degassing, and have probably remained stable since 3.5 aeons ago. The early drop in both  $T_e$  and  $T_s$  is caused by the rapid increase of both  $A$  and  $f$  in response to the atmospheric build-up. From 3.8 aeons ago the absorption spectrum would probably be dominated by water vapour. It has been assumed that  $f$  takes a value of 4 from 4 aeons ago.  $T_e$  has been drawn discontinuous (as with previous figures) indicating the change in albedo value. Initial degassing would lead to an albedo increase, but the lowered surface temperatures would probably mean that polar caps were dominating the variation in  $A$  rather than cloud amount. The albedo does not reach its present-day value of 0.33 until 2 aeons ago. The smoothed surface temperature curve illustrates the important compensatory effect of an increasing albedo and solar luminosity. This has already been discussed and demonstrated in Chapter 3 (see especially Figure 3.11). The  $T_s$  curve never drops below 276 K. Thus it has been shown that a reasonable variation in all the parameters does not lead to a global glaciation at any stage during the evolution of the Earth. A further possible modification for this calculation is the variation caused in the value of  $f$  by the capture of the Moon (see Section 3.10 and Figure 3.14).

The problems of attempting to describe the evolution of the

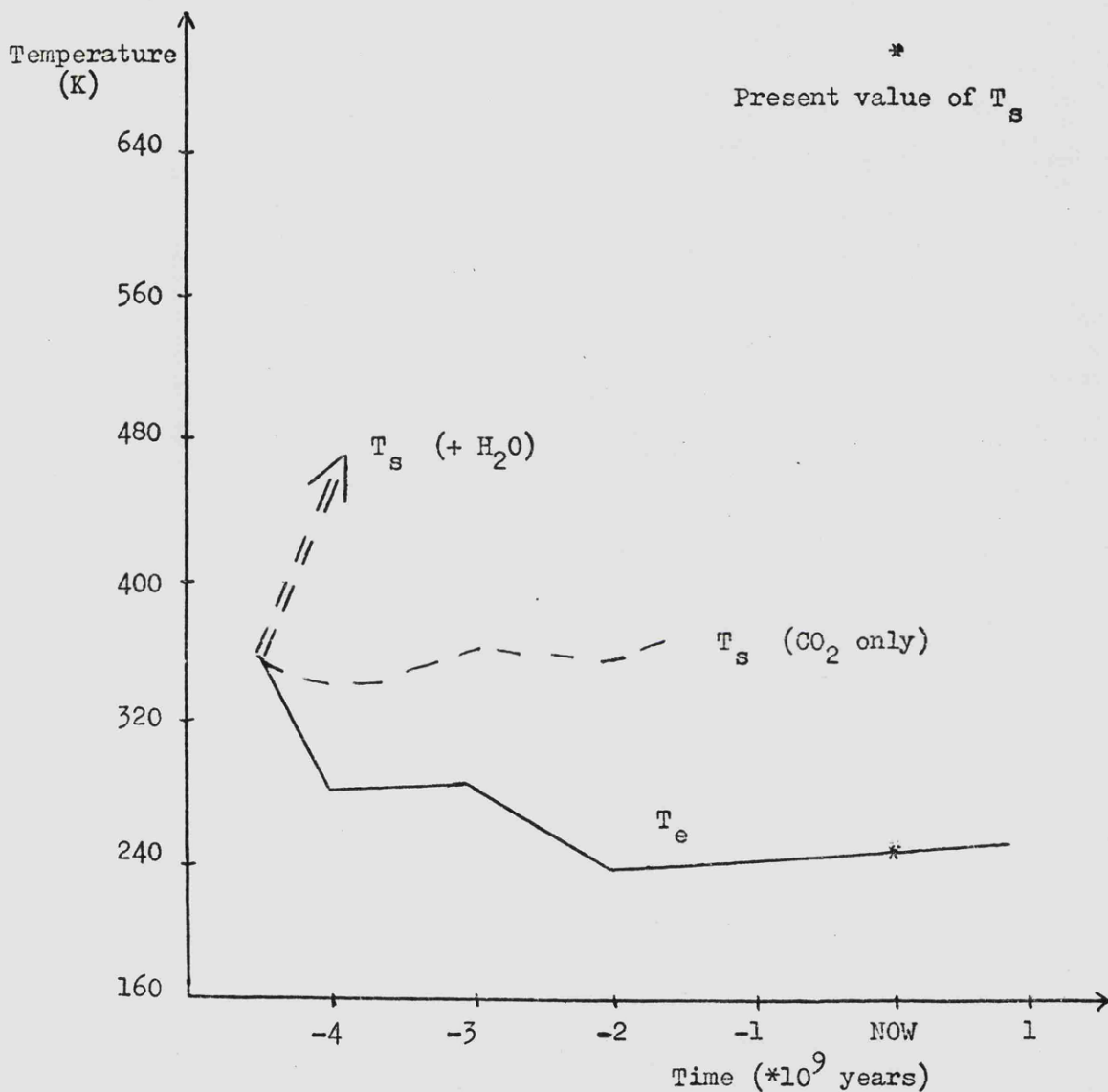
Figure 5.11



Probable evolutionary tracks of  $T_s$  and  $T_e$  for the Earth.  
 A high initial value of  $T_e$  leads to rapid degassing of both  $\text{CO}_2$  and  $\text{H}_2\text{O}$  and thus to rapid alterations in the albedo, flux factor and atmospheric absorption. The temperature is seen to stabilize within an aeon;  $T_s$  remains above 273 K.

surface temperature and atmosphere of Venus are immense. It is known to have very high surface temperatures ( $\sim 700$  K) and a high albedo ( $A \approx 0.7$ ) due to total cloud cover. The atmosphere seems to be almost entirely composed of carbon dioxide (see Table 4.2). The total amount in the Cytherean atmosphere is comparable with the total  $\text{CO}_2$  degassed from the Earth (as has already been discussed), but the lack of water vapour, at least in the observable region of the atmosphere, is difficult to explain. If a similar temperature calculation to that performed for the other planets is undertaken the effective temperature path will probably describe a curve similar to that (solid line) shown in Figure 5.12. The precise evolution of  $T_e$  is open to speculation, but since it must change from a value of approximately 255 K, 4.5 aeons ago, to its present value of approximately 245 K - forced by changes in  $A$ ,  $f$ ,  $e$  and solar luminosity - the solid curve shown is a reasonable model. The decrease in the value of  $T_e$  is because the large increases in both  $f$  (from 2 to 4) and  $A$  (from 7 per cent to 70 per cent) dominate the increasing solar luminosity. The surface temperature of Venus is much more difficult to establish for some other epoch in its evolution. In fact, the present-day observed value of approximately 700 K (indicated on Figure 5.12) is difficult to reproduce with a numerical model. The most successful such models require large amounts of water vapour below the cloud deck to increase the opacity of the atmosphere (see, e.g. Pollack and Young, 1975). Such a requirement seems to be in conflict with both the apparent lack of water vapour observed in the Venus atmosphere and with

Figure 5.12



Possible evolutionary tracks for  $T_e$  and  $T_s$  for Venus. The initial value of  $T_e$  is above 350 K and thus the general assumption is that the rapid degassing of both CO<sub>2</sub> and H<sub>2</sub>O led to a "runaway" atmosphere immediately (double dotted curve). It is possible that for some reason (possibly chemical) water vapour was not degassed immediately. The greenhouse increment caused by CO<sub>2</sub> alone is able to keep the value of  $T_s$  high enough to allow a much later degassing of H<sub>2</sub>O. If the latter history is followed the atmosphere of Venus need not be in its present chemical state for time periods close to the life-time of the planet.

the models of the chemical evolution of the atmosphere. The conflict arises from the general assumption that the "runaway greenhouse" effect took place very early in the evolution of Venus. The assumption is that as the initial surface temperature was above 350 K, an early catastrophic degassing would release both carbon dioxide and water vapour into the atmosphere. Although this would lead to a drop in effective temperature, as shown, it is generally considered (see Rasool and De Bergh, 1970 or Ingersoll, 1969) that the water vapour would not have condensed out, and so the surface temperature would have rapidly increased (shown in the figure by a double dotted curve). It is difficult to see how temperatures at the surface of above 650 K could remain stable for at least 3 aeons as required by this hypothesis.

The work of Walker (1975) makes such stability seem even more unlikely, for he considers that drastic chemical changes would take place in the atmosphere so that, in particular, the water vapour would be dissipated within one aeon of degassing.

One solution to this apparent dilemma is a much later degassing of water vapour. This is slightly more difficult to imagine, but is not unreasonable. It has already been suggested that the amount of water vapour available on Venus may be depleted compared with the Earth due to its initial formation at higher temperatures (see Anders, 1968). This, together with some degree of chemical differentiation, could produce a later degassing of water vapour. Carbon dioxide evolved into the atmosphere would keep the surface temperature high enough to ensure that water would be in its vapour phase when it was finally

degassed (the single dotted line in Figure 5.12). Thus it is just possible that the state of the atmosphere and surface of Venus today is highly unstable, and another few million years may see a return to more hospitable conditions.

The discussions presented in this section have considered primarily the role of carbon dioxide as the dominant atmospheric gas.  $\text{CO}_2$  has been shown to be particularly important for any planet with an initial temperature less than approximately 260 K, and may be the most abundant gas even in a planetary atmosphere at high temperatures (as is the case for Venus). The rapid modifications of the albedo, flux factor and surface emissivity caused by the release of water vapour into the atmosphere will cause fluctuations in the surface temperature, and once degassed the water vapour will absorb strongly. These parameters and their relationship to surface temperature will be illustrated in detail in Section 5.6. The effect of minor absorbers has not yet been discussed, and this, together with modifications in the solar luminosity curve, will be considered in the following section.

### 5.5 Modifications and Extensions

The computer model derived for this work can incorporate a wide range of input parameters. For instance, any number of absorbing and neutral gases may be input as constituents of the atmosphere and a single transmission spectrum will be derived, provided that there is a reasonable parameterization of their absorption properties available. Only two gases ( $H_2O$  and  $CO_2$ ) were considered important enough in the terrestrial planetary atmospheres for an extended parameterization to be constructed, allowing calculations of absorption beyond ranges studied in laboratory experiments (see Chapter 4, Section 4.5). However, two other gases have been considered as minor constituents in an atmosphere dominated by either  $CO_2$ ,  $H_2O$  or a neutral gas. These are carbon monoxide and methane.

Carbon monoxide is a particularly interesting secondary absorber, since it occurs in a number of situations likely to influence early planetary atmospheres: (e.g. volcanic gases on Earth, meteorites and cometary tails). It is very much more abundant on Mars (as a percentage of the total atmosphere) than on the present Earth; though the discussion in Section 4.8 of Chapter 4 and the histograms in Figure 4.40 indicate that CO would probably be the next most abundant gas in an atmosphere dominated by  $CO_2$ . To establish the effects of large mixing ratios of CO in a  $CO_2$  atmosphere a number of surface temperature calculations have been performed. Table 5.4 below lists the values derived for  $T_s$  (in terms of present-day Martian parameters - except that f was allowed to take a value of 4) for both a pure

carbon dioxide atmosphere and a combination of  $\text{CO}_2$  and CO.

Table 5.4

Effect upon Surface Temperature of Adding Carbon Monoxide  
to a Carbon Dioxide Atmosphere

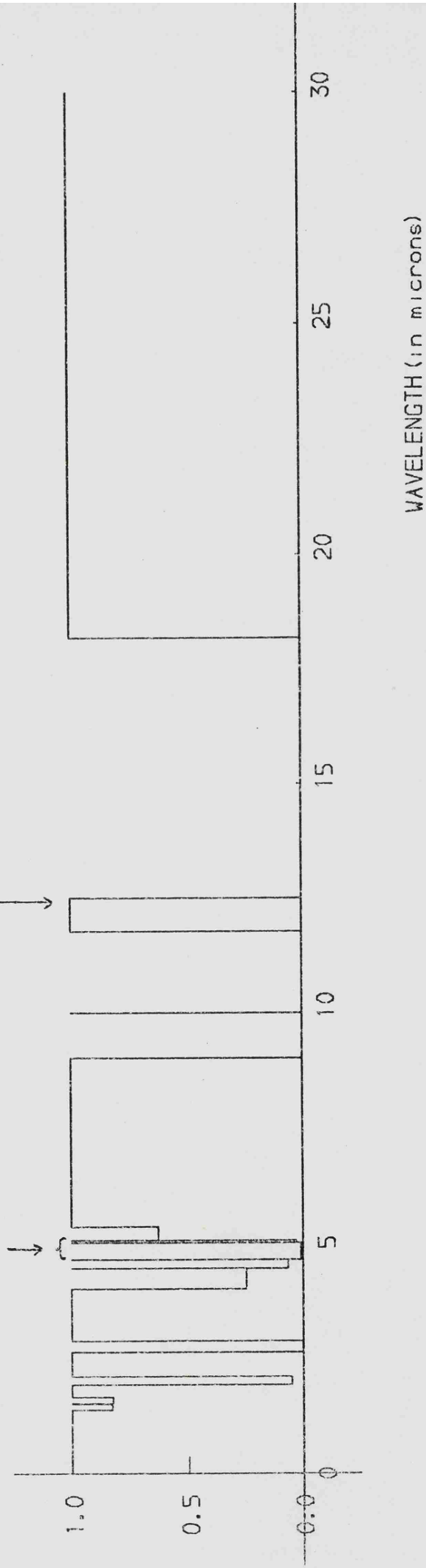
$\text{CO}_2$ (mb)	$T_s$	+ CO (mb)	$T_s$
20	232.3	0.001	232.3
20	232.3	0.01	232.4
100	241.4	0.01	241.5
100	241.4	1.0	242.0

These results underline the fact that the temperature increment due to the addition of approximately 0.1 per cent of the total atmospheric mass of carbon monoxide is almost negligible. This small effect is easily understood by reference to the position of the only infrared band strong enough to warrant consideration. This lies at approximately 4.65 microns, and so is displaced from the peak of the Planck curve for temperatures of the order of 230 K. Thus even total absorption produces little enhancement of the greenhouse effect. Figure 5.13 illustrates the combined spectrum of the last atmosphere listed in Table 5.4 (100 mb  $\text{CO}_2$  + 1 mb CO): the position of the features caused by the carbon monoxide absorption are indicated and also the position of the peak of the Planck curve for  $T = 230$  K. Thus it is reasonable to approximate the absorption features of an early atmosphere composed of both  $\text{CO}_2$  and CO by those of  $\text{CO}_2$  alone - as has already been assumed in the construction of  $T_s$  tracks for

Figure 5.13

COMBINATION OF  $\text{CO}_2$  ( $P_s = 100.0 \text{ mb}$ ), CO ( $P_s = 1.0 \text{ mb}$ ) TRUE SPECTRUM

TRANSMISSION CO features  
Peak of Planck  
curve for  $T = 230 \text{ K}$



Fractional transmission spectrum of the last atmosphere considered in Table 5.4. The major reason for the very slight temperature increase caused by the addition of CO is the position of the only band considered relative to the peak of the Planck curve.

Models I and II in Section 5.4. In fact, any effects upon the atmosphere, surface temperature and biosphere caused by an increase in the carbon monoxide mixing ratio would be due to chemical changes and toxicity, rather than its contribution to the absorption spectrum.

The contribution of methane to the absorption capacity of an atmosphere will be considerably greater than that of CO as one of the two absorption bands is centred at 7.7 microns (i.e. much closer to the peak of the Planck curve for temperatures of interest here). However the appearance of significant quantities of methane in a terrestrial planetary atmosphere is improbable on chemical grounds, particularly if the planet is sterile. In Chapter 4 there was a considered discussion of the possibility of an early reducing atmosphere around the Earth (or any of the terrestrial planets). There seems little reason to suppose that such atmospheres ever existed. Thus from both Table 4.9 and Figure 4.40 it is seen that the amount of  $\text{CH}_4$  in a neutral or oxidizing atmosphere must be small. It has been suggested by Margulis and Lovelock (1974) that production of methane by the biosphere on Earth could be the means of regulating planetary temperatures and for this reason the calculations of surface temperature performed have included higher mixing ratios of  $\text{CH}_4$  than would be stable in a sterile atmosphere. These temperatures were derived for present-day Earth parameters, except for the addition of the tabulated amounts of methane; that is, a neutral gas of approximately 1000 millibars plus the appropriate amounts of carbon dioxide and water vapour.

Table 5.5Effect upon the Surface Temperature of the Earth ofAdding Methane to the Atmosphere

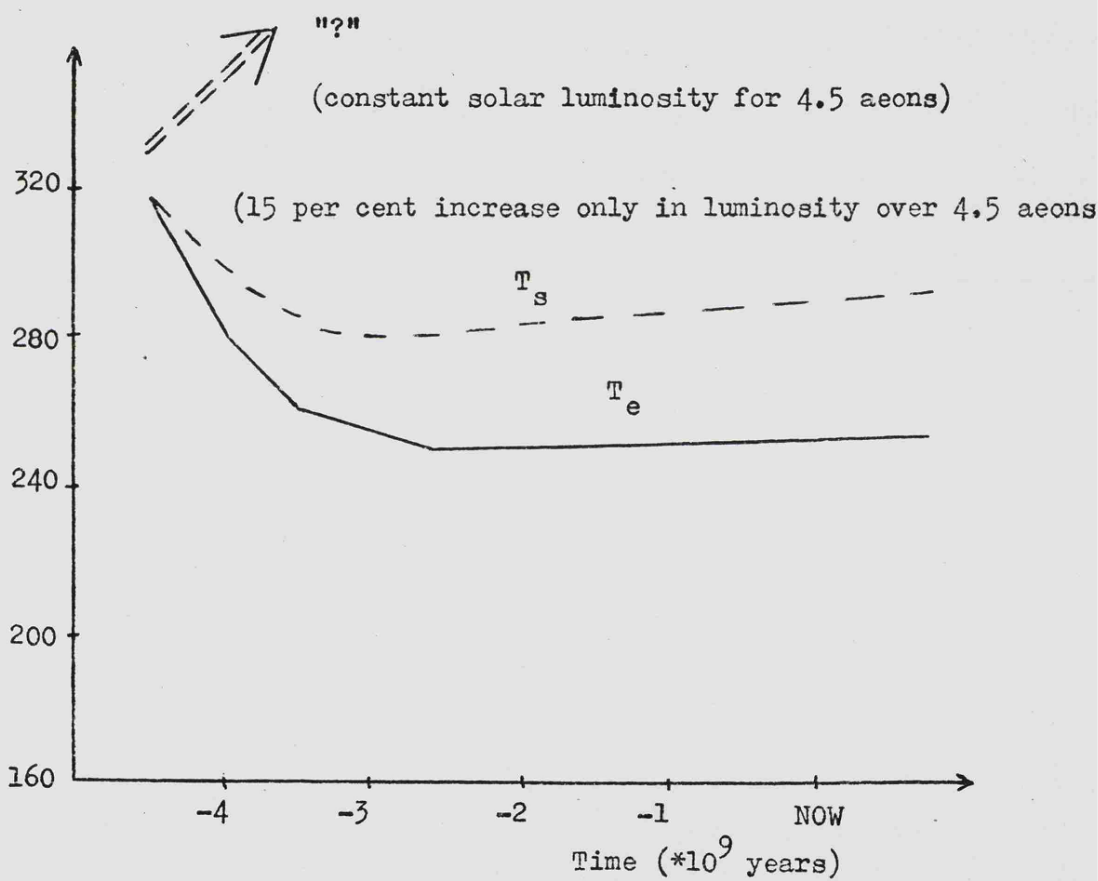
Present-day Earth's atmosphere	+ CH <sub>4</sub> (mb)	T <sub>s</sub> (k)
	0.001	285.2
	0.01	285.8
	0.1	287.7
⇒ T <sub>s</sub> ≈ 285.1 K	1.0	290.9

From these results the effect of methane absorption upon planetary temperatures is evident. The first row of the table is approximately the present-day situation for the Earth. Thus the small amount of methane present in the Earth's atmosphere is apparently responsible for a real, if small temperature increment of  $\Delta T \approx 0.1$  K. The inclusion of these minor gases in some of the surface temperature calculations has served to indicate two very important points: i) the original assumption that the greenhouse increment could be calculated for all the terrestrial planets with reference only to the amount of carbon dioxide and/or water vapour in the atmosphere is reasonable to within  $\pm 2$  K for the type of atmosphere expected; and ii) the numerical model derived in this work can be extended to incorporate any possible atmospheric constituents.

All the surface temperature curves derived in Section 5.4 of this chapter have been calculated on the assumption of a linearly increasing solar luminosity. The reasons for this assumption were given in Chapter 1. However, since the models of stellar evolution and, particularly, the evolution of the Sun are

at present undergoing investigation, it is relevant to consider other possible modes of luminosity variation. Chapter 1 discussed, at length, the long and short-term fluctuations which may have occurred in the luminosity output of the Sun. It seems unlikely that the Sun's luminosity increased very much more rapidly than the assumed rate (see Chapter 1), but it is possible that the increase was slower. The most extreme prediction is that the solar luminosity has not varied over the lifetime of the planets. This is probably much too extreme: the final theoretical curve will probably lie somewhere between this null assumption and that assumed previously. If the flux received at the Earth 4.5 aeons ago was the same as that received today, Figure 5.11 would have to be redrawn. The starting value of  $T_e \approx 332$  K might then be high enough to produce a "runaway greenhouse" on Earth. Figure 5.14 illustrates this possibility "?". From this curve it may even be possible that the studies undertaken by planetary astronomers can assist astrophysicists! If, however, only a 15 per cent (rather than the more usual 43 per cent) increase in solar luminosity over 4.5 aeons is assumed, the initial value of  $T_e \approx 320$  K (also shown in Figure 5.14) is probably low enough to avoid the "runaway" state, allowing for the rapid increases in both albedo and flux factor. These calculations illustrate the stability (within certain limits) of the surface temperature curves, and also the immense complexity involved in attempting to vary values of the five related parameters required to calculate the value of the surface temperature. The following section outlines a method of tracing the variation in  $T_s$  with changes in all these parameters.

Figure 5.14



Evolutionary curves for the Earth re-drawn for 2 other luminosity histories, (c.f. Figure 5.11). If the solar luminosity had not varied over 4.5 aeons then the initial value of  $T_e$  for the Earth may have led to a "runaway" atmosphere "?". Alternatively, a 15 per cent increase in luminosity (rather than the previously assumed 43 per cent) would probably lead to a stable temperature trend.

5.6     A Multidimensional Method of Calculating the Evolutionary  
Tracks of Surface Temperatures

The theme of this work has been the calculation of average surface temperatures for all the terrestrial planets at any stage during the past history (and future) of the Solar System. The surface temperature is a function of five parameters, four of which are interdependent, and are also functions of the value of  $T_s$ .

These parameters, which have been discussed in this thesis, are: the solar flux (incident at the planetary distance),  $S$ , the spherical albedo,  $A$ , the flux factor,  $f$ , the surface infrared emissivity,  $e$ , and the atmosphere (its total pressure, chemical composition and the partial pressures of its constituents).

The latter four are related by various feedback loops to the surface temperature. The solar flux does not depend upon  $T_s$ , but is, of course, different for different planets and at different epochs in their development. It may also be found to vary in some other unconsidered manner, when the problems of solar evolution are finally solved. A number of common-sense measures can be used to limit the combinations of parameters possible - for instance, it seems unlikely that a planet could ever take a very high value of albedo together with a low value of flux factor. This is because a high value of  $A$  (say above 40 per cent) implies a cloudy atmosphere which must mean that the "blanket effect" of the atmosphere is efficient enough to allow night-side radiation to be non-negligible. The reverse (high  $f$  and low  $A$ ) cannot be ruled out, since a rapidly rotating terrestrial planet with a tenuous atmosphere will be in this

category. The surface infrared emissivity depends upon what is likely to condense onto the surface, which, in turn, depends upon the atmospheric constituents and the surface temperature!

One method of considering the evolution of  $T_s$  is to construct a time-dependent curve for one planet (as has been done in this chapter). This cannot involve variations in the models of solar evolution, and so an alternative method is presented here. Isopleths of surface temperature have been calculated and drawn using results from the computer model. The axes chosen are incident flux at the planet (thus allowing variations in time, planetary distance and stellar model) and absorber amount in the atmosphere. The second is somewhat arbitrary, but an attempt has been made to cover most possibilities. Only carbon dioxide and water vapour have been considered. Zero absorber concentration will give the value of the effective temperature: the other discrete absorber amounts chosen are 10 millibars of  $\text{CO}_2$ , 100 millibars of  $\text{CO}_2$ , 100 millibars of  $\text{CO}_2 + 0.1$  millibars of  $\text{H}_2\text{O}$ , 100 millibars of  $\text{CO}_2 + 1$  mb of  $\text{H}_2\text{O}$  and finally 100 millibars of  $\text{CO}_2 + 10$  millibars of  $\text{H}_2\text{O}$ . If all the other parameters ( $A$ ,  $f$  and  $e$ ) are to be allowed to vary also the multi-dimensional nature of the results requires that a number of separate figures are drawn. Some parameters are more closely related than the others; in particular groups of values of  $A$ ,  $f$  and  $e$  have been considered. Table 5.6 lists the pairs of  $A$  and  $f$  values considered, and gives the value of  $e$  taken in each case (a dash indicates that the pair of  $A$  and  $f$  values were ignored as unrealistic).

Table 5.6Feasible Combinations of Flux Factor and Albedo Values

albedo: A	flux factor: f			
	2.0	2.5	3.0	4.0
0.07	e =0.90	e =0.90	-	e =0.90
0.17	e =0.93	e =0.93	e =0.93	e =0.93
0.30	-	-	e =0.95	e =0.95
0.70	-	-	-	e =0.95

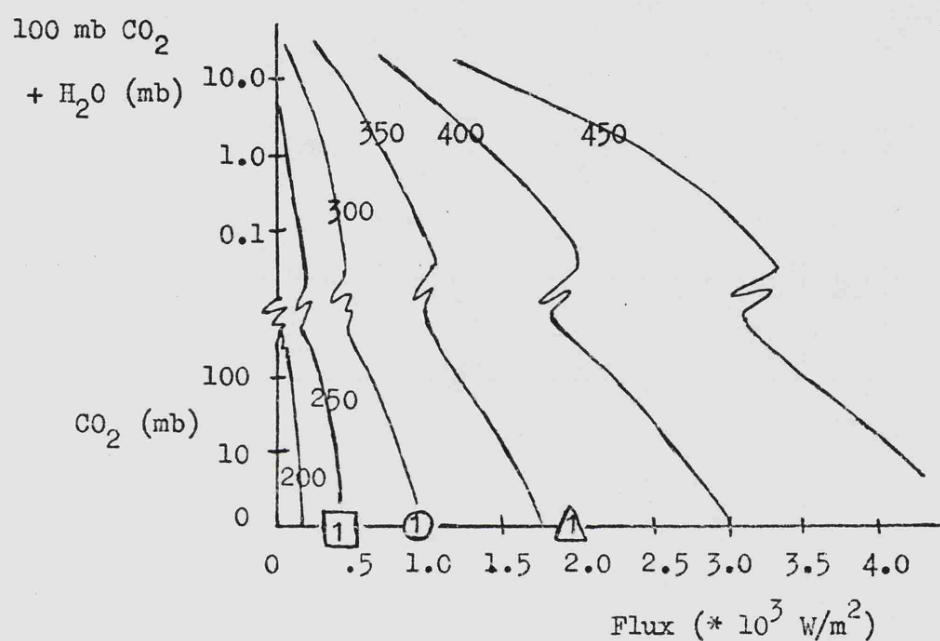
The graphs of lines of equal surface temperature were plotted for all 10 combinations of A, f and e for incident fluxes ranging from zero to  $4.0 \times 10^3 \text{ W/m}^2$  (approximately twice the flux incident at Venus now). These isopleths are displayed, in K, in Figures 5.15 to 5.19. The vertical axis (varying atmospheric composition) cannot encompass all the possible atmospheres. No consideration of neutral broadening has been included. The effect of this has already been noted. The two most important absorbing gases for all the terrestrial planets are carbon dioxide and water vapour, and thus the 'typical' atmosphere has been considered as initially dominated by CO<sub>2</sub> alone, and then CO<sub>2</sub> plus smaller amounts of water vapour. The addition of water vapour to the model atmosphere leads to a temperature discontinuity. This has been indicated by a break in both the vertical axis and the isopleths themselves. The particular combinations of CO<sub>2</sub> + H<sub>2</sub>O chosen will not apply to every planet, but the series of figures permits an interesting description of certain evolutionary tracks. The use of varying flux amount along the horizontal

axis permits a discussion either of the time evolution of one model planet (the flux variation being caused by the evolution of the Sun), or of zones of surface temperatures throughout a planetary system (this time, the flux variation is caused by differences in planetary distances). A particular zone might correspond, for instance, with a planet possessing conditions suitable for the evolution of life. This will be illustrated later.

The usefulness of this method of presentation of results will be illustrated by discussion of three planetary evolutionary tracks and also by the consideration of life-bearing conditions on these and other planets. The three model planets considered bear a significant relationship to the three terrestrial planets possessing atmospheres. Neither the fluxes, nor the atmospheres, are exactly those appropriate for Venus, the Earth or Mars; but the comparison between the evolution of these three models and the present state of the real planets is most interesting. The results are most easily followed by use of the "view-aid" which is to be found inside the back cover of this volume. Each planetary evolution is denoted by a numbered symbol (a triangle, cross circle or square) and may be followed by placing the appropriate half of the over-lay on top of the figures indicated in the description.

Figure 5.15

Upper       $f = 2.0$ ,  $A = 0.07$ ,  $e = 0.90$



Lower       $f = 2.0$ ,  $A = 0.17$ ,  $e = 0.93$

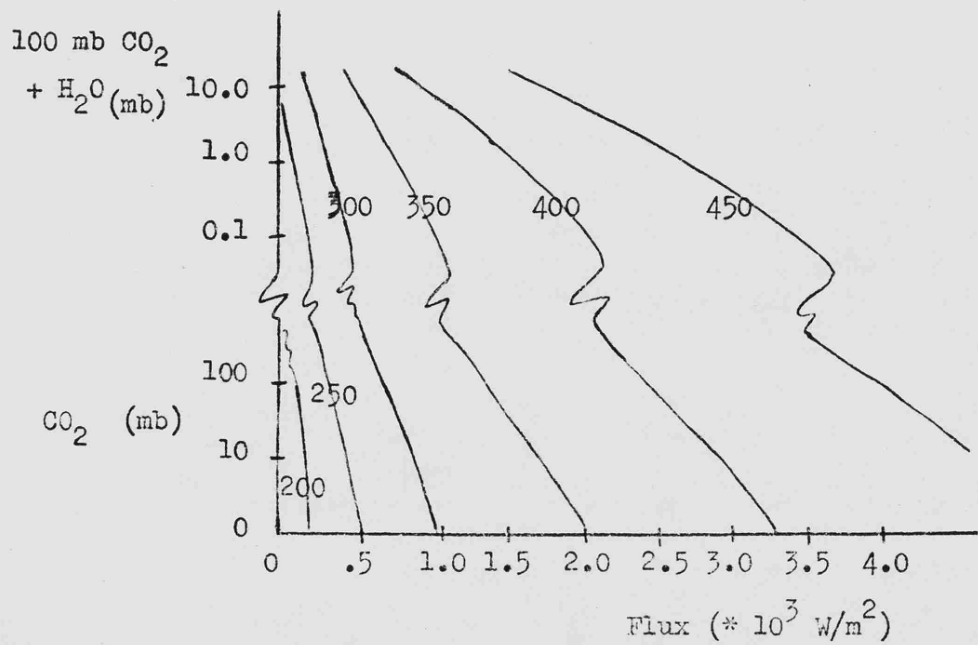
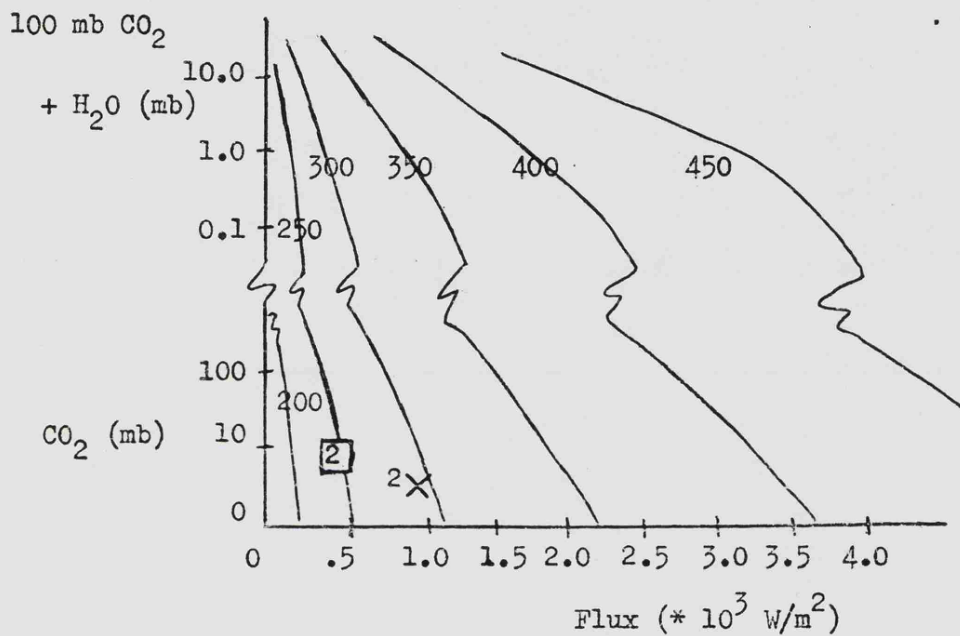


Figure 5.16

Upper       $f = 2.5, A = 0.07, e = 0.90$



Lower       $f = 2.5, A = 0.17, e = 0.93$

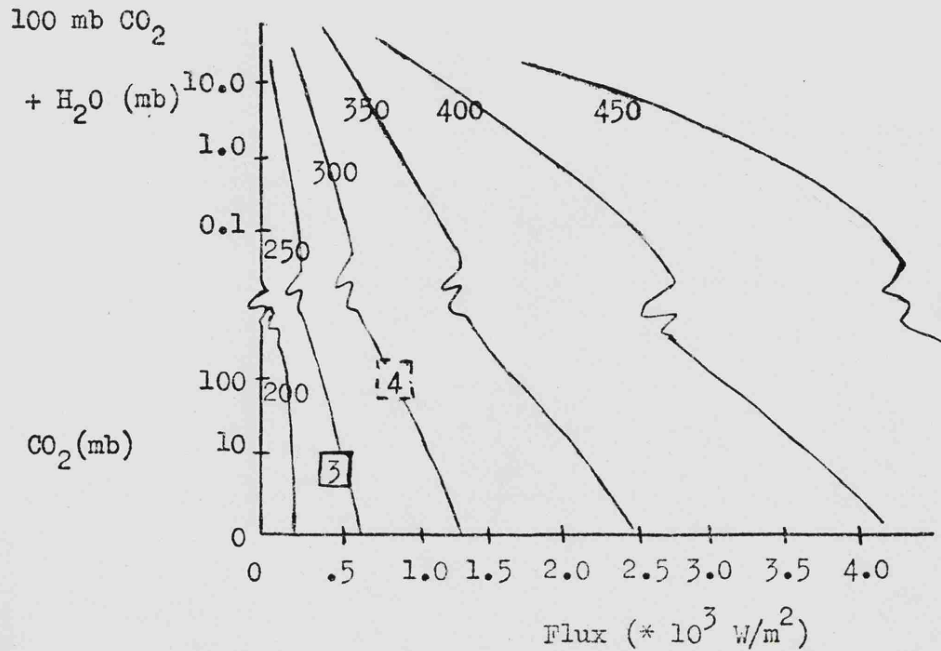
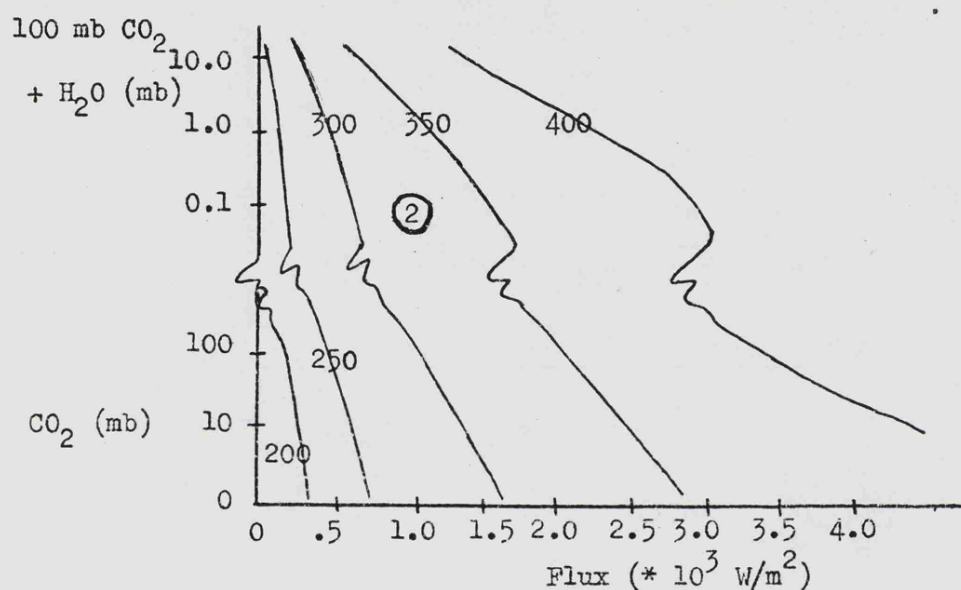


Figure 5.17

Upper       $f = 3.0$ ,  $A = 0.17$ ,  $e = 0.93$



Lower       $f = 3.0$ ,  $A = 0.30$ ,  $e = 0.95$

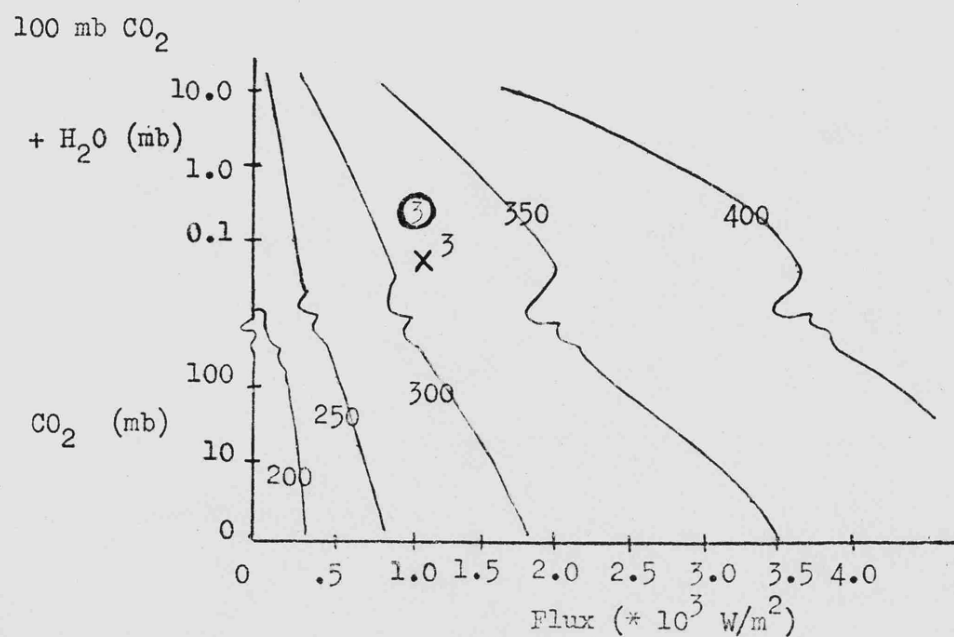
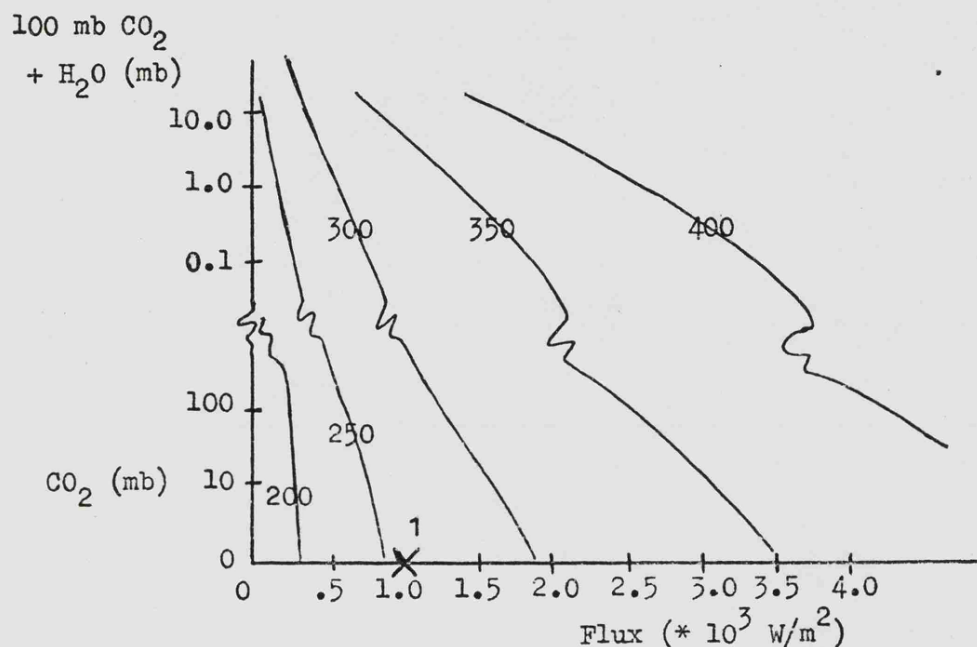


Figure 5.18

Upper       $f = 4.0, A = 0.07, e = 0.90$



Lower       $f = 4.0, A = 0.17, e = 0.93$

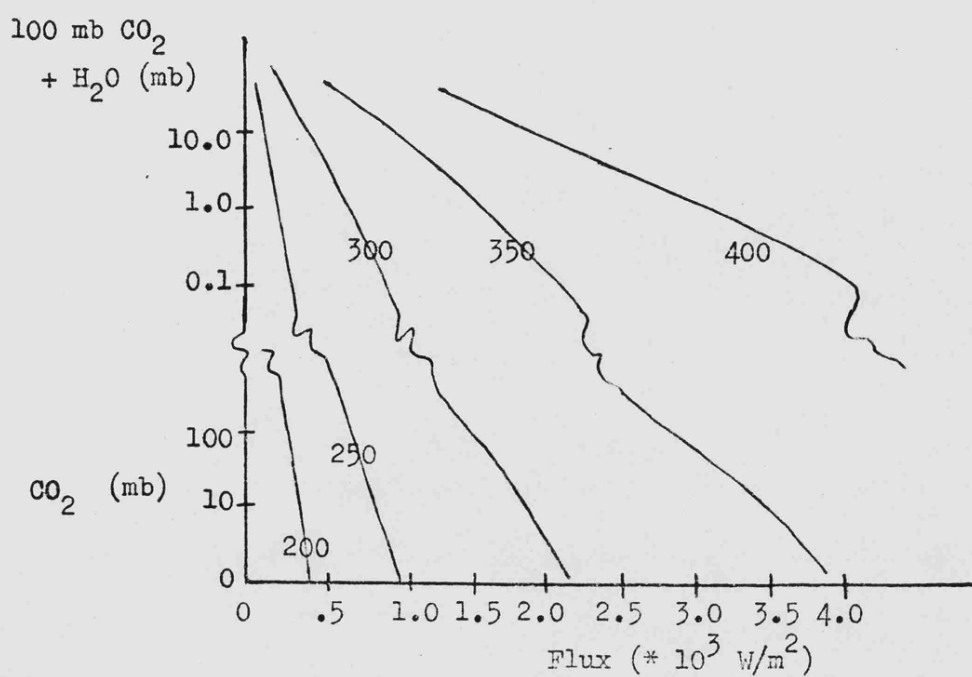
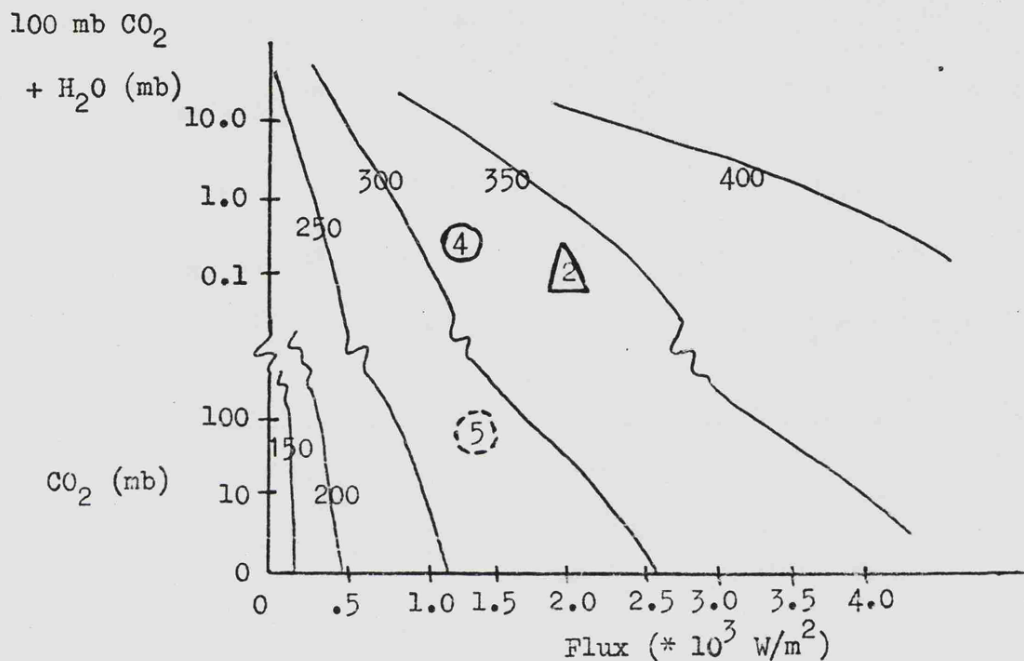
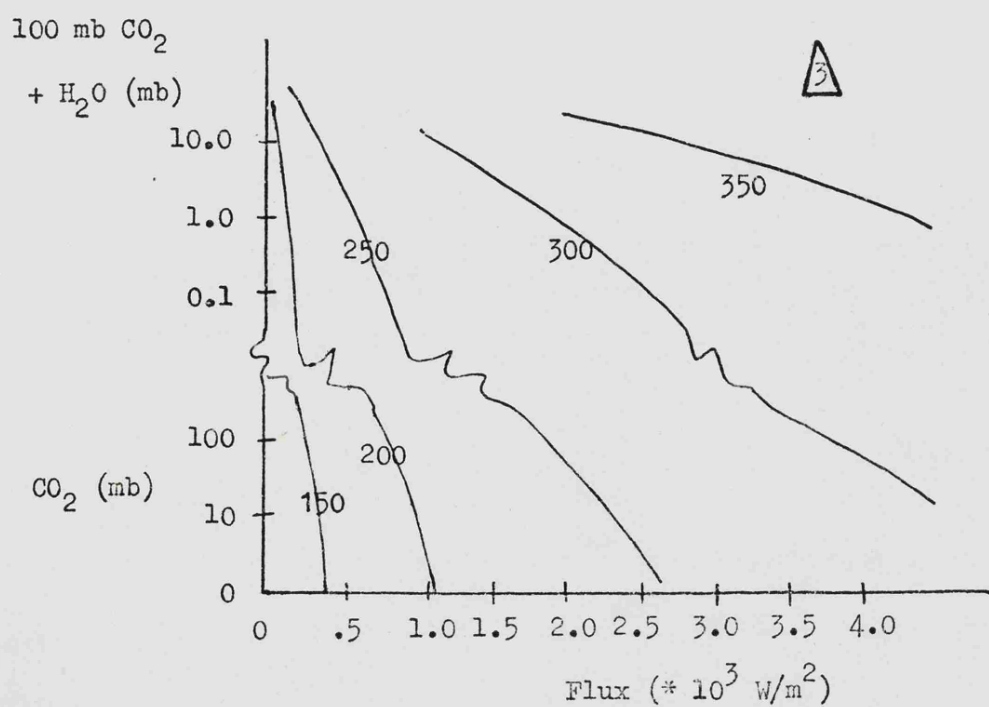


Figure 5.19

Upper       $f = 4.0, A = 0.30, e = 0.95$



Lower       $f = 4.0, A = 0.70, e = 0.95$



Model 1 A

- i) Figure 5.15 (Upper graph) - the initial conditions for this model are a flux of  $2 \times 10^3 \text{ W/m}^2$  (this is a little higher than the value of incident flux at Venus early in its evolution). The planet is assumed to have a flux factor of 2, and an albedo of 7 per cent (the surface infrared emissivity is  $e = 0.90$ ). Thus  $T_e = T_s \approx 360 \text{ K } (\Delta 1)$
- ii) Figure 5.19 (Upper graph) - such a high initial temperature would almost certainly lead to rapid degassing of both carbon dioxide and water vapour. The atmosphere would be rapidly established (so rapidly that the flux has been held constant). The flux factor now has a value of 4 and the albedo is much higher (probably close to 30 per cent) due to the large amount of water vapour available. Thus we find  $T_s \approx 340 \text{ K } (\Delta 2)$
- iii) Figure 5.19 (Lower graph) - surface temperature has remained high even without flux increase. As the Sun evolves, and the planetary temperature rises, more water vapour will be degassed and evaporated into the atmosphere. The evolution will almost certainly "run-away", finally producing a situation beyond the range of these graphs, but approximated by the last point:  $T_s \approx 500 \text{ K } (\Delta 3)$

Model 2    0

- i) Figure 5.15 (Upper graph) - the initial conditions for this model are similar to those for Model 1, except that the flux is lower (taking a value of  $1 \times 10^3 \text{ W/m}^2$ ). This leads to  $T_e = T_s \approx 300 \text{ K}$  (0 1)
- ii) Figure 5.17 (Upper graph) - early temperatures above 273 K, together with a slowly increasing flux incident on the planet, leads to considerable degassing together with the build-up of an atmosphere of carbon dioxide with small amounts of water vapour. The flux factor has a value of 3 (for a well-established atmosphere). Freezing-out of the volatiles around polar regions, or in clouds, leads to an albedo value of approximately 17 per cent and an increased surface infrared emissivity of  $\epsilon = 0.93$ . These conditions produce  $T_s \approx 325 \text{ K}$  (0 2)
- iii) Figure 5.17 (Lower graph) - temperatures remain above 300 K (but do not rise rapidly). The atmosphere would probably continue to evolve in a stable fashion under the influence of increasing solar luminosity. The albedo might increase a little, leading to a new value of  $T_s \approx 320 \text{ K}$  (0 3)
- iv) Figure 5.19 (Upper graph) - continuing atmospheric build-up would produce an increase in  $f$  (to a value of 4). Thus we have  $T_s \approx 310 \text{ K}$  (0 4)

The important and interesting factor in this evolutionary sequence is the way in which increases in incident flux have been

adequately compensated for by varying planetary characteristics. The surface temperature has remained very stable. However, this evolutionary path is unresponsive to certain features of planetary evolution. For instance, Model 2 evolution has produced stable temperatures in the range 300 K to 325 K together with large amounts of water vapour. These would almost certainly lead to surface condensation of liquid water, and possibly to loss of atmospheric carbon dioxide by solution in water and sedimentation. This has happened during the evolution of the Earth, and the remaining atmospheric  $\text{CO}_2$  contributes far less to the "greenhouse" increment than the 100 millibars standard for this model. A further calculation has been made for Model 2 allowing for this loss of  $\text{CO}_2$ .

v) Figure 5.19 (Upper graph - dotted circle)

A slight further increase in incident flux, together with the probable decrease in atmospheric carbon dioxide discussed above, renders the vertical scale on the graph inapplicable. For this reason, the resulting temperature (almost identical to that of the present-day Earth) has been indicated by a dotted circle. It is found that

$$T_s \approx 290 \text{ K} (\square 5)$$

Model 3

i) Figure 5.15 (Upper graph) - initial conditions are similar to those of Models 1 and 2, but the incident solar flux is considerably reduced. It is  $0.4 \times 10^3 \text{ W/m}^2$ . These

conditions lead to a temperature of  $T_e = T_s \approx 245$  K (□ 1)

- ii) Figure 5.16 (Upper graph) - the low value of surface temperature will initiate only slight degassing - probably only of carbon dioxide. Slight increase in atmospheric mass may raise the value of the flux factor to (say)  $f = 2.5$ . This, together with a small increase in incident flux, results in a very slight temperature change:

$$T_s \approx 249 \text{ K} \quad (\square 2)$$

- iii) Figure 5.16 (Lower graph) - continuing low temperatures combined with larger atmospheric mass may lead to freezing out of  $\text{CO}_2$  around the polar regions, and thus to an increased albedo. This almost compensates for the slowly increasing flux, giving  $T_s \approx 250$  K (□ 3)

Two most interesting points are obvious here. Firstly, this evolution (like that of Model 2) seems to be stable. The surface temperature varies little, although the parameters affecting it are changing. This may indicate that a stable surface temperature is the normal planetary condition rather than, as previously generally assumed, a phenomenon requiring complex explanation. The second point is that this final evolutionary track, which resembles that of Mars, seems to be continuing in its stable mode well below what are termed "hospitable" conditions. An interesting prediction (attempted by Sagan and Mullen, 1972) is the length of time required before a Mars-type planet will evolve to an Earth-like state (assuming, of course, that the necessary volatiles are available). To increase the surface temperature of

Model 3 from the last calculated value ( $T_s \approx 250$  K) to a value which would ensure degassing of water vapour and its partial evaporation into the atmosphere (say  $T_s \approx 300$  K) requires a huge increase in input flux. No planetary characteristics are likely to change to assist the temperature increase. This calculation has been performed for Model 3.

iv) Figure 5.16 (Lower graph - dotted square)

To increase the surface temperature to  $T_s \approx 300$  K requires an increase in the incident flux from approximately  $0.5 \times 10^3$  W/m<sup>2</sup> to  $10^3$  W/m<sup>2</sup>: that is the incident flux must double. The length of time required to produce this increase for a planet at the same distance as Mars is over 15 aeons. This is considerably longer than the time period for which the luminosity curve is applicable, and probably longer than the life-time of the Solar System. However, the long time-scale implies that, unless the evolutionary sequence for Model 3 is not applicable to Mars (they could differ if Mars is found to be suffering an intense glaciation at present), the chances of Mars naturally becoming hospitable for advanced forms of life are negligible.

One further parameter variation has to be considered. The value of the flux factor is a function of the planetary rotation rate as well as of the atmospheric mass. Planetary rotation rates are unlikely to vary greatly unless the planet is perturbed by another body of approximately planetary mass. The effect of variation in rotation rate has already been discussed for the case of the Earth in Chapter 3. Here the rotation rate may have been considerably faster before lunar capture, and thus the value of

the flux factor would be initially much higher. Model 2\* includes this possible variation.

Model 2\* X

- i) Figure 5.18 (Upper graph) -  $f = 4$  and  $A = 0.07$ , with the same incident flux as for Model 2, gives  $\underline{T_e = T_s \approx 260 \text{ K}}$  (X 1)
- ii) Figure 5.16 (Upper graph) - low surface temperature leads to little degassing, but capture of the satellite modifies the value of  $f$ . Thus we have  $\underline{T_s \approx 290 \text{ K}}$  (X 2)
- iii) Figure 5.17 (Lower graph) - higher value of  $T_s$  leads to rapid degassing and thus to increases in values of both the flux factor and the albedo. These increases combined with increasing solar flux lead to  $\underline{T_s \approx 315 \text{ K}}$  (X 3)

After this stage the evolutionary track of Model 2\* would probably follow that of Model 2 - moving to the third circle and then onwards.

A further interesting discussion which is simplified by the use of the isopleths of surface temperature presented in Figures 5.15 to 5.19 is the consideration of a specific planetary feature - say, for instance, the ability of a planetary surface/atmosphere system to support or permit the origin of life. It is possible to suggest conditions under which the origin of life and its evolution would be likely. For the discussion illustrated here the conditions chosen are that the surface temperature shall be between 270 K and 320 K and that water vapour is in the atmosphere. These are reasonable conditions, but they may be

over-restrictive (i.e. given these conditions for long enough, life stands a good chance of origin and evolution, but less hospitable conditions may not imply that life cannot exist). Zones corresponding to life-bearing conditions have been drawn on the lower half of the "view-aid". These are appropriate only for well-established atmospheric systems (i.e. only for the two of the graphs in Figure 5.19), and are labelled with the albedo values of the upper and lower graphs. A number of interesting points arise from the illustration of these zones. The fact that they are separated by only a small distance implies that, if life became established on a planet which had characteristics typical of the upper graph, it would not find it difficult to adjust if the planetary system evolved to a state typical of the lower graph. The evolutionary models described earlier are most interesting in comparison with the zones of life-bearing characteristics. The zone labelled  $A = 0.3$ , placed on the upper graph of Figure 5.19, is in a most interesting position. The fourth circle (which was the final evolutionary position of an early Earth-like planet - Model 2) lies within the life-bearing zone, whilst the second triangle (Venus-type runaway planetary evolution - Model 1) lies well outside it. Thus it seems reasonable to deduce that of the three model planets considered here, only Model 2 is a likely candidate for the origin and evolution of life!

### 5.7 Conclusions

This chapter has considered the results generated by the suite of computer programs constructed for surface temperature studies. Evolutionary tracks have been computed for two model planets, and also for the Earth, Mars and Venus. The ability of the programs to accept, as data, and produce results from, a very wide range of parameters and parameter values has been demonstrated. The usefulness of this type of computation, which does not require huge amounts of computer-time, is obvious and can, hopefully, be utilized to generate zonal and local models for any epoch, past or future.

The problem of the large number of interdependent variables has been underlined and an attempt has been made to simplify the presentation of results. The graphs presented are only a limited number from the wide range possible, but they indicate how the tracks of surface temperature may be drawn for all the terrestrial planets.

CHAPTER 6CONCLUSIONS

Planetary exploration has expanded rapidly in the last decade. Geological and climatological data from the Earth together with photographic and meteorological data from all the other terrestrial planets have stimulated theoretical studies of planetary evolution. The model described and developed here is the first theoretical model to allow for variation in all the physical parameters which must affect planetary evolution.

The model predicts the average planetary surface temperature throughout the evolutionary history of the planetary atmosphere. The numerical routines developed for, and implemented upon, the Leicester University computer take into account all possible values of all the variables required for the surface temperature calculation. Of particular importance are the spherical albedo of the planet, the flux factor (a parameter previously insufficiently considered), the infrared absorption spectrum of the atmosphere (which is a function of the chemical constituents and their partial pressures), the surface infrared emissivity and the total incident solar flux at the planet (which will depend upon the evolution of the Sun). All these parameters have been discussed in detail in this thesis. Their probable variation as the planetary atmosphere evolves has been discussed, and the calculation of the evolutionary tracks for surface temperature (described in Chapter 5) has included all the likely parametric sets. The average global nature of the temperature predictions produced represent a valuable first step towards a complete understanding of planetary climatic

regimes.

A number of original contributions have been made by this work to the understanding of planetary atmospheric evolution. The discussion of the flux factor,  $f$ , in Chapter 3 illustrates the previous confusion in the definition of effective temperature and hence in the calculation of surface temperature. The variable nature of the flux factor is important both for present-day calculations for Mars and for calculations of the evolutionary histories of surface and effective planetary temperatures. The computational model which has been developed is an efficient and accurate method for calculation of average surface temperatures. It consists of a number of routines which have been described (with the aid of flow diagrams) throughout the text. No approximations, except those described and commented upon in Chapter 2, have been used. The program should therefore be widely applicable, and can be used to predict surface temperatures for planets with any reasonable physical characteristics. A number of contributions to the Leicester University Computer Centre library of standard routines have been made as a direct result of the research undertaken for this thesis. The numerical procedures have also led to extensions of laboratory data by parameterizations which are more widely applicable. These extensions have been undertaken here for carbon dioxide and water vapour but the numerical method (described in Chapter 4) can be applied to any gas.

The calculations of surface temperatures presented in Chapters 3 and 5 are the result of the research work described in this thesis. The temperature trends have been presented in two

different and complementary ways. First, the evolution with time of a planetary atmosphere has been described both for specific planets and for model planets and the surface temperature track calculated. This produced acceptable tracks both for the Earth (see Figure 5.11) and for Mars (see Figure 3.12), and the model results for present-day conditions on both these planets agree well with available data. The surface temperature of the Earth (even allowing for the likely luminosity changes of the Sun) remains above the freezing point of water throughout its evolution, and thus the temperatures predicted by the model agree with the geological data. The exact mode of degassing is found to be important for Mars and may also be important for Venus. The surface temperature curve produced for Venus (see Figure 5.12) illustrates an interesting, and hitherto neglected, possibility. The "runaway greenhouse" effect which must have occurred may not have happened immediately after the formation of the planet, but may be a much more recent phenomenon.

The second method devised for the presentation of the results of surface temperature calculations was not intended for the evolution of any specific planet. Co-ordinates of solar flux (at a planet) and atmospheric constituents were used. Isopleths of surface temperature were plotted on graphs which took specific groups of values of planetary albedo, flux factor and surface infrared emissivity (see Figures 5.15 to 5.19). The most exciting aspect of the model planetary atmospheres described with the aid of these isopleths is the stability exhibited in the temperature evolution. This apparent stability in the surface temperature

regime of a planet has already been noted in connection with the Earth, but it was not clear whether this was a characteristic typical of most planets. The theoretical model described here seems to indicate that stable average surface temperatures over time periods of the same order as the life-time of the planet are not unusual. Another interesting consideration which was illustrated with a "view-aid" in Chapter 5 is the evolution and development of life. Zones were discussed that would probably be most hospitable to life, as we know it, and it was found that only one of the three model planets considered passed into this zone during its evolution.

The theoretical model described here is complete and well defined. It is unlikely that any physical planetary parameters of importance have been neglected. The results derived demonstrate the compensatory nature of some of the parameters considered, which tends to lead to stable temperature evolution. Improved results could be derived using the numerical model when the problem of the precise mode of solar evolution has been solved. Also data which relate to the rate and mode of degassing and atmospheric evolution would be useful and would further improve the accuracy of the predicted temperature curves. It is important to note that, although this model can calculate only average, global surface temperatures, these temperature curves could provide a valuable starting point for consideration of shorter-term temperature fluctuations. This has been well illustrated for the case of the Earth today. All climatic models start with the initial conditions given by an average regime typical of the Earth

today. Thus, presumably, it is possible to formulate other climatic models which could use as starting conditions the average surface temperatures predicted by the model described here. In this way, this simple model would be a useful tool in the prediction of climatic variations. The results produced by the model developed here are smoothed over time periods shorter than approximately  $10^8$  years. This is because the short-period feedback effects are not well understood, and, at present, it would be difficult to implement short-period perturbations without vastly increasing the computer time required for calculations. However, as has been well illustrated by the albedo calculations for both the Earth and Mars in Chapter 3, that short-period fluctuations in one or more parameters can be calculated and the resulting surface temperature fluctuations computed.

The theoretical model described here is applicable to all the terrestrial planets. At present, only data from the Earth can be obtained for earlier epochs, and these agree well with the results calculated by the model. Within the next few years, Man's ability to collect data from other terrestrial planets, using both orbiting and landing craft, will improve. These new data will revitalize thought about the present conditions of planetary surfaces and atmospheres and will also strengthen interest in the evolutionary sequences responsible for such conditions.

BIBLIOGRAPHY

- Anders E. (1968), Accts. Chem. Res. 1, 289-298, Chemical Processes in the Early Solar System as inferred from Meteorites.
- Bahcall J.N. and Davis R. Jr. (1976), Science 191, 264-267, Solar Neutrinos - A Scientific Puzzle.
- Begelman M.C. and Rees M.J. (1976), Nature 261, 298-299, Can Cosmic Clouds Cause Climatic Catastrophes?
- Benlow A. and Meadows A.J. (1976)(to be published), Ap. Space Sci. The Formation of the Atmospheres of the Terrestrial Planets by Impact.
- Berry E.X. (1974), J. Appl. Meteor. 13, 603-604, Comments on 'The "Greenhouse" Effect'.
- Blumen W. (1976), J. Atmos. Sci. 33, 161-169, 170-175, Experiments in Atmospheric Predictability I and II.
- Brancazio P.J. and Cameron A.G.W. (1964)(editors), The Origin and Evolution of Atmospheres and Oceans, John Wiley.
- Brandt J.C. and Hodge P.W. (1964), Solar System Astrophysics, McGraw-Hill.
- Brookes J.R., Isaak G.R. and Van Der Raay H.B. (1976), Nature 259, 92-95, Observations of Free Oscillations of the Sun.
- Bryson R.A. (1974), Science 184, 753-760, A Perspective on Climate Change.
- Budyko M.I. (1969), Tellus 21, 611-619, The Effect of Solar Radiation Variations on the Climate of the Earth.
- Buettner K.J.K. and Kern C.D. (1965), J. Geophys. Res. 70, 1329-1337, The Determination of Infrared Emissivity of Terrestrial Surfaces.
- Burch D.E., Gryvnak D., Singleton E.B. and France W.L. (1962), Research Report Contract A.F. 19 (604) - 2633, Ohio State University, Infrared Absorption by CO<sub>2</sub> and H<sub>2</sub>O and Minor Atmospheric Constituents.
- Burch D.E., Howard J.N. and Williams D. (1956), J. Opt. Soc. Amer. 46, 452-455, Infrared Transmission of Synthetic Atmospheres. V. Absorption Laws for Overlapping Bands.
- Cess R.D. (1975), Tellus 27, 193-198, Global Climate Change: An Investigation of Atmospheric Feedback Mechanisms.
- Cess R.D. (1976), Climatic Feedback Mechanisms, presented at the Meteorological Office, U.K., on 26 May 1976.

- Charney J.G. (1975), Quart. J. R. Met. Soc. 101, 193-202,  
Dynamics of Deserts and Drought in the Sahel.
- Christensen-Dalsgaard J. and Gough D.O. (1976), Nature 259,  
89-92, Towards a Heliological Inverse Problem.
- Chylek P. and Coakley J.A. Jr. (1975), J. Atmos. Sci. 32, 675-679,  
Analytical Analysis of a Budyko-Type Climate Model.
- Cloud P.E. (1968), Science 160, 729-736, Atmospheric and  
Hydrospheric Evolution on the Primitive Earth.
- Delsemme A.H. (1976) in Proceedings of the N.A.T.O. Advanced  
Study Institute on the Origin of the Solar System,  
Newcastle University, U.K.
- Dennison B. and Mansfield V.N. (1976), Nature 261, 32-34,  
Glaciations and Dense Interstellar Clouds.
- Donn W.L. and Shaw D. (1975), Proceedings of W.M.O./I.A.M.A.P.  
Symposium on Long Term Climatic Fluctuations, (held at  
the University of East Anglia, U.K.), 53-62, The Evolution  
of Climate.
- Falls L.W. (1974), J. Geophys. Res. 79, 1261-1264, The Beta  
Distribution: A Statistical Model for World Cloud Cover.
- Fanale F.P. (1971), Chem. Geol. 8, 79-105, A Case for Catastrophic  
Early Degassing of the Earth.
- Fanale F.P. (1976), Icarus 28, 179-202, Martian Volatiles:  
Their Degassing History and Geochemical Fate.
- Farmer C.B. (1976), Icarus 28, 279-289, Liquid Water on Mars.
- Fielder G. and Wilson L. (1975)(editors), Volcanoes of the Earth,  
Moon and Mars, Paul Elek.
- Fink U., Larson H.P., Kuiper G.P. and Poppen R.F. (1972), Icarus  
17, 617-631, Water Vapour in the Atmosphere of Venus.
- Ghil M. (1976), J. Atmos. Sci. 33, 3-20, Climate Stability for a  
Sellers-Type Model.
- Giddings J.C. (1973), Chemistry, Man and Environmental Change,  
Harper Row.
- Gierasch P., Goody R.M. and Stone P. (1970), Geophys. Fluid Dynam.  
1, 1-18, The Energy Balance of Planetary Atmospheres.
- Gribbin J. (1976), Nature 260, 396, report of meeting of Royal  
Meteorological Society.
- Goody R.M. (1964), Atmospheric Radiation. I. Theoretical Basis,  
Oxford, Clarendon Press.
- Goody R.M. and Walker J.C.G. (1972), Atmospheres. Foundations  
of Earth Science Series, Prentice Hall.

Haselgrove C.B. and Hoyle F. (1959), Mon. Not. R. Astr. Soc. 119, 112-123, Main Sequence Stars.

Henderson-Sellers A. and Henderson-Sellers B. (1975), J. Atmos. Sci. 32, 2358-2360, Comments on 'A Diffuse Thin Cloud Atmospheric Structure as a Feedback Mechanism in Global Climatic Modelling'.

Henderson-Sellers A. and Meadows A.J. (1976), Planet. Space Sci. 24, 41-44, The Evolution of the Surface Temperature of Mars.

Hill H.A. and Stebbins R.T. (1975), Ap. J. 200, 471-483, The Intrinsic Visual Oblateness of the Sun.

Holland H.D. (1962), in Petrologic Studies: A Volume in Honour of A.F. Buddington, Geol. Soc. Amer.

Holland D.M. (1975), in discussion session at N.A.T.O. Advanced Study Institute on the Early History of the Earth, Leicester University, U.K., April 1975.

Howard J.N., Burch D.E. and Williams D. (1956), J. Opt. Soc. Amer. 46, Infrared Transmission of Synthetic Atmospheres. 186-190, I, Instrumentation. 237-241, II, Absorption by Carbon Dioxide. 242-245, III, Absorption by Water Vapour. 334-338, IV, Application of Theoretical Band Models.

Hudson R.D. (1969), Infrared Systems Engineering, John Wiley, 43-44.

Hunt G.E. (1974), Proc. R. Soc. Lond. A. 341, 317-330, A New Look to the Martian Atmosphere.

Hunt G.E. (1976), The Role of Cirrus Clouds as a Climatic Variable Identified by Some Numerical Experiments, Met. Office Tech. Note.

Hunt G.E. and Mattingly S.R. (1976), J. Quart. Spectrosc. Radiat. Transfer 16, 505-520, Infrared Radiative Transfer in Planetary Atmospheres, I. Effects of Computational and Spectroscopic Economies on Thermal Heating/Cooling.

Hunten D.M. (1971), Space Sci. Rev. 12, 539-599, Composition and Structure of Planetary Atmospheres.

Hunten D.M. (1973), J. Atmos. Sci. 30, 1481-1494, The Escape of Light Gases from Planetary Atmospheres.

Ingersoll A.P. (1969), J. Atmos. Sci. 26, 1191-1198, The Runaway Greenhouse: A History of Water on Venus.

Kelly P.M. and Lamb H.H. (1976), Nature 262, 5, Prediction of Volcanic Activity and Climate.

Kondratyev K. Ya and Bunakova A.M. (1974), N.A.S.A. Tech. Transl. TT F-816, The Meteorology of Mars.

Kuiper G.P. (1953)(editor), *The Earth as a Planet (from the Solar System - Volume II)*, University of Chicago Press.

Kukla G.J. (1975), *Nature* 253, 600-603, Missing Link between Milankovitch and Climate.

Kukla G.J. and Kukla H.J. (1974), *Science* 183, 709-714, Increased Surface Albedo in the Northern Hemisphere.

Lamb H.H. (1972), *Climate: Past, Present and Future, Volume I*, Methuen and Co. Ltd.

Lee R. (1973), *J. Appl. Meteor.* 12, 556-557, The "Greenhouse" Effect.

Leighton R.B. and Murray B.C. (1966), *Science* 153, 136-144, Behaviour of Carbon Dioxide and Other Volatiles on Mars.

Levine J.S. and Riegler G.R. (1974), *Geophys. Res. Letters* 1, 285-287, Argon in the Martian Atmosphere.

Li Y-H (1972), *Amer. J. Sci.* 272, 119-137, Geochemical Mass Balance among Lithosphere, Hydrosphere and Atmosphere.

Lovelock J.E. (1975), *Proc. R. Soc. Lond. B.* 189, 167-181, Thermodynamics and the Recognition of Alien Biospheres.

Margulis L. (1976), *Nature* 259, 175-176, Report of the Second College Park Symposium held at the University of Maryland, U.S.A.

Margulis L. and Lovelock J.E. (1974), *Icarus* 21, 471-489, Biological Modulation of the Earth's Atmosphere.

Marsden B.G. and Cameron A.G.W. (1966)(editors), *The Earth-Moon System*, Plenum Press, New York.

Meadows A.J. (1972), *Phys. Letters* 5C, 199-235, The Atmosphere of the Earth and the Terrestrial Planets.

Metz W.D. (1976), *Science* 192, 454-455, Venus: Radar Maps Show Evidence of Tectonic Activity.

Milankovitch M. (1920), *Theorie Mathematique des Phenomenes Terminques Produits par la Radiation Solaire*. Belgrade.

McElhinny M.W. (1973), *Palaeomagnetism and Plate Tectonics*, Cambridge University Press.

McElroy M.B. (1972), *Science* 175, 443-445, Mars: An Evolving Atmosphere.

McElroy M.B. and Hunten D.M. (1969), *J. Geophys. Res.* 74, 1720-1739, The Ratio of Deuterium to Hydrogen in the Venus Atmosphere.

- Moore P. (1971), Quart. J. R. Astr. Soc. 12, 45-47, Transient Phenomena on the Moon.
- Moroz V.I. (1974), Izvestia, March 28, Portrait of the Planet Mars.
- Moroz V.I. (1976), Icarus 28, 159-163, Argon in the Martian Atmosphere: Do the Results of Mars 6 Agree with the Optical and Radio Occultation Measurements.
- Murray B.C., Ward W.R. and Yeung S.C. (1973), Science 180, 638-640, Periodic Insolation Variations on Mars.
- Owen T. (1974), Science 183, 763-764, Martian Climate: An Empirical Test of Possible Gross Variations.
- Owen T. (1976), Icarus 28, 171-177, Volatile Inventories on Mars.
- Ozima M. (1975), Geochim. Cosmochim. Acta. 39, 1127-1134, Ar Isotopes and Earth-Atmosphere Evolution Models.
- Plass G.N. (1960), J. Opt. Soc. Amer. 50, 868-875, Useful Representations for Measurements of Spectral Band Absorption.
- Pollack J.B. and Young R. (1975), J. Atmos. Sci. 32, 1025-1037, Calculations of the Radiative and Dynamical State of the Venus Atmosphere.
- Ramsay J.G. (1963), Trans. Geol. Soc. S. Afr. 66, 353-398, Structural Investigations in the Baberton Mountain Land, Eastern Transvaal.
- Rasool S.I. and De Bergh C. (1970), Nature 226, 1037-1039, The Runaway Greenhouse and the Accumulation of CO<sub>2</sub> in the Venus Atmosphere.
- Robinson N. (1966), Solar Radiation, Elsevier.
- Rodgers C.D. and Walshaw C.D. (1966), Quart. J. R. Met. Soc. 92, 67-92, The Computation of Infrared Cooling Rates in Planetary Atmospheres.
- Roxburgh I.W. (1974), Nature 248, 209-211, Internal Rotation of the Sun and the Solar Neutrino Flux.
- Rubey W.W. (1951), Bull. Geol. Soc. Amer. 62, 1111-1148, Geologic History of Sea Water: An Attempt to State the Problem.
- Sabu D.D. and Manuel O.K. (1976), Nature 262, 28-32, Xenon Record of the Early Solar System.
- Sagan C. and Lederberg J. (1976), Icarus 28, 291-300, The Prospects for Life on Mars: A Pre-Viking Assessment.
- Sagan C. and Mullen G. (1971), Laboratory Report; Centre for Planetary Studies, Cornell University, Ithaca, New York. The Evolution of Earth and Mars.

Sagan C. and Mullen G. (1972), Science 177, 52-56, Earth and Mars: Evolution of Atmospheres and Surface Temperatures.

Sagan C., Toon O.B. and Gierasch P.J. (1973), Science 181, 1045-1049, Climatic Change on Mars.

Schidlowski M., Eichman R. and Junge C.E. (1975), Precambrian Res. 2, 1-69, Precambrian Sedimentary Carbonates: Carbon and Oxygen Isotope Chemistry and Implications for the Terrestrial Oxygen Budget.

Schneider S.H. (1972), J. Atmos. Sci. 29, 1413-1422, Cloudiness as a Global Climatic Feedback Mechanism: The Effects on the Radiation Balance and Surface Temperature of Variations in Cloudiness.

Schneider S.H. (1975), J. Atmos. Sci. 32, 2060-2066, On the Carbon Dioxide - Climate Confusion.

Schwarzschild M., Howard R. and Harm R. (1957), Ap. J. 125, 233-241, Inhomogeneous Stellar Models. V. A Solar Model with Convective Envelope and Inhomogeneous Interior.

Schwarzschild M. (1958), Structure and Evolution of Stars, Princeton University Press.

Sellers A. and Meadows A.J. (1975), Nature 254, 44, Long Term Variations in the Albedo and Surface Temperature of the Earth.

Sellers W.D. (1973), J. Appl. Meteor. 12, 241-254, A New Global Climatic Model.

Severny A.B., Kotov V.A. and Tsap T.T. (1976), Nature 259, 87-89, Observations of Solar Pulsations.

Seyfert C.K. and Sirkin L.A. (1973), Earth History and Plate Tectonics, Harper Row, New York.

Shaw D.H. and Donn W.L. (1968), Science 162, 1270-1272, Milankovitch Radiation Variations: A Quantitative Evaluation.

Sherr P.E., Glasen A.H., Barnes J.C. and Willand J.H. (1968), Contract Report for N.A.S.A. CR-61226, Worldwide Cloud Cover Distribution for Use in Computer Simulations. (Allied Research Association Inc.).

Sylvester-Bradley P.C. (1972), The Geology of Juvenile Carbon in Exobiology, Frontiers of Biology (editor Ponnamperuma C.), North-Holland, Amsterdam.

Turekian K.K. and Clarke S.P. Jr. (1975), J. Atmos. Sci. 32, 1257-1261, The Non-Homogeneous Accumulation Model for Terrestrial Planet Formation and the Consequences for the Atmosphere of Venus.

Van Woerkom A.J.J. (1953), The Astronomical Theory of Climate Changes, in Climate Change (editor) Shapley H., Harvard University Press.

Vonder Haar T.H. and Suomi V.E. (1971), J. Atmos. Sci. 28, 305-314, Measurements of the Earth's Radiation Budget from Satellites During a Five-Year Period. Part I: Extended Time and Space Means.

Vonder Haar T.H. and Suomi V.E. (1972), J. Atmos. Sci. 29, 602-607, Reply.

Walker J.C.G. (1975), J. Atmos. Sci. 32, 1248-1256, Evolution of the Atmosphere of Venus.

Walker J.C.G. (1976) (to be published), Evolution of the Atmosphere, Hafner Press.

Walker J.C.G., Turekian K.K. and Hunten D.M. (1970), J. Geophys. Res. 75, 3558-3561, An Estimate of the Present-Day Deep-Mantle Degassing Rate from Data on the Atmosphere of Venus.

Ward W.R. (1973), Science 181, 260-262, Large Scale Variations in the Obliquity of Mars.

Weare B.C. and Snell F.M. (1974), J. Atmos. Sci. 31, 1725-1734, A Diffuse Thin Cloud Atmospheric Structure as a Feedback Mechanism in Global Climatic Modelling.

Weertman J. (1976), Nature 261, 17-20, Milankovitch Solar Radiation Variations and Ice Age Ice Sheet Sizes.

Wick G.L. (1971), Science 173, 1011-1012, Neutrino Astronomy - Probing the Sun's Interior.

Wilcox J.M. (1975), J. Atmos. Terr. Phys. 37, 237-256, Solar Activity and the Weather.

Winston J.S. (1972), J. Atmos. Sci. 29, 598-601, Comments on 'Measurements of the Earth's Radiation Budget from Satellites During a Five-Year Period. Part I: Extended Time and Space Means'.

Woichenshyn P.M. (1974), Icarus 22, 325-344, Global Seasonal Atmospheric Fluctuations on Mars.

Woolfson M.M. (1976) in Proceedings of the N.A.T.O. Advanced Study Institute on the Origin of the Solar System, Newcastle University, U.K.

PUBLICATIONS

## THE EVOLUTION OF THE SURFACE TEMPERATURE OF MARS

ANN HENDERSON-SELLERS and A. J. MEADOWS  
Astronomy Department, University of Leicester, Leicester, England

(Received in final form 18 June 1975)

**Abstract**—Changes in the average surface temperature of Mars are studied as a function of the time that has elapsed since the origin of the planet. Time variations in the factors influencing the surface temperature are investigated; and approximate methods for computing the effect of such variations are discussed. Three possible degassing sequences are postulated, and their likely effects for the presence of liquid water on the Martian surface are assessed.

### INTRODUCTION

The surface temperature of a terrestrial planet is of critical importance for the development both of its atmosphere and of its surface features. Thus the presence of liquid water (and, hence, the occurrence of surface erosion) and the rate of chemical reaction between the atmosphere and the surface both depend on this temperature. Since, however, the average surface temperature of a planet may change gradually with time, a complete picture of atmosphere-surface interaction can only be obtained by following such changes throughout the entire lifetime of a planet. In the present paper, we attempt to carry out such a study for Mars.

It must be emphasized that studies of the evolution of planetary atmospheres throughout the entire lifetime of the solar system necessarily involve the use of simplified atmospheric models. More complex models, such as are used, for example, to examine climatic change on Earth over periods of a few thousand years, cannot be applied to long-term evolution: the computational requirements would be excessive and, in any case, the necessary detailed data are lacking except for the very recent past. The resultant models are therefore subject to the same sorts of limitation that apply to stellar evolution calculations. This implies that, on the one hand, only major variations in the calculated parameters (in our case, specifically the surface temperature) can be examined: on the other, approximate, time-averaged quantities are generally sufficient for our purpose, i.e. we can ignore many shorter-period atmospheric variations.

### THE DETERMINATION OF THE EFFECTIVE TEMPERATURE

Long-term changes in the average surface temperature,  $T_s$ , of a planet with an evolving atmosphere

are most readily derived in terms of an effective temperature,  $T_e$ , defined by, in the initial state of the planet,

$$S(1 - A) = ef\sigma T_e^4,$$

where  $S$  is the solar flux, integrated over all wavelengths, at the average distance of the planet from the Sun;  $A$  is the Russell-Bond spherical albedo for the planet;  $e$  is the emissivity of the planetary surface; and  $f$  (which we shall in future call the 'flux factor') represents the ratio of the area of the planet emitting radiation to the area intercepting the solar radiation flux. All four factors  $S$ ,  $A$ ,  $e$  and  $f$  are potentially variable over the time-scale of a planet's existence. Variations in the first three of these have been recognized (though not necessarily simultaneously) in previous calculations of atmospheric evolution (e.g. Rasool and De Berg, 1970; Sagan and Mullen, 1972). We wish to point out in this section that it may also be necessary to introduce a varying flux factor, if atmospheric evolution is to be properly represented, and that this entails a further consideration of the definition of effective temperature.

The choice of a value for the flux factor is usually dismissed as elementary. For a rapidly rotating planet with a thick atmosphere it is supposed that the area emitting radiation is  $4\pi R^2$  (where  $R$  is the planetary radius), whereas for a slowly rotating planet with a thin atmosphere the emitting area is taken to be  $2\pi R^2$  (Sagan and Mullen, 1972; Hunten, 1971). Since the area receiving solar radiation is  $\pi R^2$ , the flux factors for these two cases are 4 and 2, respectively. For Mars, the choice is less than obvious: although it is a rapidly rotating planet, it possesses only a thin atmosphere. A consequent uncertainty over the value of  $f$  to be adopted can be detected in the recent literature (e.g.  $f = 4$  in Gierasch *et al.*, 1970;  $f = 2$  in Hunten, 1971). In observational terms, this problem is reflected in the

difficulty of establishing a value for the average surface temperature of Mars, owing to the large fluctuations in the surface temperature during one rotation (for details of the observations, see Kondrat'yev and Bunakova, 1974; Woichensyn, 1974). In terms of this theoretical model, it can be assumed that reasonable values for  $T_s$  can be derived by averaging for  $T_e$  either over the whole surface of the planet, or over half of its surface; but the link between  $T_e$  and  $T_s$  requires rather more consideration for Mars. The usual approach effectively assumes either that  $T_e$  is a constant over the rotation period, or that it has a square-wave variation. The obvious extension to Mars is to assume a square-wave variation again, but with a more prolonged maximum than minimum. (This corresponds physically to assuming that  $T_e$  remains at the day-side value over some specified area on the night-side.) Our task, then, is to consider what fraction of the Martian surface should be assigned a non-negligible value of  $T_e$ , and to deduce the corresponding value of  $f$  for use in our basic equation. The need to do this is not solely determined by a wish to improve agreement between theoretical and observational values of  $T_s$  for Mars. More generally, during the evolution of a planet's atmosphere, the planet may pass from an  $f = 2$  state to an  $f = 4$  state. The method we introduce here enables this transition to be carried out smoothly in the computations.

We have estimated the appropriate flux factor for the present-day Mars by working back from the observed day-time and night-time temperatures of the surface, assuming an overall radiation balance during the course of complete rotation of the planet. This leads to a value of  $f \approx 2.7$ , corresponding to  $T_e \approx 242$  K. Table 1 shows the variation of  $T_e$  and  $T_s$  for different values of  $f$ . The method for deriving  $T_s$  is described in the next section: for these computations, we have taken  $A = 17\%$ ,  $e = 0.95$ , and a solar flux at Mars =  $600 \text{ W m}^{-2}$ .

TABLE 1

Flux factor	Effective temperature (K)	Surface temperature (K)
4.0	219	228
3.0	236	235
2.7	242	252
2.0	261	270

The value we have allotted to the Martian albedo in these computations deserves a brief mention. It is a reasonable figure to use when averaging over the entire Martian orbit. But as a result of the inclina-

tion of the rotational axis and the ellipticity of the orbit of Mars, the actual value of the albedo varies round the orbit. This is a consequence of systematic changes in the surface reflectivity as a function of angle—a point we have noted for the albedo of the Earth (Sellers and Meadows, 1975). According to our estimates, the variation is from 14.8% at perihelion to 17.6% at aphelion: this difference is sufficiently large that it needs to be taken into account if mean temperatures are being calculated for a specific position in the orbit.

#### LONG-TERM EVOLUTION OF THE SURFACE TEMPERATURE OF MARS

Accepting that the Martian atmosphere has formed by degassing (cf. Meadows, 1973), we can derive values for  $T_e$  and  $T_s$  as the atmosphere builds up from zero surface pressure to the present value. The factors involved in deriving these temperatures can be divided into three groups. (i) In the defining equation for  $T_e$  we must allow for changes in  $S$ ,  $A$  and  $f$ . (The emissivity,  $e$ , is unlikely to have undergone any major change.) (ii) In deriving values for  $T_s$  we must examine the effect of increasing atmospheric mass per unit area, and allow for any changes in the chemical composition. (iii) Finally, although the sequence of change in  $T_e$  and  $T_s$  will remain the same regardless of the rate of degassing, this latter will, of course, determine the temperature reached at any epoch in the history of Mars. It must therefore be included in the calculations.

We will now examine these factors in reverse order, beginning with the rate of degassing. This is the least well-known of all the variables mentioned. For the Earth, the balance of the evidence probably points to a more rapid degassing rate early in its history (Walker, in press). However, it seems physically reasonable that the rate of degassing should be associated with the level of tectonic activity on a planet. This seems to have been high on Earth at least since the beginning of the geological record, but the Mariner data for Mars suggest that tectonic activity there is still in the growth stage. This would indicate either fairly continuous degassing of Mars throughout its history, or even that most of the atmosphere should be attributed to a relatively recent degassing episode. Nevertheless, it has also been urged (Fanale, 1971) that Mars, like the Earth, underwent most of its degassing early in its life. We must obviously conclude that the degassing rate for Mars remains uncertain: we have therefore carried out our calculations for three alternative models. For Case I, we have assumed rapid initial degassing, with the present Martian atmosphere essentially

formed by the end of the first aeon ( $1 \times 10^9$  yr) of the planet's history (taken to be 4.5 aeons long). For Case II, we have employed a constant degassing rate throughout the lifetime of the planet; and, for Case III, we have supposed a late degassing episode, with the Martian atmosphere building up from zero to the present value in the last two aeons. In each instance, we have used the additional data outlined below to trace the development of  $T_e$  and  $T_s$  for Mars over the past 4.5 aeons.

One uncertainty in linking  $T_e$  and  $T_s$  for Mars over the lifetime of the solar system derives from the need to suppose that the chemical composition of the planet's atmosphere has not changed greatly throughout its history. If this assumption is wrong, the derivation of  $T_s$  for earlier epochs will be incorrect. It is often assumed that the Earth's early atmosphere contained reduced gases: these became oxidized at a later date, and, at a still later date, free oxygen appeared in the atmosphere. Hence, the present atmospheric composition has evolved in three stages. The evidence put forward for this complex development is fairly tenuous, and there is, in any case, no reason to suppose that the Martian atmosphere has followed a parallel evolutionary path. We therefore assume in the present paper that the Martian atmosphere has always had its present chemical composition.

We turn now to possible variations of  $S$ ,  $A$  and  $f$  with time. According to theoretical models of solar evolution, the Sun's luminosity has been increasing gradually over the past 4.5 aeons: so, consequently, has  $S$ . In the present calculations we have assumed a 30% increase in solar luminosity, occurring linearly with time. This is a fairly conservative estimate, based on a number of models (e.g. Ezer and Cameron, 1965). The albedo of Mars must also have changed significantly during degassing—a point that has been overlooked in some earlier work on this topic. It would be expected that the albedo of an atmosphere-less planet with a cratered surface should be similar to present-day values for the Moon or Mercury, i.e. 7%. As we have seen, the present value for Mars is 17%. The difference can be associated with the build-up of an atmosphere on Mars: we have assumed that the albedo has increased in proportion to the atmospheric mass per unit area. We have discussed the variation of the flux factor with time in the first section of this paper. We expect it to change from a value of 2 for the atmosphere-less planet to a value of 2.7 today. In the light of our discussion it is reasonable to suppose that this change, too, will proceed in step with the increasing atmospheric mass per unit area.

## RESULTS OF CALCULATIONS

In carrying out the calculations, we have used an approach similar to that adopted by Sagan and Mullen (1972). The average surface temperature of the planet,  $T_s$ , is obtained, allowing for the 'greenhouse' effect, by dividing the emergent flux into two parts, one emitted from the surface through 'windows' in the infrared absorption spectrum and one emitted from the top of the atmosphere at a temperature of  $2^{-1/4} T_e$  (from Eddington's approximation). Thus we have

$$\frac{S}{f} (1 - A) = \sum_{\lambda_i} e B_{\lambda_i}(T_s) \Delta \lambda_i + \sum_{\lambda_j} B_{\lambda_j}(2^{-1/4} T_e) \Delta \lambda_j$$

where the infrared absorption spectrum is approximated by a step function, so that there is total absorption at the wavelengths  $\lambda_j$  and zero absorption at the wavelengths  $\lambda_i$ . The effective temperature,  $T_e$ , required in this computation can be obtained directly, since

$$\frac{S}{f} (1 - A) = \sigma T_e^4.$$

Values for  $T_e$  and  $T_s$  can thus be linked by a computer program using the data for  $S$ ,  $A$ ,  $f$ ,  $e$  and the chemical composition described in the preceding section.

Figure 1 shows the results for both  $T_e$  and  $T_s$  in Case II (linear degassing rate). The significant point to note here is the way in which the changes in the albedo and flux factor compensate for the changing solar luminosity, so that the surface temperature of Mars varies very little throughout its history.

Figure 2 shows the results for  $T_s$  obtained in Case I (early degassing) and Case III (late degassing). For both these, the degassing rate and the rate of change

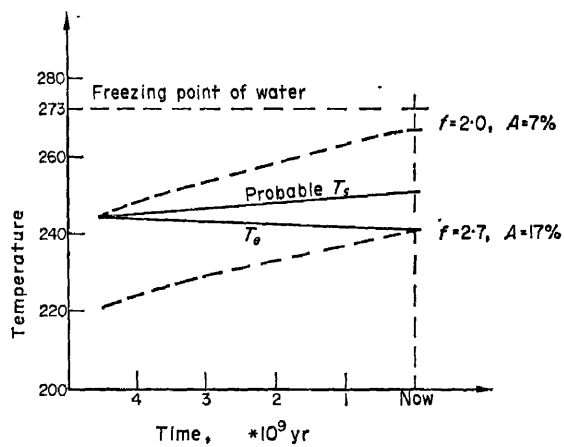


FIG. 1. THE EVOLUTION OF  $T_e$  AND  $T_s$  FOR MARS IN CASE II (A LINEAR DEGASSING RATE). THE SURFACE TEMPERATURE (IN K),  $T_s$ , IS SEEN TO VARY LITTLE THROUGHOUT THE 4.5 aeons.

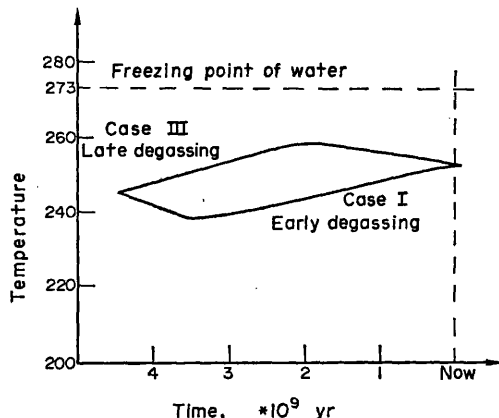


FIG. 2. THE EVOLUTION OF THE SURFACE TEMPERATURE (IN K),  $T_s$ , IN BOTH CASE I (EARLY DEGASSING) AND CASE III (LATE DEGASSING).

of the flux factor are different, so that  $T_s$  changes appreciably with time. Hence, in Case I, the surface temperature passes through a minimum value of about 239 K one aeon after the formation of Mars; whereas, in Case III, it passes through a maximum of about 261 K at the beginning of the postulated degassing episode two aeons ago.

#### CONCLUSION

Our results represent the first reasonably comprehensive study of the possible long-period changes in the surface temperature of Mars. Clearly, whatever degassing rate is assumed, the mean surface temperature of the planet remains below the freezing point of water. However, in view of the large temperature fluctuations on Mars, areas of the planet can have temperatures which are above the freezing point for an appreciable fraction of the time even when the mean temperature is below this figure. Consequently,

the occurrence of liquid water on the surface of the planet becomes increasingly possible as the mean temperature rises. It is evident from our results that a late degassing episode is especially suitable for 'switching on' a liquid water phase at a particular point in the development of Mars. The Mariner observations of the Martian surface might therefore be taken to support a link between tectonic activity and atmospheric growth in the recent history of Mars.

*Acknowledgements*—One of us (A. H.-S.) wishes to thank SRC for financial support.

#### REFERENCES

- Ezer, D. and Cameron, A. G. W. (1965). A study of solar evolution. *Can. J. Phys.* **43**, 1497.
- Fanale, F. P. (1971). History of Martian volatiles: implications for organic synthesis. *Icarus* **15**, 279.
- Gierasch, P., Goody, R. and Stone, P. (1970). The energy balance of planetary atmospheres. *J. geophys. Fluid Dyn.* **1**, 1.
- Hunten, D. M. (1971). Composition and structure of planetary atmospheres. *Space Sci. Rev.* **12**, 539.
- Kondrat'yev, K. Ya. and Bunakova, A. M. (1974). The meteorology of Mars. Nasa Tech. Transl., NASA TT F-816.
- Meadows, A. J. (1973). The origin and evolution of the atmospheres of the terrestrial planets. *Planet. Space Sci.* **21**, 1467.
- Rasool, S. I. and De Bergh, C. (1970). The runaway greenhouse and the accumulation of CO<sub>2</sub> in the Venus atmosphere. *Nature, Lond.* **226**, 1037.
- Sagan, C. and Mullen, G. (1972). Earth and Mars: Evolution of atmospheres and surface temperatures. *Science*, **177**, 52.
- Sellers, A. and Meadows, A. J. (1975). Long term variations in albedo and surface temperature of the Earth. *Nature, Lond.* **254**, 44.
- Walker, J. C. G. To be published. *Evolution of the Atmosphere*. Hafner.
- Woichenshyn, P. M. (1974). Global seasonal atmospheric fluctuations on Mars. *Icarus* **22**, 325.

## Long term variations in the albedo and surface temperature of the Earth

THE surface temperature of the Earth depends primarily on the solar constant, the Earth's albedo and the total mass and chemical composition of the terrestrial atmosphere. Studies of climate covering the past few million years have generally allowed for variations in albedo in calculating average values of the surface temperature. But over longer periods of time, however, less allowance has been made for albedo variations; it has, indeed, frequently been assumed that the albedo, when averaged over a long enough time, can be taken to be constant (see ref. 1). We wish to point out that, on the contrary, long term variations in the albedo can be expected to occur, and to produce significant changes in the average surface temperature.

The total albedo of the Earth depends on the relative proportions and dispositions of the continents and oceans and their related cloud covers. This varies both because the cross section presented to incident solar radiation by a given area depends on its latitudinal position, and because the variation in reflectivity with angle of incident radiation changes from land to ocean. Throughout much of the geological record, the relative amounts of continent and ocean do not seem to have undergone major change; but the relative disposition of the two has varied considerably because of continental drift. The amount of land area, as distinct from continental area, has certainly undergone fluctuations, but no systematic trend appears either in time, or relative to the disposition of the continents on the Earth's surface. We have estimated the average surface temperature of the Earth using a computer program which allows both for the greenhouse effect of the atmosphere and for variations in albedo resulting from different positions of the continental masses, but which assumes no significant change in the ratio of land-to-ocean area. (Surface temperatures have been computed as a function of latitude for land and ocean separately, and an average, weighted according to the areas involved, has then been calculated.)

If cloud cover is initially ignored, the important factor is the latitudinal distribution of the continents. We have therefore looked especially at two extreme cases: (1) where the continents are gathered together into a belt round the equator; (2) where they form a cap round one, or both, poles. We have constructed semi-empirical curves of reflectivity as a function of the angle of incident radiation, assuming in case (1) a covering of soil, and in case (2) an ice-snow covering. Although considerable information is available on the albedo of different types of surface, data on the variation of albedo with solar elevation are less well determined<sup>2</sup>. Fortunately, computer runs using a range of possible albedo variations with angle indicate that only minor changes are produced in the surface temperature with any reasonable functional relationship. The difference in albedo between the two models is found to change the surface temperature by more than 12 °C (the higher temperature corresponding to the equatorial position of the continents). Since the difference between a glacial and an interglacial period probably corresponds to a change in average temperature of only 5 °C (ref. 3), this albedo-dependent variation must be regarded as significant.

There are, however, two modifications that should be made. First, we have assumed extreme dispositions of the land-masses in deriving this figure for the surface temperature. More probable variations in the latitudinal position of the centre of area of the continents will still lead to differing values of the albedo, and therefore to differences in surface temperature, but

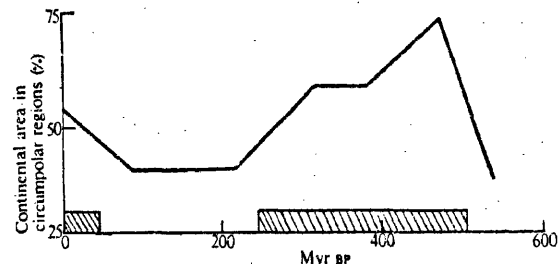


Fig. 1 Variation of continental area within 30° of poles as a function of time. The shaded parts of the time axis include all extensive glaciations<sup>4,5</sup>.

the change will be smaller than that derived above. Similarly, the effect of introducing cloud cover into the calculations, for any likely cloud distribution, is to reduce the change in albedo and so the variation in surface temperature. Nevertheless, after allowing for both these factors, the amount of latitudinal change postulated in reconstructions of continental drift still seems from our estimates to be capable of producing a variation in surface temperature of a few degrees. The effect of this would be to accentuate the prevailing climatic conditions. In particular, although a land-mass near one of the poles would, in any case, be expected to have an ice-snow cover, a resultant slight lowering of the average temperature, as a result of the albedo effect, could turn this into a major glaciation. The effects of this could then extend to appreciably lower latitudes than would otherwise be the case. Whether or not this occurs will depend on other astronomical and geological factors. What we can assert is a statement of probability: that the likelihood of extensive glaciation occurring should be greater when a higher proportion of the land mass is near the poles.

We have used the data cited by McElhinny<sup>4</sup> to derive values for the latitudinal distribution of the continents during each geological period. The results are best represented in terms of the percentage of the terrestrial surface within 30° of each pole which is covered by continent. The reason for choosing this form of presentation for the data is that continental displacements at lower latitudes, although leading to small changes in the albedo, cannot support extensive glaciation. It is the latter that can most readily be detected in the geological record.

Some of the data on continental drift remain uncertain. In particular, information on continental drift and major glaciations in the Precambrian is still inadequate for the type of comparison we wish to make here. Nevertheless, as can be seen from Fig. 1, if we separate out the periods during which extensive glaciations most commonly occurred<sup>5</sup>, these correlate reasonably well with periods when a higher percentage of the circum-polar regions was occupied by continents. Within the limits of accuracy of the data, therefore, predictions based on the albedo effect are supported by the available geological evidence.

A.S. thanks the SRC for support.

HENDERSON

ANN SELLERS

A. J. MEADOWS

Astronomy Department,  
University of Leicester, UK

Received July 18, 1974; revised January 27, 1975.

1 Sagan, C., and Mullen, G., *Science*, 177, 52 (1972).

2 Robinson, N. (ed.), *Solar Radiation*, ch. 6 (Elsevier, Amsterdam, 1966).

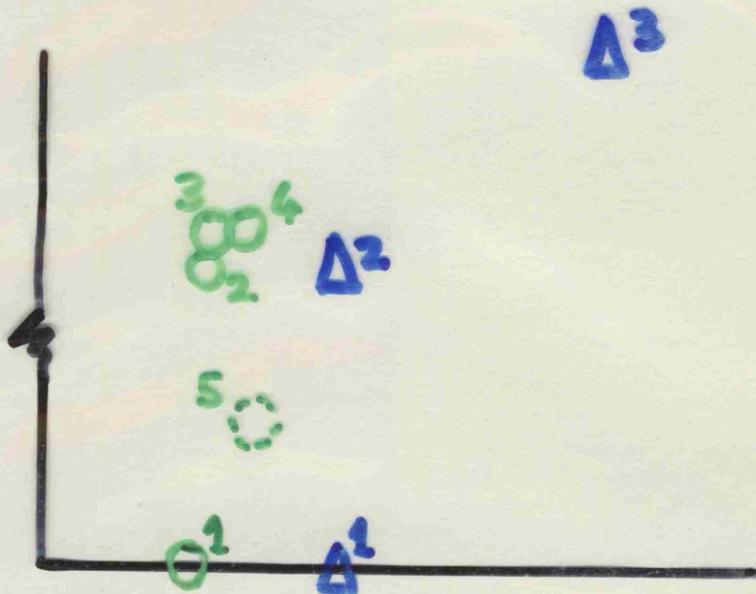
3 Bryson, R. A., *Science*, 184, 733 (1974).

4 McElhinny, M. W., *Palaeomagnetism and Plate Tectonics* (Cambridge University Press, 1973).

5 Seyfert, C. K., and Sirkin, L. A., *Earth History and Plate Tectonics*, 455 (Harper and Row, New York, 1973).

VIEW-RID. CHAPTER 5

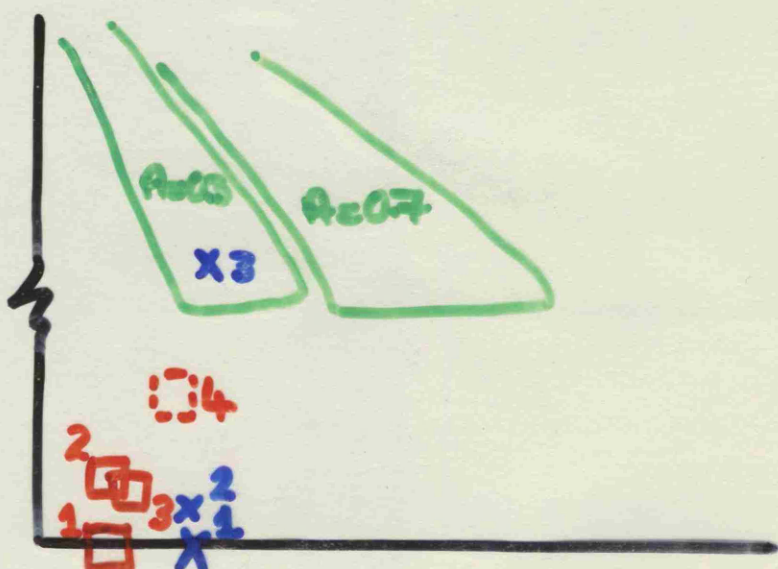
MODEL 1 A  
MODEL 2 O



MODEL 3 □

MODEL 2\* X

LIFE-BEARING ZONES (Figure 5.19)





HENDERSON-SELLERS

PH.D. THESIS 1976

ABSTRACT

A theoretical model which permits the computation of average surface temperature trends over the whole life-time of any terrestrial planet is described. The evolution of the atmosphere is considered in detail, and the changes in the physical parameters which affect the surface temperature are discussed. The variables of particular importance are the planetary albedo, the flux factor (a parameter previously considered constant), the infrared absorption spectrum of the atmosphere, the surface infrared emissivity and the probable evolutionary changes in the solar luminosity. Each of these parameters is discussed in detail and the possible feedback mechanisms which may link them to the evolution of the planetary atmosphere/surface system are considered.

The computational techniques utilized in the development of the numerical model are described. The errors are discussed and the model is found to be widely applicable and to produce smoothed temperature tracks which agree well with present-day data for both the Earth and Mars. Numerical methods are used to extend laboratory parameterizations for the variation of absorption with absorber amount and partial pressure for two gases: carbon dioxide and water vapour. Trace constituents and the effect of broadening by neutral gases are discussed.

The resulting temperature curves exhibit a number of interesting features. In particular, a number of the model planets considered are found to exhibit remarkably stable surface

temperatures as their atmospheres evolve. This stability results, in part, from the compensatory nature of the evolution of some of the planetary parameters. The rate and mode of degassing is found to be particularly important for Mars and may also be important for Venus. The temperature curve for the Earth remains above the freezing point of water throughout the life-time of the planet, and thus the predicted results agree well with geological data. Shorter-term fluctuations leading to glaciations, etc., are also discussed.

---